

# **Nucleation and Anti-Nucleation of Polyamides**

**Dissertation**

for the award of the academic degree of

Doctor of Natural Science (Dr. rer. nat.)

from the Faculty of Biology, Chemistry, and Geoscience

University of Bayreuth

submitted by

**Johannes Heigl**

born in Haßfurt

Bayreuth 2016



This doctoral thesis was prepared at the department *Macromolecular Chemistry I* at the University of Bayreuth between July 2012 and November 2016 and was supervised by Prof. Dr. Hans-Werner Schmidt.

This is a full reprint of the dissertation submitted to obtain the academic degree of Doctor of Natural Sciences (Dr. rer. nat.) and approved by the Faculty of Biology, Chemistry and Geosciences of the University of Bayreuth.

Date of submission: 09.03.2017

Date of defence: 05.09.2017

Acting dean: Prof. Dr. Stefan Schuster

Doctoral committee:

Prof. Dr. Hans-Werner Schmidt (1<sup>st</sup> reviewer)

Prof. Dr. Volker Altstädt (2<sup>nd</sup> reviewer)

Prof. Dr. Josef Breu (chairman)

Prof. Dr. Stephan Förster



## **Acknowledgement**

First of all I thank Prof. Dr. Hans-Werner Schmidt for supervising and giving me the opportunity to join his research group at the Chair Macromolecular Chemistry I. I would like to thank him for the highly interesting research topic, which allowed me to gain deep insights into fundamental as well as applied research. Furthermore, I am thankful for the scientific independence that was granted and continuous support that was given. Beyond that I am really grateful for the creative discussions and the enjoyable atmosphere at his chair.

I gratefully acknowledge Dr. Florian Richter and Dr. Arnold Schneller (BASF SE, Ludwigshafen) for fruitful discussions with respect to the work on bisureas in polyamides and the collaboration within the project anti-nucleation of polyamides.

Special thanks go to Jutta Failner, Sandra Ganzleben and Doris Hanft (technicians at Macromolecular Chemistry I) for their great support in additive synthesis and help in polymer processing. Also I would like to thank my colleague Hannes Welz for carrying out the scanning electron microscopy measurements, and Markus Langner (Macromolecular Chemistry II, Prof. Greiner) for his great support with the GCMS measurements.

For numerous productive discussions on supramolecular chemistry, and polymer processing, I would like to thank the following colleagues at Macromolecular Chemistry I: Dr. Klaus Kreger, Dr. Reiner Giesa, Dr. Christian Neuber, Dr. Philipp Knauer, Dr. Andreas Ringk, Dr. Florian Wieberger, Dr. Tristan Kolb and Christian Bartz.

Moreover, I thank my direct laboratory colleagues Dr. Andreas Haedler, Dr. Christian Probst, Christoph Steinlein, Daniel Kremer and Bastian Klose for scientific discussions and the enjoyable and cheerful atmosphere. Likewise I want to thank Petra Weiss and Christina Wunderlich for their administrative support.

I gratefully acknowledge the funding from BASF SE for the research on the nucleation and anti-nucleation of polyamides during my thesis.

Finally, my kind gratitude goes to my parents, my sister Mona, and my girlfriend Hanna who always supported me during my studies and my doctoral thesis.



*“Quod lux lumen”*

*Herbert Stangl*





## Abbreviations

°C	degree Celsius
µm	micrometer
ASTM	American Society for Testing and Materials
DMA	dynamic mechanical analysis
DMSO	dimethyl sulfoxide
DMTA	dynamic mechanic thermal analysis
DSC	differential scanning calorimetry
DTA	differential thermal analysis
e.g.	for example (exempli gratia)
et al.	and others (et alii)
eV	electron volt
g	gram
GC	gas chromatography
GC-MS	gas chromatography – mass spectrometry
h	hour
H	hydrogen
Hz	hertz
i.e.	that is (id est)
IR	infrared
J	joule
K	Kelvin
kN	kilonewton
LiCl	lithium chloride
M	molar mass
m/z	mass-to-charge ratio
mbar	millibar
mg	milligram
MHz	megahertz
min	minute
mL	milliliter
mm	millimeter
mmol	millimole
mol	mole
MPa	megapascal
MS	mass spectrometry
N	nitrogen
NE	nucleation efficiency
nm	nanometer
NMR	nuclear magnetic resonance

PA6	polyamide 6
PA66	polyamide 66
PP	polypropylene
ppm	parts per million
r	radius
rc	critical radius
rh%	relative humidity
s	second
SEM	scanning electron microscopy
subl.	sublime
$T_c$	polymer crystallization temperature
TDU	twister-desorption-liner
<i>tert-</i>	tertiary
$T_g$	glass transition temperature, glass transition temperature
TGA	thermogravimetric analysis
THF	tetrahydrofuran
$T_m$	melting temperature
UV	ultraviolet
WAXS	wide-angle X-ray scattering
wt%	weight percent
XRD	X-ray diffraction
$\Delta G$	free enthalpy
$\Delta H_f$	melt enthalpy
$\lambda$	wavelength
$\sigma$	surface tension

## Table of contents

1	Introduction .....	1
1.1	Polyamides.....	1
1.2	Crystallization of semi-crystalline polymers .....	4
2	Objectives and scope of this thesis.....	9
3	Properties of the neat polyamide 6 grade.....	15
3.1	Compounding and sample preparation.....	17
3.2	Influence of processing conditions on thermal behavior of PA6 .....	20
3.3	Self-nucleation of PA6.....	33
3.4	Crystal modification and degree of crystallinity.....	35
3.5	Glass transition temperature.....	39
3.6	Summary .....	41
4	Nucleation and clarification of polyamide 6.....	43
4.1	Thermal stability and properties of a bisurea additive .....	52
4.1.1	Thermal properties of the bisurea additive .....	56
4.1.2	Nucleation and optical properties of PA6.....	58
4.1.3	Nucleation and optical properties of PA6 under various processing conditions .....	63
4.1.4	Investigation of temperature stability of the bisurea under processing conditions .....	69
4.1.5	Morphology of PA6 at the nanoscale.....	73
4.2	Bisthiourea additives .....	76
4.2.1	Synthesis and characterization of bisthioureas .....	78
4.2.2	Thermal properties of bisthioureas .....	80
4.2.3	Nucleation and optical properties of PA6.....	82
4.2.4	Morphology of injection molded PA6 samples.....	88

4.2.5	Crystal modification and degree of crystallinity .....	90
4.2.6	Water absorption and mechanical properties .....	93
4.3	Summary .....	96
5	Anti-nucleation of polyamides.....	99
5.1	Nigrosine as commercial anti-nucleating agent for PA6 .....	103
5.1.1	Properties of Nigrosine.....	104
5.1.2	Anti-nucleation of PA6 by Nigrosine .....	106
5.1.3	Properties of PA6 containing Nigrosine .....	116
5.2	Salts as anti-nucleating agents.....	120
5.2.1	Lithium chloride.....	121
5.2.2	Ammonium salts.....	126
5.3	Azine dyes as anti-nucleating agents for PA6 .....	138
5.3.1	Properties of azine dyes .....	141
5.3.2	Anti-nucleation of PA6 by azine dyes.....	146
5.4	Neutral Red as anti-nucleating agent for PA6 .....	154
5.4.1	Properties of Neutral Red.....	155
5.4.2	Anti-nucleation of PA6 by Neutral Red .....	157
5.4.3	Properties of PA6 containing Neutral Red .....	167
5.5	Improving anti-nucleating agents by LiCl.....	171
5.6	Water absorption and mechanical properties.....	179
5.7	Anti-nucleation of polyamide 66 .....	183
5.8	Summary .....	188
6	Summary .....	191
7	Zusammenfassung .....	195
8	Experimental part .....	201
8.1	Materials and equipment.....	201

8.2	Methods and procedures .....	204
8.3	Synthesis and characterization of bithiourea derivatives.....	213
9	Literature .....	217



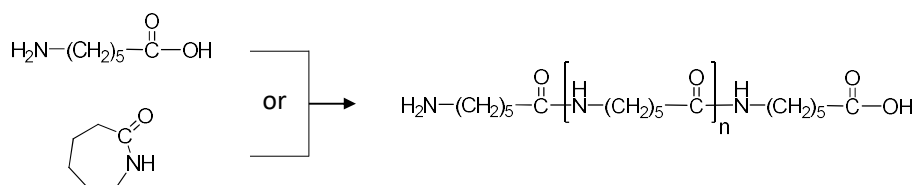
# 1 Introduction

## 1.1 Polyamides

The origin of polyamides dates back to the 1930s. In the course of basic research, Carothers and his coworkers discovered polyamides incidentally and patented polyamide 66 (PA66) in 1935, and polyamide 6 (PA6) in 1938.<sup>[1]</sup> Nowadays, polyamides belong to one of the most important technical polymers for industrial applications. Among all polyamide types, PA6 and PA66 are the most commonly used nylon resins with a market share of 90%, followed by specific polyamide resins such as PA11 and PA12 (7%).<sup>[2]</sup>

Polyamides can be categorized into two main types, which are differentiated because of their monomers. The AB type is synthesized by polymerization via ring opening polymerization of lactams or polycondensation of amino acids. The AABB type is synthesized by polycondensation of diamines and dicarboxylic acids. Both routes are schematically shown in Figure 1. For example, PA6 is mainly synthesized via ring opening polymerization of  $\epsilon$ -caprolactam, whereas PA66 is obtained by a polycondensation reaction of hexamethylenediamine and adipic acid.<sup>[2]</sup>

### AB type:



### AABB type:

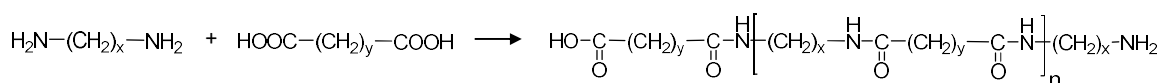


Figure 1. Synthetic routes to polyamides of the AB type such as PA6 and AABB type such as PA66.

PA6 and PA66 are distinguished by a large number of advantageous properties, such as high toughness, and high temperature resistance, which guarantee them an important market position in the engineering thermoplastics sector.<sup>[3]</sup> In contrast to other thermoplastics, polyamides tend to absorb high amounts of moisture. Depending on the polyamide type, 10% water uptake is possible.<sup>[2]</sup> Thus, swelling values of up to 0.3% per 1.0% water uptake may occur and have to be considered. In order to prevent negative effects, polyamides have to be dried prior to processing and finished components have to

be conditioned. Moreover, polyamides are polar and thus resistant to diluted bases, hydrocarbons, esters, ketones, alcohols and oils. They are unstable in the presence of strong bases and acids, as well as chlorinated hydrocarbons. At elevated temperatures, hydrolysis may occur.<sup>[3]</sup>

Main consumer of polyamides is the automotive industry. Due to their strong mechanical load capability, polyamides have replaced several metal parts in cars or trucks, such as gears, bearings and coil forms among others.<sup>[2]</sup> Especially the resistance to oil and the thermal stability in combination with weight reduction awards polyamides unique properties for numerous industrial applications.

One major benefit of polyamides, and in general for all polymers, is that their properties can be influenced by additives in order to obtain tailored materials for specific applications. Nowadays, numerous additives are used to control the crystallization process and with that the properties of the polymer. The main classes of additives include antioxidants,<sup>[4]</sup> UV-stabilizers,<sup>[5]</sup> flame retardants,<sup>[6]</sup> processing aids,<sup>[7]</sup> colorants,<sup>[8]</sup> optical brighteners,<sup>[9]</sup> nucleating<sup>[10]</sup> and anti-nucleating agents.<sup>[11]</sup> The latter two are known to influence the crystallization behavior of the polymers.

*Nucleating agents* act as nucleation sites inducing polymer crystallization.<sup>[12,13]</sup> As consequence, the polymer crystallization temperature is increased and the spherulite size reduced, beneficially improving for example cycle times during injection molding and mechanical properties. In rare cases nucleating agents can also act as clarifiers to improve the optical properties significantly.<sup>[2,10,14]</sup> In contrast, *anti-nucleating agents* retard the crystallization process of the polymers.<sup>[11,15]</sup> Consequently, the polymer crystallization temperature is decreased and the spherulite size increased, leading to good fluidity, molding precision during injection molding, and enhanced surface gloss of components.<sup>[11,16,17]</sup> Both additive classes significantly influence the crystallization process of the polymer.

In the following, the terms “nucleating agent” and “anti-nucleating agent” are defined regarding their meaning within this work:

**Nucleating agent:** A polymer additive which is capable of increasing the polymer crystallization temperature is henceforth referred to as nucleating agent. Nucleating agents can lead to enhanced properties such as optical or mechanical properties.<sup>[14,18]</sup>



*Anti-nucleating agent:* A polymer additive which is capable of decreasing the polymer crystallization temperature is henceforth referred to as anti-nucleating agent. Anti-nucleating agents do not eliminate the polymer crystallization process but rather retard the polymer crystallization.<sup>[19]</sup> Hence, the result is a polymer with a lower crystallization temperature compared to the neat polymer. Ideally, anti-nucleating agents do not influence further polymer properties, such as the melting temperature or the degree of crystallinity.

### 1.2 Crystallization of semi-crystalline polymers

Semi-crystalline polymers consist of long molecule chains, which occur in crystalline and amorphous regions. In the polymer melt, these polymer chains are present as entangled coils. Upon cooling, the polymer chains start to arrange regularly leading to a partial formation of crystalline structures. The crystalline structures on the macroscale are called spherulites.<sup>[20,21]</sup> The detailed morphology of a spherulite is schematically presented in Figure 2.<sup>[22]</sup>

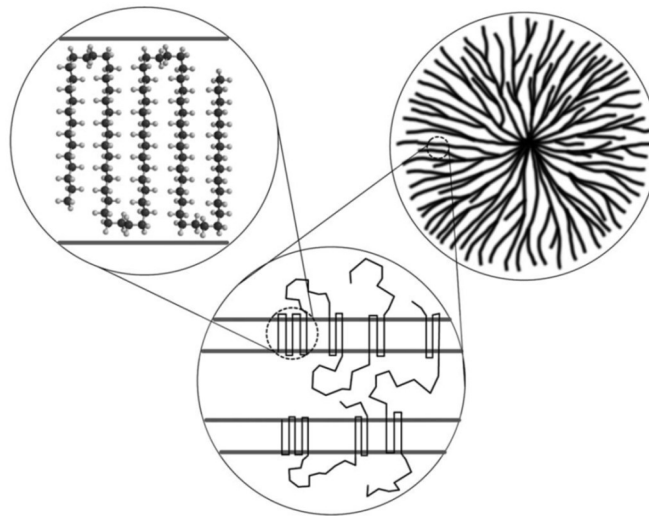


Figure 2. Schematic representation of a semi-crystalline polymer according to Milner.<sup>[22]</sup> Chain-folded crystalline lamellae (top left) lie adjacent to amorphous regions of comparable thickness at the nanoscale (bottom). These lamellae are organized radially into spherulites at the micron scale (top right).

During the crystallization process of semi-crystalline polymers, the polymer chains arrange by folding back and forth vertical to the crystallization plane, resulting in a folded chain crystal (Figure 2, top left image). These chain crystals arrange into lamellar crystallites (bottom), which start to grow from the nucleation site and are separated by amorphous regions. The lamellae are finally organized radially into spherulites at the micron scale (top right).<sup>[20–23]</sup>

For polymer crystallization, the following requirements must be met:<sup>[10]</sup>

- The molecular structure of the polymer must allow crystalline ordering. Therefore, a certain regularity is required.
- The crystallization temperature of the polymer has to be in between the melting temperature and the glass transition temperature of the polymer.
- Nucleation must occur prior to crystallization.
- The crystallization rate should be sufficiently high.

The crystallization of semi-crystalline polymers essentially takes place in two steps, namely *primary and secondary crystallization*. The *primary crystallization* can be divided into nucleation and crystal growth. In the following, the basics of the crystallization of semi-crystalline polymers are revealed.

The driving force of a phase transformation is the difference of the free enthalpy of the initial phase and the final phase. Thermodynamically, a change of the free enthalpy  $\Delta G$  of the system takes place. This process only occurs when the free enthalpy  $\Delta G$  is reduced. During the formation of nuclei, parts of molecules arrange themselves to crystalline structures, and hence release energy. However, in order to form a new phase, energy is required to generate the interface between both phases. Consequently, the overall change of the free enthalpy  $\Delta G$  is composed of a volume fraction  $\Delta G_{\text{volume}}$ , which releases energy, and a surface fraction  $\Delta G_{\text{surface}}$ , which requires energy to generate the interface. This results in the following equation:<sup>[10,20,23]</sup>

$$\Delta G = \Delta G_{\text{volume}} + \Delta G_{\text{surface}} \quad (1)$$

The released energy is proportional to the volume of the nuclei, whereas the required energy is proportional to its surface. Assuming a spherical nuclei with a radius  $r$ , the following equation is applicable:<sup>[10,20,23]</sup>

$$\Delta G = -\frac{4}{3}\pi r^3 \cdot \Delta G_v + 4\pi r^2 \sigma \quad (2)$$

with  $\Delta G_v$  as free enthalpy per volume unit of the nuclei during the phase transition and  $\sigma$  as the surface tension of the melt. Figure 3 presents schematically the primary nucleation of a spherical nuclei.<sup>[23]</sup>

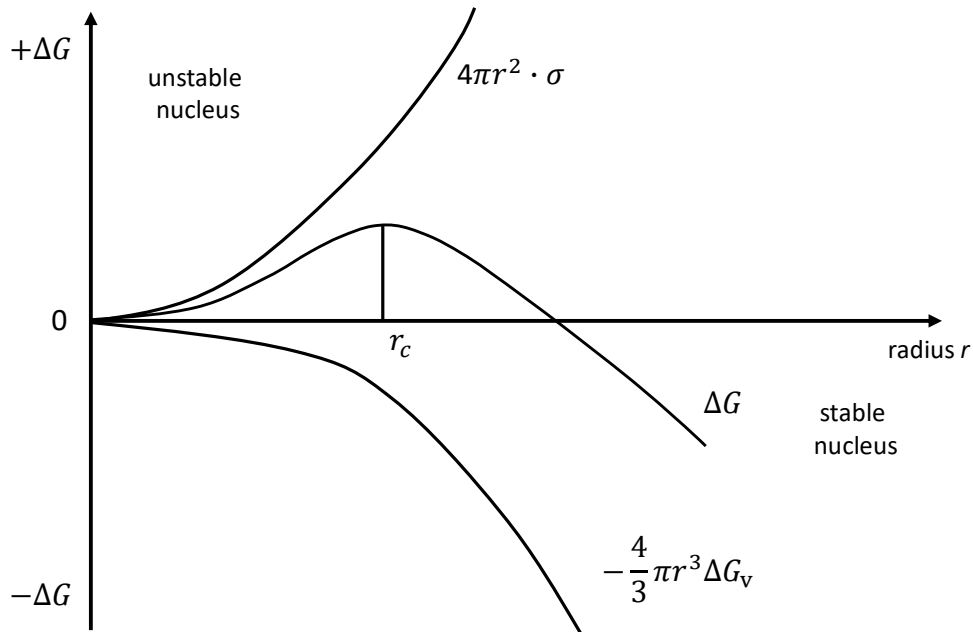


Figure 3. Schematic presentation of primary nucleation of a spherical nuclei (reproduced from Menges).<sup>[23]</sup>

As Figure 3 clearly shows, energy is required to generate a stable nucleus.<sup>[10]</sup> The crystal growth starts not until a nucleus is formed which overcomes the critical nuclei radius  $r_c$ . Nuclei which are smaller than the critical radius minimize their energy by dissolving. The nuclei are only stable when  $\Delta G$  becomes negative. This phenomenon is called primary nucleation which is followed by crystal growth.<sup>[10,23]</sup>

Figure 4 reveals that the rate of nucleation and the rate of crystal growth differ concerning their maximum. When the polymer melt is cooled fast, a high rate of nucleation and a low rate of crystal growth lead to a high nuclei density, and hence smaller spherulites are obtained. Whereas slow cooling from the melt leads to a fast rate of crystal growth and less nuclei due to a low rate of nucleation. Consequently, larger spherulites are obtained. In the metastable region, the rate of nucleation is extremely low, which can be explained by the dissolving of the nuclei. With decreasing temperature the nucleation rate, as well as the rate of crystal growth, increase. When the temperature is getting close to the glass transition temperature  $T_g$  of the polymer, the rate of nucleation decreases due to an increase of the viscosity of the polymer melt.<sup>[10,23]</sup>

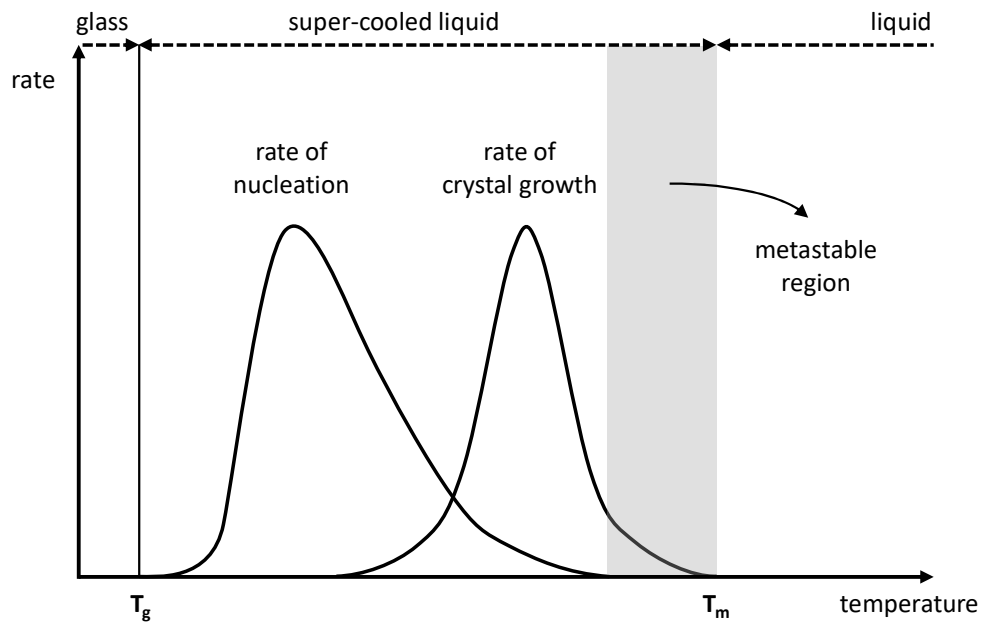


Figure 4. Schematic representation of the rate of nucleation and the rate of crystal growth as a function of the temperature (reproduced from Amos).<sup>[10]</sup>

With respect to primary nucleation, there are three different nucleation mechanisms that can occur during polymer crystallization.<sup>[10]</sup> First, *homogeneous nucleation* occurs spontaneously in the super-cooled melt without further influences. Second, *orientation induced nucleation* occurs in many polymer processes such as extrusion or injection molding. It is caused by orientation of the polymer chains due to flow and shear directions during polymer processing and is known to increase the crystallization rate and the degree of crystallinity.<sup>[24–27]</sup> Third, *heterogeneous nucleation* occurs at the interface of a foreign phase such as impurities, substrates, or nucleating agents. Heterogeneous nucleation is of fundamental interest for industrial applications. By the use of nucleating agents the crystallization behavior and morphology of a polymer can be controlled, and the polymer crystallization temperature easily increased.<sup>[14,28–30]</sup> Furthermore, many macroscopic polymer properties, such as optical and mechanical properties, depend on the morphology and spherulite size, respectively.<sup>[2]</sup> By influencing the crystallization behavior and morphology of polymers, these properties can be set to the desired values for specific applications.

In this thesis the main chapters (3, 4 and 5) are introduced by specific preambles summarizing literature and discussing the state of the art



## 2 Objectives and scope of this thesis

The objectives and scope of this thesis are to explore and develop new additives for technically important semi-crystalline polyamides, and in particular polyamide 6. The principle aim is to influence the polymer crystallization behavior, to control the polymer morphology, and to improve macroscopic properties. In order to obtain the fundamental basis for the experiments in this thesis, *polyamide 6* is investigated in detail and its characteristic properties are determined. The second part of this work deals with *nucleation and clarification of polyamide 6*, followed by a part addressing the issue of *anti-nucleation of polyamides*.

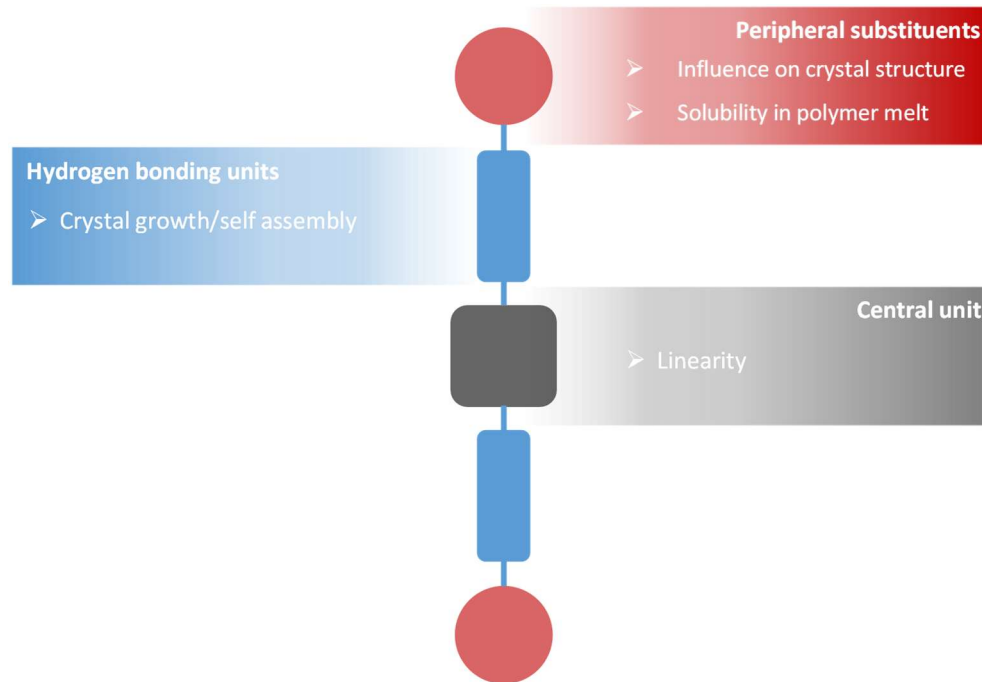
### **Properties of the neat polyamide 6 grade**

In the first part the fundamental properties of the neat polyamide 6 grade used in this work are revealed. Here, polymer processing and sample preparation for subsequent characterizations will be described in order to understand the neat material first, before studying the crystallization behavior influenced by additives. Therefore, the following issues have to be addressed:

- In order to reveal suitable *processing conditions* and *sample preparation methods* within this work, standard conditions and procedures have to be optimized.
- Different processing conditions for a polymer can lead to varying polymer properties. Therefore, the *influence of processing conditions on thermal behavior of PA6* is investigated by means of differential scanning calorimetry (DSC) and gas chromatography – mass spectrometry (GC-MS).
- To calculate the nucleation efficiency of additives *self-nucleation experiments* of neat PA6 have to be conducted to obtain the maximum polymer crystallization temperature.
- Finally, characteristic values such as *crystal modification*, *degree of crystallinity* and *glass transition temperature* of the neat resin are determined.

## Nucleation and clarification of polyamide 6

Building on the work of Richter et al.<sup>[14]</sup>, the second part of this thesis deals with supramolecular additives as nucleating and clarifying agents for PA6. These additives are linear compounds consisting of a central unit substituted symmetrically with two hydrogen bonding units. The hydrogen bonding units are responsible for the crystal growth (self-assembly), preferable in sheet-like morphologies.



The presented research in this thesis is beyond the results of Richter et al.<sup>[14]</sup>, and mainly focuses on thermal stability and additive efficiency under elevated polymer melt temperatures during processing of a selected bisurea compound. The aim is to examine ideal processing conditions and to achieve optimal additive efficiencies. Therefore, the following research is conducted:

- *Thermal properties* of the neat additive are determined by thermogravimetric analysis (TGA) and polarized light microscopy.
- In order to further support the results from Richter et al.<sup>[14]</sup>, *nucleation and optical properties* of additivated PA6 are investigated at standard processing conditions. Polymer crystallization is monitored by DSC and optical properties (clarity and haze) are determined.



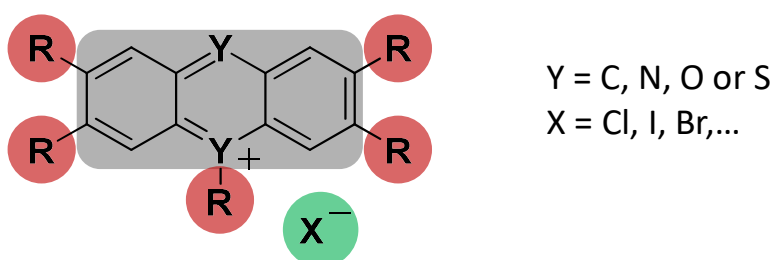
- *Nucleation and optical properties under various processing conditions* are examined and *investigations of temperature stability of the bisurea* under these conditions are conducted to detect ideal processing parameters.
- A further aim of this chapter is to get detailed understanding of the influence of a supramolecular additives on the *morphology of PA6 at the nanoscale*. To visualize the spherulitic morphology scanning electron microscopy is applied.

Additionally, based on the concept of supramolecular additives, a *new class of nucleating and clarifying agents*, tailored for PA6, is developed. The linear *bisthiourea molecules* consist of a central unit being substituted symmetrically with two hydrogen bonding units. Equally to bisurea compounds, bisthiourea derivatives form hydrogen bonds causing self-assembly into nano-objects. These nano-objects may act as nucleation sites for PA6 and may improve the crystallization behavior and the optical properties.

- The synthesis of a series of novel bisthiourea derivatives with varying substituents is carried out.
- In order to characterize the compounds, standard methods such as NMR-spectroscopy, mass spectrometry, thermogravimetric and differential thermal analysis are applied.
- To determine the influence of the bisthiourea compounds on the *polymer crystallization temperature* of PA6, and to calculate the nucleation efficiency, DSC measurements are conducted. Furthermore, *optical properties* are measured on injection molded samples.
- The influence of the bisthioureas on the *morphology of PA6* is explored by polarized light microscopy.
- Moreover, characteristic values such as *crystal modification* and *degree of crystallinity* are determined by means of wide angle X-ray scattering (WAXS) and DSC.
- Additionally, the *water absorption* and the *mechanical properties* of neat PA6 and PA6 comprising a selected bisthiourea additive are determined by means of water absorption experiments and tensile tests.

### Anti-nucleation of polyamides

The aim of the third part is to investigate the phenomenon of anti-nucleation and to develop structure-property relations and a possible mechanism explaining this almost unknown effect. The objective is to develop new anti-nucleating agents for PA6 and PA66 based on published knowledge from the literature.<sup>[11,15,19,31–33]</sup> Anti-nucleating agents for polyamides, such as Nigrosine, often consist of an anthracene-like heterocyclic scaffold. This rigid and planar central unit can bear various substituents and charges which may interact with the polymer chain, and hence influence the polymer crystallization temperature.



Currently, a prediction of anti-nucleation based on the molecular structure of an additive is not possible. Therefore, a systematical approach is adopted by exploring different anti-nucleating agents known from the literature and deducing molecular structural units which might be responsible for the anti-nucleation effect. On this basis, several approaches are pursued and the following research is conducted:

- At first, commercially applied *Nigrosine*<sup>[11]</sup> as reference material is investigated in detail. The polymer crystallization and melting temperatures are determined and the influence on the morphology of PA6 is investigated by polarized light microscopy.
- In order to develop a colorless anti-nucleating agent *LiCl* and several ammonium salts are investigated concerning their anti-nucleating ability in PA6.
- The class of *azine dyes* exhibits compounds with planar structures and charges, and hence combines the features of Nigrosine and salts. A large number of *azine dyes* are tested with respect to their influence on the thermal behavior of PA6.
- *Neutral Red* as representative compound of the class of *azine dyes* is investigated concerning the *influence of processing conditions* on the anti-nucleation efficiency of Neutral Red. Additionally, the influence of Neutral Red on properties of PA6 such

as morphology, glass transition temperature, crystal modification and degree of crystallinity are examined.

- Furthermore, a new concept is developed to enhance the additive efficiencies of hardly soluble anti-nucleating agents by introducing LiCl as co-additive.
- Additionally, the water absorption and the mechanical properties of neat and anti-nucleated PA6 are determined. Therefore, the water absorption of injection molding platelets is monitored and tensile tests are conducted.
- Finally, *anti-nucleation of polyamide 66* is investigated with selected anti-nucleating agents.



### 3 Properties of the neat polyamide 6 grade

In this work, polyamide 6 was investigated. The focus was set on nucleating and anti-nucleating agents as additives to alter the crystallization behavior. However, nowadays there are plenty of polyamide grades available which differ significantly from each other. Deviations in melting and crystallization temperatures, mechanical and optical properties for one type of polymer are usual. Therefore, the neat polymer has to be investigated very well before the additivation experiments. Characteristic values of the reference material have to be determined to see a change of properties of the material by additivation. Furthermore, the appropriate polymer processing conditions are very important and have to be identified. To ensure perfect dispersion or solubility of an additive in the polymer melt, processing conditions must be adjusted. Figure 5 shows an excerpt from the data sheet of the investigated PA6 grade (Ultramid® B27 E) provided by BASF SE.<sup>[34]</sup>

® = registered trade mark of  
BASF SE

## Ultramid® B27 E

#### Product description

Ultramid® B27 E is a polyamide 6 grade of low viscosity that is well suited for compounding and the production of monofilaments.

Specification	Test method	Unit	Value
Relative Viscosity (RV) 1% [m/v] in 96% [m/m] sulfuric acid	According to ISO 307 (calculated by Huggins method)		2.62 - 2.83
Viscosity Number (VN) 0,5% [m/v] in 96% [m/m] sulfuric acid	According to ISO 307	ml/g	142 - 158
Moisture content	According to ISO 15512	% [m/m]	max. 0.10
Extractables	According to ISO 6427- chips not ground/16h	% [m/m]	max. 0.6

#### General properties

Test method	Unit	Typical value
Melting point	°C	220
Density	g/cm <sup>3</sup>	1.12 - 1.15
Bulk density	kg/m <sup>3</sup>	780
Pellet size	mm	2 - 2.5
Pellet shape		round
Water absorption, 23°C/50% rh	%	2.2
Water absorption, saturation in water 23°C	%	8.5

Figure 5. Data-sheet excerpt of the polyamide 6 grade Ultramid® B27 E.<sup>[34]</sup>

In the following chapter characteristic values of Ultramid® B 27 E are presented and the polymer processing as well as the sample preparation for subsequent characterization used in this thesis are described.

First, the melting and crystallization temperatures under varying processing conditions are examined. For this purpose, three compounding experiments were conducted:

- standard processing conditions according to Richter et al.<sup>[14]</sup>
- variation of processing time
- variation of melt temperature during processing (processing temperature)

In addition, samples of this set of experiments were investigated by gas chromatography-mass spectrometry (GC-MS) to examine potential degradation products and check the purity of the PA6 grade.

In order to calculate the efficiency of nucleating agents, the maximum possible crystallization temperature of neat PA6 has to be determined. For this purpose self-seeding experiments as described in the literature<sup>[14,35]</sup> were conducted.

By additivation of polymers almost all properties can be influenced. In order to reveal those changes, the crystal modification, degree of crystallinity, and the glass transition temperature of neat PA6 were investigated by means of wide-angle X-ray scattering (WAXS), differential scanning calorimetry (DSC) and dynamic mechanic thermal analysis (DMTA). The influence on optical properties (haze and clarity) as well as mechanical properties (elastic modulus, ultimate strength, rupture strength) and water absorption are discussed later.

### 3.1 Compounding and sample preparation

Hydrogen bonds strongly influence the properties of polyamides in the solid state as well as in the polymer melt. Miri et al.<sup>[36]</sup> and Richter et al.<sup>[14]</sup> describe an orientation induced chain alignment in polyamide melts during processing. Under specific processing conditions, hydrogen bonds can even be preserved in the polymer melt. This phenomenon is called "memory effect".<sup>[37]</sup> Before conducting any measurements the polymer has to be compounded to erase the thermal history. Samples have to be prepared under identical processing conditions to guarantee their comparability. Melt temperatures during processing for PA6 range typically from 238 °C to 270 °C.<sup>[2]</sup>

To guarantee easy filling of the polymer to the micro-compounder and homogeneous melting while compounding, the polymer granulate was first pulverized with a freezer mill. The polyamide powder was dried for at least 24 h at 80 °C before compounding with a co-rotating twin screw compounder (DSM Xplore 15 mL) under nitrogen atmosphere. Figure 6 shows an inside view of the compounder with three heating zones and the sensor for the measurement of the melt temperature  $T_p$ .

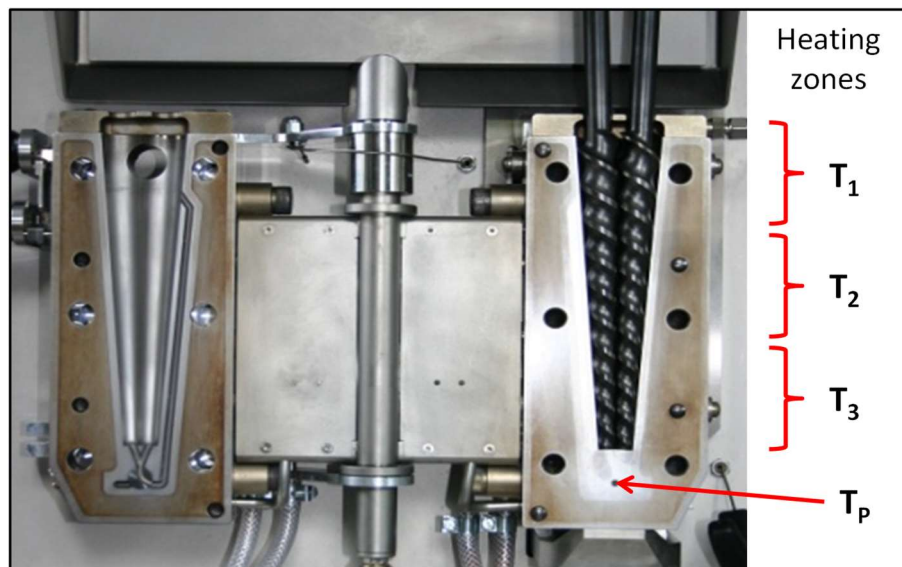


Figure 6. DSM Xplore 15 mL micro-compounder with the heating zones  $T_1$ ,  $T_2$  and  $T_3$  and the sensor for measuring the melt temperature  $T_p$  during processing.

The standard processing parameters are reported in Table 1. These parameters have already been established by Richter et al.<sup>[14]</sup> In the course of this thesis some parameters were changed to optimize the effect of various additives.

The micro-compounder has three heating zones which can be controlled separately. In order to prevent the material melting partially and from adhesion to the feeding hopper, the temperature in heating zone 1 ( $T_1$ ) was lower than in heating zones 2 and 3 ( $T_2$  and  $T_3$ ). The heating zones were adjusted to result in a processing temperature (melt temperature during processing) of 245 °C as listed in Table 1. After a standard compounding time of 5 minutes, the melt was discharged and collected either as a polymer strand or transferred directly to the injection molding unit.

Table 1. Standard processing parameters for PA6 and its measured melt temperature during processing.

Polymer	Temperature profile ( $T_1$ - $T_2$ - $T_3$ ) [°C]	Melt temperature during processing [°C]	Compounding time [min]	Rotational speed [rpm]
PA6	230-260-260	245	5	50

Injection molding platelets with a thickness of 1.1 mm were produced using a DSM Xplore 12mL injection molding machine. With these specimen optical properties, morphology investigations or WAXS measurements were conducted. Figure 7 shows the injection molding machine, the injection mold and an injection molding specimen.



Figure 7. DSM Xplore 12mL injection molding machine (left), injection mold with a thickness of 1.1 mm (middle) and injection molding specimen with a diameter of 25 mm and a thickness of 1.1 mm (right).

As described above, the barrel of the injection molding unit was directly filled with the discharged polymer melt from the twin-screw compounder. Specimen with a diameter of 25 mm and a thickness of 1.1 mm were prepared under nitrogen atmosphere using a polished injection mold with a thickness of 1.1 mm (Figure 7). The standard injection molding conditions are listed in Table 2.



Table 2. Standard injection molding conditions for PA6.

Polymer	Barrel temperature [°C]	Mold temperature [°C]	Injection pressure [bar]	Injection time [sec]	Holding time [sec]
PA6	250	100	6	10	10

To study the thermal properties of the compounded polymer, DSC measurements were conducted. Those samples were taken either from the polymer strand or from the sprue of the injection molding platelets. For this purpose, a part (5 to 7 mg) was clipped off (Figure 8).

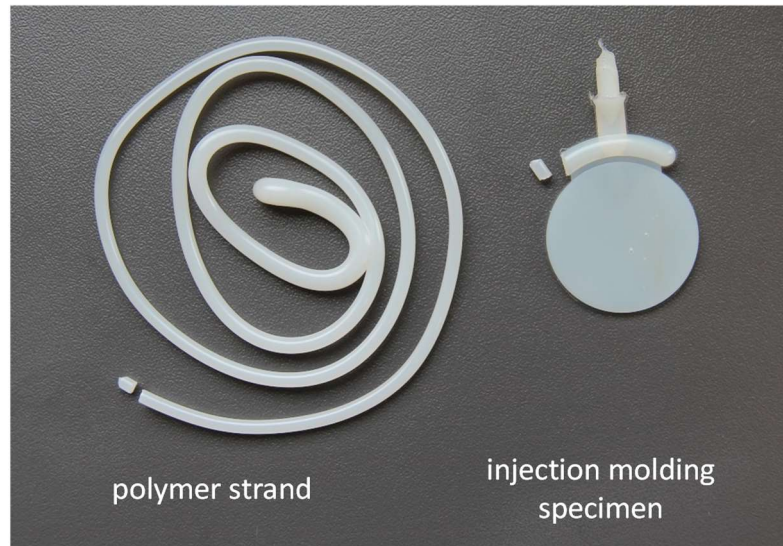


Figure 8. Polymer strand after discharge from the compounder (left) and injection molded specimen (right).

### 3.2 Influence of processing conditions on thermal behavior of PA6

To classify an additive, especially a nucleating or anti-nucleating agent, the melting and particularly the crystallization temperatures are important. Those characteristic temperatures can help judging whether a compound is a suitable additive. To compare the additives and to estimate their efficiency, melting and crystallization temperatures of the neat polymer have to be determined first. As known from the literature, the thermal behavior of a polymer can differ depending on varying processing conditions.<sup>[38]</sup> In this work three different compounding experiments were conducted to study the influence of the processing conditions on the thermal behavior of PA6. In the following these three types of experiments are explained for neat PA6.

#### *Standard processing conditions*

In the course of this thesis, PA6 was compounded with various additives of different concentrations. For this purpose, concentration series with up to nine additive concentrations were processed within one extrusion experiment. In the case of a concentration series, after every compounding run some polymer remains in the dead volume of the compounder. The remaining polymer in the dead volume corresponds to 5.4 g for PA6. To explore possible changes of melting or crystallization temperatures of the neat polymer due to the retention time in the extruder, a blank concentration series without any additive was conducted.

First, 14 g pulverized polymer were filled in the compounder. After 5 min at 245 °C, the melt was discharged and discarded for cleaning purposes. The material in the dead volume of 5.4 g remains in the compounder. 8.6 g polymer was refilled to the compounder and the melt was discharged and collected after 5 min compounding as first sample. This procedure was repeated nine times. The initial weights and the experiment sequence are reported in Table 3.

Table 3. Initial weights for a blank concentration series of PA6.

Run	Comment	$m_{\text{PA6}}$ [g]
0	cleaning	14.0
1	1st sample	8.6
2	2nd sample	8.6
3	3rd sample	8.6
4	4th sample	8.6
5	5th sample	8.6
6	6th sample	8.6
7	7th sample	8.6
8	8th sample	8.6
9	9th sample	8.6

Finally, nine samples were obtained. To determine the melting and crystallization temperatures, DSC measurements were conducted on a Perkin Elmer Diamond DSC with autosampler under nitrogen atmosphere at standard heating and cooling rates of 10 K/min. To erase the thermal history, samples were heated to 250 °C for 5 min before each cooling run. For each sample two heating and cooling scans were performed. The starting and end temperatures for PA6 samples are presented in Table 4. Values for the polymer crystallization temperatures ( $T_c$ ) were determined at the exothermic peak minimum in the second cooling scan. Melting temperatures ( $T_m$ ) were determined at the maximum of the endothermic peak of the second heating scan.

Table 4. Starting and end temperatures for the DSC measurements of PA6. For each sample two heating and cooling scans were performed under nitrogen at 10 K/min. Samples were held at the end temperature for 5 min before each cooling run.

Starting temperature [°C]	End temperature [°C]	Heating rate [K/min]
50	250	10

Figure 9 shows the second heating and cooling curves of each sample. The dashed line indicates the peak maxima of the melting peaks and the peak minima of the crystallization peaks, respectively. There is no significant change of the peaks and the corresponding enthalpies among all samples meaning no degradation or change in the sample is visible.

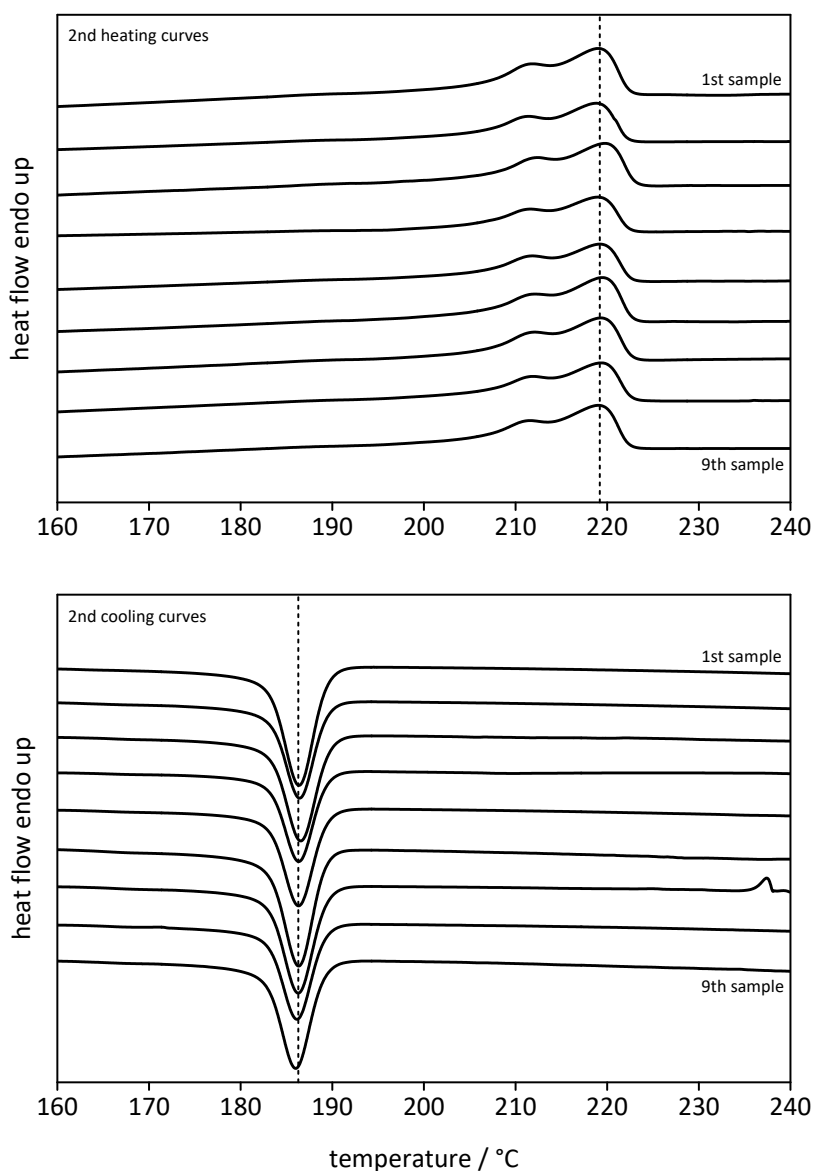


Figure 9. Second heating curves (top) and second cooling curves (bottom) of neat PA6. For each run the samples were compounded for 5 min at 245 °C. DSC heating and cooling rate: 10 K/min.

The melting curves of PA6 exhibit double melting peaks. Todoki et al. considered that the double melting peaks are the result of superposition of three processes which occur in sequence during heating: *Perfection of the original crystals, melting of the perfected crystals concurrently with recrystallization, and melting of the recrystallized crystals.*<sup>[39]</sup>

Figure 10 presents the peak values for the melting and crystallization temperatures of Figure 9 versus the corresponding sample number. All measured temperatures are within 0.5 °C. No significant changes of the melting or crystallization temperature with increasing sample number could be detected. The mean values were calculated as the average of all nine samples and are listed in Table 5.

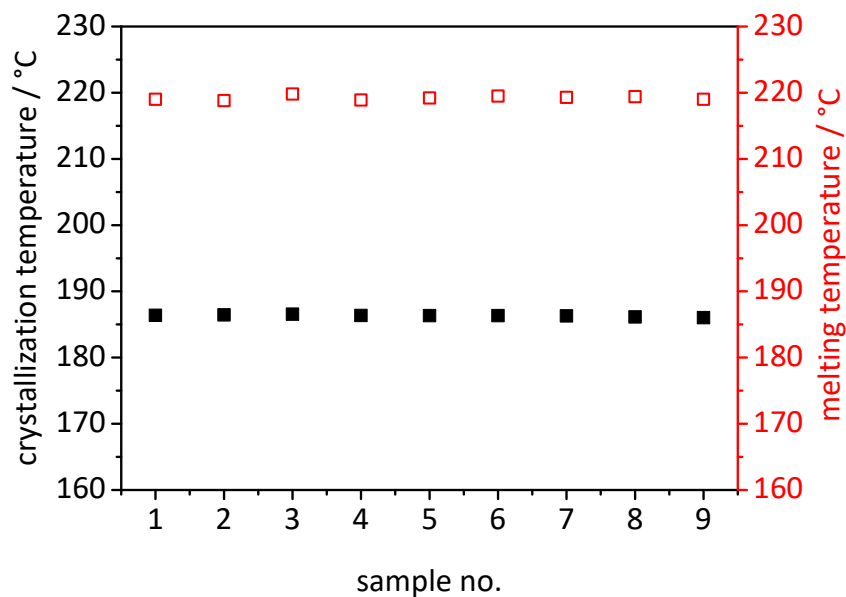


Figure 10. Crystallization temperatures (black, filled squares) and melting temperatures (red, blank squares) of neat PA6 versus the number of processing runs. For each run the samples were compounded for 5 min at 245 °C. DSC heating and cooling rate: 10 K/min.

Table 5. Calculated mean values and standard deviation of melting and crystallization temperatures of neat PA6 compounded at 245 °C measured by DSC.

	Mean value	Standard deviation
Melting temperature	219.2 °C	0.3 °C
Crystallization temperature	186.3 °C	0.2 °C

Throughout this work values measured by DSC are reported without any decimal place due to a measurement accuracy of  $\pm 0.5$  °C for DSC measurements.

*Processing conditions with varying processing time*

The compounding time plays often an important role to improve the effect of polymer additives due to increased solubility and perfect dispersion in the polymer melt.<sup>[40]</sup> Therefore, the influence of the compounding time on the melting and crystallization temperatures was investigated.

For this purpose, a method was developed to prepare samples with different compounding times within one compounding experiment. The way of proceeding is explained below:

The compounder was charged with 14.0 g of polymer. The temperature controls were set to a resulting melt temperature of 245 °C (see Table 6). After 5 min of compounding, about 0.5 g polymer melt (enough for a DSC measurement) was discharged and collected (first sample: 5 min). After another 5 min, 0.5 g polymer melt was discharged and collected, again. Consequently, this sample was compounded for 10 min overall (second sample: 10 min). This procedure was repeated for the compounding times listed in Table 6. Eventually, five samples with total processing times of 5, 10, 20, 30 and 60 min were obtained.

Table 6. Processing parameters for extrusion experiments with varying processing time and constant melt temperature during processing.

Temperature profile (T <sub>1</sub> -T <sub>2</sub> -T <sub>3</sub> ) [°C]	Melt temperature during processing [°C]	Processing time [min]	Rotational speed [rpm]
		5	
		10	
230-260-260	245	20	50
		30	
		60	

Results of the extrusion experiment with varying processing times for neat PA6 are shown in Figure 11. Both, melting and crystallization temperatures, show no significant change by varying processing time which leads to the assumption that no degradation processes of neat PA6 occurred. Thermal stability up to 60 min processing time with a melt temperature of 245 °C is possible. The values of melting and crystallization temperatures for neat PA6 at varying processing times are summarized in Table 7. A comparison with the crystallization

and melting temperature of the concentration series of neat PA6 shows no changes at extended processing times.

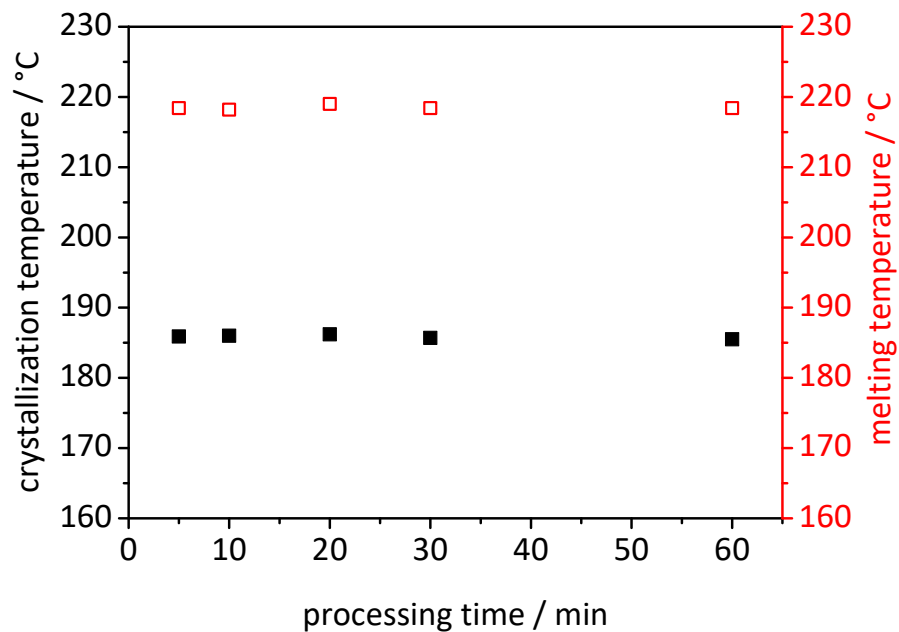


Figure 11. Crystallization (black, filled squares) and melting (red, blank squares) temperatures of neat PA6 as function of the processing time. The processing time is defined as time how long the polymer remains in the extruder during compounding. DSC heating and cooling rate: 10 K/min.

Table 7. Melting and crystallization temperatures of neat PA6 for different processing times measured by DSC.

Processing time [min]	Melting temperature [°C]	Crystallization temperature [°C]
5	218	186
10	218	186
20	219	186
30	218	186
60	218	185

#### *Processing conditions with varying melt temperature during processing*

Besides the processing time, the influence of the melt temperature during processing plays an important role. Too low melt temperatures may lead to too high viscosities of the polymer melt and incomplete solubility in case of additives and can cause problems while processing. Whereas, too high melt temperatures during processing can evoke thermal degradation, leading to partial loss of certain properties. To determine the influence of

various melt temperatures on the thermal behavior of PA6, an experiment was developed to screen different melt temperatures during processing. The way of proceeding is explained below:

**1st run (cleaning run):** 14.0 g pulverized polymer was filled to the compounder. After 5 min compounding at 245 °C, the melt was discharged and discarded. A dead volume of 5.4 g remains in the compounder.

**2nd run (sample run):** 8.6 g pulverized polymer was refilled to the compounder and the melt was discharged and collected after 5 min compounding at 245 °C as first sample run. After this run, the heating zone temperatures were set to a resulting melt temperature of 259 °C (see Table 8).

**3rd run (cleaning run):** 8.6 g pulverized polymer was refilled to the compounder and after 5 min compounding at 259 °C, the melt was discharged and discarded. A dead volume of 5.4 g remains in the compounder.

**4th run (sample run):** 8.6 g pulverized polymer was refilled to the compounder and after 5 min compounding at 259 °C, the melt was discharged and collected as first sample run. After this run the heating zone temperatures were set to a resulting melt temperature of 273 °C (see Table 8).

Steps **3** and **4** were repeated for two times with processing temperatures of 273 °C and 283 °C as listed in Table 8. At the end four sample runs at four different melt temperatures were prepared within one extrusion experiment.



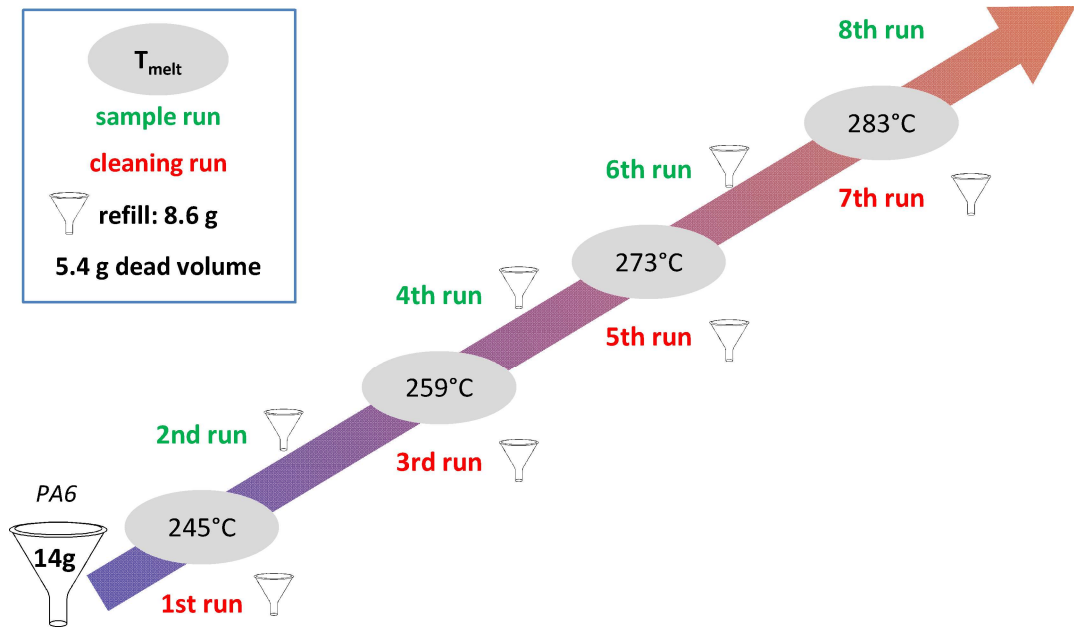


Figure 12. Schematic illustration of the sequence for an extrusion experiment with varying melt temperatures during processing. The melt temperature was increased after two extrusion runs. The uneven runs were cleaning runs and the even runs were sample runs. Four sample runs at four different melt temperatures during processing were prepared by this method.

Table 8. Adjusted processing parameters for the extrusion experiment with varying melt temperatures during processing and constant compounding time.

Temperature profile ( $T_1$ - $T_2$ - $T_3$ ) [°C]	Melt temperature during processing [°C]	Compounding time [min]	Rotational speed [rpm]
230-260-260	245		
240-275-275	259	5	50
250-290-290	273		
270-300-300	283		

Figure 13 presents the crystallization and melting temperatures of neat PA6 at melt temperatures during processing of 245 °C, 259 °C, 273 °C and 283 °C.

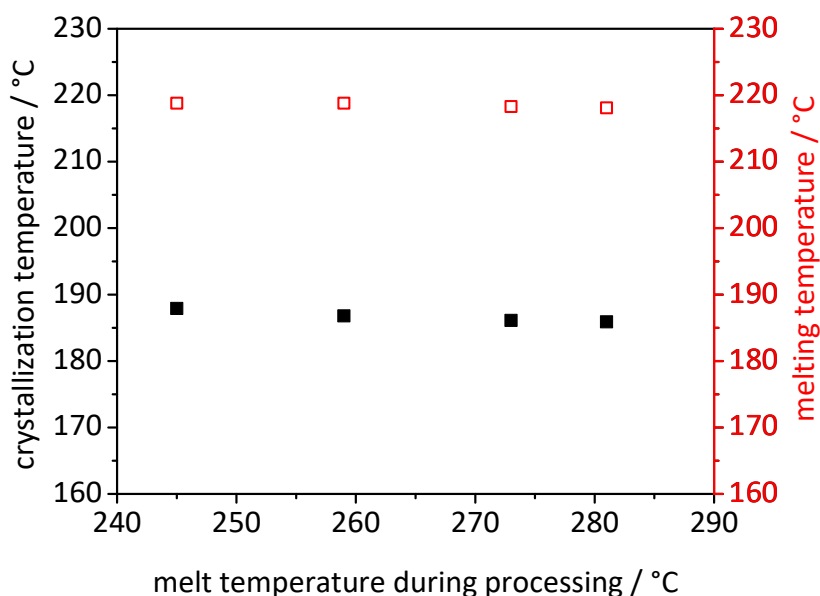


Figure 13. Crystallization temperatures (black, filled squares) and melting temperatures (red, blank squares) of neat PA6 as function of the melt temperature during processing. DSC heating and cooling rate: 10 K/min.

As shown in Figure 13, no significant influence of the melt temperature during processing on the melting or crystallization temperature of PA6 could be observed. Both, melting and crystallization temperatures, are mainly within 1 °C when compared to the values at different processing temperatures. There is merely 1 °C difference between samples of 245 °C and 259 °C compared to the samples prepared at 273 °C and 283 °C which is within the limit of accuracy of the DSC.

Table 9 summarizes the melting and crystallization temperatures at different melt temperatures during processing.

Table 9. Melting and crystallization temperatures of neat PA6 at different melt temperatures during processing measured by DSC. DSC heating and cooling rate: 10 K/min.

Melt temperature during processing [°C]	Melting temperature [°C]	Crystallization temperature [°C]
245	219	187
259	219	187
273	218	186
283	218	186

The results present almost constant thermal properties of neat PA6 in a temperature range between 245 °C and 283 °C. This fact is of particular importance, as in the following course of the thesis the influence of the melt temperature during processing on the performance of various additives will be investigated. Besides temperature-sensitive additives, which have their performance optimum at lower melt temperatures, there are additives which require high melt temperatures during processing to reach their maximum effect.<sup>[41]</sup> Richter et al. prepared the PA6 compounds only at melt temperatures of 245 °C.<sup>[14]</sup> Within the frame of this work open questions concerning the influence of the melt temperature during processing on additives should be answered as well. To reply those questions, higher melt temperatures during processing are necessary to study the additive stability under increased processing temperatures. Furthermore, the solubility of additives in the polymer melt was tested at different melt temperatures to enhance the efficiency of certain additives. In order to exclude any influences or changes in the neat polymer at elevated melt temperatures, the above described experiment was conducted for neat PA6.

#### *GC-MS measurements*

On the basis of the DSC data, it is difficult to determine thermal degradation or the like at elevated melt temperatures during processing. For this purpose, also a gas chromatography–mass spectrometry (Agilent 5977A MSD with Gerstel Autosampler) was used. Gas chromatography–mass spectrometry (GC-MS) combines the features of gas chromatography and mass spectrometry in one machine. This analytical method makes it possible to identify various substances and verify the purity within one test sample at different measuring temperatures. Figure 14 shows the sample setup for analyzing the polyamide samples.

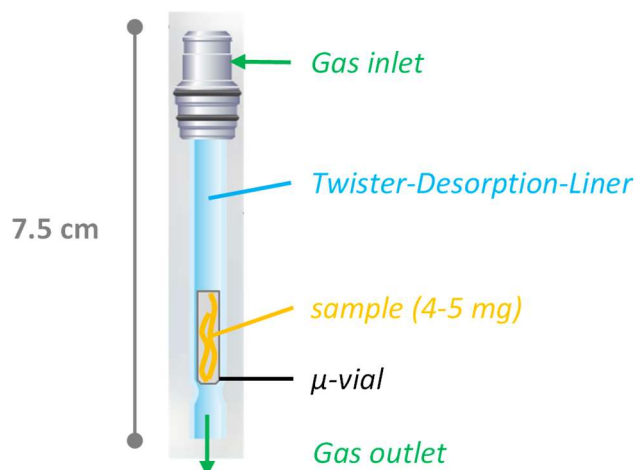


Figure 14. Sample setup for the GC-MS experiments. The sample (4 – 5 mg) is placed in a  $\mu$ -vial which is positioned in a twister-desorption-liner (TDL).

Initially, 4 -5 mg polymer strand was placed in a  $\mu$ -vial. This  $\mu$ -vial was inserted to a glass capillary called “twister-desorption-liner” (TDL) and stored in the autosampler of the GC-MS machine (see Figure 15). The TDL was heated to the requested temperature and held there for 5 min. After 5 min, the TDL was purged with helium gas (1 mL/min) to transfer substances degassed from the sample to the gas chromatography column ((5%-Phenyl)-methylpolysiloxane column). A chromatogram was recorded for 38 min. The eluat was analyzed by mass spectrometry with a rate of seven mass spectra per second. Any peak from the chromatogram could be selected separately and by evaluating the corresponding mass spectra the volatile compounds of a sample could be identified. Measurements at different temperatures were conducted with the same sample. For this purpose, the sample was heated to the lowest required measuring temperature, held there for 5 min and then cooled to room temperature. After 38 min, when the first measurement was finished, the sample was heated to the second lowest measuring temperature. This procedure was repeated for each temperature ending with the highest measuring temperature.

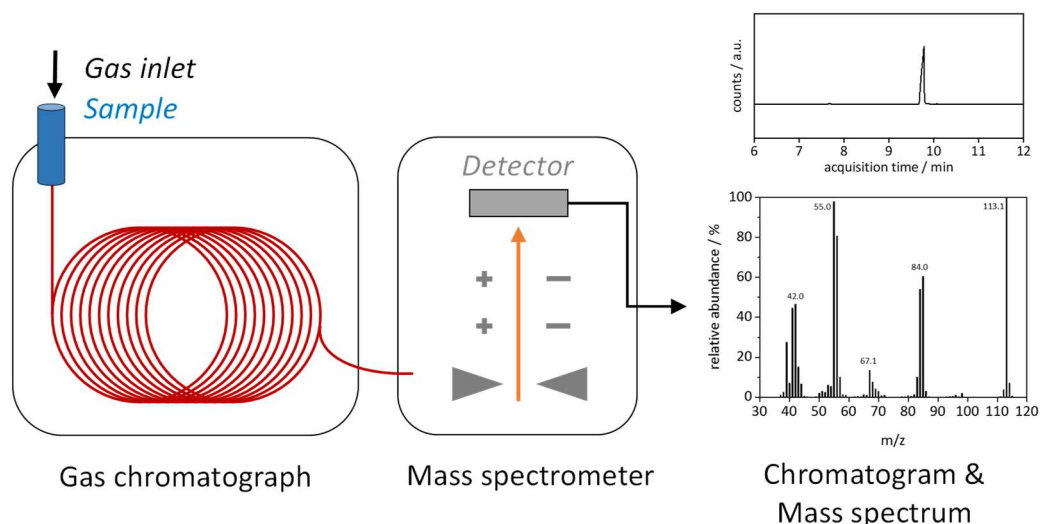


Figure 15. Schematic setup of the GC-MS machine (Agilent 5977A MSD with Gerstel Autosampler) consisting of a sample holder, gas chromatograph and mass spectrometer with detector.

Figure 16 shows the chromatograms of PA6 measured at different temperatures. With increasing temperature the peak increases as well. Evaluating the mass spectrum of the detected peak clearly showed that this peak can be referred to  $\epsilon$ -caprolactam.

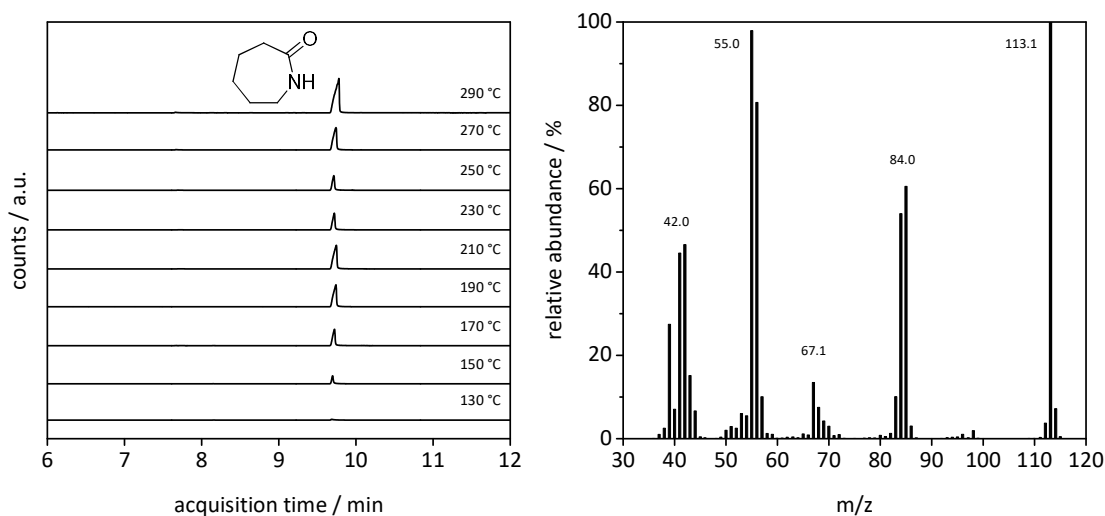


Figure 16. Chromatograms of neat PA6 at different holding temperatures as indicated (left) and mass spectrum of the peak measured in PA6. The peak can be referred to  $\epsilon$ -caprolactam with a molar mass of 113.16 g/mol (right).<sup>[42]</sup>

It is shown that with increasing temperature more  $\epsilon$ -caprolactam migrates from the solid to the gas phase. PA6 is polymerized via ring-opening polymerization of  $\epsilon$ -caprolactam. In the literature it is well known that PA6 contains  $\epsilon$ -caprolactam from synthesis<sup>[2,43,44]</sup> and was already detected by gas chromatography<sup>[45,46]</sup>, differential refractometry<sup>[47]</sup> or IR spectroscopy<sup>[48]</sup>. So it can be assumed that the detected  $\epsilon$ -caprolactam originates from

synthesis as well. In order to confirm these assumptions, thermal investigations of neat  $\epsilon$ -caprolactam were conducted. Figure 17 shows the thermogravimetric analysis and simultaneous thermal analysis of  $\epsilon$ -caprolactam.

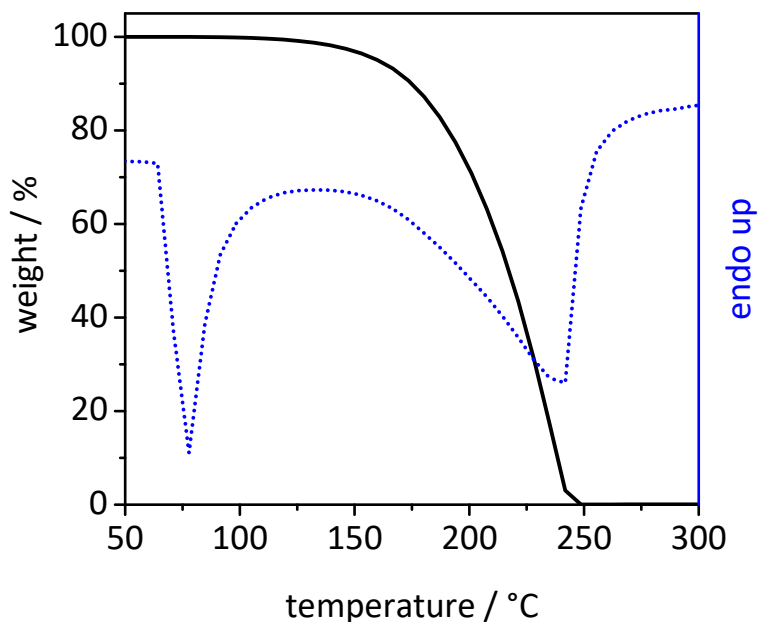


Figure 17. Thermogravimetric analysis (solid line) and simultaneous differential thermal analysis (dotted line) of  $\epsilon$ -caprolactam, measured under nitrogen atmosphere at a heating rate of 10 K/min.

Figure 17 revealed a melting point at 75 °C, followed by weight loss starting above 100 °C. The previous GC-MS measurements showed the appearance of the  $\epsilon$ -caprolactam peak at 150 °C with increasing intensity at elevated temperatures. Finally, the results are largely consistent with those obtained by the TGA/DTA measurement and also with those known from the literature.<sup>[42]</sup>

### 3.3 Self-nucleation of PA6

To determine the maximum polymer crystallization temperature of the neat PA6 grade used in this work, self-seeding experiments as established by Lotz et al. for polypropylene<sup>[35]</sup> and already conducted by Richter et al. for polyamides<sup>[14]</sup> were performed. This involves the partial melting of the polymer at a temperature  $T_s$ . This temperature is located between the inflection point of the 2nd derivation of the melting peak and its offset (shaded region in Figure 18). In this region unmolten, remaining crystal fragments can act as perfect nuclei for the crystallization of the polymer and increase the crystallization temperature.

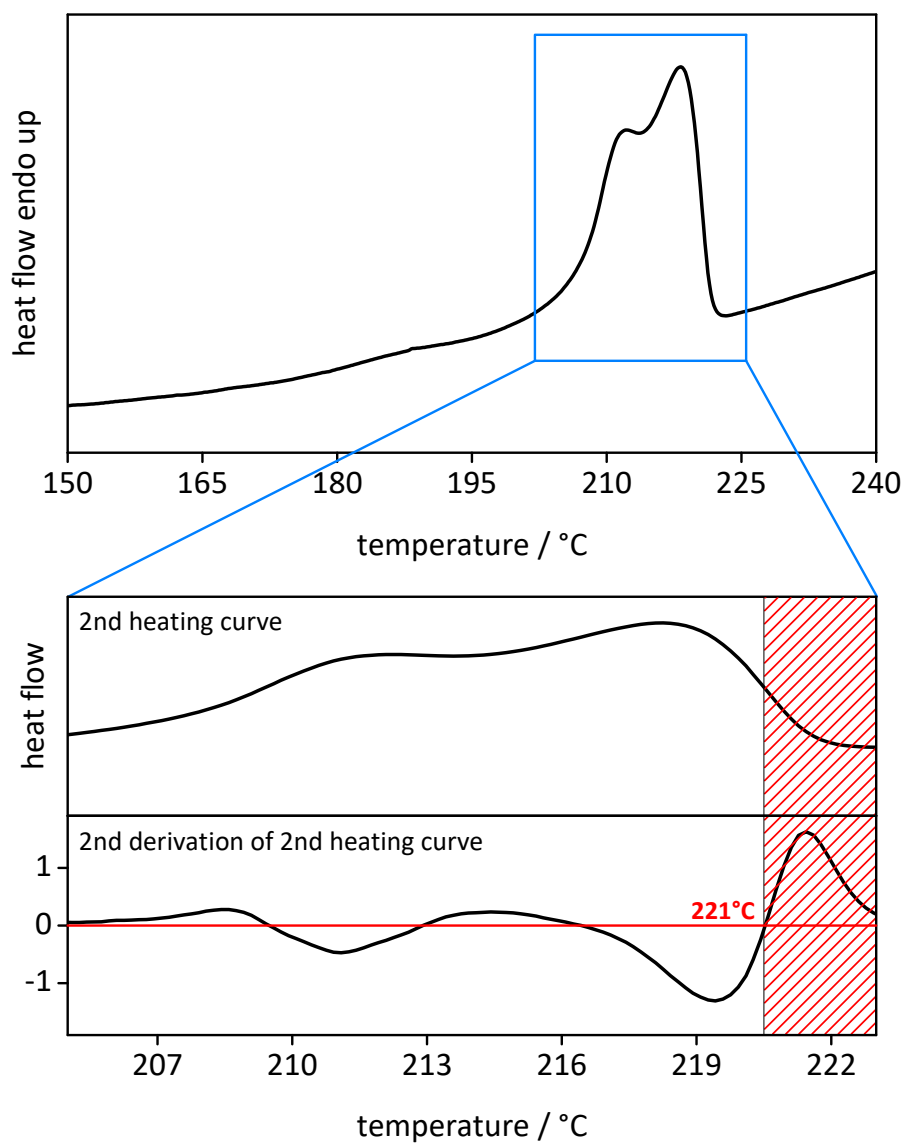


Figure 18. Melting endotherm of PA6 (top) and indication of the partial melting range (shaded region) used for self-nucleation experiments (bottom).

The first step of a self-seeding experiment involves the complete erasure of the thermal history of the polymer. Therefore, the polymer is heated to 250 °C for 5 min to avoid the nucleation at unmolten sites acting as self-nuclei upon cooling. After that, an initial standard state is created by cooling the “erased” melt at 10 K/min.

To determine the maximum polymer crystallization temperature  $T_{c(\text{maximum})}$  for a polymer, various  $T_s$  values were tested as shown in Figure 19.

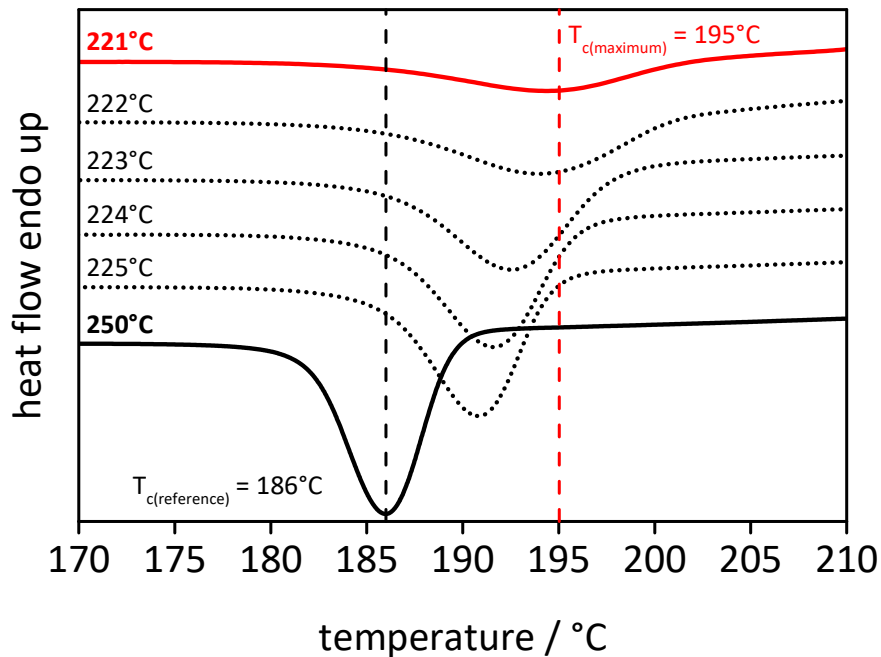


Figure 19. Crystallization exotherms of melt processed neat PA6 for different self-nucleation temperatures  $T_s$ . A maximum polymer crystallization temperature  $T_{c(\text{maximum})}$  of 195 °C was determined. DSC heating and cooling rate: 10 K/min.

A maximum self-nucleation of PA6 was induced after melting for 5 min at 221 °C. Here, a maximum polymer crystallization temperature  $T_{c(\text{maximum})}$  of 195 °C was obtained. As a result, the polymer crystallization temperature of this PA6 grade can be increased by 9 °C maximally.



### 3.4 Crystal modification and degree of crystallinity

Polyamides can crystallize due to hydrogen bonding between amide groups. Depending on the processing conditions, three main polymorphs, the  $\alpha$ -,  $\gamma$ - and the metastable  $\beta$ -phase can occur. The  $\alpha$ - and  $\gamma$ -form are the most prominent modifications.<sup>[2,49–51]</sup> The  $\alpha$ -phase is mainly obtained after annealing or crystallization at elevated temperatures. However, the  $\gamma$ -form is received at lower temperatures.<sup>[2]</sup> The structures and hydrogen-bonding pattern of the  $\alpha$ - and  $\gamma$ -form are presented in Figure 20.<sup>[51]</sup>

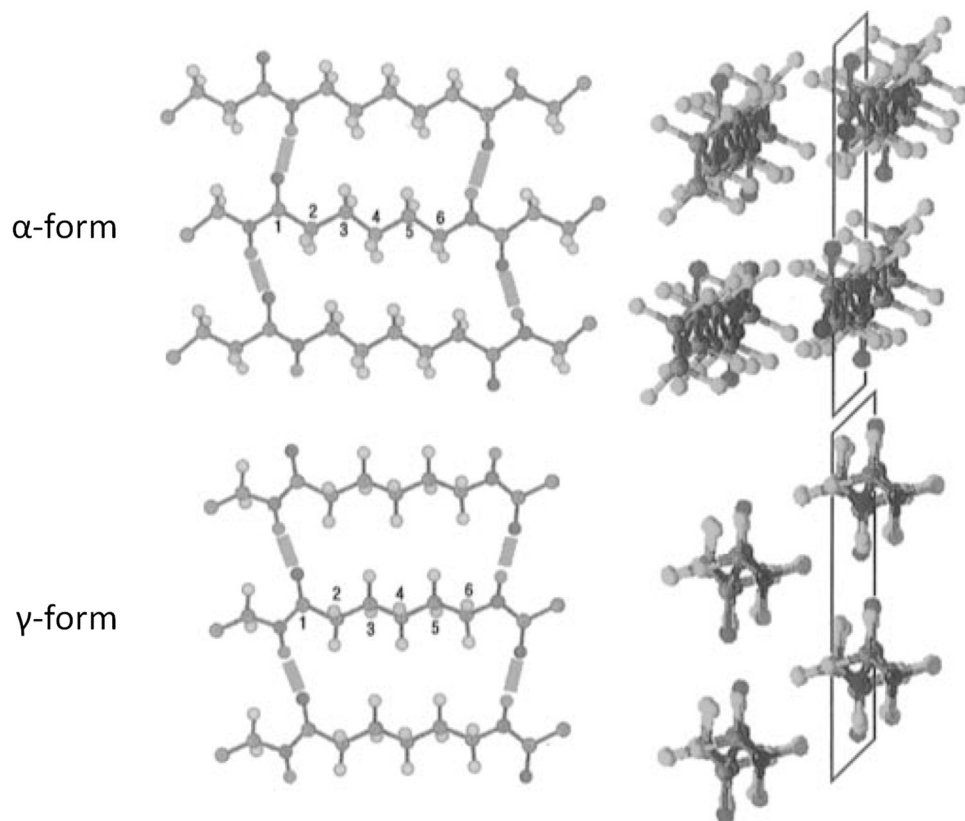


Figure 20. Structures of the  $\alpha$ - and  $\gamma$ -forms of PA6 according to Dasgupta.<sup>[51]</sup> The left side shows the view of the hydrogen-bonding planes, and the right side shows the view down the chain axis. For the  $\alpha$ -form, the adjacent chains are antiparallel and the hydrogen bonding is between adjacent chains within the same sheet. For the  $\gamma$ -form, the chains are parallel and the hydrogen bonding is between chains in adjacent sheets.

It is well known that both polymorphs differ concerning their mechanical and thermal properties.<sup>[38,50,52]</sup> Besides achieving a favored crystal modification by specific polymer processing, additives can influence the crystallization process of a polymer as well, and generate a favored modification as described by Richter et al. and Xue et al.<sup>[14,30]</sup>

### *Crystal modification*

Wide-angle X-ray diffractometry (WAXS) is a common method to characterize the crystal modifications of a polymer. In this thesis WAXS measurements were conducted on 1.1 mm thick injection molding platelets with diameters of 25 mm with a Bruker D8 Advance X-ray diffractometer using  $\text{CuK}\alpha$  radiation ( $\lambda = 1.54 \text{ \AA}$ ). Data were recorded in the range of  $5\text{-}40^\circ$  ( $2\theta$ ) with a step size of  $0.025^\circ$  and a step time of 10 sec. Figure 21 shows the WAXS pattern of an injection molded specimen of neat PA6 processed at  $245^\circ\text{C}$  which crystallizes predominantly in the  $\gamma$ -phase.

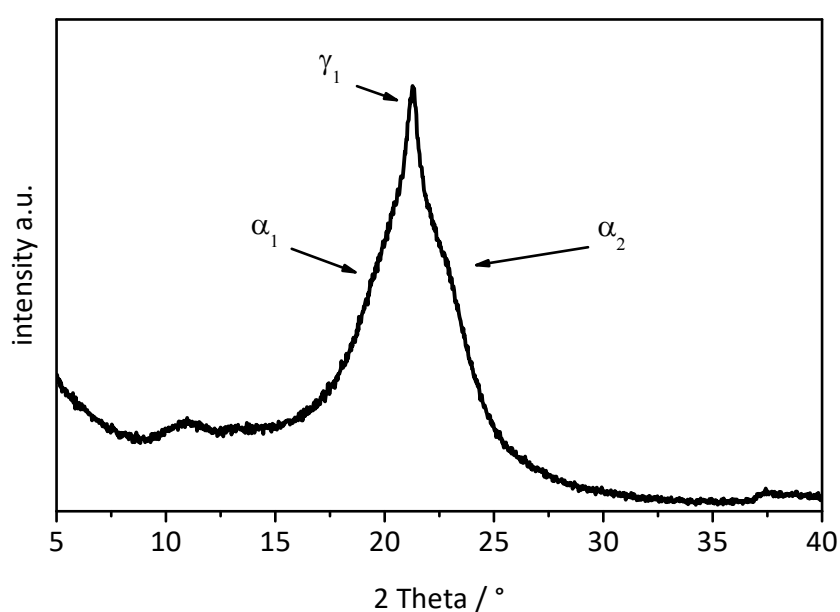


Figure 21. WAXS pattern of an injection molded PA6 specimen (1.1 mm thickness) processed at  $245^\circ\text{C}$ .

As mentioned above, processing conditions can influence the crystal modification of polyamides. WAXS measurements of samples processed at melt temperatures of  $283^\circ\text{C}$  showed no change of the diffraction pattern. In this case the varying processing conditions had no influence on the crystal modification of PA6.

### *Degree of crystallinity*

In addition to the crystal modification of a polymer, the degree of crystallinity is another important parameter, especially for semi-crystalline polymers. The degree of crystallinity is defined as percentage of ordered molecules or the amount of crystalline fraction in a polymer. Polyamides are polymers of intermediate crystallinity and can be varied over a relatively wide range.<sup>[2]</sup>

Common methods for determining the degree of crystallinity are density measurements<sup>[53]</sup>,

differential scanning calorimetry (DSC)<sup>[53]</sup>, X-ray diffraction (XRD)<sup>[54,55]</sup>, infrared spectroscopy<sup>[53]</sup> and nuclear magnetic resonance (NMR)<sup>[2,56]</sup>. The measured values deviate between the methods used. So it is important to compare only values obtained by the same method.

Within the frame of this work the degree of crystallinity was determined using differential scanning calorimetry. For this purpose, the enthalpy of the endothermic peak ( $\Delta H_f$ ) of the first heating scan was used (Figure 22). With the value of a 100% crystalline PA6 sample ( $\Delta H_{f(100\%)} = 188 \text{ J/g}$ )<sup>[57,58]</sup> the degree of crystallinity can be calculated by equation 3:<sup>[38,59,60]</sup>

$$\text{degree of crystallinity} = \frac{\Delta H_f}{\Delta H_{f(100\%)}} \cdot 100\% \quad (3)$$

Hereafter, the determination of the degree of crystallinity is presented for PA6 processed at a melt temperature of 245 °C. The DSC curve in Figure 22 shows the enthalpy as area below the melting peak, which is 65 J/g. Using equation 3, a degree of crystallinity of 34% can be calculated.

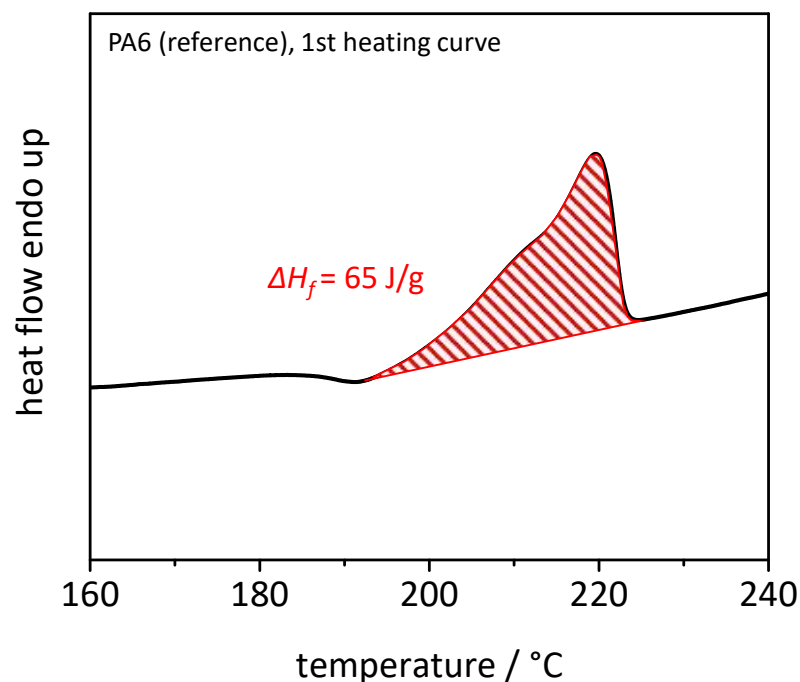


Figure 22. First heating curve of neat PA6 processed at a melt temperature of 245 °C with a melt enthalpy  $\Delta H_f$  of 65 J/g. DSC heating and cooling rate: 10 K/min.

Furthermore, the influence of elevated melt temperatures during processing on the degree of crystallinity was investigated. Equally to the crystal modification, no significant change of the crystallinity could be observed with increased melt temperatures during processing as shown in Table 10.

Table 10. Melt enthalpy and degree of crystallinity of neat PA6 at various melt temperatures during processing. DSC heating and cooling rate: 10 K/min.

Melt temperature during processing [°C]	$\Delta H_f$ [J/g]	Degree of crystallinity [%]
245	65	34
259	68	36
273	66	35
283	68	36

### 3.5 Glass transition temperature

The glass transition temperature is the reversible transition in amorphous or semi-crystalline polymers from a hard and brittle state into rubber-like state with increasing temperature. The glass transition temperature determines the continuous service temperature of a polymer and consequently the field of application.

Typical values of the glass transition temperature for PA6 range from - 32 °C for samples at a relative humidity of 100 rh% up to 75 °C for dried specimen.<sup>[2]</sup> This reveals that the effect of water absorption on the glass transition temperature is of fundamental importance and has to be considered when measuring the glass transition temperature. Furthermore, the glass transition temperature varies significantly concerning the technique of measurement as well as the cooling rate and can be influenced by additives.<sup>[61,62]</sup>

One method for the determination of the glass transition temperature is DSC.<sup>[62]</sup> In the case of the PA6 grade used in this work it was hardly possible to measure the glass transition temperature by DSC. It is well known that DSC often lacks the sensitivity to adequately identify the glass transition temperature.<sup>[63]</sup>

An alternative method for measuring the glass transition temperature is dynamic mechanic thermal analysis (DMTA). During a DMTA measurement a sinusoidal deformation is applied to a sample of known geometry. The sample can be exposed to a controlled stress or a controlled strain. For a known stress, the sample deforms a certain amount, which can be related to its stiffness.<sup>[64]</sup> DMTA measures stiffness and damping, which are reported as modulus and tan delta. Because of the sinusoidal force, the modulus can be expressed as an in-phase component, namely storage modulus, and an out of phase component, namely loss modulus. The storage modulus  $E'$  is the dimension of the elastic behavior of the sample. The ratio of the loss to the storage is tan delta. It is a measure of the energy dissipation of a material.<sup>[64]</sup>

The specimen for DMTA measurements were punched out from an injection molding platelet resulting in a sample with dimensions of 1.11 mm x 10.00 mm x 1.96 mm. The samples were conditioned at 70 °C and 62 rh% for 4 days corresponding to DIN ISO 527-2.<sup>[65]</sup> DMTA measurements were conducted with a DMTA IV from Rheometric Scientific.

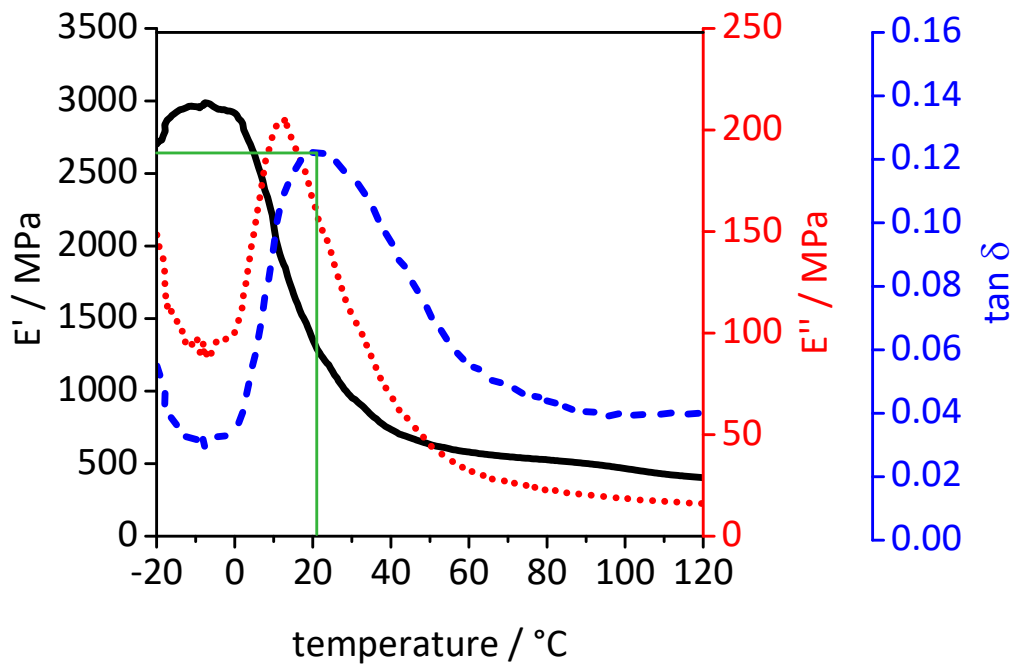


Figure 23. DMTA measurement of neat PA6 after equilibrium water uptake (70 °C, 62 rh%, 4 days) measured at 1 Hz and 2 K/min. Black line: storage modulus  $E'$ ; Red line: loss modulus  $E''$ ; Blue line: loss factor  $\tan \delta$ . The green line indicates the glass transition temperature determined from the maximum of  $\tan \delta$ .

Figure 23 shows a typical plot of the storage modulus  $E'$ , loss modulus  $E''$  and loss factor  $\tan \delta$  as a function of temperature for neat PA6 after equilibrium water uptake measured at a frequency of 1 Hz and a heating rate of 2 K/min. The blue curve shows the loss factor  $\tan \delta$ . The ratio between the loss modulus and the storage modulus is defined as  $\tan \delta$ , and represents the relative contribution of the viscous versus elastic properties.<sup>[63]</sup> The value for the glass transition temperature is determined either from the onset of the  $E'$  drop, the peak of the  $E''$  curve or the peak of  $\tan \delta$ .<sup>[64]</sup> In this work the glass transition temperature is defined as the peak maximum of  $\tan \delta$ . The green line in Figure 23 indicates the glass transition temperature of neat PA6 at 20 °C.

### 3.6 Summary

Nowadays, plenty of polymer grades with different properties such as melting and crystallization temperatures or optical and mechanical properties are available. Those grades show quite huge differences regarding their characteristic values. Furthermore, processing and measuring conditions can have a large influence on those parameters. In order to compare all experiments and samples within this thesis, neat PA6 was investigated first. Table 11 summarizes the characteristic values for PA6 (Ultramid B27 E) processed at a melt temperature of 245 °C. The variation of the melt temperature during processing as well as the processing time revealed no significant influence on the investigated properties of the polymer, such as melting and crystallization temperature, degree of crystallinity, glass transition temperature and crystal modification. Consequently, the neat polymer can be processed between 245 °C and 283 °C without significant changes of the above mentioned properties.

Table 11. Summary of characteristic values for Ultramid B27 E. processed at 245 °C.

	PA6 (reference)
Melting temperature $T_m$	218 °C
Crystallization temperature $T_c$	186 °C
Degree of crystallinity	35%
Glass transition temperature $T_g$ *	20 °C
Main crystal modification	$\gamma$ -modification

\*only measured for PA6 processed at 245 °C.





## 4 Nucleation and clarification of polyamide 6

Properties of semi-crystalline polymers are largely governed by the degree of crystallinity and the size of the crystalline units. Especially macroscopic properties such as mechanical or optical properties are related to these microscopic features of the polymer. Nowadays, polymers are applied in nearly every industrial field. To meet the challenges demanded by industry, polymers must exhibit specific characteristics. Controlling the macroscopic properties by controlling its crystallization process became a key factor for technical polymers.

### *Nucleation*

The limiting step of crystallization is the nucleation of a polymer. Nucleation starts at temperatures well below the melting temperature of the material and requires large undercooling. It can be differentiated between two main nucleation processes:

1. *Homogenous nucleation* takes place when adjacent polymer chains stick together and induce polymer crystallization. However, this process only happens when the formed nuclei exceed a critical size. Otherwise these nuclei get resolved due to thermodynamic instability.<sup>[10]</sup>
2. *Heterogeneous nucleation* is induced due to impurities, unmolten polymer fragments or additives. This process is of fundamental importance for industrial applications.<sup>[2,12,13,56]</sup>

Nowadays, a bunch of additives are used to control the crystallization process and with that the properties of the polymer. So-called nucleating agents are widely used in semi-crystalline thermoplastics. They act as heterogeneous nucleation sites inducing polymer crystallization.<sup>[12,13]</sup> As a consequence, the polymer crystallization temperature is increased. Additionally, the spherulite size is reduced. Thus, cycle times during injection molding<sup>[66,67]</sup> as well as mechanical and optical properties can be improved.<sup>[2,14,28,30,68–74]</sup>

Xue et al. showed the influence of nucleating agents on the morphology of PA6 by means of polarized light microscopy (Figure 24). The spherulite size of neat PA6 (left) is strongly reduced by the addition of 0.3 wt% nucleating agent (right) and the amount of spherulites is strongly increased.<sup>[30]</sup>

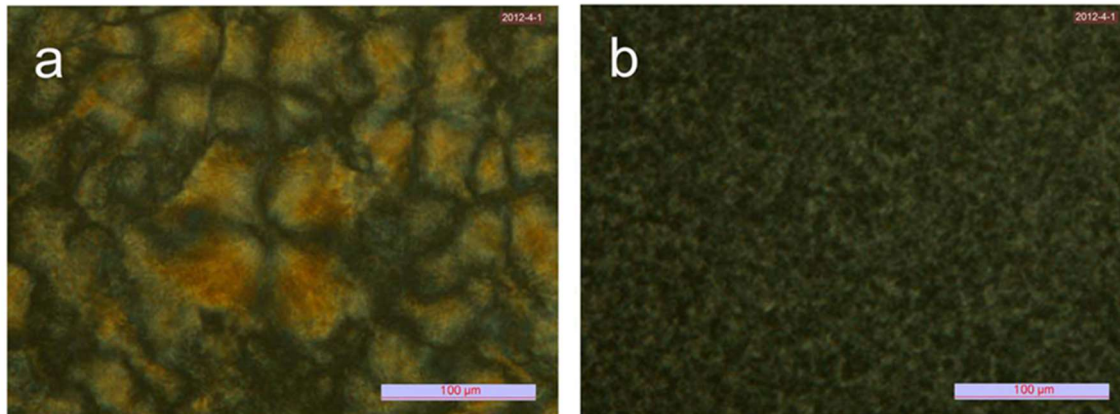


Figure 24. Polarized optical micrographs of (a) virgin PA6 and (b) PA6 comprising 0.3 wt% nucleating agent according to Xue et al.<sup>[30]</sup>

To reach the entire potential of a nucleating agent, fine dispersion, solubility and compatibility with the polymer must be ensured. The latter requires an epitaxial match of the nucleating agent and the polymer to guarantee nucleation induced by the additive.<sup>[12]</sup> Similar crystalline structures, or surface features of the additive and the polymer can promote epitaxial growth.<sup>[75,76]</sup> Moreover, the crystallization temperature of the nucleating agent should be higher than the polymer crystallization temperature in order to act as nucleation site for polymer crystallization.<sup>[73]</sup> Finally, thermal stability of the additives must be warranted to avoid side reactions or thermal degradation during polymer processing.<sup>[77]</sup> As mentioned above, a large undercooling of the polymer melt is required to initiate nucleation and subsequent crystallization processes. Due to nucleating agents the polymer crystallization temperatures are shifted to higher temperatures compared to the neat polymer. A common method for the determination of temperature transitions of polymers, especially for crystallization temperatures, is differential scanning calorimetry (DSC).<sup>[59]</sup> Figure 25 shows the thermographs of neat PA6 and PA6 comprising different concentrations of a bisurea compound investigated by Richter et al.<sup>[14]</sup> It could be demonstrated in a certain concentration regime that an increasing amount of additive leads to higher polymer crystallization temperatures.<sup>[14]</sup> However, an increase of the additive concentration does not necessarily lead to a higher crystallization temperature. At high additive concentrations, phase separation between additive and polymer can occur. Furthermore, undissolved additive cannot contribute to polymer nucleation.<sup>[78]</sup>

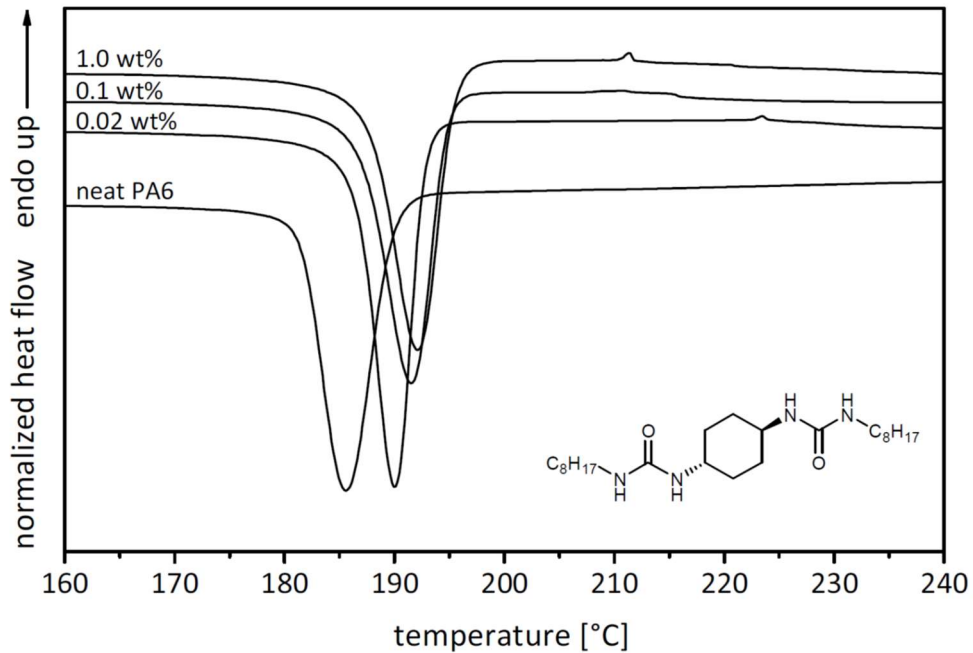


Figure 25. Differential scanning thermographs of neat PA6 and PA6 comprising different concentrations of a bisurea compound with cooling rates of 10 K/min according to Richter et al.<sup>[14]</sup>

In order to calculate the efficiency of nucleating agents, the increase of the crystallization temperature induced by a nucleating agent is compared to a sample nucleated by its own crystal fragments (self-seeding experiment; see chapter 3.3)<sup>[35]</sup>. The nucleation efficiency (NE) is calculated by equation 4:<sup>[79]</sup>

$$NE(\%) = 100 \cdot \left( \frac{T_{c(nucleated)} - T_{c(reference)}}{T_{c(maximum)} - T_{c(reference)}} \right) \quad (4)$$

with  $T_{c(nucleated)}$  being the crystallization temperature of the polymer induced by a nucleating agent,  $T_{c(reference)}$  being the crystallization temperature of the neat polymer and  $T_{c(maximum)}$  being the maximum crystallization temperature obtained by self-seeding experiments.<sup>[35,79]</sup>

In recent years, a large number of studies focused on inorganic particles and organic salts as nucleating agents for polyamides.<sup>[2,56,80]</sup> For example inorganic sodium phenylphosphinate<sup>[80]</sup>, kaolin, talc<sup>[80,81]</sup> and salts of benzoic acid<sup>[13]</sup> were found to be nucleating agents for polyamides. Furthermore, Mudra et al. compared the efficiency of several potential and commercial nucleating agents in PA6.<sup>[80]</sup> Additionally, several publications deal with polymeric materials as nucleating agents for polyamides. For example PA4.6 efficiently nucleates both PA6 and PA66.<sup>[82]</sup> Furthermore, Du et al. described the use of maleated poly(ethylene-co-vinyl acetate) as nucleating agent for PA6.<sup>[83]</sup>

However, inorganic nucleating agents cause problems due to insolubility in the polymer melt, and consequently have to be finely dispersed during polymer processing. Poorly dispersed particles can state a major problem for the nucleation efficiency of an additive. Recently, these dispersion issues could be eliminated by organic nucleating agents. Depending on the chemical structure, the additives can be soluble in the polymer melt, self-assemble upon cooling into supramolecular nano-objects, and induce polymer crystallization. These additives are called supramolecular polymer additives.<sup>[14,73]</sup>

Figure 26 presents a schematic structure of supramolecular additives. The structure consists of a central unit connecting two units capable of forming hydrogen bonds which are responsible for crystal growth and self-assembly behavior, respectively. Furthermore, the crystal structure and the dissolution properties in the polymer melt of an additive can be influenced by variation of the peripheral substituents.<sup>[14,73]</sup> By modifying and adjusting these units, tailored additives can be synthesized. Hence, the dissolution behavior of the additives can be adapted to a certain polymer and the surface of the supramolecular nano-objects can be tuned to support epitaxial growth of the designated polymer.

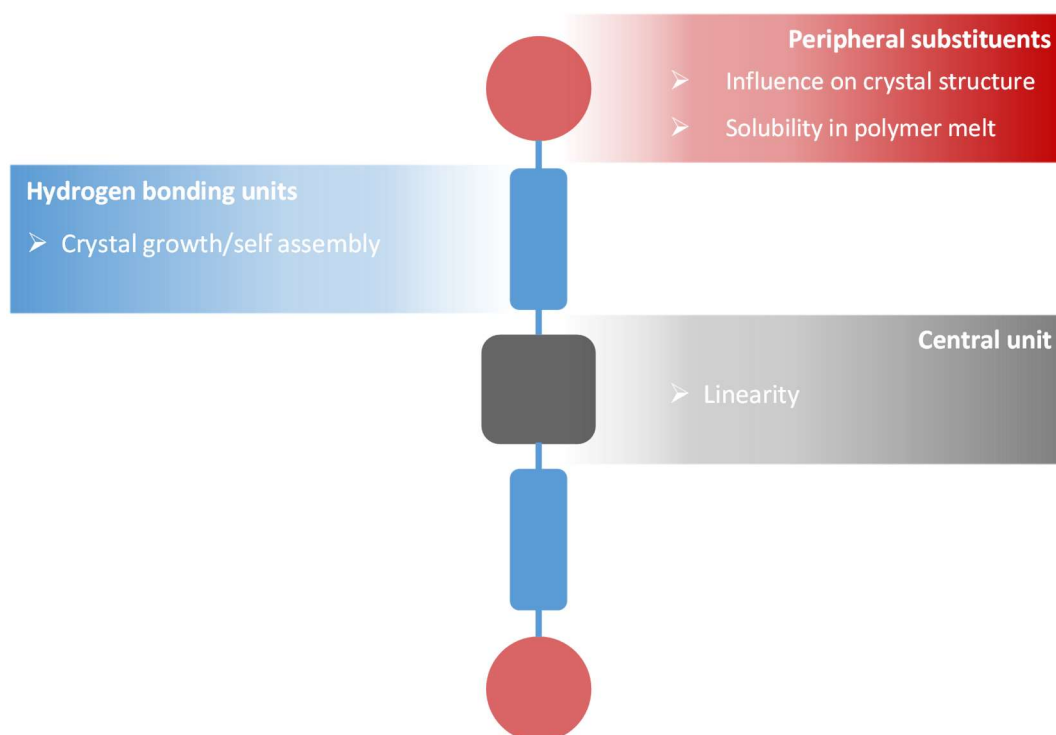


Figure 26. Schematic structure of linear supramolecular additives consisting of a central unit, two hydrogen bonding units and peripheral substituents. (reproduced from Richter et al.<sup>[14]</sup>)

With appropriate epitaxy those supramolecular aggregates exhibit an extremely high density of nucleation sites due to their high surface-to-volume ratio.<sup>[75]</sup> To develop effective and well-performing supramolecular polymer additives some requirements have to be fulfilled:<sup>[18,73,84]</sup>

- *Self-assembly* of additive molecules due to structural moieties has to be ensured.
- *Solubility* of the additive at the desired melt temperatures during processing.
- *Insolubility* of the additive above the crystallization temperature of the neat polymer upon cooling from the melt.
- *Suitable surface* for epitaxial growth of the polymer.

In order to understand the way of functioning of supramolecular additives, Figure 27 presents a scheme of the self-assembly concept of supramolecular nucleating agents during polymer processing.

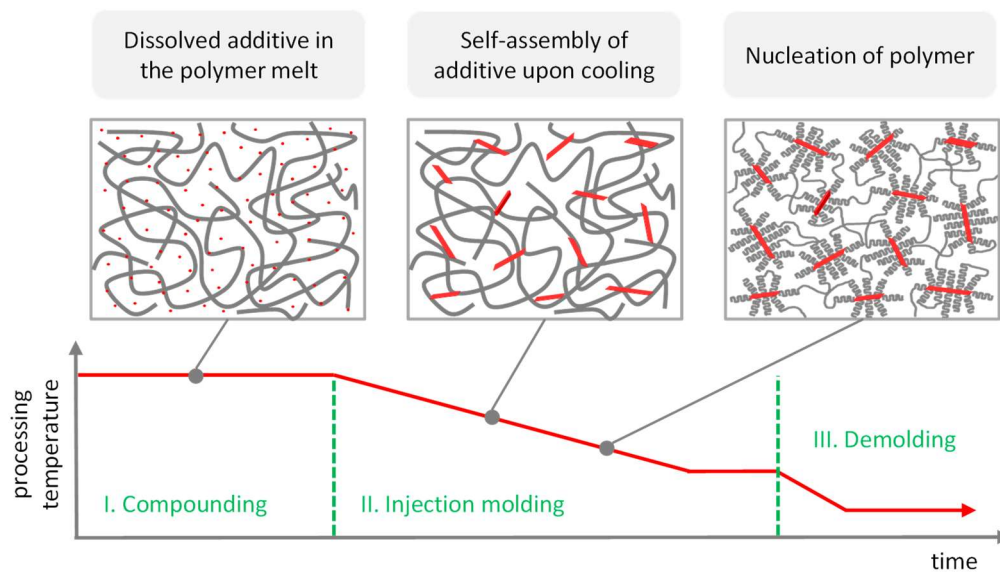


Figure 27. Schematic thermoreversible self-assembly process of supramolecular nucleating agents during polymer processing. The red dots indicate additive molecules whereas the red bars indicate the supramolecular nano-objects. The bottom graph schematically describes a typical temperature profile during polymer processing (red line).

First, the additives are dissolved in the polymer melt and thus well distributed. Here, appropriate melt temperatures during processing are of high importance to guarantee ideal solubility, while avoiding thermal degradation of the additives. Upon cooling, the additive molecules self-organize into so-called supramolecular nano-objects due to intermolecular forces (e.g. hydrogen bonding). In the end, these nano-objects are capable

of providing an appropriate surface for the nucleation of the polymer. This process is fully reversible without any losses.<sup>[14]</sup>

Due to their ability to eliminate the dispersion issues, organic supramolecular additives gained growing interest. Supramolecular additives for polypropylene are applied commercially for several years now. Dibenzylidene sorbitol<sup>[69,85]</sup> and 1,3,5-benzenetrisamide derivatives<sup>[73,78,86–88]</sup> were developed with regard to the nucleation of isotactic polypropylene. Furthermore, trisamides were found to be capable as nucleating agents for polyvinylidene fluoride<sup>[29]</sup> and polybutylene terephthalate.<sup>[71]</sup> Recently, Richter et al. transferred the concept of supramolecular nucleating agents to semi-crystalline polyamides.<sup>[14]</sup> He developed a new class of supramolecular nucleating agents on the structural motif of 1,4-cyclohexane bisureas specifically for polyamides. Figure 28 shows three examples for supramolecular nucleating agents.

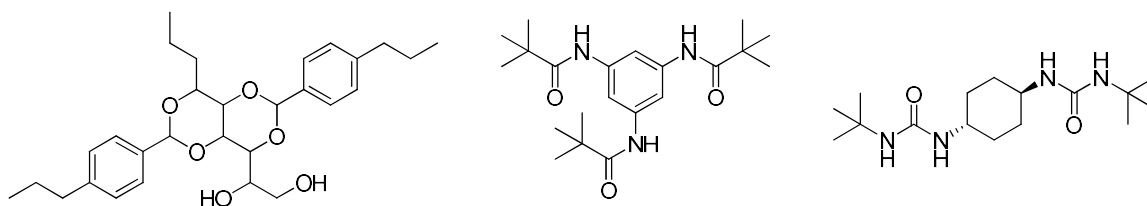


Figure 28. Chemical structures of supramolecular nucleating agents. Left: 1,2,3-trideoxy-4,6:5,7-bis-O-[(4-propylphenyl)methylene]-nonitol (TBPMN, NX8000, Miliken Chemical); middle: 1,3,5-tris(2,2-dimethylpropionylamino)benzene (Irgaclear XT 386, BASF); right: 1,1'-(*trans*-1,4-cyclohexylene)bis(3-*tert*-butylurea). NX8000 and Irgaclear XT 386 are commercial nucleating agents for PP, whereas the bisurea compound efficiently nucleates polyamides.

### Clarification

Usually, semi-crystalline polymers appear opaque or milky. They are not transparent due to light scattering at the interfaces between crystalline and amorphous regions. However, the optical properties of those polymers can also be tuned by additives.<sup>[14,28,73,74,89]</sup> Those additives are called clarifying agents and are considered as a subcategory of nucleating agents. They can efficiently improve optical properties of a polymer such as transparency, haze and clarity. According to ASTM D 1003, *the standard test method for haze and luminous transmittance of transparent plastics*, haze and clarity values can be measured by means of a hazemeter.<sup>[90]</sup> The haze value is referred to the amount of transmitted light, which is scattered in angles larger than 2.5°, and indicates the cloudiness of a sample. Polymers with a haze of 100% strongly scatter light and appear “milky”, whereas polymers

with a haze value of 0% appear clear as glass. Clarity is the amount of transmitted light that is scattered in angles smaller than  $2.5^\circ$ , where low clarity values cause a loss of sharpness of an image. A clarity value of 0% indicates a total loss of sharpness, whereas a clarity value of 100% means that an image is displayed completely sharp. Figure 29 shows the influence of haze and clarity on an image and on the visual appearance of transparent objects.<sup>[91]</sup>

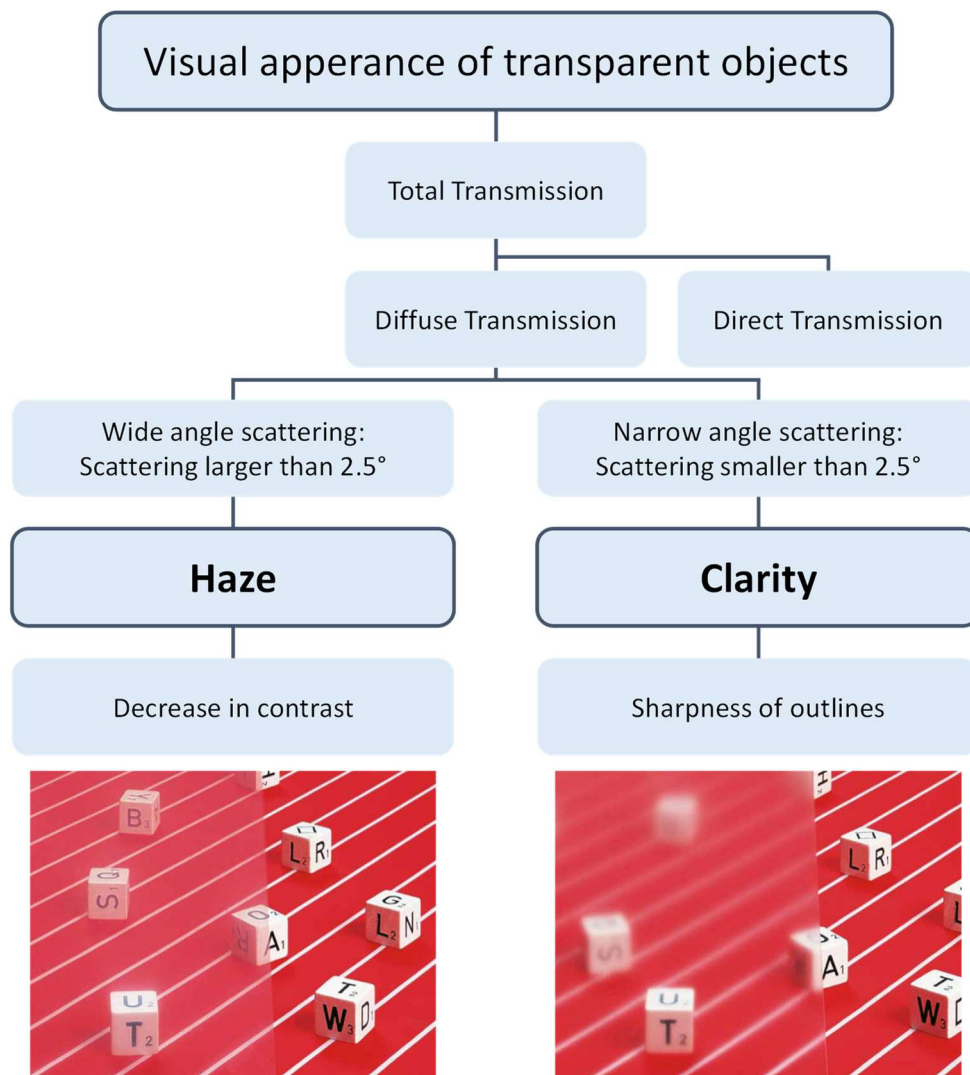


Figure 29. Haze and clarity. Top: Definition. Bottom: Visualization of the influence of the haze and clarity of transparent polymer specimens on the visual appearance of objects. (reproduced from BYK<sup>[91]</sup>)

As mentioned above, semi-crystalline polymers exhibit crystalline and amorphous phases with different refractive indices for each phase. This mismatch leads to scattering which reduces the transparency of a specimen. Additionally, semi-crystalline polymers partly consist of anisotropic structures (i.e. spherulites) emerging from crystallization. Those structures lead to an increase of haze values, and thus a decline of the optical properties at the same time. By adding additives the spherulite size can be decreased and the amount of

scattered light reduced which can lead to improved optical properties.<sup>[28]</sup> The effect of the addition of a clarifying agent on the visual appearance of injection molded specimen is presented in Figure 30.<sup>[14]</sup>



Figure 30. Effect of the addition of a bisurea additive on the visual appearance of injection molded specimen. Left: PA6 (reference); middle: PA6 + 0.2 wt% additive; right: PA6 + 1.3 wt% additive.<sup>[14]</sup>

Figure 30 visually demonstrates the influence of the addition of a nucleating agent to a polymer. With an increasing amount of additive, the optical properties, haze and clarity, as well as transparency, were enhanced significantly. In the presence of the clarifying agent, the amount of spherulites within the polymer was increased, while the size of the spherulites was decreased coincidentally. The size of the spherulites is assumed to be smaller than the wave length of visible light. Consequently, less scattering occurs, which leads to enhanced optical properties.

Nevertheless, a reduction of the crystallite size cannot be regarded as the only reason for the enhancement of optical properties.<sup>[73,78]</sup> As stated above, Xue et al. demonstrated the decrease of spherulites of PA6 by nucleating agents without observing an enhancement of the optical properties.<sup>[30]</sup> Moreover, it is well known from the literature that talc is a very good nucleating agent for a plenty of polymers but shows no positive influence on the optical properties of polymers.

However, in recent years several patents and publications dealing with clarifying agents for isotactic polypropylene were released. Sorbitol and trisamide derivatives are common clarifying agents for polypropylene and have been commercially applied for years.<sup>[67,69,70,72,73,78,86]</sup> Kristiansen et al. investigated sorbitol/i-PP systems. They observed that haze and clarity of injection-molded i-PP specimens are strongly dependent on the additive concentration.<sup>[67]</sup> Furthermore, a strong influence of cooling kinetics on the optical properties of the clarified i-PP was detected.<sup>[69]</sup> Abraham et al. made similar



observations.<sup>[78]</sup> Therefore, additive concentrations and processing conditions play an important role in the field of nucleating and clarifying agents.

For the first time, Richter et al. was able to clarify a semi-crystalline polymer other than polypropylene. He synthesized a new class of bisurea additives, and thus was able to improve the optical properties of polyamides remarkably. A reduction of haze values to less than 20% with additive concentrations of 1.0 wt% was observed. This outstanding work was patented in 2013.<sup>[14,89,92]</sup>

The following chapter will address detailed investigations of the thermal stability of a bisurea compound at various melt temperatures during processing and the development of a new nucleating and clarifying agent for polyamide 6.

## 4.1 Thermal stability and properties of a bisurea additive

Most bisurea molecules discussed in this work consist of a central unit, two urea linkages, which are responsible for hydrogen bonding, and peripheral substituents. The detailed functions of each group are explained in frame of the introduction of this chapter. The schematic structure of linear bisureas is presented in Figure 31.

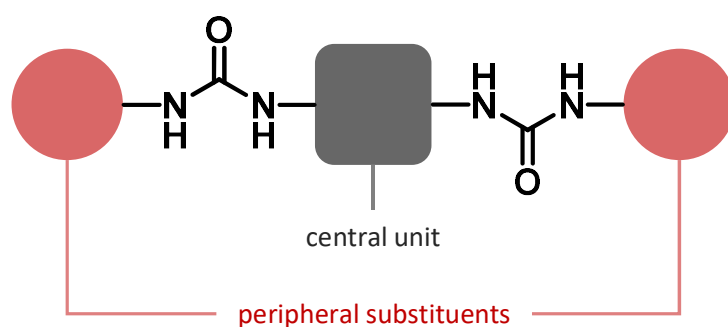


Figure 31. Schematic structure of a linear bisurea molecule consisting of a central unit, two urea linkages, and peripheral substituents.

Bisurea compounds are widely known to the literature and applied in a number of different fields.<sup>[93–104]</sup> The two main sectors deal with the formation of organo and hydrogels due to hydrogen bonding interactions of the urea groups<sup>[93,94,100,101,104]</sup> and the formation of polymeric assemblies.<sup>[95–98,102]</sup> Recently, the use of bisurea structures as supramolecular polymer additives and nucleating agents has been reported.<sup>[14,30,89,92]</sup> Richter et al. were the first developing several bisurea derivatives as supramolecular polymer additives for polyamides, followed by Xue et al. who also found bisureas as nucleating agents for PA6<sup>[30]</sup> and Xu et al. who were able to nucleate poly(l-lactid acid) with organic bisurea compounds.<sup>[103]</sup>

It is well known that bisurea compounds are capable of self-assembling into nano-objects. For example, Schmidt et al. conducted NMR-crystallographic studies of two-dimensionally self-assembled compounds.<sup>[99]</sup> In this work the crystal structures and morphology of three supramolecular compounds were determined. Among others, one bisurea compound, namely 1,1'-(cyclohexane-*trans*-1,4-diyl)bis(3-*tert*-butylurea) originally developed by Richter et al.<sup>[14]</sup> was investigated. The structural formula and morphology is presented in Figure 32.

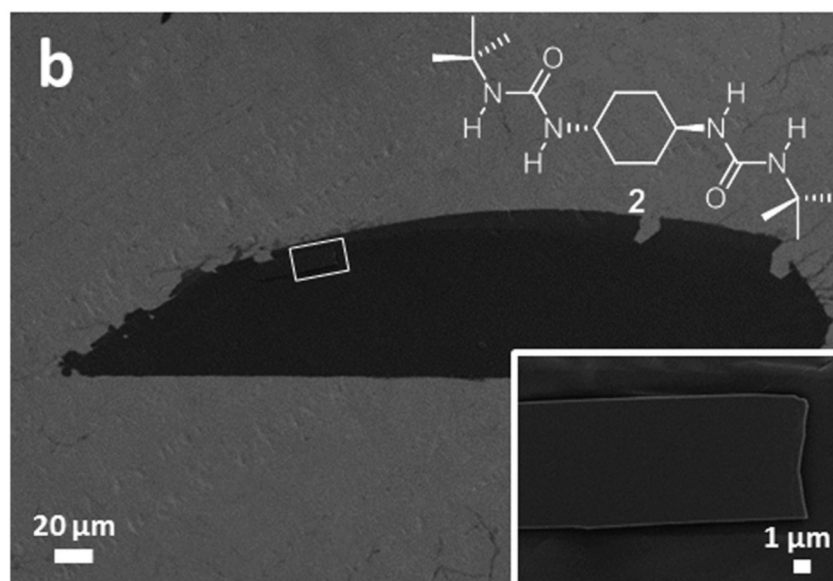


Figure 32. SEM image of the two-dimensional structure of 1,1'-(cyclohexane-*trans*-1,4-diyl)bis(3-*tert*-butylurea) (200 ppm) formed in butan-2-one. The region where the magnified image (inset) was collected is marked using the white box. This compound was originally developed and synthesized by Richter et al.<sup>[14]</sup> and the image is an excerpt from Schmidt et al.<sup>[99]</sup>

As shown in Figure 32, the bisurea compound forms sheet-like structures when crystallized from butan-2-one. Moreover, powder X-ray diffraction as well as 1D and 2D multinuclear solid-state NMR spectroscopy revealed a “pseudo-biaxial” hydrogen bond system where each molecule is directly connected to four neighboring molecules via hydrogen bonds resulting in two-dimensional nanosheets.<sup>[99]</sup> Figure 33 shows two nano-sheets consisting of bisurea molecules formed due to hydrogen bonds lying on the top of each other.

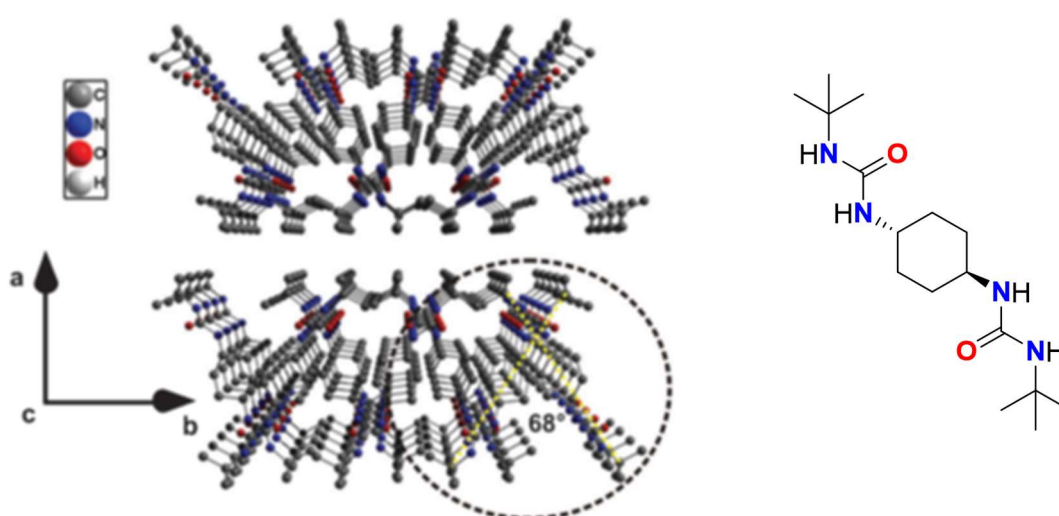


Figure 33. Extended crystal packing plot and structure of 1,1'-(cyclohexane-*trans*-1,4-diyl)bis(3-*tert*-butylurea) investigated by Schmidt et al. (figure reproduced from Schmidt et al.<sup>[99]</sup>).

It is well known that polyamides also crystallize in sheet-like structures which are favored due to hydrogen bonds.<sup>[51,105–107]</sup> These intermolecular hydrogen bonds connect neighboring chains and form extended planar sheets. These sheets dominate the molecular structure of polyamides.<sup>[2]</sup> Hence, it can be assumed that sheet-like structures have the ability to promote the nucleation of polyamides. For example, Masahito et al. showed the epitaxially growth of PA6 on a nano-sheet of graphite.<sup>[108]</sup>

As demonstrated by Schmidt et al., bisurea compounds exhibit sheet-like structures due to hydrogen bonds. Richter et al. investigated three classes of bisurea compounds, namely symmetrical *cis*-1,4-cyclohexane bisurea derivatives, asymmetric *trans*-1,4-cyclohexane bisurea derivatives and symmetrical *trans*-1,4-cyclohexane bisurea derivatives, regarding their nucleation potential. One example for each of the three classes is shown in Figure 34.

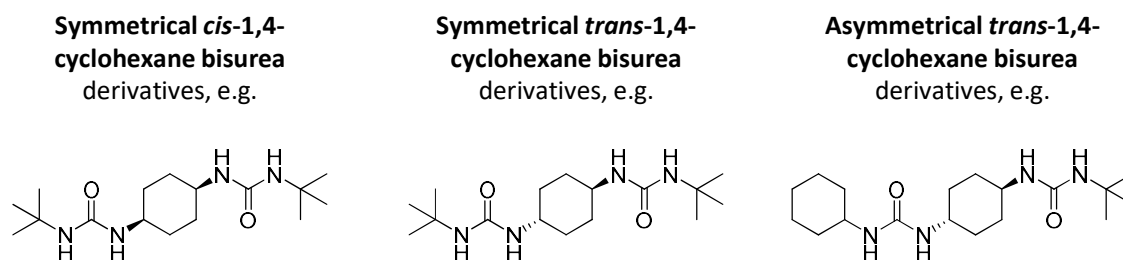


Figure 34. Examples for the three classes of bisurea derivatives investigated by Richter et al.<sup>[14]</sup>

In total, 29 derivatives were investigated by Richter et al. with respect to their nucleation behavior in PA6.<sup>[14]</sup> All derivatives showed good nucleation properties with some additives exhibiting nucleation efficiencies up to 90% at additive concentrations of just 0.2 wt%. Furthermore, for some nucleating agents a change of the crystal modification of PA6 from  $\gamma$ -phase to  $\alpha$ -phase was observed. Besides good nucleation properties, the asymmetric *trans*-1,4-cyclohexane bisurea derivatives and especially the symmetric *trans*-1,4-cyclohexane bisurea derivatives exhibit excellent clarifying properties. Haze values of less than 20% at additive concentrations below 1.0 wt% were observed. Due to a conformational change in the central unit, the *cis*-derivatives showed lower nucleation efficiencies and no enhancement of the optical properties. Furthermore, the mechanical properties of PA6 were significantly increased by the use of certain bisurea additives.<sup>[89,92]</sup> In addition to Richter et al., Xue et al.<sup>[30]</sup> synthesized an ureido mixture which is also capable of nucleating PA6 (Figure 35). Furthermore, the mechanical properties were improved notably and a change of the crystal modification from the  $\alpha$ - to the  $\gamma$ -phase with increasing

additive content was observed. In contrast to Richter et al., no enhancement of the optical properties was observed.

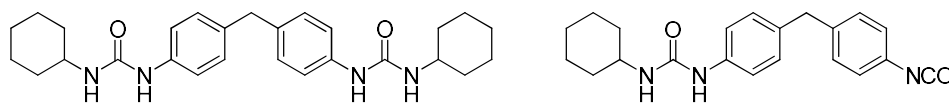


Figure 35. Ureido mixture as nucleating agent investigated by Xue et al.<sup>[30]</sup>

Richter et al. mainly focused on structure-property relations of bisurea compounds and their nucleating and clarifying effect in semi-crystalline polyamides. Investigations of the influence of the processing temperature on the effect of the additives were not part of the work. Both, Richter et al. and Xue et al., worked with temperatures at the lower end of the processing range for polyamides. Knowledge about thermal stability of these additives for industrial applications at higher melt temperatures during processing are not available yet, but are of fundamental importance for industrial benefit.

The following chapter deals with investigations about the thermal stability of an efficient bisurea compound and its behavior at elevated melt temperatures during processing. Primarily, the neat additive is studied regarding its thermal stability and the results of Richter et al. are reproduced and verified. Furthermore, the influence of nucleation on the morphology was evaluated. Afterwards, correlations between melt temperature during processing and additive efficiency are examined by varying the processing temperatures systematically. The compounds were investigated in a temperature range from 245 °C to 283 °C and compared with respect to their nucleation efficiency and their influence on the optical properties.

Figure 36 shows the investigated bisurea compound **1**, namely 1,1'-(cyclohexane-*trans*-1,4-diyl)bis(3-*tert*-butylurea). This additive was originally developed and synthesized by Richter et al. at the chair of macromolecular chemistry I at the University of Bayreuth. For the subsequent investigations the batch already synthesized by Richter et al.<sup>[14]</sup> was used.

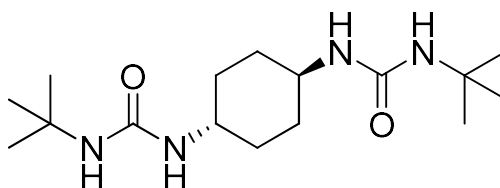


Figure 36. Chemical structure of investigated bisurea compound **1** (1,1'-(cyclohexane-*trans*-1,4-diyl)bis(3-*tert*-butylurea)).

## 4.1.1 Thermal properties of the bisurea additive

The thermal properties of 1,1'-(cyclohexane-*trans*-1,4-diyl)bis(3-*tert*-butylurea) **1** were already determined by Richter et al.<sup>[14]</sup> To guarantee reproducibility and to avoid mistakes, measurements of the thermal properties were conducted by means of combined thermogravimetric (TGA) and simultaneously differential thermal analysis (DTA) and complemented by polarized light microscopy.

TGA measurements of the dried bisurea were performed between 30 °C and 700 °C with a heating rate of 10 K/min under nitrogen atmosphere. Figure 37 shows the thermogravimetric analysis (solid line) and simultaneous thermal analysis (dotted line) of compound **1**.

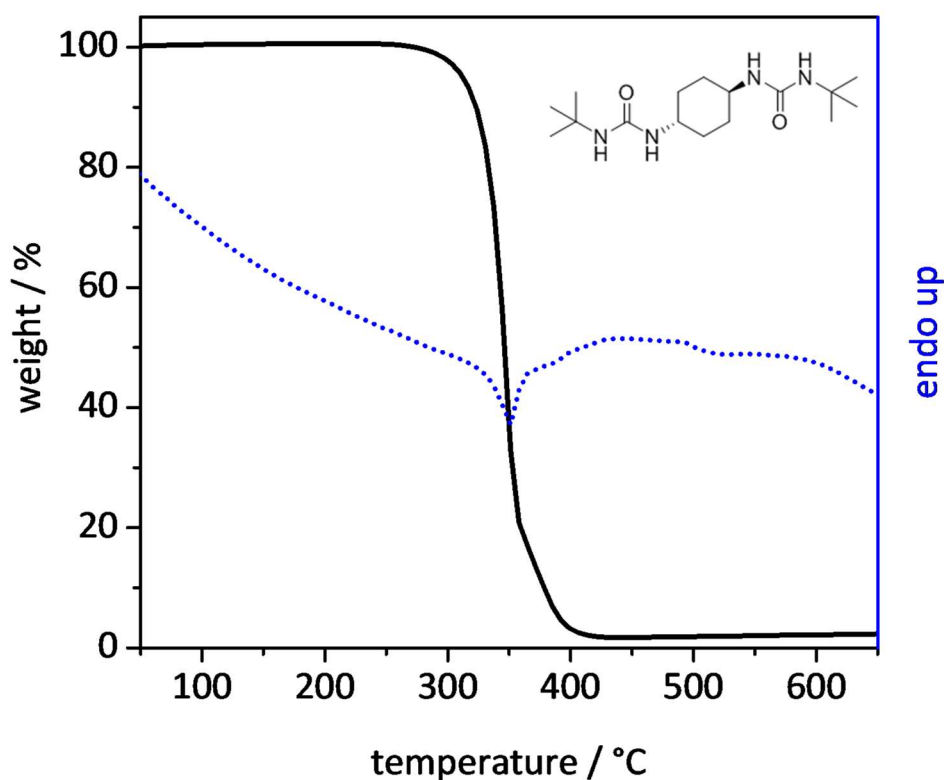


Figure 37. Thermogravimetric analysis (solid line) and simultaneous differential thermal analysis (dotted line) of 1,1'-(cyclohexane-*trans*-1,4-diyl)bis(3-*tert*-butylurea), measured under nitrogen atmosphere at a heating rate of 10 K/min.

It clearly shows up that no melting endotherm, but sublimation with subsequent thermal decomposition of the bisurea occur. Bisurea **1** exhibits a weight loss of 5% at 310 °C. Sublimation starts at around 280 °C and thermal decomposition appears above 350 °C indicated by a kink of the TGA curve. At higher temperatures sublimation and thermal degradation interfere and a residual weight of 2% is the result.

TGA measurements register only the weight loss of the measured sample. To get further information, polarized light microscopy was conducted. Therefore, a few milligram of bisurea **1** were placed between two glass slides, inserted to a hot stage and observed at different temperatures while heating with 10 K/min. Figure 38 presents images obtained from polarized light microscopy of compound **1**.

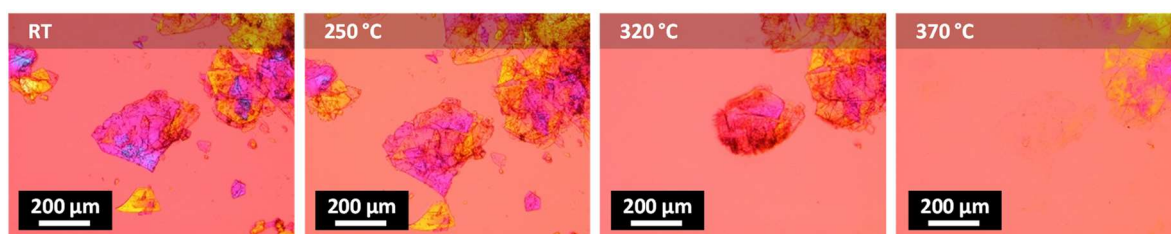


Figure 38. Polarized light microscopy of compound **1** viewed through a  $\lambda/4$  platelet at various temperatures while heating with 10 K/min.

With increasing temperature the platelets start to sublime and finally disappear. At some spots the platelets get brownish before disappearing, which can be referred to degradation of the bisurea compound. Complete sublimation of the bisurea could not be observed due to a limited temperature range of the hot stage (maximum temperature: 375 °C).

These results are in good agreement with those determined by TGA measurements. Both experiments revealed no change up to a temperature of 250 °C. At temperatures around 320 °C, the TGA curve starts to drop and the optical micrographs showed a reduction of the platelets. Additionally, the brown color at the edges of the platelets indicate thermal degradation, which could be confirmed by the kink of the TGA curve at 350 °C. Moreover, a large amount of the sample disappeared in both experiments. However, the TGA experiment revealed no weight loss of 100%, which is a further sign for thermal degradation at elevated temperatures.

### 4.1.2 Nucleation and optical properties of PA6

In the following, the influence of bisurea **1** on the polymer crystallization temperatures and the optical properties at different additive concentrations were investigated. Richter et al. investigated the bisurea compounds only at processing temperatures below 250 °C. In frame of this work higher melt temperatures during processing are discussed. In order to ensure the comparability of all experiments and to guarantee consistent handling for all samples, first of all bisurea **1** was compounded as reference with processing parameters used by Richter et al.<sup>[14]</sup>

First, the additive was ground and filled with the pulverized polymer powder into a bottle. To get a homogenous distribution, the powder/powder blend was mixed with a tumble mixer for at least 12 h and dried at 80 °C overnight. Afterwards, the obtained blend was compounded with a co-rotating twin-screw compounder (DSM Xplore 15 mL) under nitrogen atmosphere. Detailed processing parameters are listed in chapter 3.1.



Figure 39. Tumble mixer with bottles for the preparation of polymer powder/additive powder blends.

The additive was investigated in a concentration range from 1.5 wt% to 0.1 wt%. The different concentrations were prepared by diluting the initial additive/polymer mixture (1.5 wt%) with a mixture of the initial PA6/additive powder and neat PA6 powder, yielding the following dilution series: 1.5 wt%, 1.3 wt%, 1.0 wt%, 0.8 wt%, 0.6 wt%, 0.4 wt%, 0.2 wt% and 0.1 wt%. The preparation steps and initial weights for a concentration series are shown in Table 12 and are explained below.

For the cleaning run and the first sample run a mixture with a concentration of 1.5 wt% additive was used. For the following runs the initial additive concentration was diluted by



neat PA6 and the initial powder mixture to obtain the requested concentrations. With a dead volume of 5.4 g the exact additive concentrations of the extrudates could be calculated according to Richter et al.:<sup>[14]</sup>

With an initial additive concentration of 1.5 wt% and a dead volume of 5.4 g (for PA6 and the compounder used for this work), the amount of additive within the dead volume is 0.081 g. To obtain an additive concentration of 1.3 wt%, 6.8 g of the initial powder mixture with 1.5 wt% of additive and 1.8 g of neat PA6 are added. The amount of additive in 6.8 g of the initial powder mixture is 0.102 g. Consequently, the total amount of additive within the compounder in the first dilution run is 0.183 g. The exact additive concentration results from the total amount of additive divided by the amount of polymer:

$$\left( \frac{0.081 \text{ g} + 0.102 \text{ g}}{5.4 \text{ g} + 6.8 \text{ g} + 1.8 \text{ g}} \right) \cdot 100\% = \left( \frac{0.183 \text{ g}}{14 \text{ g}} \right) \cdot 100\% = 1.31\% \quad (5)$$

Table 12 summarizes the initial weights and resulting additive concentrations for a concentration series in PA6.

Table 12. Initial weights and additive concentration for a concentration series in PA6.

Run	Comment	$m_{\text{powder mixture}}$ [g]	$m_{\text{neat polymer}}$ [g]	$C_{\text{additive}}$ [wt%]
1	cleaning	14.0	0.0	1.50
2	1st sample	8.6	0.0	1.50
3	1st dilution	6.8	1.8	1.30
4	2nd dilution	4.7	3.9	1.00
5	3rd dilution	3.9	4.7	0.80
6	4th dilution	2.7	5.9	0.60
7	5th dilution	1.6	7.0	0.40
8	6th dilution	0.5	8.1	0.20
9	7th dilution	0.2	8.4	0.10

Subsequent experiments were conducted with the compounding and injection molding parameters already listed in chapter 3.1. The polymer melt temperature during processing was 245 °C. In order to investigate the influence of the additive on the optical properties,

injection molding specimen with a thickness of 1.1 mm were prepared and clarity and haze were measured according to ASTM D-1003. To study the crystallization behavior of the compounded polymer, DSC measurements were performed and the polymer crystallization temperatures were obtained from the exothermic minimum of the second cooling curves. Figure 40 shows the DSC cooling curves of neat PA6 and PA6 comprising 1.0 wt% bisurea **1**. The addition of the bisurea additive leads to an increase of the polymer crystallization temperature due to initiation of nucleation at temperatures above the original crystallization temperature of the reference.

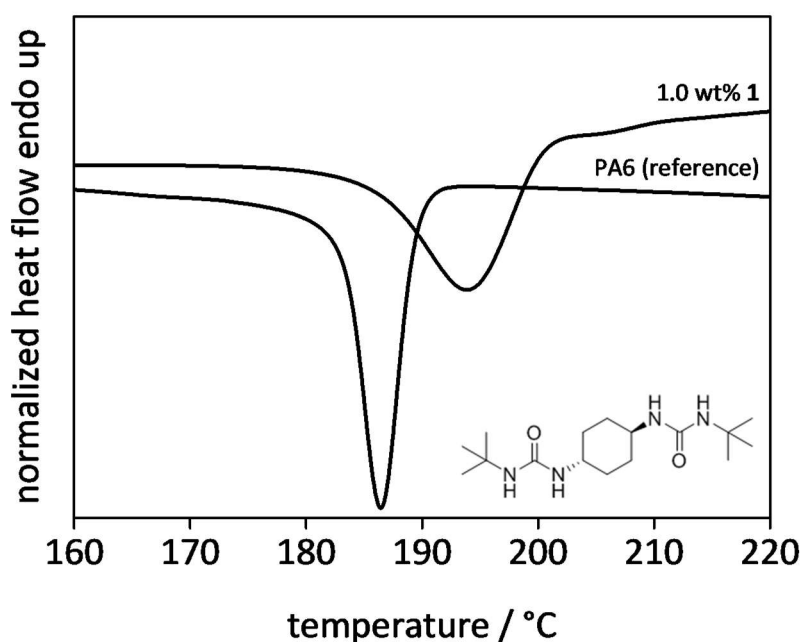


Figure 40. Differential scanning exotherms of neat PA6 and PA6 comprising 1.0 wt% bisurea **1**. The neat polymer has a polymer crystallization temperature of 186 °C and the additivated polymer has a polymer crystallization temperature of 194 °C. Polymer melt temperature during processing: 245 °C. DSC heating and cooling rate: 10 K/min.

In order to compare various additives with each other and to estimate the potential of a nucleating agent, the nucleation efficiency of an additive can be calculated by equation 6:

$$NE(\%) = \left( \frac{T_{c(\text{additive})} - T_{c(\text{reference})}}{T_{c(\text{maximum})} - T_{c(\text{reference})}} \right) \cdot 100\% = \left( \frac{194\text{ }^{\circ}\text{C} - 186\text{ }^{\circ}\text{C}}{195\text{ }^{\circ}\text{C} - 186\text{ }^{\circ}\text{C}} \right) \cdot 100\% = 89\% \quad (6)$$

with  $T_{c(\text{additive})}$  being the crystallization temperature of the additivated polymer,  $T_{c(\text{reference})}$  being the crystallization temperature of the neat polymer and  $T_{c(\text{maximum})}$  being the maximum crystallization temperature obtained by self-seeding experiments according to Lotz et al.<sup>[35]</sup> Consequently, a nucleation efficiency of 89% for PA6 comprising 1.0 wt%

bisurea **1** was achieved.

In order to evaluate the ideal additive concentration for further experiments, a concentration series of PA6 with bisurea **1** was reproduced from Richter et al.<sup>[14]</sup> Figure 41 presents the polymer crystallization temperature (top) and the optical properties clarity and haze (bottom) as function of the additive concentration.

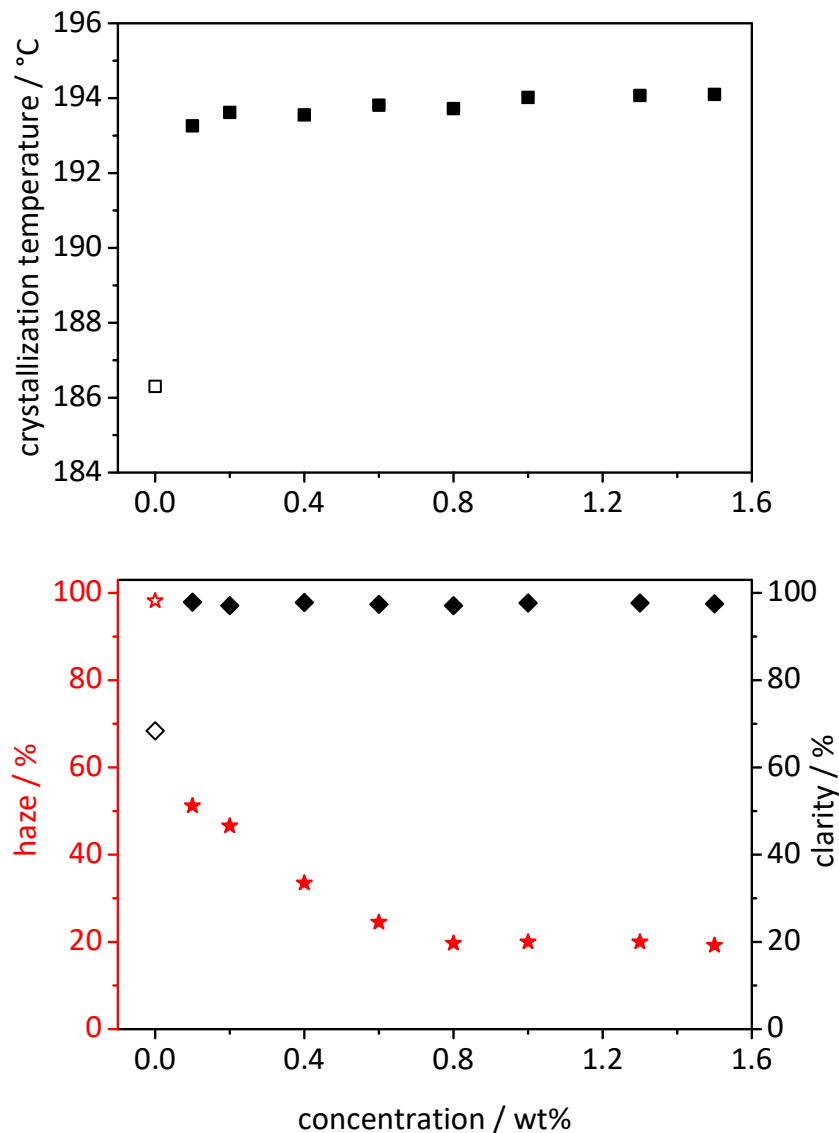


Figure 41. Polymer crystallization temperatures (top graph) and the optical properties haze (★) and clarity (◆) (bottom graph) of PA6 comprising bisurea **1** as function of the additive concentration. The blank symbols indicate the values for neat PA6. DSC heating and cooling rate: 10 K/min.

As presented in the top graph of Figure 41, the crystallization temperature is increased significantly even at an additive concentration of 0.1 wt%. However, with increasing additive concentration a slight increase of the polymer crystallization temperature can be observed with a maximum crystallization temperature of 194 °C at 1.0 wt% revealing a

nucleation efficiency of 89%.

The bottom graph of Figure 41 presents the optical properties clarity and haze as function of the additive concentration. The clarity values increase from 68% to 98% at the lowest concentration of 0.1 wt% and stay constant within all concentrations. Whereas the haze values decrease from 98% to around 20% at a concentrations of 0.8 wt% and stay constant at 20% with increasing additive concentrations.

Comparing nucleation efficiencies and optical properties of the concentration series, an additive concentration of 1.0 wt% emerges to be the optimal concentration for further experiments. The additive reveals the best nucleation efficiency as well as the best optical properties at this concentration. To study the influence of processing parameters on the thermal stability of the additive this is the best concentration to easily detect a change of the additive performance.

#### 4.1.3 Nucleation and optical properties of PA6 under various processing conditions

As already mentioned, the nucleation and clarification ability of supramolecular polymer additives strongly depends on the individual chemical structure of the additive. Besides the chemical properties, the processing parameters are of huge importance. In general, additives exhibit a certain temperature until their thermal stability is not guaranteed anymore. The bisurea additives are thermally stable up to 250 °C before detecting a weight loss by TGA measurements. However, PA6 is usually processed in a temperature range of 238 °C to 270 °C.<sup>[2]</sup> In most cases industrial compounding takes place at elevated melt temperatures and increased friction and shear occur in contrast to a compounder on the laboratory scale.

In order to get knowledge about the performance at varying processing parameters, the following chapter approaches the influence of the processing time and temperature of the *tert*-butyl substituted bisurea **1** on the efficiency concerning nucleation and optical properties. Information about a decline of the additive performance at certain processing parameters were examined. Furthermore, the ideal processing parameters for compound **1** were figured out.

##### *Influence of processing time*

On the one hand, the processing time can play an important role to improve the effect of polymer additives due to increased solubility and dispersion in the polymer melt. On the other hand, the thermal load can cause degradation and lead to a decline of the additive efficiency. Therefore, the influence of the processing time on the nucleation and clarification effect of PA6 comprising compound **1** was investigated.

The following experiments were conducted with PA6 comprising 1.0 wt% bisurea **1**. This composition was investigated at a constant melt temperature during processing of 245 °C with varying processing times of 5 min, 10 min, 20 min, 30 min and 60 min. The way of proceeding is explained below:

First, 14.0 g of PA6 comprising 1.0 wt% bisurea **1** was filled in the compounder. After 5 minutes, the melt was discharged and discarded (cleaning run). Up next, 8.6 g of the polymer/additive composition was filled in the compounder, mixed for the requested time and transferred to the injection molding machine to prepare injection molding platelets.

Figure 42 presents the polymer crystallization temperatures, and optical properties (haze

and clarity) of PA6 comprising 1.0 wt% bisurea **1** as function of the processing time.

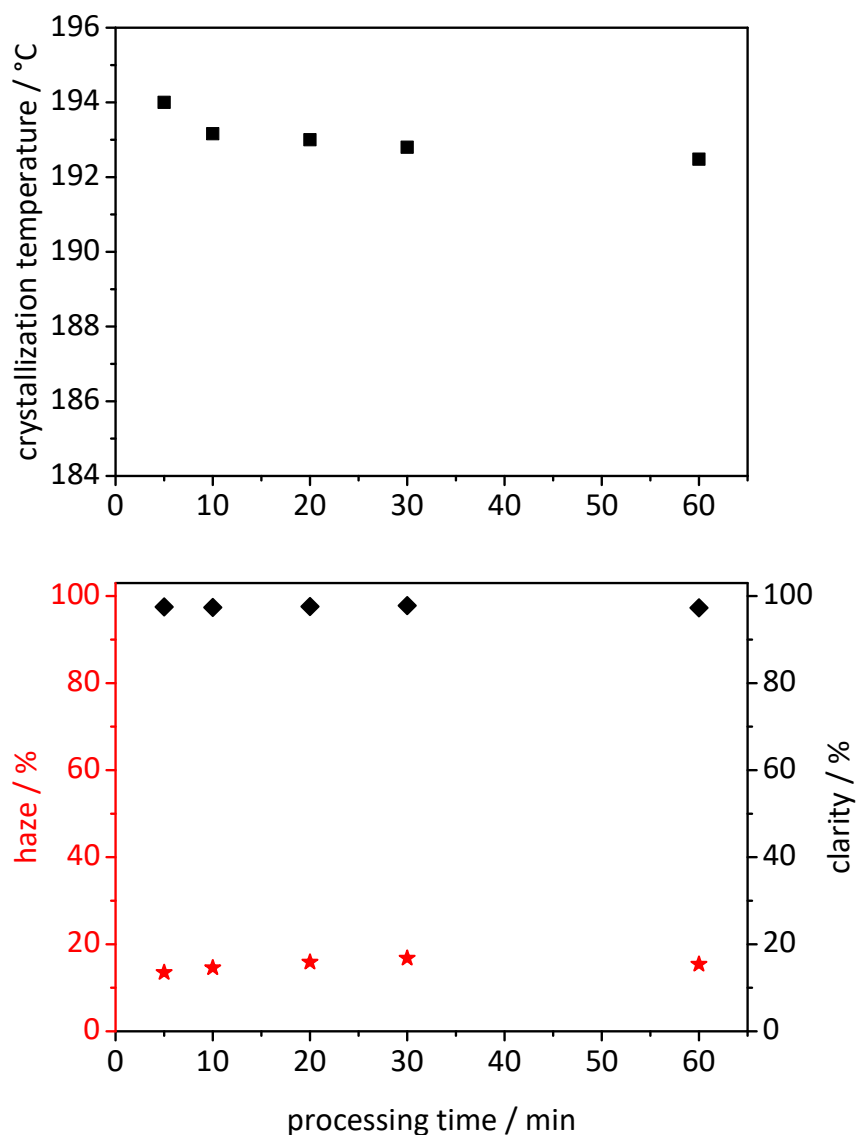


Figure 42. Polymer crystallization temperatures (top graph) and the optical properties haze (★) and clarity (◆) (bottom graph) of PA6 comprising 1.0 wt% of bisurea **1** as function of the processing time. The processing time is defined as the time the polymer remains in the extruder during compounding. Melt temperature during processing: 245 °C.

The polymer crystallization temperature after a processing time of 5 minutes is slightly increased compared to the other processing times (top graph, Figure 42). Similar observations were made for the neat polymer as well (see chapter 3.2). However, this deviation is in the range of the measuring accuracy of the DSC apparatus. Thus, the crystallization temperature of the additivated polymer is unaffected by the processing time.

The bottom graph of Figure 42 shows the influence of the processing time on the optical properties haze and clarity. No significant shift of the values by varying processing time can be recognized. Both, haze and clarity values, stay constant with increased processing time. Figure 43 shows the optical properties of neat PA6 as function of the processing time for comparison. Haze values stay almost constant at around 100% with extended processing time, whereas clarity values are fluctuating between 50% and 70%.

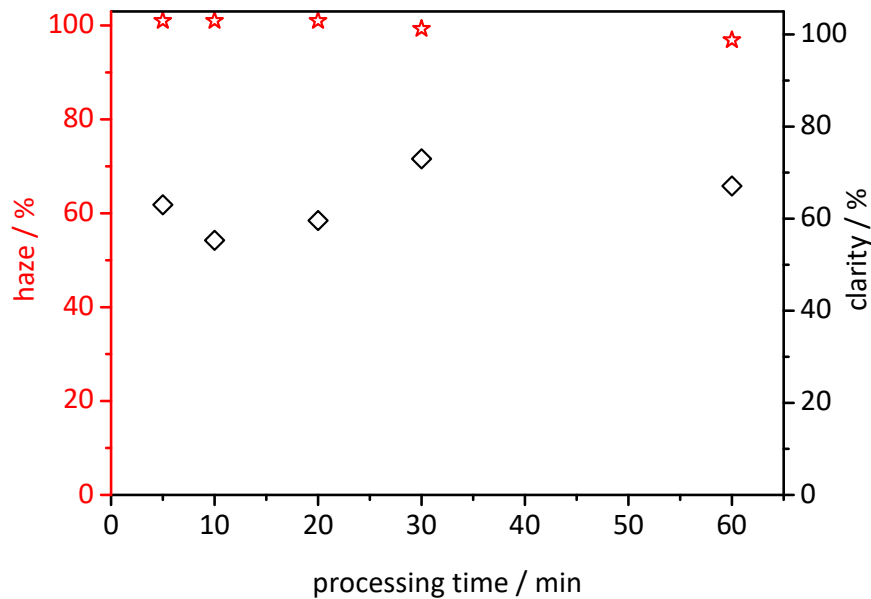


Figure 43. Optical properties haze (☆) and clarity (◇) of neat PA6 as function of processing time. The processing time is defined as time how long the polymer remains in the extruder during compounding. Melt temperature during processing: 245 °C.

All in all, no influence of the processing time on the nucleation and optical properties at melt temperatures during processing of 245 °C were found. Therefore, the following section addresses the influence of the melt temperature during processing.

*Influence of melt temperature during processing*

Increased melt temperatures during processing can lead to a better dissolution and dispersion of an additive but can also cause thermal degradation with simultaneous decline of the nucleation efficiency and optical properties. In order to determine the influence of the melt temperature during processing on the performance of bisurea **1**, various melt temperatures were tested. The following experiments were conducted with PA6 comprising 1.0 wt% bisurea **1** at melt temperatures of 245 °C, 259 °C, 273 °C and 283 °C and a processing time of 5 minutes. The detailed way of proceeding is explained below and the parameters are summarized in Table 13.

Table 13. Initial weights, melt temperature and additive concentration for a temperature dependent extrusion experiment of additivated PA6.

Run	Comment	$m_{\text{powder mixture}}$ [g]	Melt temperature during processing [°C]	$C_{\text{additive}}$ [wt%]
1	cleaning	14.0	245	1.0
2	sample	8.6		1.0
3	cleaning	8.6	259	1.0
4	sample	8.6		1.0
5	cleaning	8.6	273	1.0
6	sample	8.6		1.0
7	cleaning	8.6	283	1.0
8	sample	8.6		1.0

First, 14.0 g of PA6 comprising 1.0 wt% bisurea **1** was filled in the compounder. After 5 minutes, the melt was discharged and discarded (cleaning run). Next, 8.6 g of the polymer/additive composition was filled in the compounder, mixed for the requested time and transferred to the injection molding machine to prepare injection molding platelets. Lastly, both, the compounder and injection molding machine, were cleaned and ready for the next processing temperature. At the end, four samples at four different melt temperatures were prepared.



Figure 44 presents the polymer crystallization temperatures and optical properties haze and clarity of PA6 comprising 1.0 wt% bisurea **1** as function of the melt temperature during processing.

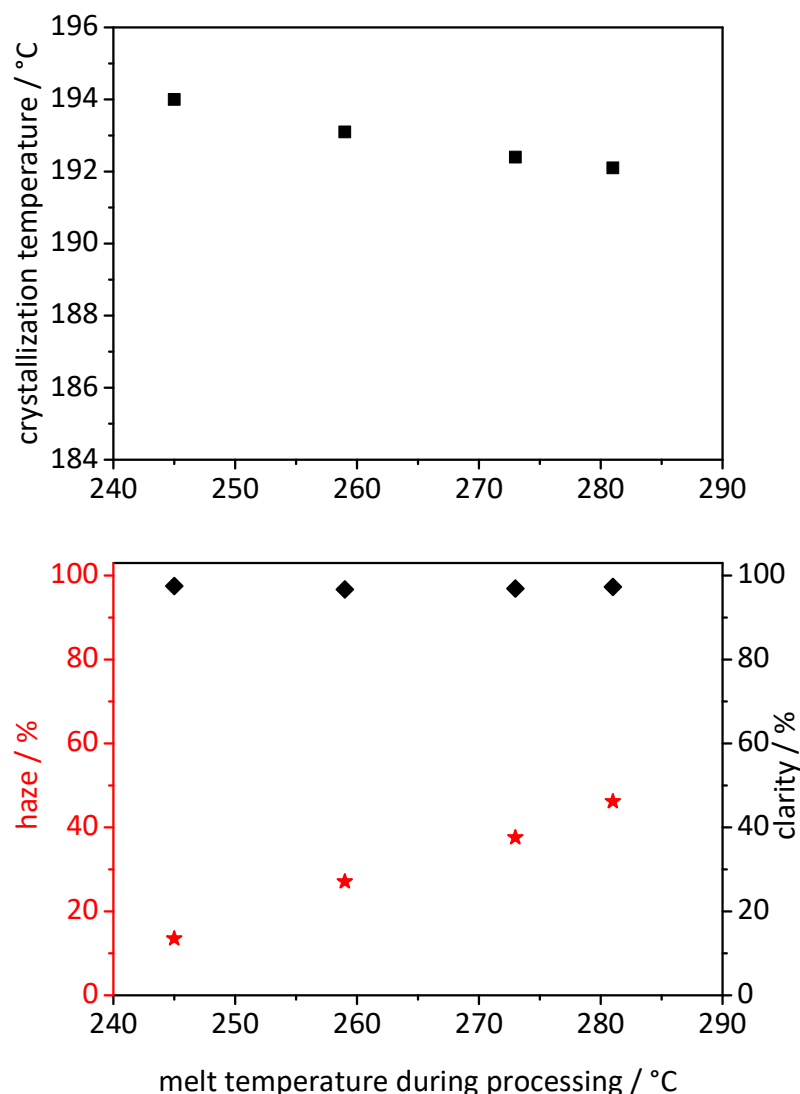


Figure 44. Polymer crystallization temperatures (top graph) and the optical properties haze (★) and clarity (◆) (bottom graph) of PA6 comprising 1.0 wt% of bisurea **1** as function of melt temperature during processing.

The polymer crystallization temperatures show a slight decrease with increasing melt temperature during processing. The polymer crystallization temperature decreased from 194 °C at a melt temperature of 245 °C to a polymer crystallization temperature of 192 °C at 283 °C. Similar shifts of the crystallization temperatures were observed for the neat polymer at elevated melt temperatures during processing as well (see chapter 3.2). Thus, the crystallization temperature of the additivated polymer is largely unaffected by the melt temperature during processing.

The bottom graph of Figure 44 presents the optical properties haze and clarity as function of the melt temperature during processing. In contrast to the polymer crystallization temperature, a significant influence of the melt temperature during processing on the optical properties of the additivated polymer could be observed. The haze values increase linearly from below 20% at 245 °C to almost 50% at 283 °C. Clarity values still remain constant at around 100%.

Figure 45 shows the optical properties of neat PA6 at different melt temperatures during processing.

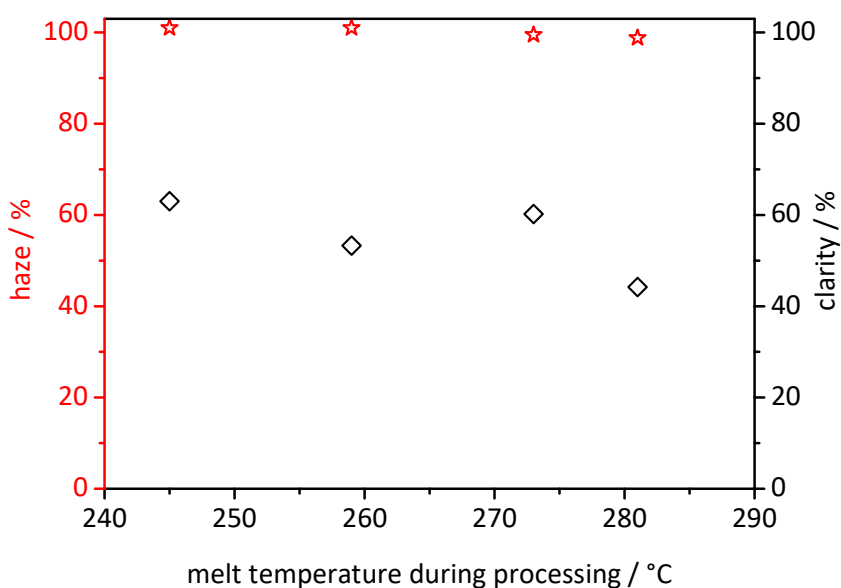


Figure 45. Optical properties haze (★) and clarity (◇) of neat PA6 as function of the melt temperature during processing.

Haze values of neat PA6 stay almost constant at around 100% with increasing melt temperature during processing, whereas clarity values are fluctuating between 45% and 65%. Due to the fact that no significant influence of the melt temperature during processing on the optical properties of the neat polymer could be observed, the decline of the optical properties have to come along with the bisurea additive. By a release of possible degradation products of the bisurea additive at higher melt temperatures during processing, which might be insoluble in the polymer melt, increased light scattering and thus a decline of the optical properties may occur.

In order to analyze possible degradation products of the additive at elevated melt temperatures during processing, the following chapter will discuss the above stated assumptions in detail with the help of GC-MS measurements of the compounds.

## 4.1.4 Investigation of temperature stability of the bisurea under processing conditions

Previous investigations revealed that the optical properties of clarified PA6 decline with increasing melt temperatures during processing. Thermal investigations of the bisurea additive showed thermal stability up to 250 °C, but the processing temperatures for industrial applications usually exceed this temperature.

In order to elucidate the behavior of the bisurea additive at elevated melt temperatures during processing GC-MS measurements were conducted. Therefore, bisurea **1** was measured in a temperature range from 230 °C up to 290 °C. Detailed sample preparation for the GC-MS measurements was already explained in chapter 3.2.

In order to understand the process of decomposition for bisurea **1** and in order to identify possible elimination products, first a conventional mass spectrum was recorded (Figure 46).

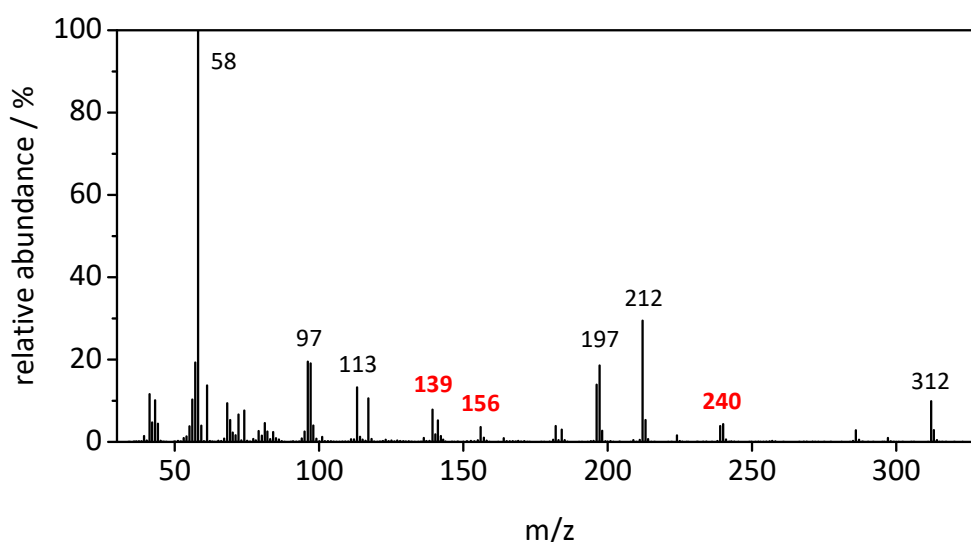


Figure 46. Conventional mass spectrum of bisurea **1** (molecule peak:  $m/z = 312$ ) exhibiting the fragment peaks at  $m/z = 139$ , 156 and 240. These peaks were also detected via GC-MS.

Figure 46 presents the fragmentation process of bisurea **1** with the following fragments: MS (70 eV),  $m/z$  (%): 312 (18); 240 (7); 212 (44); 197 (32); 156 (5); 139 (10); 97 (25); 61 (15); 58 (100).

To gain information about the thermal stability and behavior of bisurea **1** at elevated temperatures GC-MS measurements were conducted. Figure 47 presents the chromatograms of compound **1** at 230 °C, 250 °C, 270°C and 290 °C. Three peaks at 9.2 min (**a**), 10.4 min (**b**) and 17.0 min (**c**) could be detected. Peak **c** is many times higher and broader than peaks **a** and **b**. Also a significant increase of the detected peaks with increasing measuring temperature is observed.

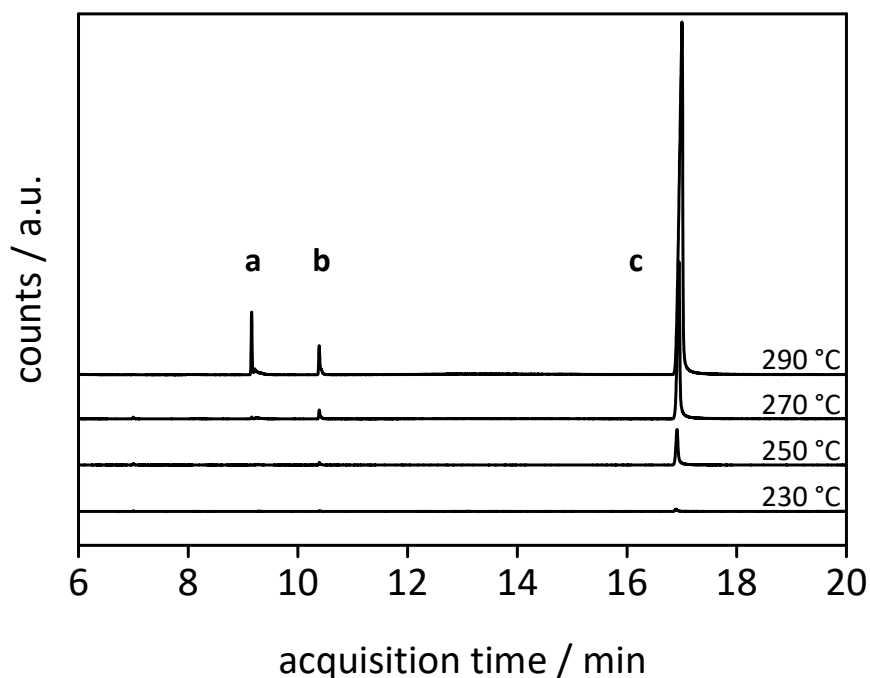


Figure 47. Chromatograms of bisurea **1** at various temperatures measured by GC. Three peaks at 9.2 min (**a**), 10.4 min (**b**) and 17.0 (**c**) could be detected. Mobile phase: helium gas (1 mL/min); Gas chromatography column: ((5%-Phenyl)-methylpolysiloxane column).

Three compounds with molecule peaks of  $m/z = 156$ , 139 and 240 (**a**, **b** and **c**) occur. The molecule peaks observed by GC can also be observed when examining the conventional mass spectrum of bisurea **1**, and hence correspond to molecule fragments.

Figure 48 shows schematically the chemical structures of possible fragments of bisurea **1** for the  $m/z$  values of 139, 156 and 240.

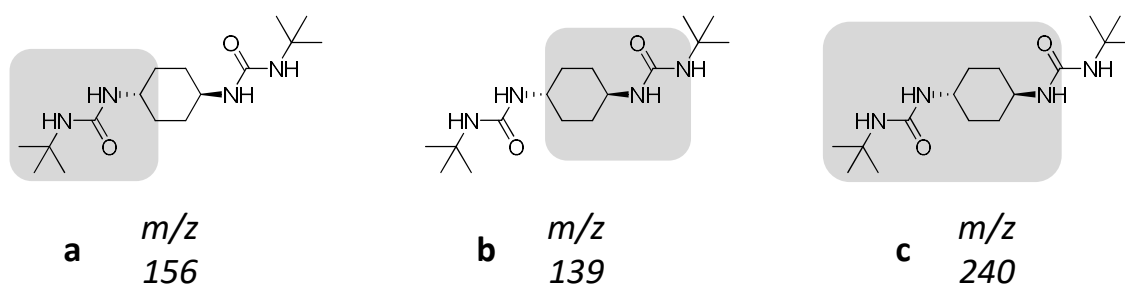


Figure 48. Possible fragments (highlighted in grey) and corresponding molpeaks of peaks (**a**, **b** and **c**) detected during GC-MS measurements.

In the case of the conventional mass spectrometry these fragments originate from ionization. Whereas for the GC-MS measurements the detected peaks must come along with thermal treatment of the sample. Upon heating, the sample starts to sublime and/or degrade. After that, the gassy substances are transferred to the chromatography column and are separated. At the end of the column the individual fractions are ionized and

measured by the mass spectrometer. The fact that the peaks first occur at 250 °C and then begin to increase with increasing measuring temperature is indicative that the additive starts to degrade and the detected substances are thermal decomposition products. Previously, the TGA curve revealed a weight loss of bisurea **1** starting at 250 °C. Finally, the  $m/z$  values of the detected peaks are in accordance with the peaks of the conventional mass spectrum.

The above described investigations were carried out for the neat additive. In order to explore the behavior of the additive in the polymer under processing conditions, GC-MS measurements were conducted with PA6 comprising bisurea **1**.

Figure 49 presents the chromatograms of PA6 comprising 1.0 wt% bisurea **1** at 230 °C, 250 °C, 270 °C and 290 °C. In contrast to the neat additive only two peaks at 7.6 min (**d**) and 9.8 min (**e**) could be detected.

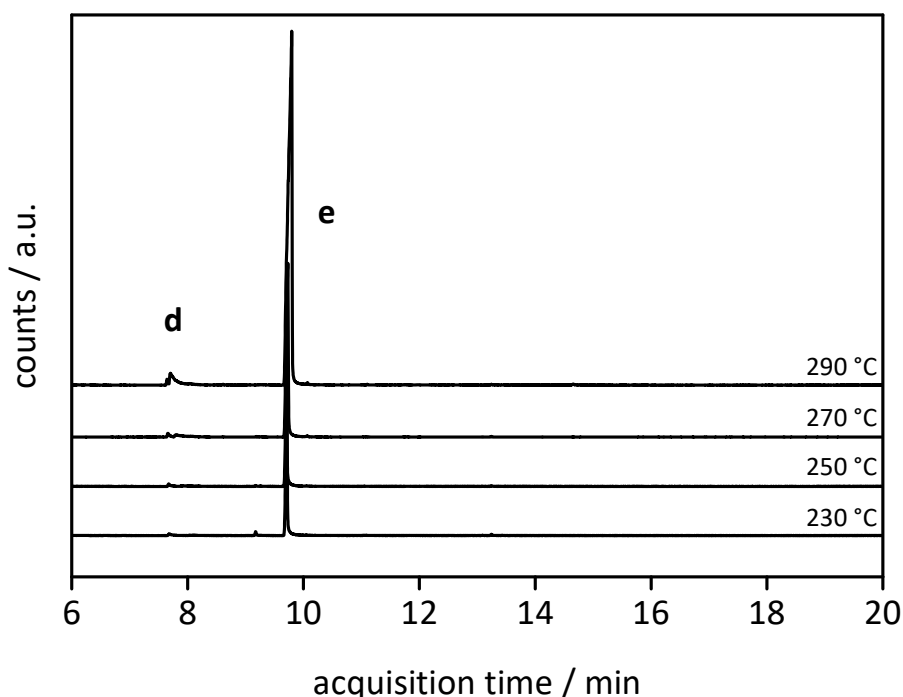


Figure 49. Gas chromatograms of PA6 comprising 1 wt% bisurea **1** measured at temperatures as indicated. Two peaks at 7.6 min (**d**) and 9.7 (e) could be detected. Mobile phase: helium gas (1 mL/min); Gas chromatography column: ((5%-Phenyl)-methylpolysiloxane column).

Peak **e** is more distinct than peak **d**. By evaluating the mass spectra of **e** and comparison with the GC-MS measurements of the neat polymer in chapter 3.2, this peak can be referred to  $\epsilon$ -caprolactam which originates from polymer synthesis.

Peak **d** appears at 270 °C for the first time. The mass spectra show a molecule peak at  $m/z$  of 114 which can be referred to cyclohexane diamine and can be assumed to be a degradation product from the bisurea additive.

The results of the GC-MS investigations of PA6 comprising the bisurea additive **1** strongly differ from those conducted for the neat additive. No similar peak occurs comparing both measurement series. This may be caused by interaction of the additive molecules and the polymer chains due to hydrogen bonds. However, it is very difficult to make a declaration how exactly the degradation process takes place and if there is a difference between the neat additive and the additive embedded to a polymer matrix. Nevertheless, possible degradation products occur at high melt temperatures during processing which might be the reason for the decline of the optical properties. Therefore, melt temperatures during processing around 250 °C should be selected for bisurea **1** to clarify PA6 without any losses for the optical properties.

## 4.1.5 Morphology of PA6 at the nanoscale

As already mentioned in frame of the introduction of this chapter, the morphology of polymers is strongly influenced by nucleating agents. Therefore, the influence of the *tert*-butyl substituted *trans*-bisurea **1** on the macroscopic morphology is investigated on injection molded samples by polarized light microscopy. Additionally, thin films are investigated by scanning electron microscopy (SEM) to study the influence of the nucleating agent on the morphology of PA6 at the nanoscale.

In order to explore the morphology of injection molding samples by polarized light microscopy, thin sections with a thickness of 10  $\mu\text{m}$  were cut parallel to the direction of injection (flow direction). These thin sections were placed between two object slides and fastened with an adhesive tape (Figure 50).

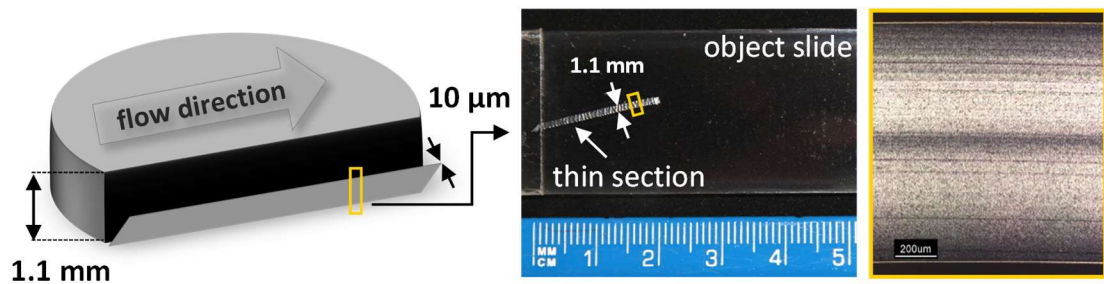


Figure 50. Thin section (10  $\mu\text{m}$  thick) from injection molded specimen cut parallel to the flow direction (left), sample for morphology investigations of injection molded specimen (middle) and corresponding polarized optical micrographs of thin section.

Figure 51 presents the thin sections already applied by Richter et al.<sup>[14]</sup> The images were merged from two separate pictures to present the complete cross section of the injection molding sample. The haze values of the samples are quoted in the right top corner of the images. Both samples exhibit oriented skin layers and a less oriented spherulitic core region. These effects were already described by Richter et al. and are explained by the temperature gradient of the injection mold from the outside to the inside, and hence varying cooling rates within the injection molding specimen. Furthermore, the black stripe in the middle of the specimens was attributed to the injection molding process and the thin stripes oriented parallel to the cutting direction originate from the cutting process.<sup>[14]</sup> Comparing neat PA6 (left) and PA6 comprising 1.0 wt% bisurea **1** clearly shows that the spherulite size decreases due to the presence of the additive, and hence decreases the haze value from 98% for neat PA6 to 20% for the additivated sample.

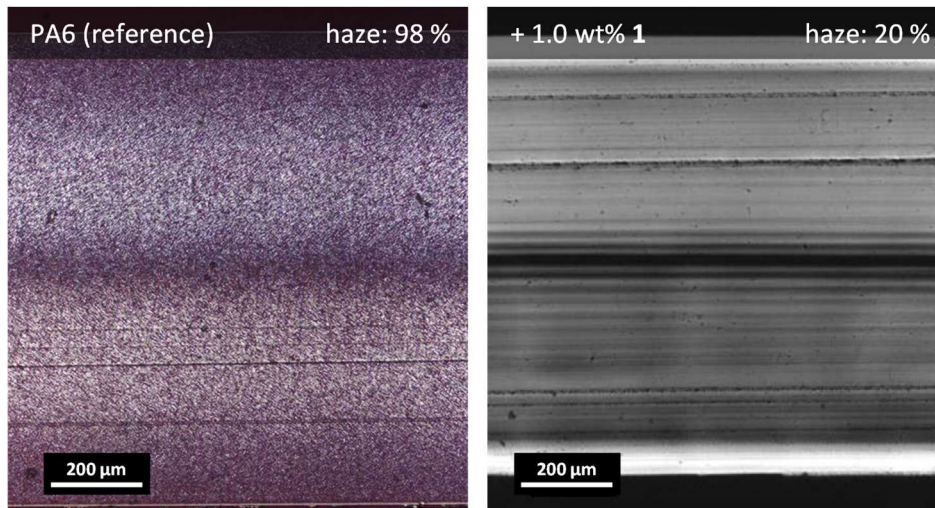


Figure 51. Thin sections of injection molded samples (thickness 1.1 mm) parallel to the flow direction and the corresponding haze values of neat PA6 (left) and PA6 comprising 1.0 wt% bisurea **1**. The images presented consist of two separate pictures taken between crossed polarizers and are reproduced from Richter et al.<sup>[14]</sup>

However, it is hardly possible to clearly see any spherulites in detail with polarized light microscopy. To get a better insight and to verify the results of Richter et al., the reduction of the spherulite size due to nucleating agents was investigated by SEM.

For this purpose thin films were prepared. PA6 was dissolved in formic acid and afterwards dropcast on a silicon wafer. The wafer was shortly placed on a hot stage at 250 °C and quenched to room temperature to obtain a homogenous film. For the additivated film as little as possible of the additive was placed onto the molten film by a pin and quenched to room temperature after 60 seconds.



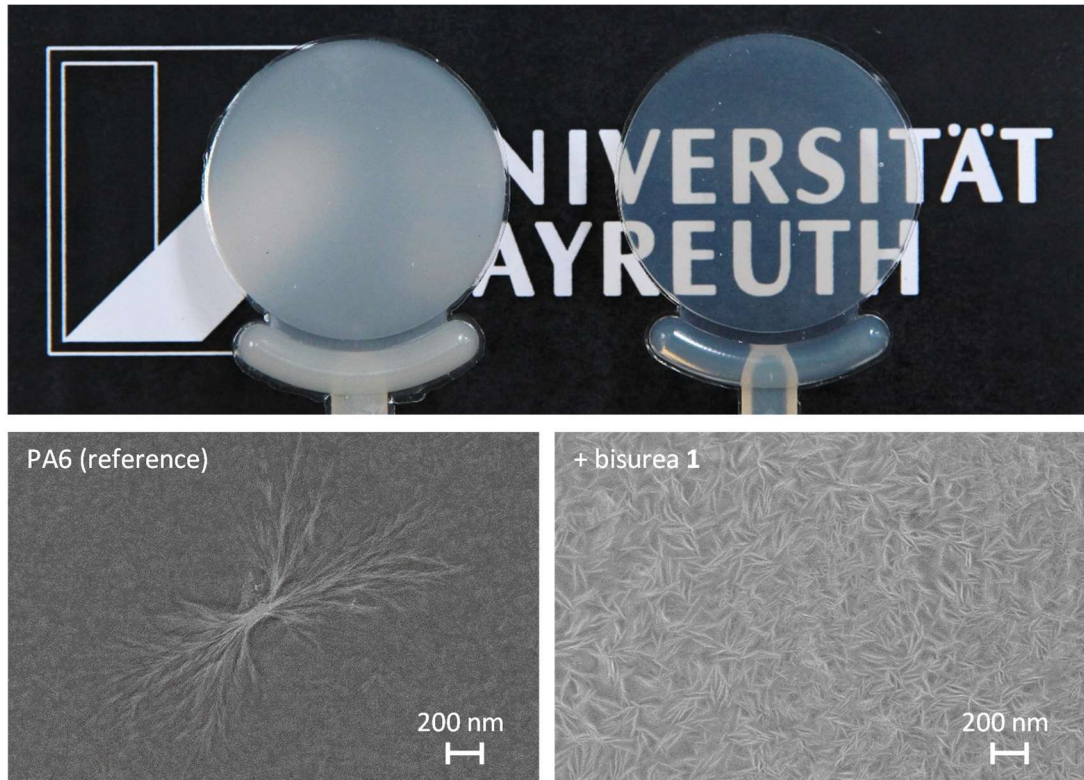


Figure 52. Emblem of the University of Bayreuth viewed through injection molded platelets of PA6 (thickness 1.1 mm) containing 0.0 and 1.0 wt% of **1** (top) and SEM images of PA6 without additive (left) and PA6 comprising bisurea **1** (right) after quenching from the melt to room temperature.

Figure 52 presents injection molded platelets and SEM images of thin films of neat PA6 (left) and PA6 comprising bisurea **1**. The injection molded samples distinctly illustrate the clarifying effect of the bisurea additive. This macroscopic clarifying effect can be explained by morphology changes at the nanoscale. As well as the injection molding samples, the SEM images look completely different. The neat sample shows a huge spherulite with a diameter of several hundred nanometers. In contrast, the additivated sample exhibits considerably more and much smaller structures which also can be referred to spherulites. Due to the fact that the spherulites of the clarified sample are less than 100 nm in diameter and the spectrum of visible light ranges from 400 nm to 700 nm,<sup>[109]</sup> it can be assumed that almost no refraction or scattering of visible light occurs and the sample appears transparent. In contrast to that, the neat polymer exhibits spherulites with diameters above 400 nm which scatter visible light, and hence the sample does not appear transparent.

The investigations above clearly show that the morphology of PA6 is influenced significantly by the bisurea additive. The size of the spherulites is decreased while their number is significantly increased in the presence of the bisurea additive **1**. This leads to reduced refraction and scattering resulting in a transparent, semi-crystalline polyamide 6.

## 4.2 Bisthiourea additives

Thiourea compounds are widely known for their biological activities such as antibacterial, antithyroid, hypnotic, anesthetic, antiviral, anticancer and anticonvulsant properties.<sup>[110–116]</sup> Moreover, in recent years plenty of studies addressed thiourea derivatives as organocatalysts for non-stereoselective and stereoselective applications in organic synthesis<sup>[117–121]</sup> or as corrosion inhibitors for metal surfaces.<sup>[122]</sup> Besides thiourea derivatives, also bisthiourea compounds attracted great attention. They are applicable as chiral solvating agents for NMR spectroscopy,<sup>[123,124]</sup> organocatalysts<sup>[125]</sup> or as non-linear optical materials,<sup>[126,127]</sup> to name just a few examples.

Bisthioureas exhibit a quite similar structural motif to bisurea derivatives. Merely the carbonyl oxygens are substituted by sulphur atoms. Thiourea and bisthiourea derivatives, for instance, have a reputation for the formation of intra- and intermolecular hydrogen bonds of the nitrogen protons to sulfur atoms.<sup>[111,128,129]</sup> The interactions between the molecules enable the formation of nano-objects via self-assembly.<sup>[130]</sup> The surface of these nano objects can be appropriate for inducing polymer nucleation.

Equally to the bisurea derivatives, bisthiourea derivatives might have the ability to nucleate and possibly clarify PA6. So far, there is no evidence in the literature referring bisthioureas as nucleating or clarifying agents for PA6. That is why several bisthiourea compounds are investigated in the following to examine their potential as polymer additives for PA6 compared to the similar bisurea additives. Therefore, several bisthiourea derivatives have been synthesized consisting of a central unit, two urea linkages, which are responsible for hydrogen bonding, and peripheral substituents. The detailed functions of each group were explained in frame of the introduction of this chapter. The schematic structure of linear bisthioureas is presented in Figure 53.

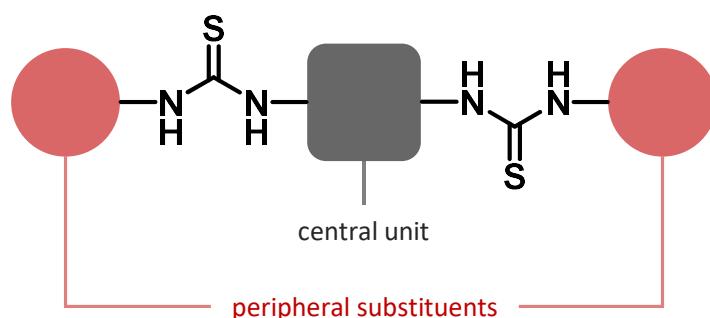


Figure 53. Schematic structure of a linear bisthiourea molecule consisting of a central unit, two thiourea linkages and peripheral substituents.

The following chapter deals with the synthesis, characterization and subsequent investigations about thermal stability, nucleation efficiency and clarification of four bithiourea derivatives as polymer additives for PA6. Furthermore, the influence of nucleation on the morphology, crystal modification and degree of crystallinity is evaluated.

## 4.2.1 Synthesis and characterization of bithioureas

In the frame of this work, symmetric bithiourea derivatives were synthesized based on 1,4-substituted *trans*-cyclohexane central units. The synthesized compounds were characterized using  $^1\text{H-NMR}$  spectroscopy, mass spectrometry and thermogravimetric analysis. A summary of the characterization data for each compound is given in the experimental section in chapter 8.3 of this thesis.

*Synthesis*

The bithiourea derivatives were synthesized via an addition reaction of commercially available *trans*-1,4-diaminocyclohexane and the corresponding thioisocyanates in dry THF under dry and inert conditions. Figure 54 presents the reaction pathway.

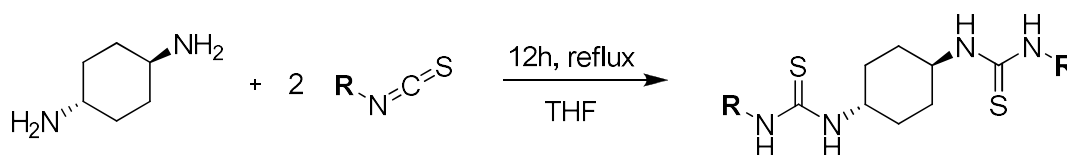
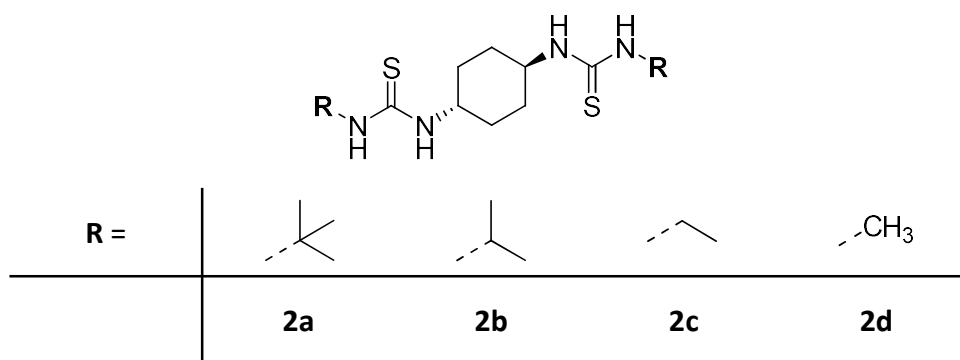


Figure 54. Synthetic route to *trans*-1,4-cyclohexyl-bithiourea derivatives starting from *trans*-1,4-diaminocyclohexane.

The following *trans*-1,4-cyclohexyl-bithiourea derivatives were synthesized:



### NMR characterization

As an example, the results of the spectroscopic characterization of the bithiourea **2a** will be discussed. The spectroscopic data of all synthesized bithiourea compounds are summarized in the experimental section.

The  $^1\text{H-NMR}$  spectrum of 1,1'-(*trans*-1,4-cyclohexane)bis(3-*tert*-butylthiourea) **2a** measured in dimethyl sulfoxide (DMSO) is shown in Figure 55. All signals could be clearly assigned to the corresponding protons. The equatorial and axial protons of the cyclohexane core could be referred to the signals **1** at 1.1 ppm and 1.95 ppm. The signal of the CH-group **2** is located at 3.95 ppm and the methyl groups **5** are assigned to 1.45 ppm. The N-H protons of the thiourea groups **3** and **4** are dedicated to the signals in the range of 6.95 to 7.05 ppm.

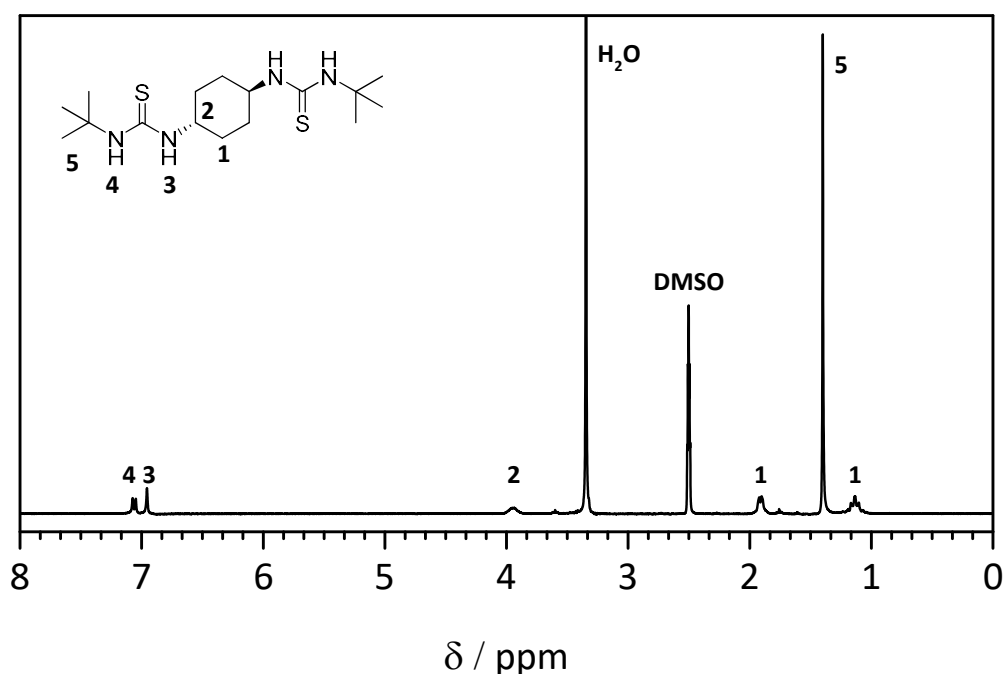


Figure 55.  $^1\text{H-NMR}$  spectrum of **2a** ( $(\text{CD}_3)_2\text{SO}$ ).

## 4.2.2 Thermal properties of bithioureas

The thermal properties of the bithiourea derivatives were simultaneously determined by means of combined thermogravimetric (TGA) and differential thermal analysis (DTA).

TGA measurements of the dried bithioureas were performed between 30 °C and 700 °C with a heating rate of 10 K/min under nitrogen atmosphere. Figure 56 shows the thermogravimetric analysis (solid lines) and simultaneous thermal analysis (dotted lines) of all synthesized bithiourea compounds.

It clearly shows up that no melting endotherms, but sublimation with subsequent thermal decomposition of all bithiourea derivatives occur. At higher temperatures sublimation and thermal degradation interfere and residual weights are the result. Compounds **2a** and **2d** exhibit a weight loss of 5% at around 240 °C, whereas compounds **2b** and **2c** are more stable with 5% weight loss above 265 °C. For compounds **2a**, **2b** and **2c** decomposition starts around 300 °C indicated by a kink of the TGA curve. Compound **2d** seems to sublime without decomposition which can be explained by the straight drop of the TGA curve to a weight loss of nearly 100%.

Table 14 summarizes the results from TGA/DTA measurements. All bithiourea compounds are thermally stable above 240 °C, and hence suitable for the additivation of PA6. Furthermore, no correlation between varying substituents and thermal stability could be determined.

Table 14. Investigated bithioureas, their melting temperatures  $T_m$  (DTA) and temperatures at 5% weight loss  $T_{-5 \text{ wt\%}}$  (TGA, N<sub>2</sub> atmosphere, 10 K/min).

Compound	$T_m$ [°C]	$T_{-5 \text{ wt\%}}$ [°C]
<b>2a</b>	sublimation	241
<b>2b</b>	sublimation	269
<b>2c</b>	sublimation	265
<b>2d</b>	sublimation	242

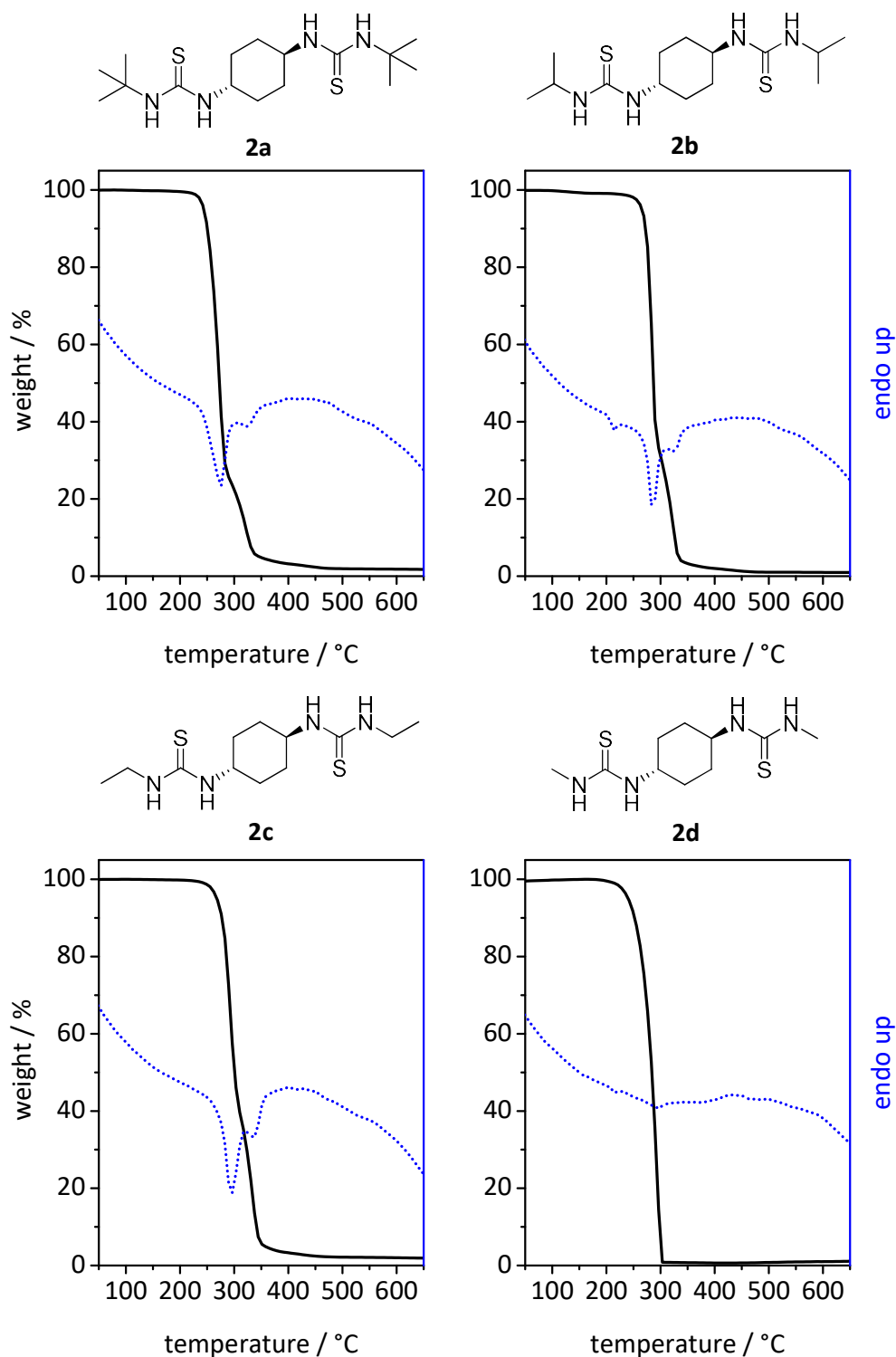


Figure 56. Thermogravimetric (solid lines) and simultaneous differential thermal analysis (dashed lines) of investigated bistioureas, measured under nitrogen atmosphere at a heating rate of 10 K/min.

#### 4.2.3 Nucleation and optical properties of PA6

As mentioned above, the nucleation efficiency of supramolecular additives depends on the individual chemical structure, their solubility and self-assembly ability in the polymer melt. Nucleating agents provide surfaces which act as nucleation sites for epitaxial growth of the polymer. In addition, the additive concentration in the polymer melt has a strong influence on the efficiency of an additive. The optical properties of semi-crystalline polymers are governed by light scattered at the interfaces of the crystalline and amorphous phases of a polymer. By adding specific additives, the spherulite size of those polymers can be decreased and the amount of scattered light reduced which can lead to improved optical properties. These additive are called “clarifiers” and are a subcategory of nucleating agents. In the following, the influence of the bistiourea derivatives on the polymer crystallization temperature and the optical properties of PA6 will be discussed in detail. The additives were compounded at 245 °C and investigated in concentrations from 1.5 wt% to 0.1 wt%. The different concentrations were prepared by diluting the initial additive concentration of 1.5 wt% with a mixture of the initial PA6/additive powder blend and neat PA6, yielding the following dilution series: 1.5 wt%, 1.3 wt%, 1.0 wt%, 0.8 wt%, 0.6 wt%, 0.4 wt%, 0.2 wt% and 0.1 wt%. The preparation steps and initial weights for a concentration series are explained and listed in chapter 4.1.2. Optical properties were measured on injection molded platelets with a thickness of 1.1 mm. To study the crystallization behavior of the compounds, DSC measurements were performed and the polymer crystallization temperatures were obtained from the exothermic minimum of the second cooling curves. Figure 57 shows exemplarily the DSC cooling curves of neat PA6 and PA6 comprising 1.0 wt% bistiourea **2d**. The addition of the bistiourea additive leads to an increase of the crystallization temperature due to nucleation at temperatures above the initial crystallization temperature of the reference. The polymer crystallization temperature of the neat polymer is 186 °C and for the additivated polymer 191 °C. The nucleation efficiency for 1.0 wt% bistiourea **2d** is 56% and was calculated by the following equation:

$$NE(\%) = \left( \frac{T_{c(\text{additive})} - T_{c(\text{reference})}}{T_{c(\text{maximum})} - T_{c(\text{reference})}} \right) \cdot 100\% = \left( \frac{191\text{ }^{\circ}\text{C} - 186\text{ }^{\circ}\text{C}}{195\text{ }^{\circ}\text{C} - 186\text{ }^{\circ}\text{C}} \right) \cdot 100\% = 56\% \quad (7)$$



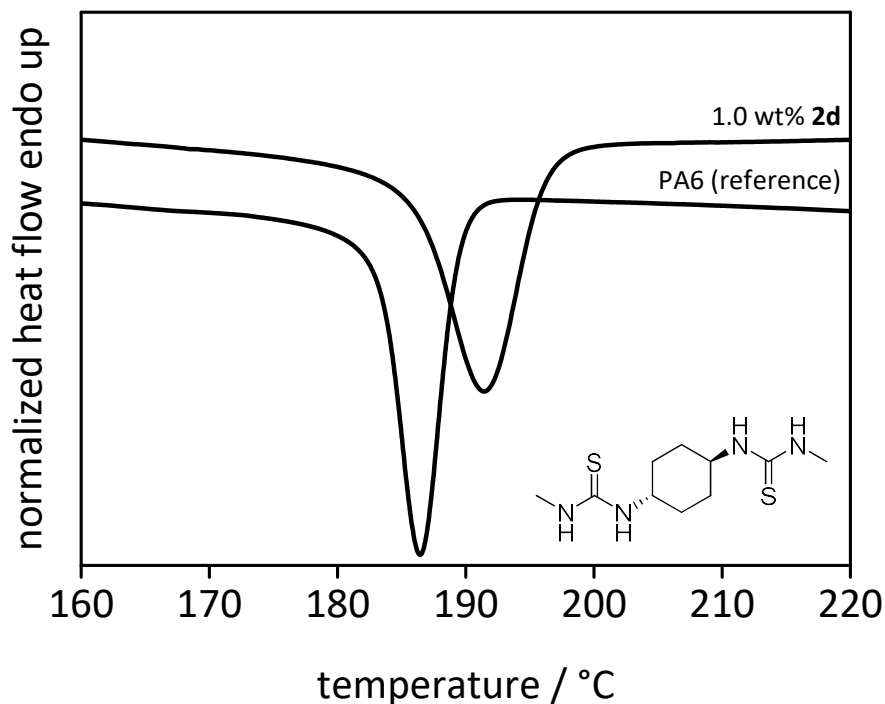


Figure 57. Differential scanning exotherms of neat PA6 and PA6 comprising 1.0 wt% bistiourea **2d**. The neat polymer has a polymer crystallization temperature of 186 °C and the additivated polymer has a polymer crystallization temperature of 191 °C. Polymer melt temperature during processing: 245 °C. DSC: 10 K/min, N<sub>2</sub>.

The optical properties were measured on injection molded platelets with a thickness of 1.1 mm according to ASTM D-1003. Figure 58 demonstrates the effect of bistiourea **2a** on the visual appearance of injection molded PA6. The transparency of the additivated sample (right) was enhanced remarkably compared to neat PA6 (left). The color of the injection molding specimen changed from colorless for neat PA6 to yellowish for PA6 comprising the bistiourea compound. This effect may be referred to the yellowish sulfurous bistiourea compound, as the corresponding whitish bisurea compound **1** revealed no discoloration of PA6.

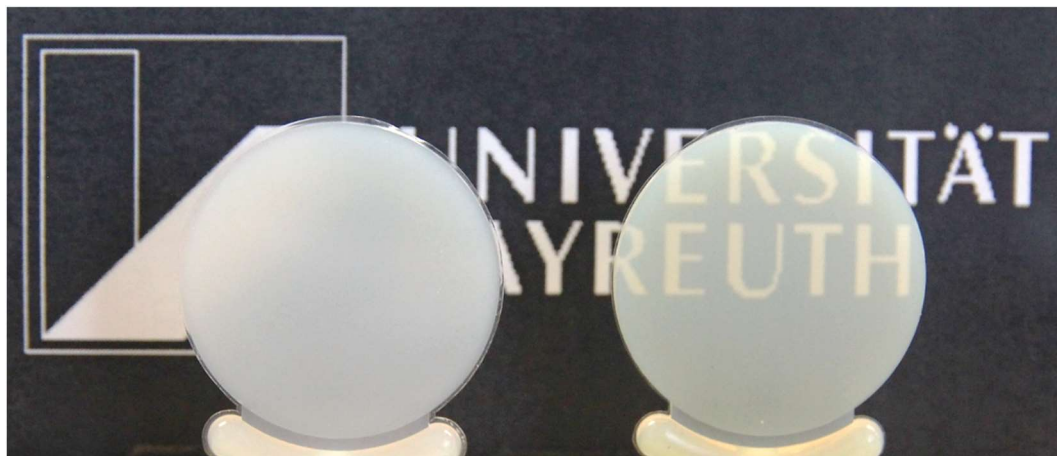


Figure 58. Effect of the addition of **2a** on the visual appearance of injection molded PA6 specimen. Left: neat PA6; Right: PA6 comprising 1.5 wt% bistiourea **2a**.

The chemical structures of the bistiourea derivatives **2a** -**2d**, their nucleation ability in PA6 and their influence on the optical properties (haze and clarity) of PA6 are compared and presented in Figure 59 and Figure 60. The substituents were varied from *tert*-butyl **2a**, isopropyl **2b**, ethyl **2c** and methyl **2d**. The blank symbols indicate the values for neat PA6. All compounds were processed at a melt temperature of 245 °C.

Figure 59 presents the nucleation and optical properties for the *tert*-butyl **2a** and isopropyl **2b** substituted bistioureas.

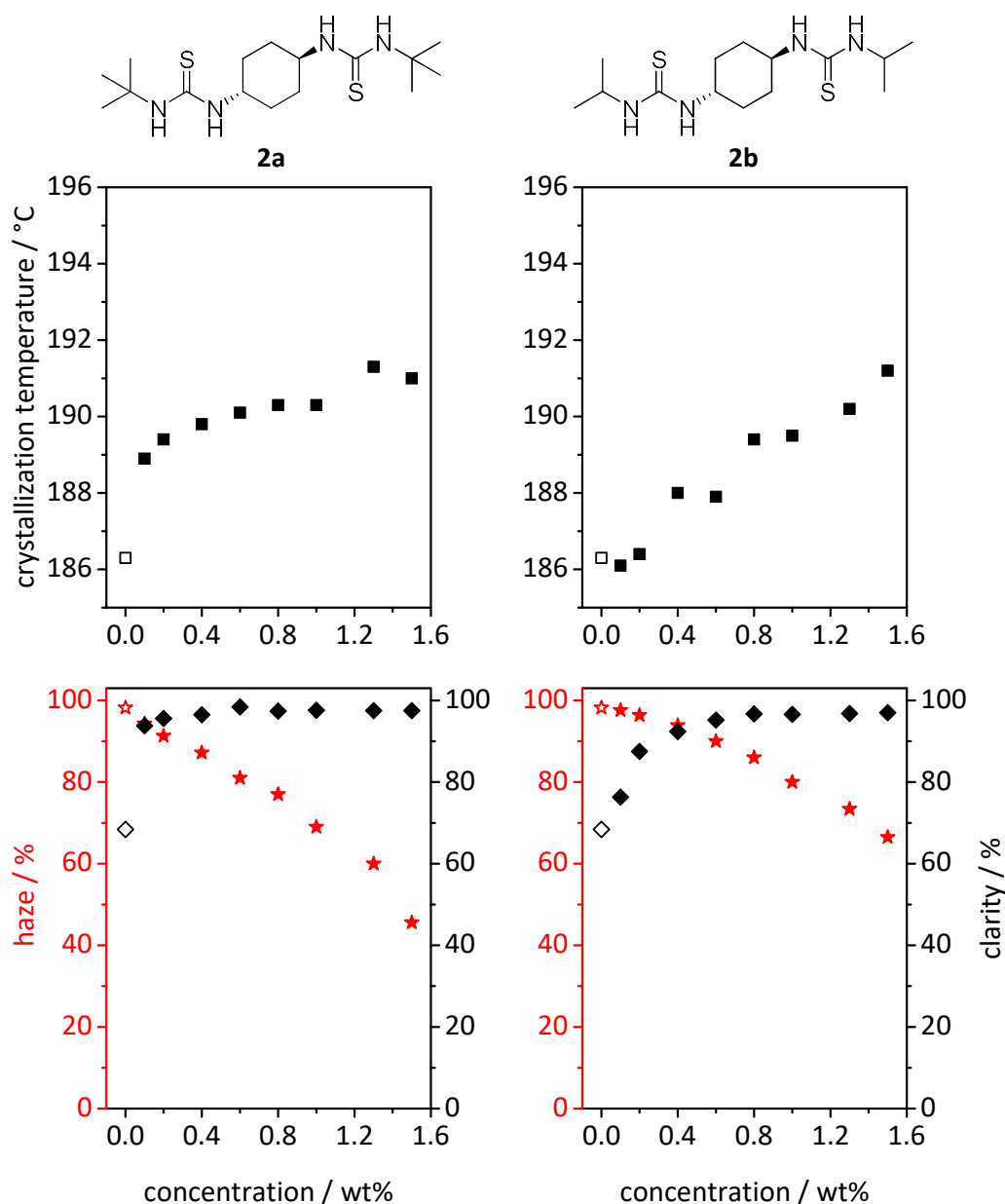


Figure 59. Polymer crystallization temperatures (top graphs) and the optical properties haze (★) and clarity (◆) (bottom graphs) of PA6 comprising the bistioureas **2a** and **2b** as function of the additive concentration. The blank symbols indicate the values of the neat polymer. DSC heating and cooling rate: 10 K/min.

Both bistioureas showed nucleation efficiencies of up to 60% at additive concentrations above 1.0 wt%. Compound **2a** exhibits quite high nucleation efficiencies even at low additive concentrations compared to bistiourea **2b**. A nucleation efficiency of 33% at an additive concentration of 0.1 wt% was reached for **2a**, whereas compound **2b** showed no increase of the polymer crystallization temperature at low additive concentrations. Both compounds showed a significant enhancement of the optical properties with increasing additive concentration. An almost linear decrease of the haze values with increasing additive concentration was observed for both compounds. Bistiourea **2a** reduced the haze

value from nearly 100% to 45% and **2b** induced a reduction of the haze value to 65% at an additive concentration of 1.5 wt%. Clarity values increased for both compounds even at low concentrations to almost 100%.

Figure 60 presents the nucleation and optical properties for the ethyl **2c** and methyl **2d** substituted bistioureas.

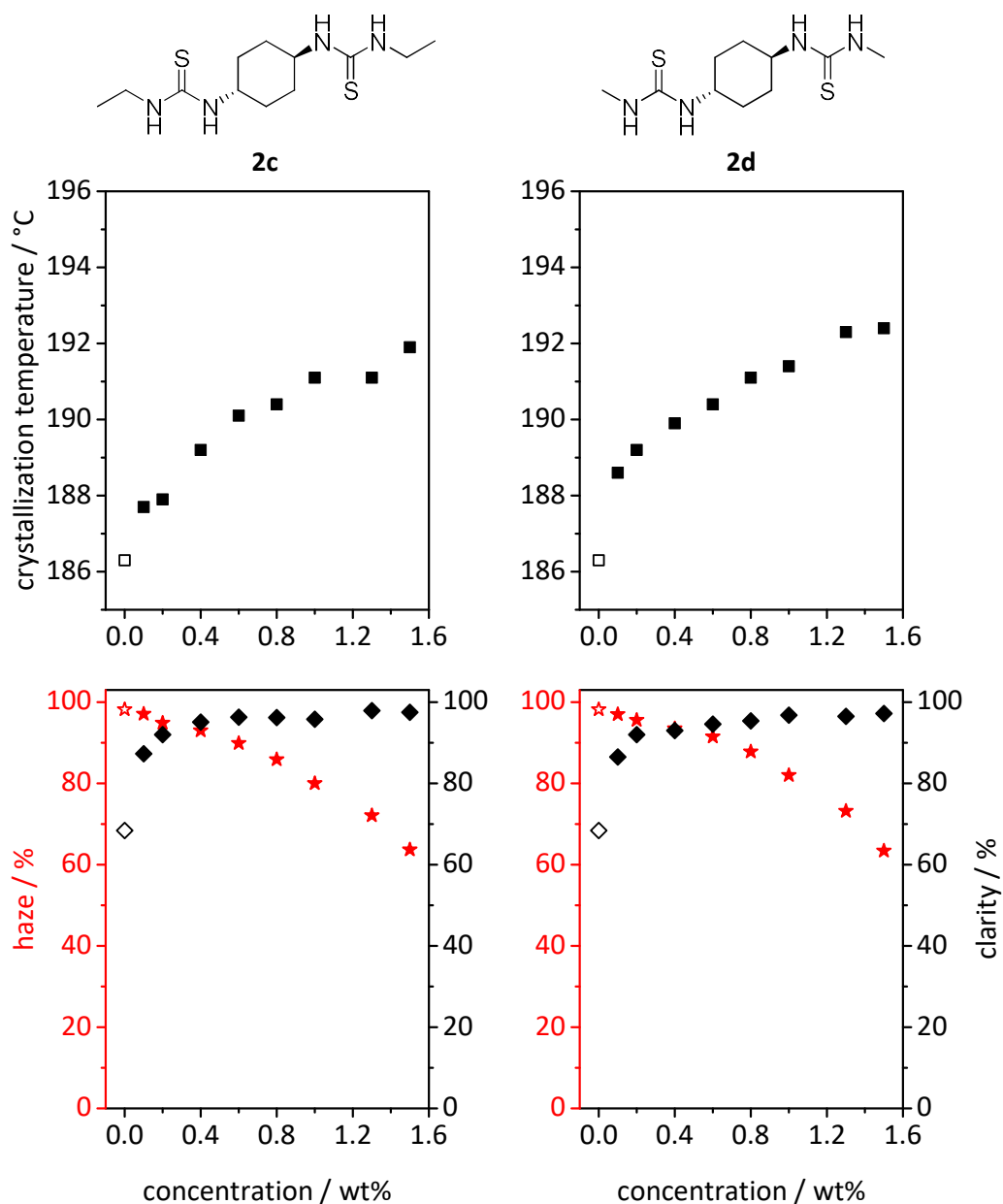


Figure 60. Polymer crystallization temperatures (top graphs) and the optical properties haze (★) and clarity (◆) (bottom graphs) of PA6 comprising the bistioureas **2c** and **2d** as function of the additive concentration. The blank symbols indicate the values of the neat polymer. DSC heating and cooling rate: 10 K/min.

Both derivatives, bistiourea **2c** and **2d**, show very similar nucleation properties. The polymer crystallization temperatures increased with increasing additive concentrations.

Nucleation efficiencies above 70% at additive concentrations of 1.5 wt% were reached. Both compounds showed a significant enhancement of the optical properties with increasing additive concentration. An almost linear decrease of the haze values with increasing additive concentration was observed for both compounds. A reduction of haze values of almost 100% to nearly 60% at additive concentrations of 1.5 wt% was realized for both additives. Furthermore, clarity values increased for both compounds even at low concentrations to almost 100%.

In order to establish a connection between the measured values haze and clarity and the macroscopic injection molding samples, Figure 61 illustrates the optical effect of the addition of **2a** on injection molded platelets of PA6. With increasing additive concentration a significant enhancement of the optical properties can be observed leading to a transparent sample with a haze value around 45%.

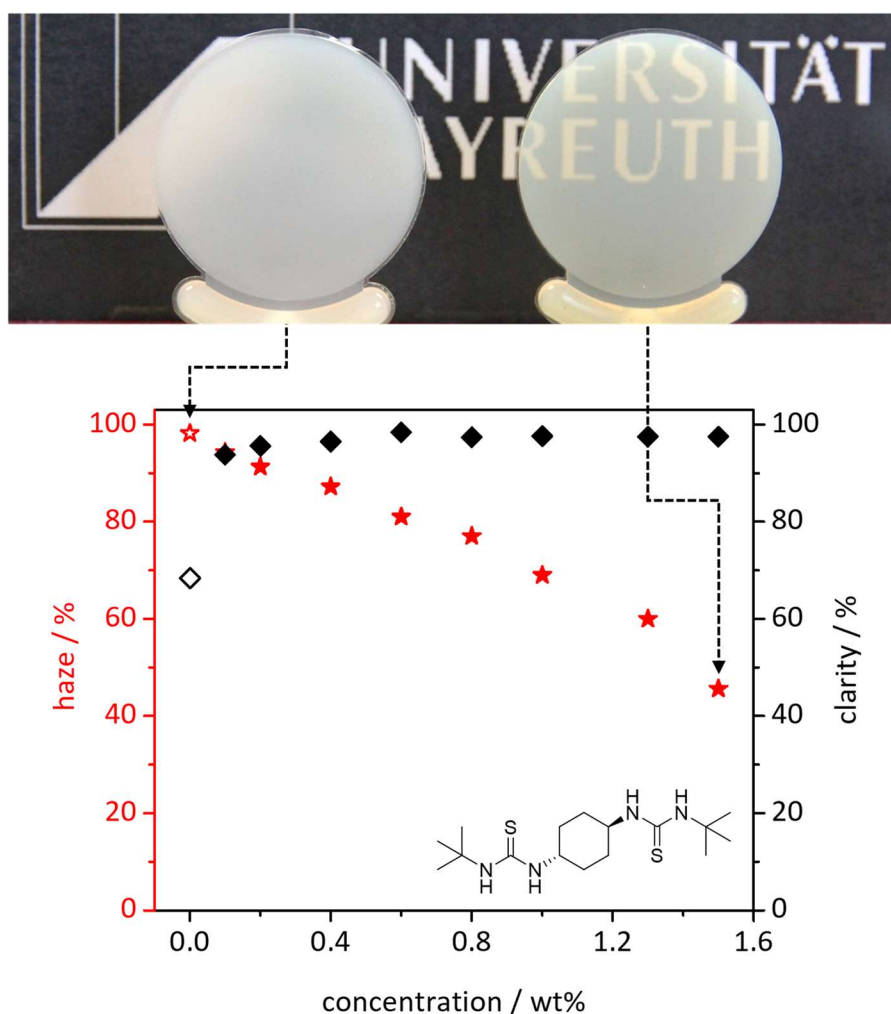


Figure 61. Emblem of the University of Bayreuth viewed through injection molded platelets of PA6 (thickness 1.1 mm) containing 0.0 wt% and 1.5 wt% of **2a** (top).

#### 4.2.4 Morphology of injection molded PA6 samples

As already described in chapter 4.1 the morphology of polymers is strongly influenced by nucleating agents. In the following, the influence of the *tert*-butyl substituted bistiourea **2a** on the morphology of PA6 is investigated. Therefore, injection molded samples with a thickness of 1.1 mm were cut parallel to the direction of injection (flow direction) to obtain thin sections with a thickness of 10  $\mu\text{m}$ . These thin sections were placed between two object slides and examined by polarized light microscopy.

Figure 62 presents the thin sections of neat PA6 (left) and PA6 comprising 1.5 wt% bistiourea **2a** (right). The images were merged from two separate pictures to present the complete cross section of the injection molding sample. The haze values of the samples are quoted in the right top corner of the images.

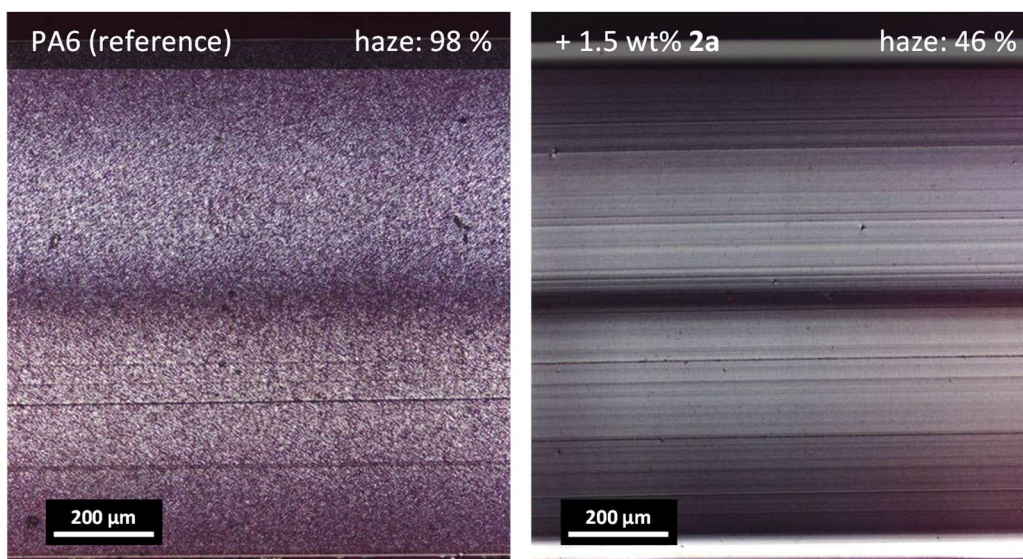


Figure 62. Thin sections of injection molded samples (thickness 1.1 mm) parallel to the flow direction and the corresponding haze values of neat PA6 (left) and PA6 comprising 1.5 wt% **2a**. The images presented consist of two separate pictures taken between crossed polarizers.

Polyamides mostly crystallize in spherulitic structures. These structures are relatively fine and homogeneous, and hence a determination of specific values of the crystallite size or amount by polarized light microscopy is unusual. Due to extremely fast cooling rates during injection molding these structures get even much smaller and more homogenous.<sup>[2]</sup>

Figure 62 presents the images of the spherulitic structures of neat PA6 (left) and PA6 comprising 1.5 wt% bistiourea **2a** (right). Both samples exhibit oriented skin layers and a less oriented spherulitic core region. These effects were already described in chapter 4.1.5.

The comparison of neat PA6 (left) and additivated PA6 (right) clearly shows that the spherulitic morphology was significantly influenced by the addition of the bistiourea. The spherulites become very small due to additivation so that no single crystallite can be recognized by polarized light microscopy. The haze value of this sample was reduced from 98% for neat PA6 to 46%.

In summary it was shown that bistioureas influenced the morphology of PA6 and decreased the spherulite size. Hence, the amount of scattered light is reduced leading to improved optical properties.

## 4.2.5 Crystal modification and degree of crystallinity

Polyamides can crystallize due to hydrogen bonding between amide groups. Depending on the processing conditions, three main polymorphs, the  $\alpha$ -,  $\gamma$ - and the metastable  $\beta$ -phase can occur.<sup>[2,49–51]</sup> Both, Richter et al. and Xue et al., observed a change of the crystal modification of PA6 due to bisurea additives.<sup>[14,30]</sup> Furthermore, the degree of crystallinity is a characteristic parameter for semi-crystalline polymers and can influence density, optical transparency and mechanical properties of a polymer.

Both, crystal modification and the degree of crystallinity, can be modified by nucleating agents. In the following, the influence of bistiourea additives on the crystal modification and degree of crystallinity of PA6 are determined by means of WAXS and DSC.

*Crystal modification*

In order to investigate the influence of the bistiourea derivatives on the crystal modification of PA6, WAXS measurements were conducted on 1.1 mm thick injection molding platelets with diameters of 25 mm with a Bruker D8 Advance X-ray diffractometer using  $\text{CuK}\alpha$  radiation ( $\lambda = 1.54 \text{ \AA}$ ). Data was recorded in the range of  $10\text{--}35^\circ$  (2 Theta) with a step size of  $0.025^\circ$  and a step time of 10 seconds. Figure 63 shows the WAXS patterns of injection molded specimen of neat PA6 and PA6 comprising the bistioureas **2a** – **d** all processed at  $245^\circ\text{C}$ .

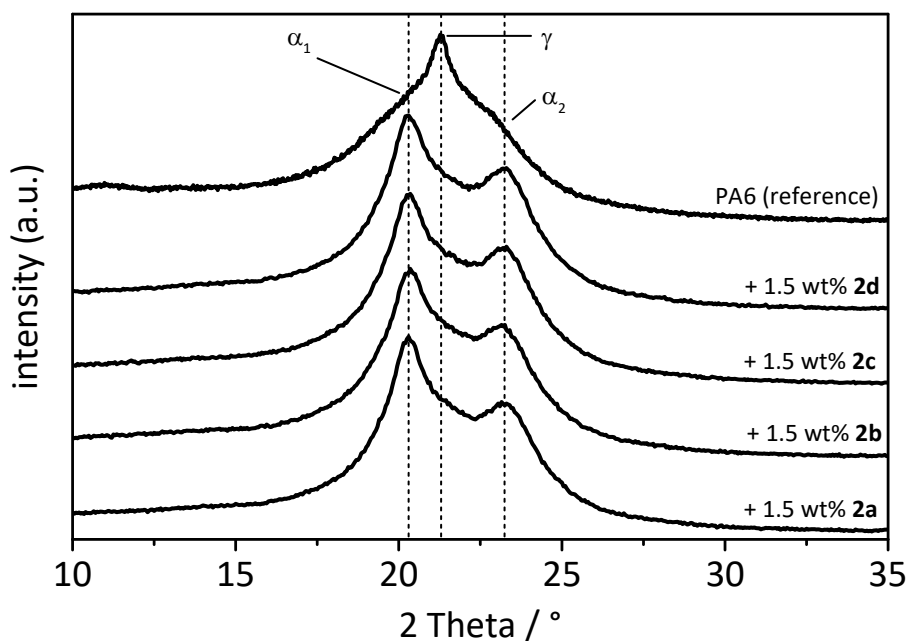


Figure 63. Diffractometer scans of neat PA6 and PA6 comprising the bistioureas **2a** – **d** with a concentration of 1.5 wt%. Measurements were conducted on 1.1 mm thick injection molding samples which were prepared under equal processing conditions at  $245^\circ\text{C}$ .



The diffractometer scans in Figure 63 show a significant distinction between neat PA6 and PA6 comprising bistiourea additives. PA6 predominantly crystallizes in the  $\gamma$ -form, whereas the additivated PA6 crystallized in the  $\alpha$ -form under equal processing conditions. It is well known that the  $\alpha$ -phase is mainly obtained from crystallization at elevated temperatures.<sup>[2]</sup> Due to the nucleation effect of the bistiourea additives, the polymer crystallization temperature was increased and thus, the polymer may tend to crystallize in the  $\alpha$ -form. A similar effect was observed by Richter et al. for bisurea additives.<sup>[14]</sup> A correlation between the chemical structures of the additives and the change of the crystal modification cannot be determined. The XRD patterns of PA6 comprising the different bistioureas look almost coincident.

Furthermore, the effect of bistiourea **2a** at different concentrations on the crystal modification of PA6 was studied and is shown in Figure 64. Even at a very low additive concentration of 0.1 wt% a significant difference of the XRD pattern compared to neat PA6 can be observed. The additive **2a** promotes the formation of  $\alpha$ -form crystals even at low concentrations and thus acts as  $\alpha$ -nucleator for PA6.

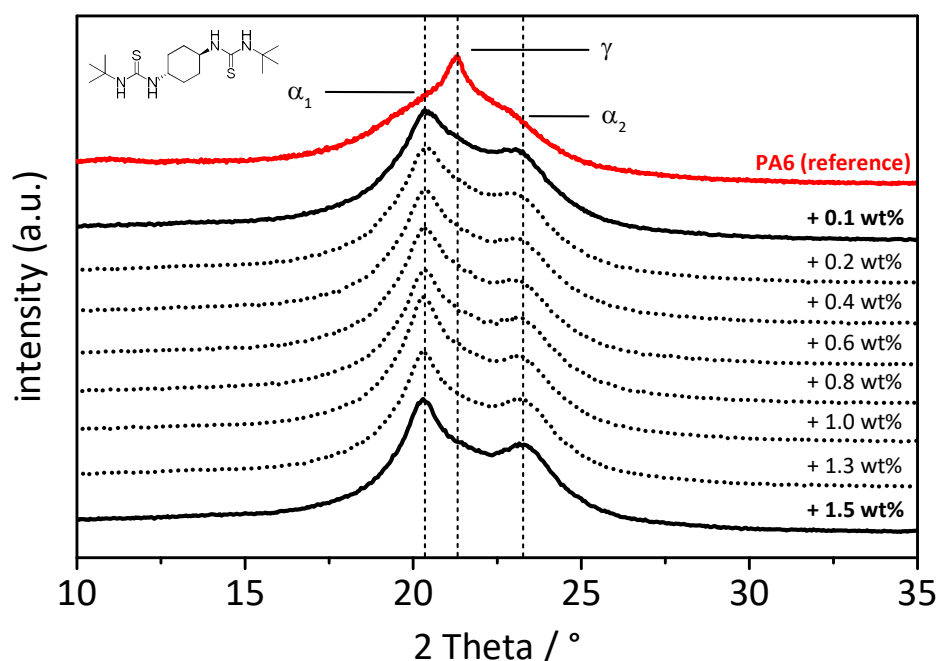


Figure 64. Diffractometer scans of PA6 comprising different concentrations of **2a**. Measurements were conducted on 1.1 mm thick injection molding samples which were prepared under same processing conditions at 245 °C.

*Degree of crystallinity*

The degrees of crystallinity of PA6 comprising bistiourea derivatives **2a** – **d** were determined using differential scanning calorimetry (DSC). For this purpose, the enthalpies of the endothermic peaks ( $\Delta H_f$ ) of the first heating scans were used. With the value of a 100% crystalline PA6 sample ( $\Delta H_{f(100\%)} = 188 \text{ J/g}$ )<sup>[57,58]</sup> the degree of crystallinity was calculated by equation 3, as already described in chapter 3.4.<sup>[38,59,60]</sup>

The degrees of crystallinity for neat PA6 and PA6 comprising 1.5 wt% bistiourea additives are summarized in Table 15. The additivation of PA6 with the investigated bistiourea compounds showed no significant change of the degree of crystallinity.

Table 15. Degrees of crystallinity of neat PA6 and PA6 comprising 1.5 wt% bistiourea additive. DSC heating and cooling rate: 10 K/min.

Sample	$\Delta H_f$ [J/g]	degree of crystallinity [%]
PA6 (reference)	65	34
+ 1.5 wt% <b>2a</b>	61	33
+ 1.5 wt% <b>2b</b>	61	33
+ 1.5 wt% <b>2c</b>	60	32
+ 1.5 wt% <b>2d</b>	61	33

In summary it was shown that the additivation of PA6 with bistioureas caused a change of the crystal modification from the  $\gamma$ - to the  $\alpha$ -phase with a consistent degree of crystallinity.

#### 4.2.6 Water absorption and mechanical properties

Polyamides crystallize due to hydrogen-bonds between the polymer chains. These hydrogen bonds can be influenced by the addition of additives. In the case of supramolecular nucleating agents the polymer crystallizes at an epitaxially appropriate surface provided by the nucleating agent. The additive stays in the crystalline phase of the polymer. This modification might lead to an influence of the polymer properties. Polyamides are known to absorb water in a certain amount, depending on the polyamide type, temperature, crystallinity and sample dimensions. By addition of additives, the affinity to absorb water might be influenced. Particularly the mechanical properties, such as the elastic modulus, are strongly governed by the amount of water.<sup>[2,131]</sup> Therefore, the influence of bithiourea **2a** on the water absorption and the mechanical properties of PA6 are studied.

##### *Water absorption*

Water absorption experiments were conducted on 1.1 mm thick injection molded platelets with diameters of 25 mm. Samples were dried for 8 days at 80 °C under vacuum. The dried samples were weighed and stored at 30 °C and 50 rh% in a thermocabinet. In the following, samples were weighed every 24 h until saturation was reached.

Figure 65 presents the water uptake of injection molded platelets of neat PA6 and PA6 comprising 1.5 wt% **2a** as function of the time stored at 30 °C and 50 rh%. In the period of the first three days an almost linear increase of water uptake up to 1.25 % for both samples was observed. With increasing storage time the process flattens and the water uptake reached a plateau after 30 days. Neat PA6 revealed a water uptake by 3.1% and PA6 comprising the nucleating agent **2a** showed a value of 3.0%.after 36 days.

All in all, in consideration of the measuring error, no significant deviations of the water absorption could be observed among neat PA6 and PA6 comprising the bithiourea **2a**.

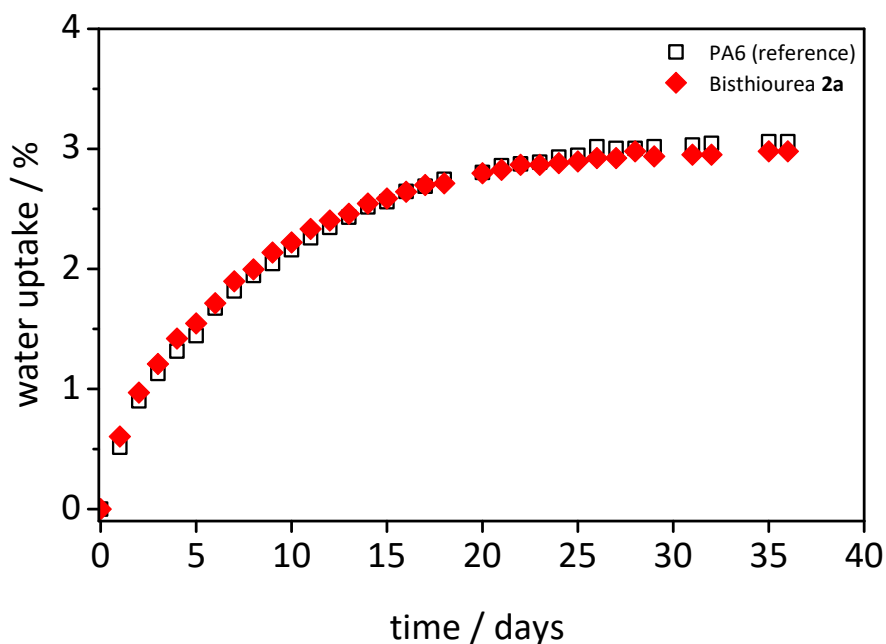


Figure 65. Water uptake of dried injection molding platelets (1.1 mm thickness; 25 mm diameter) of neat PA6 and PA6 comprising 1.5 wt% **2a** as function of the time at 30 °C at 50 rh%.

### *Mechanical properties*

Tensile tests were conducted on conditioned specimen (4 days, 70 °C, 62 %rh) by an Instron 5565 universal tester with a camera (Instron 2663-821 Advanced Video Extensometer), pneumatic clamps and a 1 kN load cell. Tensile rods with a measuring section of 30 mm x 5 mm x 2 mm were tested at an initial strain rate of 0.3 mm/s (up to 0.5% strain; video measurement) and then increased to 50.0 mm/s. The reported moduli were calculated from the initial slope between 0.15% and 0.35%. The average of at least four samples is reported. Figure 66 presents a typical stress-strain curve of a conditioned PA6 specimen with characteristic values as indicated.

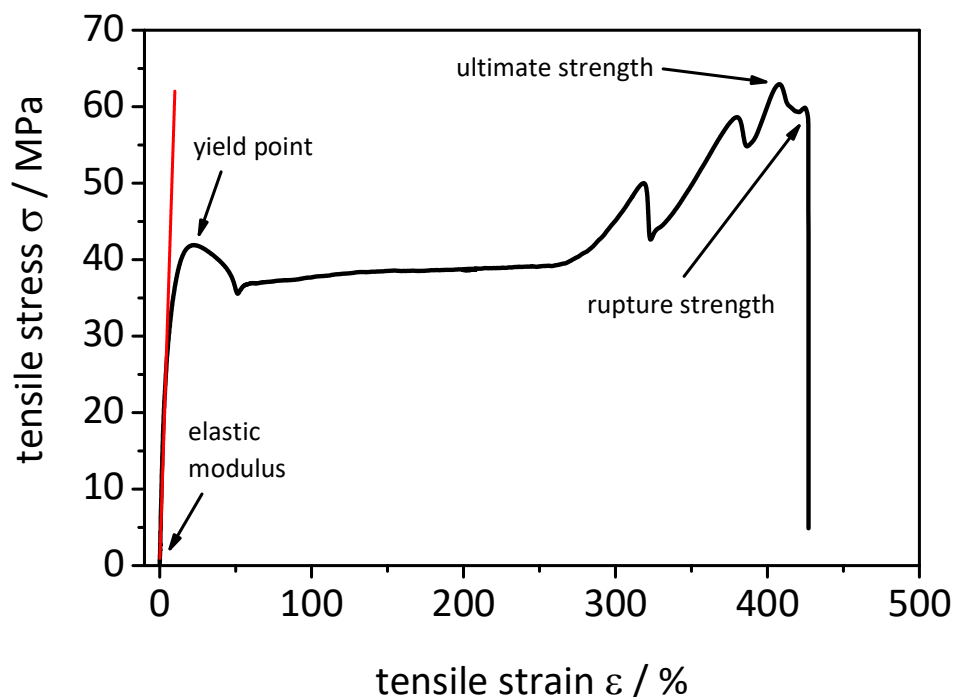


Figure 66. Typical stress-strain curve of a conditioned PA6 specimen with characteristic measurable values: Elastic modulus, yield point, ultimate strength and rupture strength.

The characteristic values for neat PA6 and PA6 comprising 1.5 wt% bistiourea **2a** are summarized in Table 16. The elastic modulus for PA6 comprising **2a** is significantly higher than for neat PA6. The values for the ultimate strength, rupture strength and elongation at break are almost in the same range for both compounds. Similar observation were made by Gabriel et al. for PA6 comprising bisurea additives.<sup>[92]</sup>

Table 16. Summary of the tensile properties of neat PA6 and PA6 comprising bistiourea **2a**. All samples were conditioned prior to the experiments. The average of at least four samples is reported.

Compound	Elastic modulus [MPa]	Ultimate strength [MPa]	Rupture strength [MPa]	Elongation at break [%]
PA6 (reference)	633 ± 25	69 ± 4	66 ± 5	499 ± 48
+ 1.5 wt% bistiourea <b>2a</b>	717 ± 12	70 ± 2	69 ± 1	486 ± 23

### 4.3 Summary

In the first part of this chapter the influence of elevated processing conditions on the thermal stability of a bisurea compound, and hence the nucleation and clarification efficiency in PA6 was investigated in detail.

An enhancement of almost all parameters listed in Table 17 was realized due to the bisurea additive at a processing temperature of 245 °C. However, it was observed that increasing melt temperatures during processing induced a slight decrease of the haze value. GC-MS investigations revealed thermal degradation of the bisurea additive **1** at elevated temperatures. Based on these investigations, processing temperatures around 245 °C turned out to be best to clarify PA6 without an increase of the haze value. Additionally, for the first time, the influence of a nucleating agent on the spherulitic morphology of PA6 was observed at the nanoscale by scanning electron microscopy of thin films.

Table 17 summarizes characteristic parameters of neat PA6 and PA6 comprising 1.0 wt% bisurea **1** processed at 245 °C and 283 °C.

Table 17. Summary of characteristic values of neat PA6 and PA6 comprising 1.0 wt% bisurea **1** processed at a melt temperature of 245 °C and 283 °C.

	PA6 (reference)	+ 1.0 wt% bisurea <b>1</b> @ 245 °C	+ 1.0 wt% bisurea <b>1</b> @ 283 °C
Melting temperature	218 °C	218 °C	218 °C
Crystallization temp.	186 °C	194 °C	192 °C
Nucleation efficiency	-	89%	67%
Haze	98%	18%	46%
Clarity	68%	98%	97%
Degree of crystallinity	34%	33%	33%

Furthermore, a new class of clarifying agents for polyamides was developed. The concept and structural motif of bisurea compounds was transferred to a related class of bistioureas. Four bistiourea derivatives were synthesized, characterized and investigated with regard to their nucleation and clarification ability in PA6. Nucleation efficiencies up to

70% at concentrations of 1.5 wt% were achieved. Additionally, an enhancement of the optical properties (haze and clarity) was achieved by all investigated compounds. For example, 1,1'-(trans-1,4-cyclohexane)bis(3-tert-butylthiourea) **2a** at an concentration of 1.5 wt% gained a reduction of the haze value from 98% to 45% for a 1.1 mm thick sample. Furthermore, morphology investigations showed a significant decrease of the spherulite size and the initial  $\gamma$ -modification transferred to the  $\alpha$ -form for PA6 comprising these bithiourea additives. Mechanical investigations revealed an increase of the elastic modulus from 633 MPa to 717 MPa for PA6 comprising 1,1'-(trans-1,4-cyclohexane)bis(3-tert-butylthiourea) **2a**.

Table 18 summarizes characteristic parameters of neat PA6 and PA6 comprising the investigated bithiourea additives.

Table 18. Summary of properties of neat PA6 and PA6 comprising 1.5 wt% of the bithioureas **2a** – **2d**. Melt temperature during processing for all data was 245 °C.

	PA6 (reference)	<b>2a</b>	<b>2b</b>	<b>2c</b>	<b>2d</b>
Melting temperature / °C	218	217	218	217	217
Crystallization temp. / °C	186	191	191	192	192
Nucleation efficiency / %	-	56	56	67	67
Haze / %	98	46	67	64	63
Clarity / %	68	98	97	98	97
Degree of crystallinity / %	34	33	33	32	33
Main crystal modification	$\gamma$	$\alpha$	$\alpha$	$\alpha$	$\alpha$
Elastic modulus / MPa	633 ± 25	717 ± 12	-	-	-
Ultimate strength / MPa	69 ± 4	70 ± 2	-	-	-
Rupture strength / MPa	66 ± 5	69 ± 1	-	-	-
Elongation at break / %	499 ± 48	486 ± 23	-	-	-





## 5 Anti-nucleation of polyamides

Polyamides are characterized by a large number of beneficial properties, such as excellent mechanical properties, high temperature and chemical resistance and good processability by extrusion and injection molding, which guarantee them a secure market position in the engineering thermoplastics sector. These basic properties of the polymer can be influenced and improved by the addition of fillers or additives.<sup>[2,132]</sup>

As already described in chapter 4, nucleating agents are commonly used to improve the crystallization process of polymers. Nucleating agents accelerate the generation of the crystalline nucleus, enhancing the crystallization rate, making the crystal homogeneously fine, and consequently increasing the crystallization temperature of the polymer. For instance, nucleating agents for polyamides usually include inorganic particles, organic salts and polymeric nucleating agents, all being insoluble in the polymer melt, and hence have to be finely dispersed during processing.<sup>[2]</sup>

However, not only nucleation of polymers is a way to influence the crystallization behavior of polymers. The opposite of nucleation is so-called “*anti-nucleation*”. In contrast to nucleating agents, anti-nucleating agents decrease the polymer crystallization temperature. Important is, that anti-nucleation agents should not sacrifice other polymer properties such as melting temperature or degree of crystallinity. Those anti-nucleating agents are of growing interest because of applications requiring lower polymer crystallization temperatures than the neat polymer. For example, the control of the polymer crystallization is of particular significance to provide a specific influence on properties such as shrinkage or impact strength.<sup>[15,132]</sup> Particularly for film blowing, polyamides with lower crystallization temperatures and enhanced fluidity than conventional polyamide are necessary to extend the processing time and ensure flexibility of the polymer before the film reaches too high degrees of crystallization.<sup>[16,132]</sup> Additionally, good fluidity and molding precision were observed due to the application of anti-nucleating agents.<sup>[11,132]</sup> Furthermore, anti-nucleating agents are able to improve the surface gloss and texture of injection molded products, and hence unique selling properties of reinforced polyamides with high quality surfaces for visible parts in automotive and furniture industry can be reached.<sup>[11,16,17]</sup>

To classify a nucleating agent, the nucleation efficiency of an additive can be calculated as already described in chapter 4. In the case of anti-nucleation there is no possibility to calculate an anti-nucleation efficiency, because it is not feasible to evaluate the lowest polymer crystallization temperature which might be reached by a perfect anti-nucleation agent. Consequently, there is no reference to calculate an exact efficiency for a certain anti-nucleating agent. However, it is merely possible to calculate the shift of the polymer crystallization temperature of an additivated sample  $T_{c(\text{additive})}$  compared to the polymer crystallization temperature  $T_{c(\text{reference})}$  of the neat polymer. With the help of following equation a value  $\Delta T_c$  can be calculated:

$$\Delta T_c = T_{c(\text{additive})} - T_{c(\text{reference})} \quad (8)$$

$\Delta T_c$  can attain a positive, a negative, or a zero value. A zero value shows neither nucleation nor anti-nucleation. A positive value indicates nucleation, whereas a negative value signals anti-nucleation. Since the DSC has an error of  $\pm 0.5$  °C, anti-nucleation is assumed not before a  $T_c$  shift by a minimum of 2 °C. With the help of these values a simple method is established to draw a comparison between crystallization temperatures of additivated and neat polymer samples. Figure 67 shows the graphical presentation of calculation of  $\Delta T_c$  by DSC thermograms for neat (black) and anti-nucleated (red) PA6.

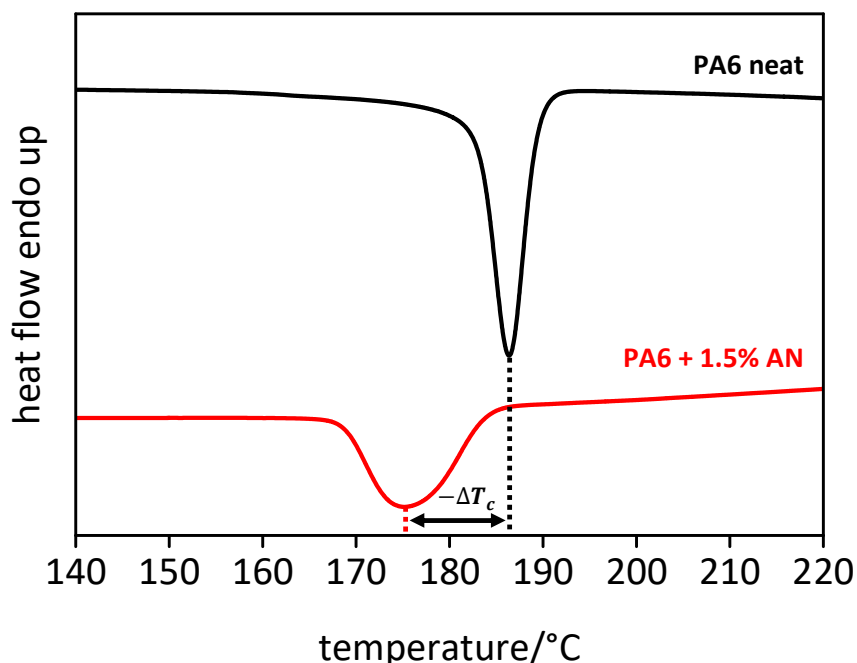


Figure 67. DSC cooling curves of neat PA6 (black) and anti-nucleated PA6 (red). The polymer crystallization temperature is shifted to lower temperatures for anti-nucleated PA6. Heating and cooling rate: 10 K/min.

Up to now, the phenomenon “anti-nucleation of polymers” is only described for polyamides and only a few scientific publications can be found. The first evidence of anti-nucleation in the literature was reported by Valenti et al. in 1973. They described that inorganic salts, such as LiBr, LiCl or KCl, continuously depressed the melting temperature of PA6 with an increasing salt content and drastically slowed down the crystallization rate.<sup>[133]</sup> A few years later, Siegmann et al. also observed a strong depression of the polymer melting temperature, a retardation of the crystallization rate and decrease of the polymer crystallization temperature of PA6 with increasing content of metal halides.<sup>[31,32]</sup> However, all of these investigations showed a significant decrease of the polymer melting temperature.

In 2002 Hayashi et al. patented Nigrosine as nucleation suppressor for polyamides which is commercially applied since then. The addition of the dye lowers the polymer crystallization temperature with substantially no shift in the melting temperature and improves the fluidity and surface gloss of polyamides.<sup>[11,19,134]</sup> Moreover, Sukata et al. discusses the thermal behavior of PA66 containing Nigrosine on the basis of differential scanning calorimetry (DSC), dynamic mechanical analysis (DMA) and X-ray diffraction (XRD) studies. They also observed that the addition of Nigrosine reduced the crystallization rate and the crystallization temperature of PA66 and additionally increased the glass transition temperature.<sup>[19]</sup> Up to now, Nigrosine represents the only commercially applied anti-nucleating agent. Therefore, the importance of Nigrosine and its properties will be discussed in chapter 5.1 in detail.

Furthermore, Takeuchi et al. patented about 200 polycyclic structures wherein three or more 4-membered or higher cyclic structures are condensed. Those derivatives exhibit anti-nucleation effects in PA66. Besides lowering the crystallization temperature of PA66, morphology investigations were conducted. Here, an increasing spherulite size and decreasing number of spherulites with increasing additive concentration compared to the neat polymer could be observed. Figure 68 presents a exemplarily selection of these polycyclic structures.<sup>[15]</sup>

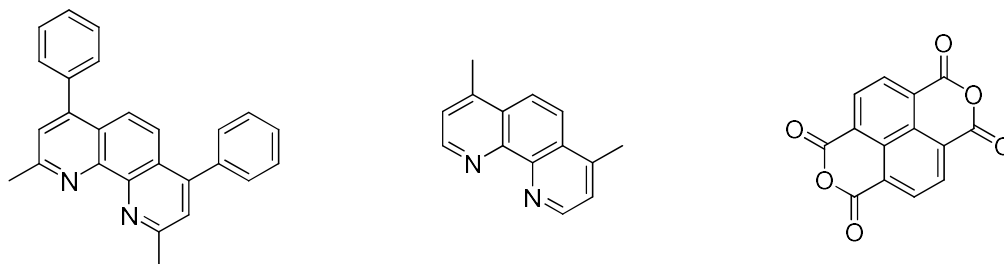


Figure 68. Polycyclic structures patented by Takeuchi et al. as nucleating-effect-suppressor for polyamides.<sup>[15]</sup>

Also Lin et al. described that some metal complex acid dyes reduced the crystallization temperature of PA66 with substantially no decrease of the melting temperature, and Topoulos et al. reported that tripentaerythritol slows down crystallization rates of polyamides.<sup>[16,33]</sup> Furthermore, McAdam and Kamal investigated PA6 comprising clay and observed a reduction of the crystallization rate of the nanocomposite due to hindered chain mobility of the polymer chains.<sup>[135,136]</sup>

Besides additives as small molecules, several publications and patents describe a reduction of the polymer crystallization temperature of polyamides by blending with other polymers such as polystyrene, polyoxymethylene or acrylonitrile butadiene styrene.<sup>[137–146]</sup>

According to the current state of the art, a prediction of the anti-nucleation ability based on the molecular structure of an additive is not possible yet. Therefore, a systematical approach is adopted by exploring Nigrosine and further anti-nucleating agents known from the literature to understand the almost unexplored effect of anti-nucleation. Therefore, structural components which are responsible for the anti-nucleation effect are deduced and the development of new anti-nucleating agents is carried out. Here, it is particularly important that no other polymer properties, such as i.e. degree of crystallinity, crystal modification or polymer melting temperature, are affected.

### 5.1 Nigrosine as commercial anti-nucleating agent for PA6

Nigrosine is one of the oldest synthetic dyes and was discovered by Coupier in 1867.<sup>[147]</sup> Nigrosine is known to reduce the polymer crystallization temperature of polyamides since several years now.<sup>[19,148]</sup> This effect was patented by Hayashi et al. in 2002.<sup>[11,134]</sup> Due to the fact that only a small number of compounds are known to act as anti-nucleating agents for semi-crystalline polymers, up to now, Nigrosine is the leading product and the only commercially applied anti-nucleating agent.

Hence, just a few patents can be found dealing with the anti-nucleation of PA66 and particularly Nigrosine.<sup>[11,134,149]</sup> Moreover, merely one scientific publication can be found discussing the influence of Nigrosine on the thermal behavior of PA66 in detail.<sup>[19]</sup> No further publications are available approaching the anti-nucleation of PA6 and Nigrosine.

Therefore, in the following chapter the anti-nucleation effect of Nigrosine on the thermal behavior of PA6 is investigated in detail. Hence, Nigrosine can serve as a model compound to examine the almost unexplored mechanism of the anti-nucleation of semi-crystalline polyamides. Besides the properties of neat Nigrosine and its anti-nucleation effect on PA6, the influence of Nigrosine on the morphology, crystal structure, degree of crystallinity and glass transition temperature of PA6 is investigated for the first time. Understanding the way of functioning of an anti-nucleating agent is the first step towards developing new compounds capable of reducing the polymer crystallization temperature.

5.1.1 Properties of Nigrosine

Nigrosines are black or dark blue powders which represent extremely complex structural mixtures of phenazine dyes.<sup>[147]</sup> After literature search, three main types of Nigrosine could be figured out. These types are different in terms of their chemical structure and consequently their solubility. Figure 69 presents the chemical structures of the main components of water soluble (Acid Black 2), alcohol soluble (Solvent Black 5) and oil soluble (Solvent Black 7) Nigrosines.<sup>[150-153]</sup>

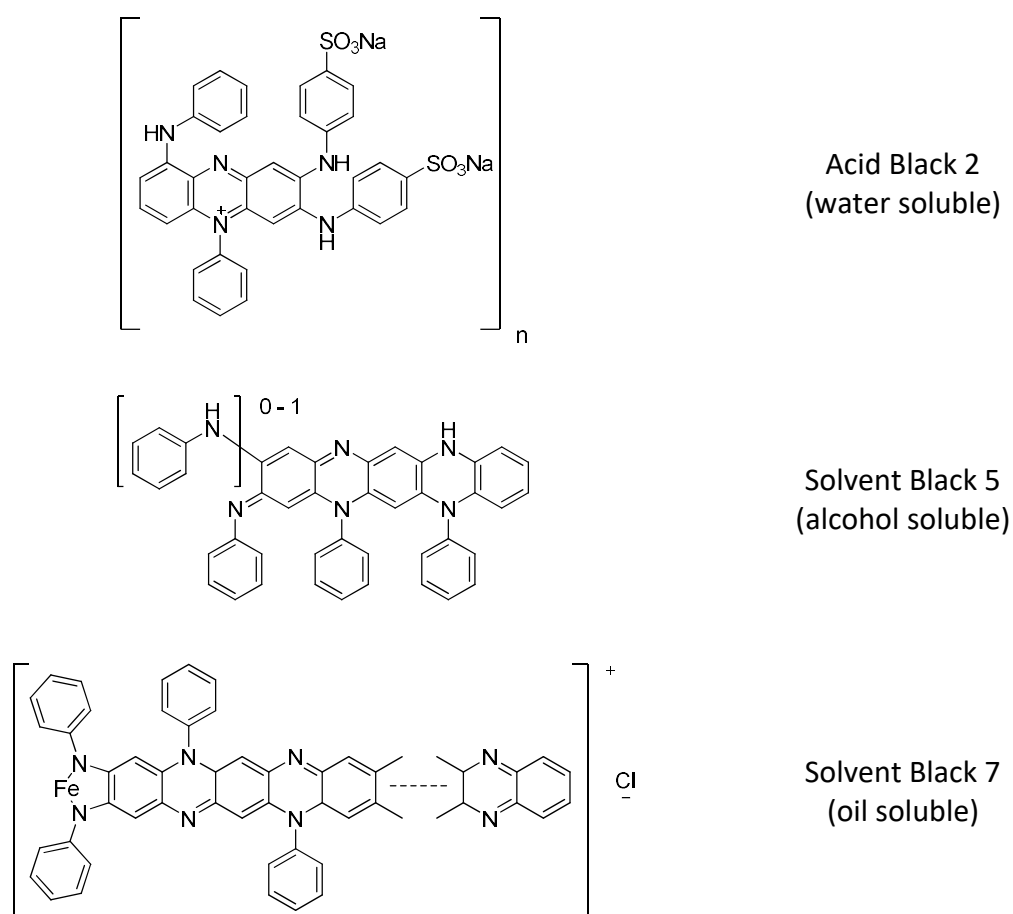


Figure 69. Structures, names and attributes of the three main Nigrosine types.<sup>[151-153]</sup>

The alcohol and oil soluble types are synthesized in a complicated process out of nitrobenzene or nitrophenol/nitrocresols, aniline, and aniline hydrochloride in the presence of an iron or copper catalyst at 180-200 °C.<sup>[11,19,147,150]</sup> Sulfonation of the alcohol soluble Nigrosine leads to a water soluble Nigrosine type.<sup>[147,150]</sup>

The water soluble Acid Black 2 is mainly used for leather, wool or silk dyeing and has also been used as a negative stain for spirochetes, bacteria, protozoa and fungi.<sup>[147,150,151]</sup> Solvent Black 5, which is also known as Nigrosine spirit soluble, is insoluble in water but

soluble in ethanol, benzene, toluene and various acids. This type of Nigrosine is especially used to color alcoholic solvents, vanishes, lacquers, wood stains and marker-pencil or printing inks. Moreover, it is used for coloring resins including phenolic resins, styrenes, polyamides and urea resins.<sup>[147,150]</sup> Solvent Black 7 is an oil soluble Nigrosine type and has similar properties and fields of application as Solvent Black 5.<sup>[153]</sup> All further experiments within this work are conducted with Colorant Black 500, which is an alcohol soluble Nigrosine type distributed by Orient Chemicals.

Thermal stability and behavior of additives are of great importance to avoid side reactions or degradation of the additive while processing. Furthermore, side-reactions with the polymer itself should be avoided not to influence the polymer properties in a worse way. Therefore, the thermal properties were simultaneously determined by means of combined thermogravimetric analysis (TGA) and differential thermal analysis (DTA). Figure 70 shows the thermogravimetric analysis (solid line) and differential thermal analysis (dotted line) of Colorant Black 500.

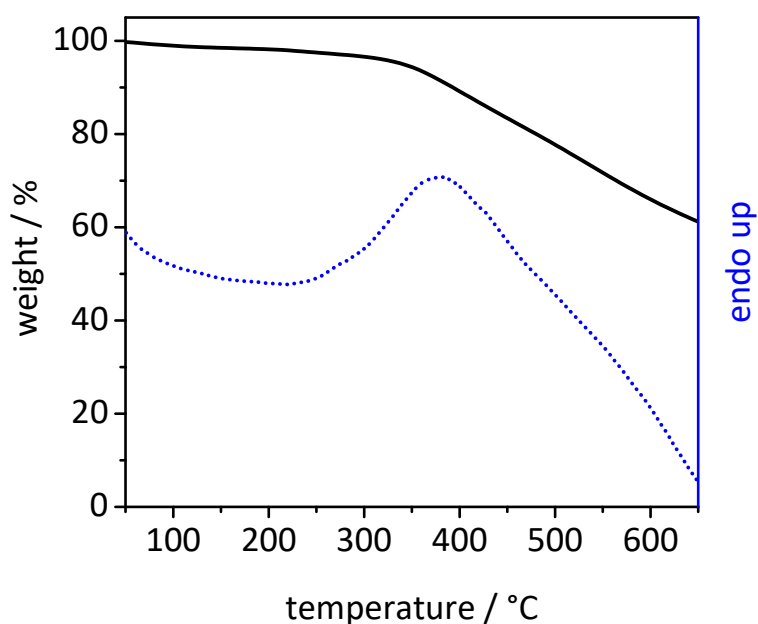


Figure 70. Thermogravimetric analysis (solid line) and simultaneous differential thermal analysis (dotted line) of Colorant Black 500, measured under nitrogen atmosphere at a heating rate of 10 K/min.

The thermal analysis of Colorant Black 500 revealed a slight weight loss at temperatures at around 100 °C which drastically increased at temperatures above 350 °C. The weight loss at lower temperatures may be ascribed to volatile low molecular compounds or solvent residuals, whereas the weight loss at elevated temperatures indicates thermal degradation of the Nigrosine compound. Furthermore, no melting could be observed.

5.1.2 Anti-nucleation of PA6 by Nigrosine

In order to visualize the anti-nucleation ability of Nigrosine, an additive screening process established by Abraham et al. was applied.<sup>[29]</sup> For this purpose samples were prepared by melting a polymer pellet between two glass slides at 250 °C. Afterwards, the sample was pressed for 2 minutes at 250 °C and quenched to room temperature. Up next, the cover glass was removed and a small amount of Nigrosine was positioned in the middle of the film. The whole setup was covered again and inserted to a hot stage under a polarized optical microscope. The sample was heated well above the melting temperature of the polymer for 5 min while the additive partly dissolves and diffuses into the surrounding polymer melt. This setup was slowly cooled at 10 K/min to monitor the crystallization process of the polymer. The sample preparation is schematically shown in Figure 71.

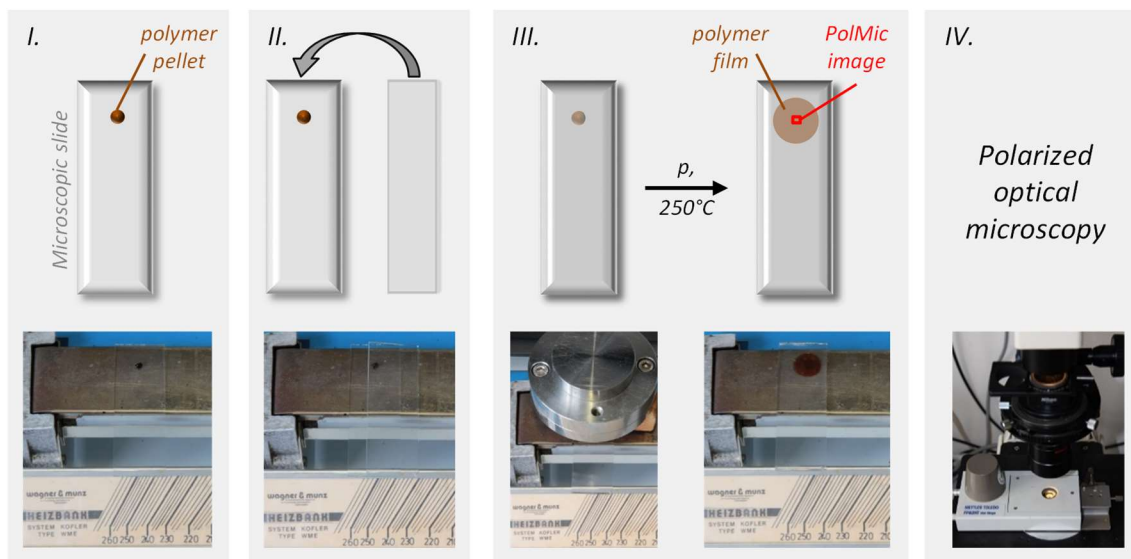


Figure 71. Preparation process for films and screening samples. At the beginning a polymer pellet was molten between two glass slides. Afterwards, the sample was pressed for 2 minutes at 250 °C and quenched to room temperature.

Figure 72 presents micrographs of PA6 partly comprising Colorant Black 500 recorded between crossed polarizers at temperatures as indicated. The image at 188 °C shows molten PA6 starting to crystallize in the left bottom corner. The black regions correspond to the optical isotropic polymer melt. The dissolved Nigrosine in the top right corner is not visible due to its black color. Upon cooling, the polymer crystallizes starting in the region without Colorant Black 500 (left bottom corner). Below a temperature of 186 °C the region without additive is fully crystallized. The region containing Nigrosine reveals just a few spherulites (top right corner). Upon further cooling, spherulites slowly emerge in the



additive rich section. At a temperature of 173 °C almost the whole sample is crystallized.

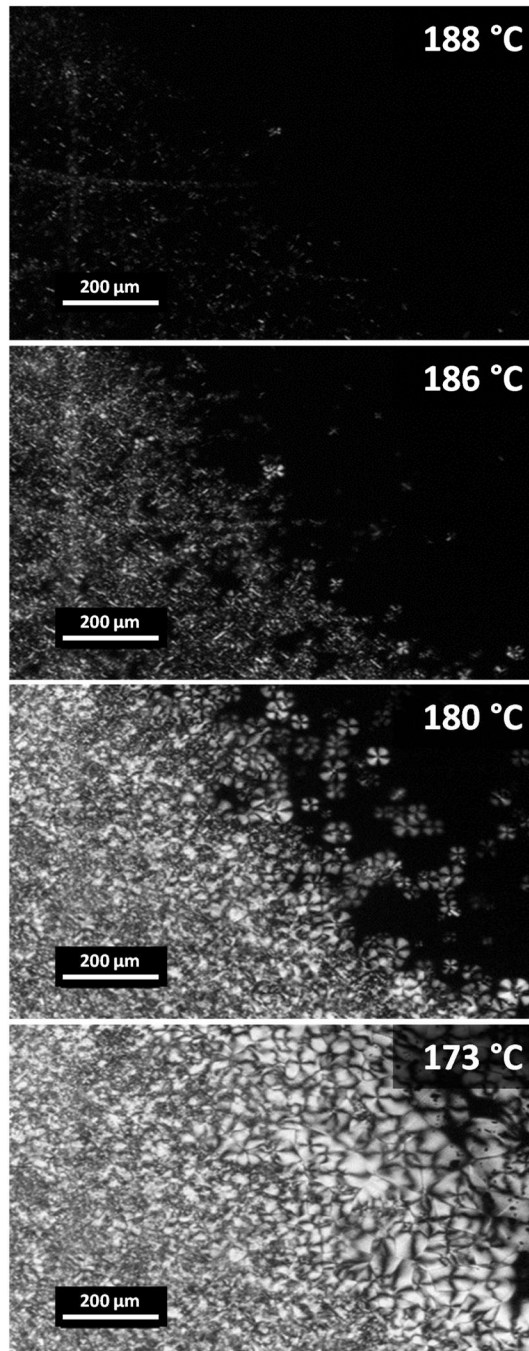


Figure 72. Optical micrographs from polarized light microscopy of a PA6 film with a small amount of Colorant Black 500. Samples were heated, kept at 250 °C for 5 minutes, cooled with a rate of 10 K/min and observed at different temperatures. The additive is dissolved and not visible in the top picture. The additive does not crystallize upon cooling. Areas where the additive is dissolved crystallize at much lower temperatures than areas where no additive is available.

The addition of Nigrosine caused a retardation of the polymer nucleation. It can clearly be seen that less nuclei are available for the polymer to crystallize. Hence, the spherulites become distinctly larger in the additive rich section before their growth is stopped by

colliding with adjacent spherulites. Similar observations were made by Takeuchi et al. for PA66 comprising polycyclic structures as anti-nucleating agents.<sup>[15]</sup>

In the following, the anti-nucleation effect of Nigrosine (Colorant Black 500) in PA6 will be discussed in detail. To study the influence of the processing conditions, various compounding temperatures were applied. The polymer crystallization temperatures were obtained from DSC measurements, reported as the temperature at the exothermic minimum upon cooling from the melt. Furthermore, the influence of Nigrosine on the polymer morphology of PA6 was examined by means of polarized light microscopy. For experimental parameters and details refer to chapter 4 and 8.

#### *Standard processing conditions*

Figure 73 presents the polymer crystallization temperatures of PA6 comprising Colorant Black 500 as function of the additive concentration processed at a measured melt temperature of 245 °C.

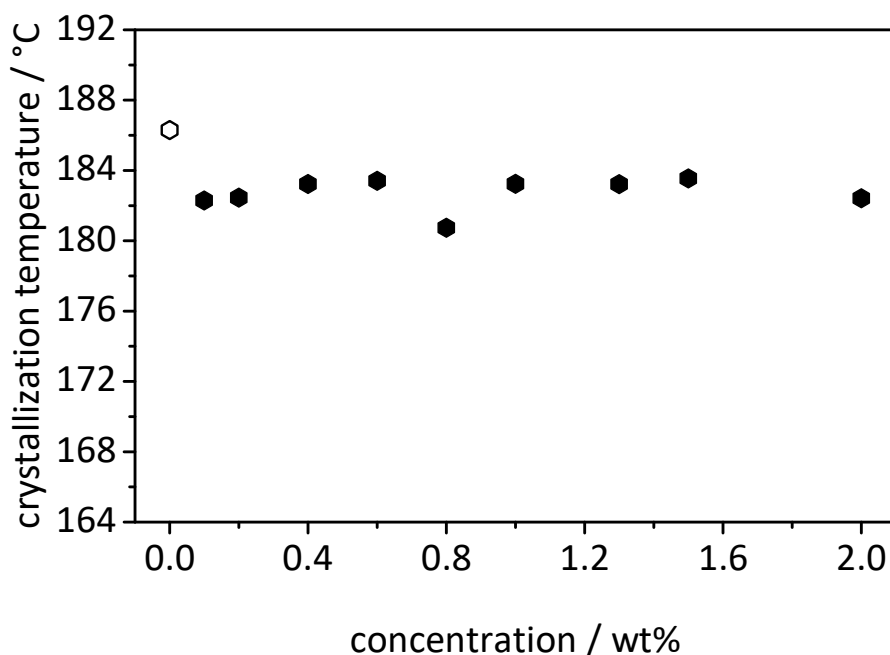


Figure 73. Polymer crystallization temperatures of PA6 comprising Colorant Black 500 as function of the additive concentration. The blank hexagon indicates the polymer crystallization temperature of neat PA6 (reference). Polymer melt temperature during processing: 245 °C. DSC heating and cooling rate: 10 K/min.

It clearly shows up that in the presence of Nigrosine the polymer crystallization temperature was reduced. The values for the polymer crystallization temperatures dropped from 186 °C for neat PA6 to 182 °C for the additivated polymer. Merely the measuring point at 0.8 wt% indicates a polymer crystallization temperature of 180 °C. No

significant enhancement of the anti-nucleation effect with increasing additive concentration could be observed. Lately, a reduction of 3-4 °C of the crystallization temperature could be realized at a processing temperature of 245 °C.

#### *Processing conditions with varying melt temperature during processing*

Besides temperature-sensitive additives, which have their performance optimum at low processing temperatures, there are additives which require elevated processing temperatures to reach their maximum effect.<sup>[41]</sup> In order to improve the additive performance of Nigrosine, the processing parameters were adapted. Due to elevated melt temperatures during processing, enhanced solubility of the additive in the polymer melt may be achieved. Thermal investigations of Colorant Black 500 revealed a thermal stability up to 350 °C. In order to improve the anti-nucleation effect of Nigrosine in PA6, higher melt temperatures during processing were applied. Therefore, PA6 comprising 1.5 wt% Colorant Black 500 was processed at 245 °C, 259 °C, 273 °C and 283 °C. Figure 74 presents the crystallization and melting temperatures of the additivated samples as well as the neat PA6 samples as function of the melt temperature during processing.

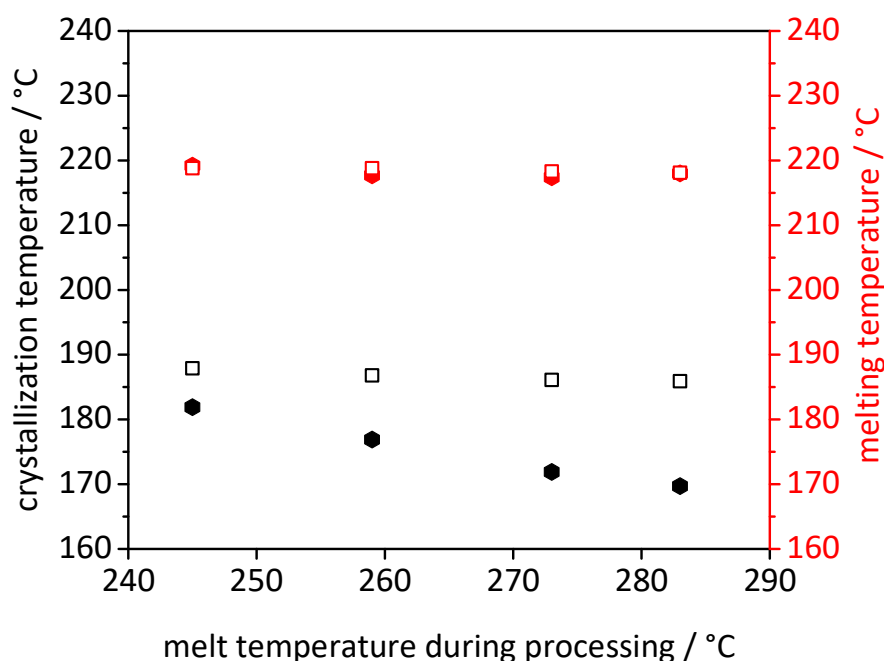


Figure 74. Crystallization and melting temperatures of neat PA6 (□ crystallization, □ melting) and PA6 containing 1.5 wt% Colorant Black 500 (● crystallization, ● melting) as function of the melt temperature during processing. DSC heating and cooling rate: 10 K/min.

As shown in Figure 74 a significant influence of the processing temperature on the crystallization temperature of PA6 comprising Colorant Black 500 was observed. The polymer crystallization temperatures of the additivated samples were linearly reduced from 182 °C at a melt temperature of 245 °C to a polymer crystallization temperature of 170 °C at a melt temperature of 283 °C. This means a reduction of 12 °C due to an elevated processing temperature without changing the amount of additive. Neat PA6 served as reference and revealed almost no change of the polymer crystallization temperature at different melt temperatures during processing. It can be assumed that elevated melt temperatures lead to a better dissolution of the Nigrosine compound which results in an enhanced anti-nucleation effect. Besides a reduction of the polymer crystallization temperature, a retention of the melting temperature for the additivated PA6 at elevated melt temperatures during processing was observed.

These results were confirmed on the basis of a further concentration series of PA6 comprising Colorant Black 500 at 283 °C. Figure 75 shows a concentration series compounded at 245 °C compared to a concentration series processed at 283 °C.

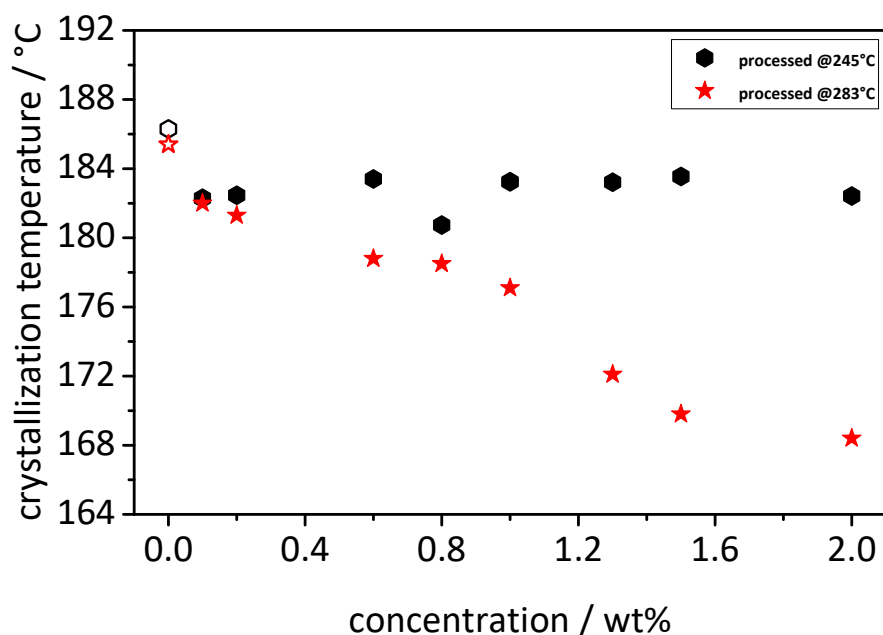


Figure 75. Crystallization temperatures of PA6 containing Colorant Black 500 as function of the additive concentration. Different symbols indicate different polymer melt temperatures during processing: 245 °C (hexagons) and 283 °C (stars). DSC heating and cooling rate: 10 K/min.

At low additive concentrations of 0.1 and 0.2 wt% almost no difference between the polymer crystallization temperatures of both experiments could be recognized. However,

with increasing additive concentration a significant improvement of the additive performance was observed at a processing temperature of 283 °C.

These results lead to the conclusion that a small portion of Nigrosine is soluble in the polymer melt at a processing temperature of 245 °C. Consequently, a slight anti-nucleation effect was observed. However, the results clearly show that the majority of the Nigrosine compound might be soluble at elevated processing temperatures which leads to a significant enhancement of the additive performance. Hence, a reduction of the polymer crystallization temperature of PA6 by 18 °C was achieved.

#### *Crystallization behavior and morphology of PA6 comprising Nigrosine*

As already presented above, the spherulitic morphology of PA6 was strongly influenced by Nigrosine. Therefore, the influence of Colorant Black 500 on the crystallization behavior of PA6 was studied isothermally by DSC and polarized light microscopy. Additionally, the macroscopic morphology of PA6 comprising Nigrosine was studied on 2.0 mm thick injection molded samples.

Polyamides are known to crystallize fast upon cooling. This leads to a relatively fine and homogenous spherulitic morphology. Isothermal experiments at temperatures above the polymer crystallization temperature provide an opportunity to slow down the crystallization process and investigate the crystallization behavior of PA6 more precisely. For this purpose, both, isothermal DSC measurements, and isothermal microscopy experiments were conducted. Samples of neat and additivated PA6 were taken from the polymer strand of the extruded polymer. For the microscopy experiments, thin films of the extruded neat, as well as the extruded and additivated polymer, were pressed as already explained above. First, the samples were heated quickly to 250 °C, held there for 5 min and cooled at a rate of 10 K/min to an isothermal end temperature of 200 °C. The samples were left at 200 °C until fully crystallized. Both, DSC samples and microscopy samples, were treated equally concerning the temperature program. All parameters are summarized in Table 19.

Table 19. Starting and end temperatures as well as the cooling rate and holding time for the isothermal DSC measurements and microscopy experiments of PA6.

Starting temperature [°C]	End temperature [°C]	Cooling rate [K/min]	Holding time [°C]
250	200	10	5

Figure 76 presents the micrographs obtained by polarized light microscopy of a neat PA6 film at 200 °C after 1 min, 3 min, 4 min and 7 min and the corresponding isothermal DSC curve.

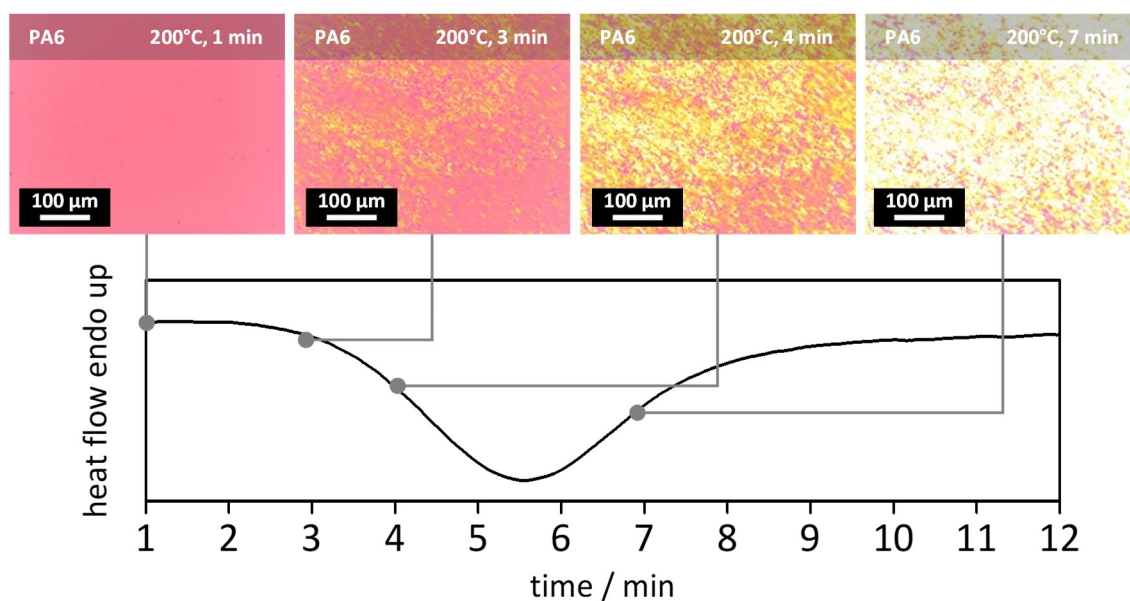


Figure 76. Top: Polarized optical micrographs (with a  $\lambda/4$  platelet) of a neat PA6 film at 200 °C after 1 min, 3 min, 4 min and 7 min. The polymer film pressed out of an extruded polymer pellet was heated, kept at 250 °C for 5 min and cooled to 200 °C with 10 K/min. Bottom: Isothermal DSC curve at 200 °C of neat PA6.

The image after 1 min shows the optical isotropic polymer melt which appears pink due to the  $\lambda/4$  platelet. The yellowish appearing areas after 3 min originate from spherulites which became visible due to birefringence of the crystalline structures. At this point, the corresponding DSC curve starts to drop which describes the onset of the crystallization process of the polymer. With proceeding time an increasing amount of crystalline structures was observed. At 7 min the micrograph shows an almost fully crystallized polymer film. The endset of the crystallization peak of the DSC measurement is around 9 min. Despite of the isothermal crystallization, neat PA6 crystallizes rather fast and exhibits very fine and homogenous spherulites which can hardly be identified.

Figure 77 presents the micrographs obtained by polarized light microscopy of PA6 comprising 2.0 wt% Colorant Black 500 at 200 °C after 0 min, 17 min, 25 min, 40 min, 90 min and 150 min and the corresponding isothermal DSC curve.

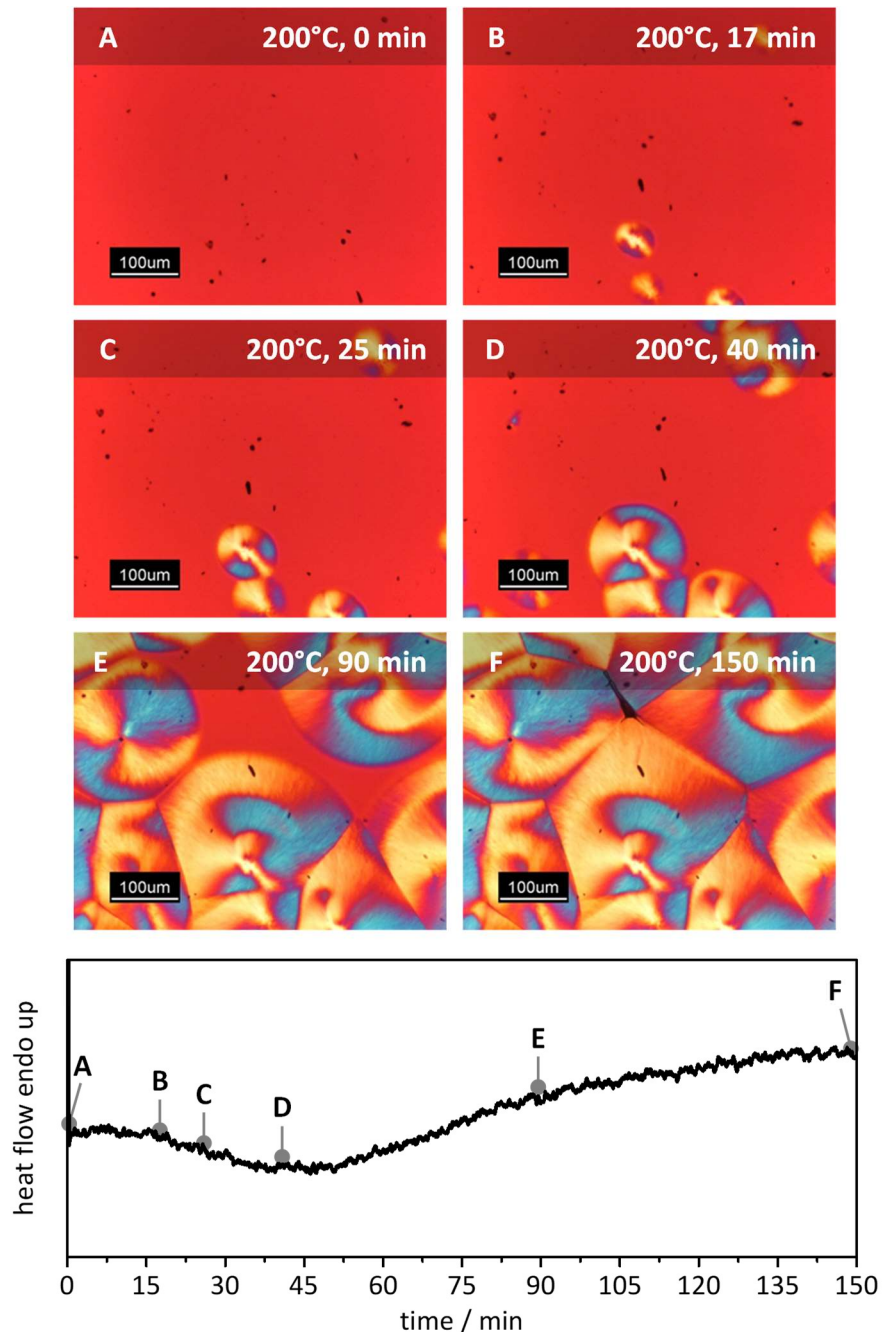


Figure 77. Top: Polarized optical micrographs of a PA6 film comprising 2.0 wt% Colorant Black 500 at 200 °C after 0 min, 17 min, 25 min, 40 min, 90 min and 150 min. The compounded polymer pellets were heated and pressed, kept at 250 °C for 5 min and cooled to 200 °C with 10 K/min. Bottom: Isothermal DSC curve at 200 °C of PA6 comprising 2.0 wt% Colorant Black 500 processed at 283 °C.

The image at 0 min shows the optical isotropic polymer melt which appears pink due to the  $\lambda/4$  platelet and some dark dots which originate from poorly dissolved Colorant Black 500.

The second image after 17 min shows three yellowish and purplish structures which can be attributed to spherulites. The corresponding DSC curve starts to drop at 14 min which describes the onset of the crystallization process of the polymer. After 40 min, merely six spherulites showed up within the observed image section. As it appears from the images, the growth rate of the spherulites is very slow and very little nuclei were formed. This incident leads to huge spherulites which are almost not limited in their expansion. These spherulites reached diameters of several hundreds of microns before the growth was stopped by collision with adjacent spherulites. At 150 min the micrograph shows an almost fully crystallized polymer film and the endset of the crystallization peak of the DSC measurement is at around 140 min.

These experiments clearly show the influence of Nigrosine on the crystallization behavior and also on the spherulitic morphology of PA6. The images present vividly the partial suppression of forming nuclei and hence the retardation of polymer crystallization due to the addition of Nigrosine as anti-nucleating agent. Moreover, the visual results were confirmed by isothermal DSC measurements of the same compounds under equal temperature conditions.

In order to show the influence of Nigrosine on the macroscopic morphology of PA6 injection molded samples with a thickness of 2.0 mm were cut parallel to the direction of injection (flow direction) to obtain thin sections with a thickness of 10  $\mu\text{m}$ . These thin sections were placed between two object slides and examined by polarized light microscopy. Figure 78 presents the thin sections of neat PA6 (left) and PA6 comprising 1.5 wt% Colorant Black 500 (right). The images were merged from three separate pictures to present the complete cross section of the injection molding sample.

Both samples exhibit smaller spherulites near the skin layers and major spherulites in the core regions. These effects were already described by Richter et al.<sup>[14]</sup> and were explained by the temperature gradient of the injection mold from the outside to the inside, and hence varying cooling rates within the injection molding specimen. Furthermore, the black areas of the neat PA6 originate from impurities due to the cutting process.



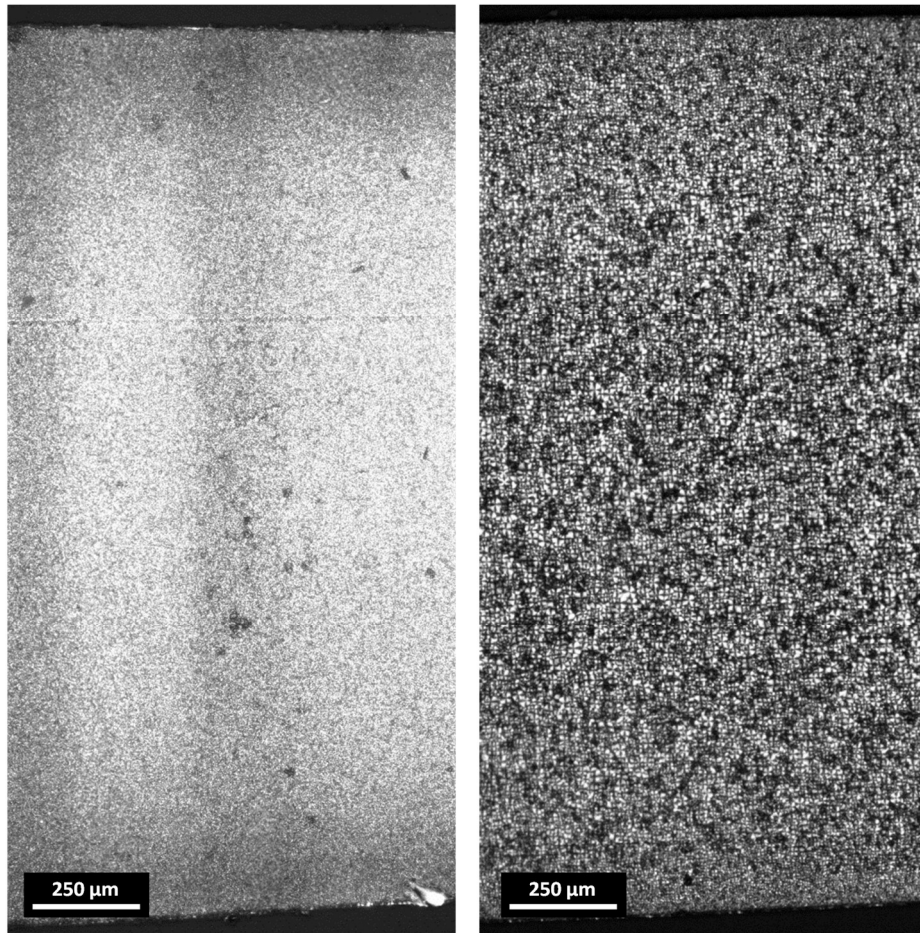


Figure 78. Optical micrographs from polarized light microscopy of cross-sections of tension rods of neat PA6 (left) and PA6 comprising 1.5 wt% Colorant Black 500 (right).

By comparing neat PA6 (left) and additivated PA6 (right) it can be shown that the spherulitic morphology was significantly influenced by the addition of Nigrosine. The spherulites are distinctly larger due to the additivation, even at very fast cooling rates during injection molding. This effect may have significant influence on further polymer properties and will be investigated in the following.

## 5.1.3 Properties of PA6 containing Nigrosine

Polyamides crystallize due to hydrogen bonds between amide groups of the polymer chains. These hydrogen bonds are the leading element for nearly every feature of the polymer. By influencing the pattern of these hydrogen bonds, the properties of the polymer can be influenced significantly. This can be effected by particular polymer processing or specific additives. Certainly, it is of great importance not to downgrade the properties of the polymer by additivation. As already shown above, Nigrosine has a significant influence on the morphology of PA6. Therefore, the following chapter will examine the influence of Nigrosine on important parameters of PA6 such as crystal modification, degree of crystallinity and glass transition temperature. Therefore, methods such as WAXS, DSC and DMTA were applied.

*Crystal modification*

In order to figure out the crystal modifications, WAXS measurements were conducted. Figure 79 shows the WAXS pattern of 1.1 mm thick injection molded platelets of neat PA6 and PA6 comprising 1.5 wt% Colorant Black 500.

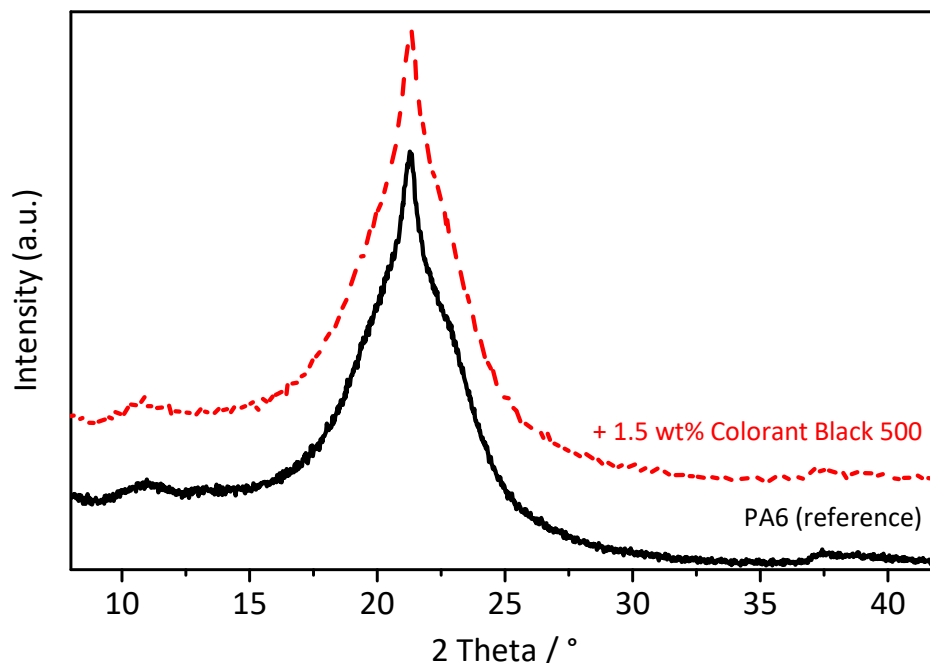


Figure 79. WAXS pattern of neat PA6 (line) and PA6 containing 1.5 wt% Colorant Black 500 (dashed line). Measurements were performed at room temperature on 1.1 mm thick injection molded specimen.

As already described in chapter 3.4, PA6 can crystallize into  $\alpha$ -,  $\gamma$ - or the metastable  $\beta$ -phase. As apparent from Figure 79 both compounds, neat PA6 and PA6 comprising

Nigrosine, crystallized predominantly in the  $\gamma$ -phase. The WAXS pattern of neat PA6 shows a hint of the  $\alpha$ -peak around  $23^\circ$ , whereas for PA6 comprising Colorant Black 500 almost no  $\alpha$ -peak is visible. All in all, no significant variations of the crystal modification were observed.

### *Degree of crystallinity*

In addition to the crystal modification, the degree of crystallinity is another important parameter, especially for semi-crystalline polymers. Therefore, the degree of crystallinity was determined by DSC. The detailed procedure is explained in chapter 3.4. As presented in Table 20, the degree of crystallinity just varied slightly from each other for neat PA6 and PA6 comprising Colorant Black 500.

Table 20. Melt enthalpies  $\Delta H_f$  and degree of crystallinity of neat PA6 and PA6 comprising 1.5 wt% Colorant Black 500 determined by DSC. Both samples were processed at  $283^\circ\text{C}$ . DSC heating and cooling rate: 10 K/min.

Compound	$\Delta H_f$ [J/g]	Degree of crystallinity [%]
PA6 (reference)	68	36
+ 1.5 wt% Colorant Black 500	66	35

### *Glass transition temperature*

A further very important property of polymers is the glass transition temperature. The glass transition is defined as the temperature when the chain mobility of the polymer chains drastically increases, and hence the polymer becomes soft. Besides additives, water absorption has a great influence on the glass transition temperature.<sup>[2]</sup> Therefore, throughout the whole work samples were measured after equilibrium water uptake ( $70^\circ\text{C}$ , 62 rh%, 4 days), with a frequency of 1 Hz and a heating rate of 2 K/min. Figure 80 presents the plot of the storage modulus  $E'$  and loss factor  $\tan \delta$  as a function of the temperature for PA6 comprising 1.5 wt% Colorant Black 500. The value for the glass transition temperature was determined from the peak of  $\tan \delta$ . The red line indicates the glass transition temperature of PA6 comprising 1.5 wt% Colorant Black 500. The conducted measurements revealed a glass transition temperature of  $22^\circ\text{C}$ . By comparison, neat PA6 exhibits a glass transition temperature of  $20^\circ\text{C}$  under the same storing and measurement conditions. Consequently, the addition of Nigrosine showed no significant influence on the glass transition temperature of PA6.

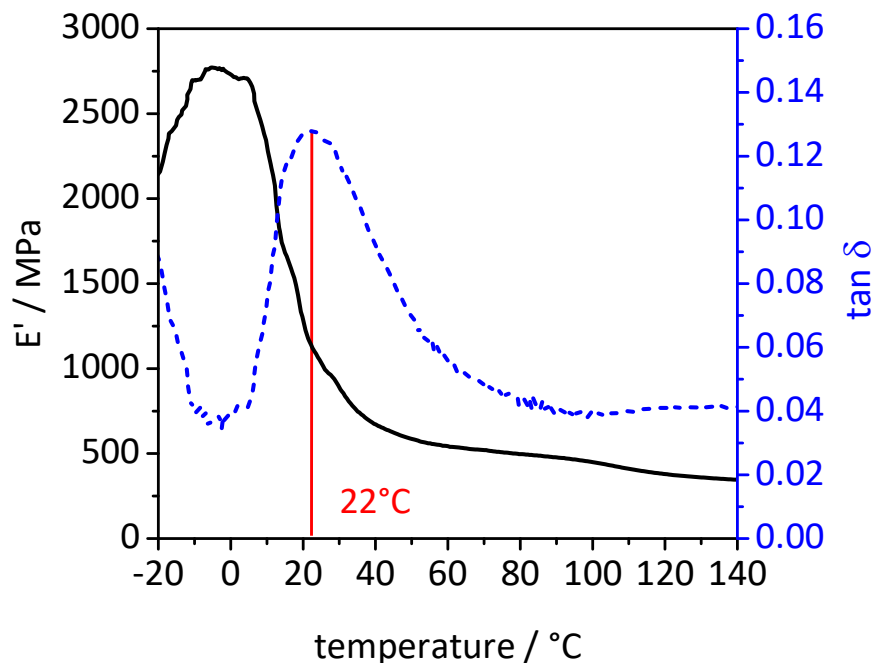


Figure 80. DMTA measurements of PA6 comprising 1.5 wt% Colorant Black 500 after equilibrium water uptake (70 °C, 62 rh%) measured at a frequency of 1 Hz, and a heating rate of 2 K/min. Solid, black line: storage modulus  $E'$ ; Dashed, blue line:  $\tan \delta$ . The red solid line indicates the glass transition temperature determined from the maximum of  $\tan \delta$ .

All in all, a significant decrease of the polymer crystallization temperature by the addition of Colorant Black 500 could be observed. By adapting the melt temperatures during processing an enhanced solubility of the additive and a coincident significant reduction of the polymer crystallization temperature could be achieved, while no change of the melting temperature was observed. Characteristic properties such as crystal modification, degree of crystallinity and glass transition temperature were mainly unaffected and showed almost the same values as for the neat polymer.

In conclusion, Nigrosine acts as an excellent anti-nucleating agent having no negative influence on the properties of PA6. Moreover, it is a cheap and commercially available compound. Nevertheless, Nigrosine is a mixture of various azine dyes which can hardly be extracted. Furthermore, the applications of anti-nucleated polyamides are limited due to the black color of Nigrosine, and hence no free choice of color for a certain application is possible. In addition to that, solubility problems of Nigrosine in PA6 were revealed. By solving these solubility problems, Nigrosine would become much more efficient and less additive would be needed for the same effect.

Table 21 summarizes the characteristic values examined within this work for neat PA6 and PA6 comprising Colorant Black 500.

Table 21. Summary of characteristic values of neat PA6 and PA6 comprising 1.5 wt% Colorant Black 500. Melt temperature during processing for all data was 283 °C.

	PA6 (reference)	+ 1.5 wt% Colorant Black 500 @ 283 °C
Melting temperature $T_m$	218 °C	218 °C
Crystallization temperature $T_c$	186 °C	170 °C
Degree of crystallinity	36%	35%
Glass transition temperature $T_g$	20 °C	22 °C
Main crystal modification	$\gamma$ -modification	$\gamma$ -modification

### 5.2 Salts as anti-nucleating agents

In order to develop new anti-nucleating agents, leading elements of the commercially applied Nigrosine are investigated concerning their anti-nucleation effect on polyamides. Nigrosine usually exhibits charges which might be responsible for disturbing the hydrogen bonds between the polymer chains, and hence retard the crystallization process. Long before Nigrosine, the influence of salts on the crystallization behavior of PA6 was reported by Valenti et al. in 1973. They described that inorganic salts, such as LiBr, LiCl or KCl, drastically slowed down the crystallization rate.<sup>[133,154]</sup> These investigations were one of the first evidences for the phenomenon of anti-nucleation. A few years later, Siegmann et al. also observed a decrease of the polymer crystallization temperature of PA6 with increasing content of metal halides, but also noted a strong depression of the polymer melting temperature.<sup>[31,32]</sup> Both, Valenti et al. and Siegmann et al., investigated inorganic salts in concentration ranges above 2.0 wt% and observed a significant decrease of the melting temperature of PA6. Recently, Tian et al. showed a similar effect for PA6 additivated with ionic liquids.<sup>[155]</sup> This type of influence on the polymer properties is a miserable condition and leads to a decrease of the mechanical properties.<sup>[156]</sup> Thus, this effect has to be strictly avoided. However, salts exhibit advantages as well. The investigated salts are cheap, commercially available and colorless which makes them a candidate to open a wide field of new applications for anti-nucleating agents.

In the following chapter, detailed investigations on the influence of LiCl are conducted at concentrations below 2.0 wt% which were not investigated so far. As mentioned above, ionic liquids also revealed a decrease of the polymer crystallization temperature of polyamides. Ammonium salts can be attributed to ionic liquids as well, but are more thermally stable and solid at room temperature.<sup>[157]</sup> Therefore, several ammonium salts with varying counter ions and different alkyl chain lengths are systematically tested with respect to their anti-nucleation ability in PA6 in order to develop a colorless anti-nucleation agent. The anti-nucleation effect was recorded by DSC measurements, and the influence on the crystal structure of PA6 was determined by WAXS. Furthermore, the influence on the macroscopic morphology of PA6 was studied on injection molded samples.

## 5.2.1 Lithium chloride

Based on the work of Valenti et al., on the bulk properties of synthetic polymer-inorganic salt systems, LiCl was evaluated with respect to its anti-nucleation ability in PA6 at low additive concentrations. The concentrations reached from 0.1 wt% to 2.0 wt%. Furthermore, the crystal modification and morphology of PA6 of additivated samples were investigated.

First of all, the thermal properties of neat LiCl were determined. Figure 81 shows the thermogravimetric analysis (solid line) and simultaneous thermal analysis (dotted line) of LiCl.

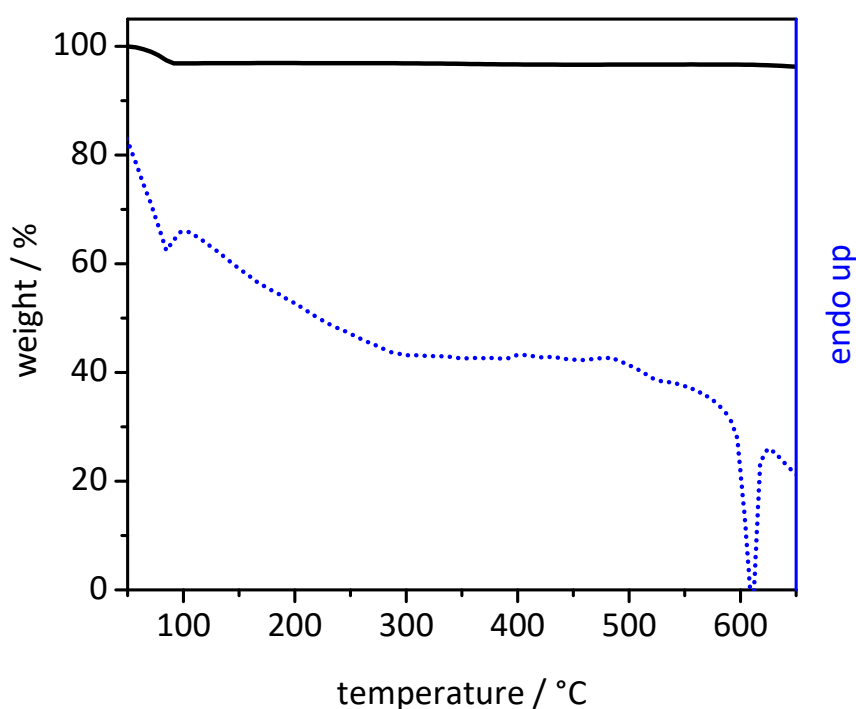


Figure 81. Thermogravimetric analysis (solid line) and simultaneous differential thermal analysis (dotted line) of LiCl, measured under nitrogen atmosphere at a heating rate of 10 K/min.

The thermal analysis of LiCl revealed a weight loss at a temperature of 100 °C which can be attributed to water. Furthermore, no melting was observed and sublimation occurred first above 700 °C. LiCl is thermally stable and suitable for the additivation of PA6. However, it has to be considered that LiCl is highly hygroscopic and hence have to be dried before compounding.

In order to examine the anti-nucleation ability of LiCl, a concentration series in PA6 was prepared. Figure 82 presents the crystallization and melting temperatures of PA6 comprising LiCl as function of the additive concentration in the range of 0.1 – 2.0 wt%.

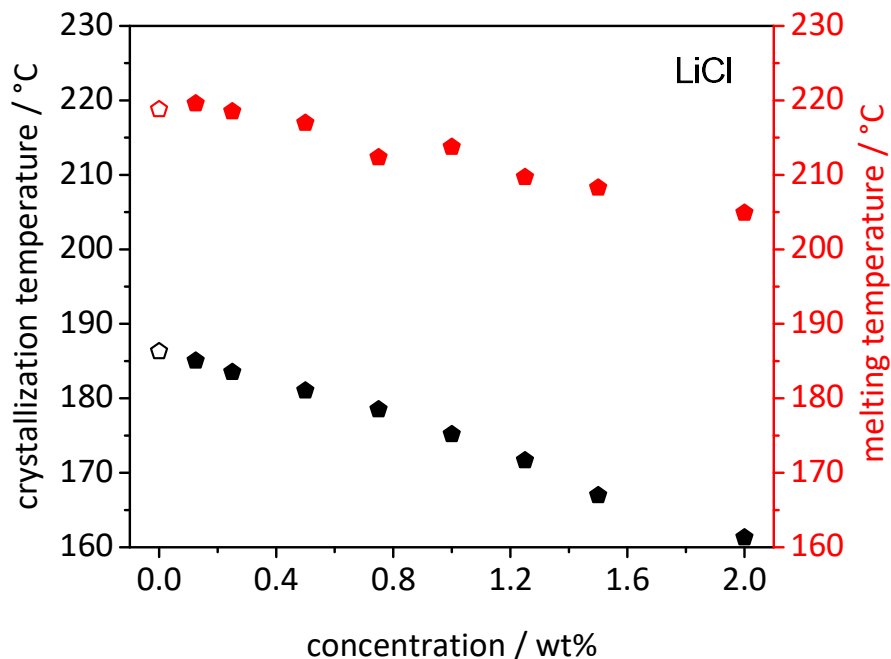


Figure 82. Crystallization and melting temperatures of PA6 comprising LiCl as function of the additive concentration. Polymer melt temperature during processing: 245 °C. DSC heating and cooling rate: 10 K/min.

As shown in Figure 82, a significant influence of the additive concentration of LiCl on the crystallization temperature of PA6 was observed. The polymer crystallization temperature was almost linearly reduced from 186 °C for neat PA6 to 161 °C at an additive concentration of 2.0 wt%. At the same time, a strong reduction of the melting temperature of PA6 could be observed. At concentrations below 0.25 wt%, no significant change of the melting temperature of PA6 was observed, whereas with increasing additive content, a strong reduction of the polymer melting temperature occurred. The melting temperature of neat PA6 decreased from 218 °C to 205 °C for an additive concentration of 2.0 wt%. Similar results were made prior to this work for concentrations above 2.0 wt%. However, these results shows that concentrations of LiCl up to 0.25 wt% lead to a reduction of the polymer crystallization temperature up to 3 °C without affecting the melting temperature of the polymer. Consequently, LiCl can be used as polymer additive at relatively low amounts. However, it has to be kept in mind, that concentrations above 0.25 wt% lead to a drastically decrease of the melting temperature and may influence the properties of the polymer. Therefore, the influence of LiCl on the crystal modification and on the macroscopic morphology of PA6 is demonstrated using a sample of PA6 comprising 2.0 wt% LiCl. Figure 83 shows the WAXS pattern of injection molded specimen of neat PA6 and PA6 comprising 2.0 wt% LiCl.



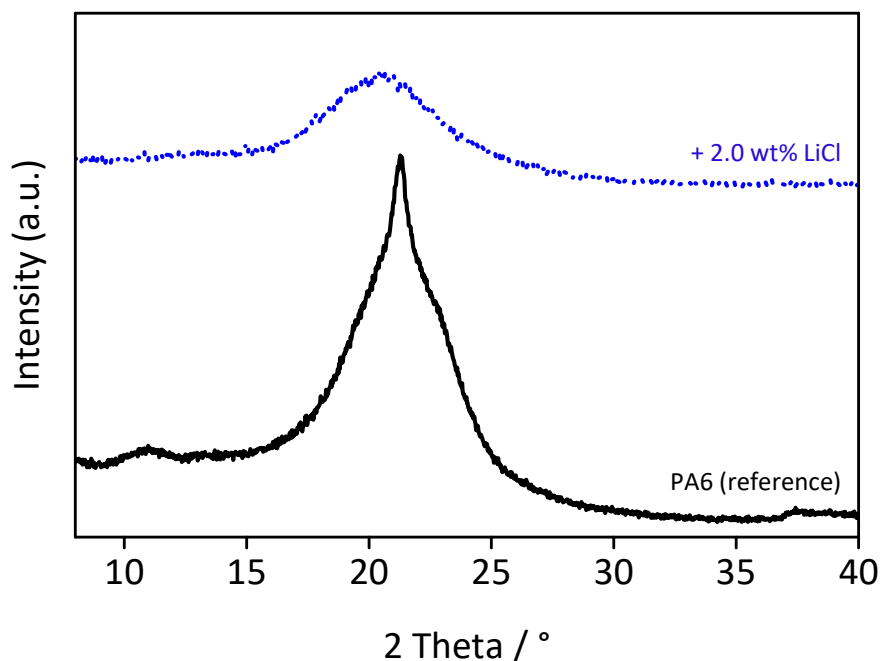


Figure 83. WAXS pattern of neat PA6 (line) and PA6 containing 2.0 wt% LiCl (dashed line). Measurements were performed at room temperature on 1.1 mm thick injection molding specimens.

As apparent from Figure 83, neat PA6 crystallizes predominantly in the  $\gamma$ -phase, whereas the WAXS pattern of PA6 comprising LiCl appears blurred and shows no defined peaks. This was to be expected and confirms the strong influence of LiCl on the polymer crystallization. The crystal modification of PA6 is strongly affected by the addition of LiCl. It can be assumed that there is a strong interaction of PA6 and LiCl. For this reason, large amounts of LiCl remained in the crystalline phase during and past the crystallization process. Ciferri et al. and Siegmann et al. explained the change of the crystallization data of PA6 by addition of various salts with complex building of the salts and the polymer.<sup>[154,156]</sup> As a result, the polymer is not capable of crystallizing in the usual way, and hence no defined WAXS pattern can be measured. These explanations confirm the cause of the decline of the melting temperature of PA6 at high additive concentrations.

Another explanation might be a loss of the degree of crystallinity with a coincident increase of the amorphous phase of the polymer. This leads to a pronounced amorphous halo and a loss of the crystalline peaks within the WAXS pattern.

Therefore, the degree of crystallinity of PA6 comprising different concentrations of LiCl was determined by DSC. The results are summarized in Table 22.

Table 22. Melting enthalpies  $\Delta H_f$  and degree of crystallinity and melting temperature of neat PA6 and PA6 comprising different concentrations of LiCl determined by DSC. All samples were processed at 245 °C. DSC heating and cooling rate: 10 K/min.

Compound	$\Delta H_f$ [J/g]	Degree of crystallinity [%]	Melting temperature [°C]
PA6 (reference)	65	34	218
+ 0.125 wt% LiCl	62	33	219
+ 0.25 wt% LiCl	56	30	218
+ 0.5 wt% LiCl	52	28	217
+ 0.75 wt% LiCl	51	27	212
+ 1.0 wt% LiCl	49	26	214
+ 1.25 wt% LiCl	46	24	210
+ 1.5 wt% LiCl	41	22	208
+ 2.0 wt% LiCl	38	20	205

As already demonstrated by the WAXS measurements, also the degree of crystallinity was significantly influenced by the addition of LiCl at high additive concentrations. The degree of crystallinity was reduced from 34% for neat PA6 to 20% for PA6 comprising 2.0 wt% LiCl.

In order to visualize the influence of LiCl on the macroscopic morphology of PA6, injection molded platelets with a thickness of 1.1 mm were cut parallel to the direction of injection (flow direction) to obtain thin sections with a thickness of 10  $\mu\text{m}$ . These thin sections were placed between two object slides and examined by polarized light microscopy. Figure 84 presents the thin sections of neat PA6 (left) and PA6 comprising 2.0 wt% LiCl. The images were merged from two separate pictures to present the complete cross section of the injection molding platelet.

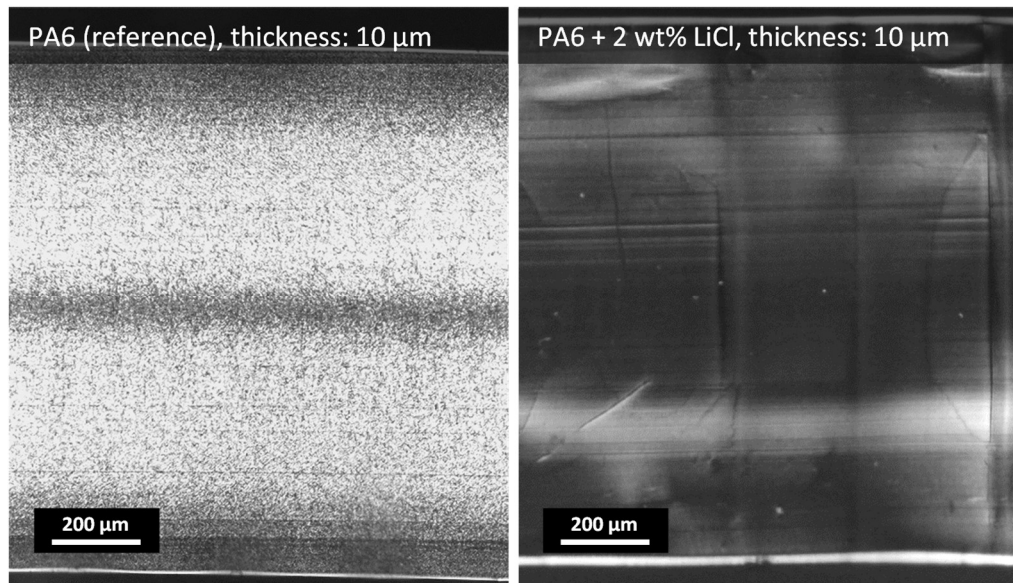


Figure 84. Thin sections (10 μm thick) of neat PA6 (left) and PA6 comprising 2.0 wt% LiCl from injection molded specimen cut parallel to the flow direction.

By comparing neat PA6 (left) and additivated PA6 (right) it becomes clear that the spherulitic morphology was significantly influenced by the addition of LiCl. In the case of PA6 comprising LiCl, no spherulitic morphology can be observed and the sample appears almost transparent. Furthermore, several folds and wrinkles emerged during the cutting process which also can be ascribed to the decreased degree of crystallinity and possibly to a decline of the mechanical properties.

In conclusion, LiCl significantly effects major properties of PA6. Besides a strong reduction of the crystallization temperature, a massive decline of properties such as melting temperature, crystal modification and degree of crystallinity were observed even at concentrations below 2.0 wt%. The investigations revealed that LiCl might be capable as additive for PA6 only at concentrations of 0.25 wt% or below. In this region a slight anti-nucleation effect of 3 °C was observed with almost unchanged properties of the polymer, as far as investigated.

## 5.2.2 Ammonium salts

As revealed in the previous chapter, inorganic salts such as LiCl are capable of reducing the polymer crystallization temperature of PA6. Unfortunately, this effect also comes along with a decline of several properties of the polymer. However, as learned from the literature, as well as presented in previous investigations, charged compounds might be the key to anti-nucleate polyamides. Besides inorganic salts, organic salts represent a huge class of charged compounds. These include, among others, organic ammonium salts. Depending on the number of organic groups, the ammonium cation is called a primary, secondary, tertiary, or quaternary cation. Quaternary ammonium cations are stable and thus inert. Salts of quaternary ammonium cations are often used as disinfectants, surfactants, fabric softeners, antistatic agents or for antibacterial applications.<sup>[158–162]</sup> Figure 85 presents the chemical structure of a quaternary ammonium salt.

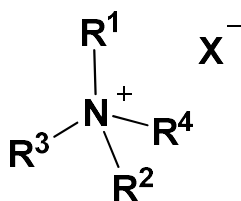


Figure 85. Chemical structure of a quaternary ammonium salt. The R groups may be the same or different alkyl groups. The X indicates the anionic group such as chloride, iodide or bromide.

By varying the alkyl chain length of the cationic group and the choice of a suitable anion, properties such as solubility or melting temperature of the ammonium salt can be controlled and adjusted. Further advantages are that the compounds are mostly colorless, commercially available and cheap. Since there is no evidence in the literature concerning the influence of organic ammonium salts on the crystallization behavior of polyamides, this chapter discusses several organic ammonium salts with respect to their anti-nucleation ability. To establish structure-property relations concerning the anti-nucleation of PA6, the alkyl chain lengths are systematically varied as well as the counter ions are changed. The polymer crystallization temperatures are determined by DSC and the thermal properties of the pure ammonium salts are analyzed by thermogravimetric analysis and simultaneous thermal analysis.

In order to test the capability of ammonium salts to anti-nucleate polyamides, the additive screening process already described in chapter 5.1 was applied. Figure 86 presents

micrographs of PA6 partly comprising Tetrabutylammonium hexafluorophosphate **3a** recorded between crossed polarizers at temperatures as indicated.

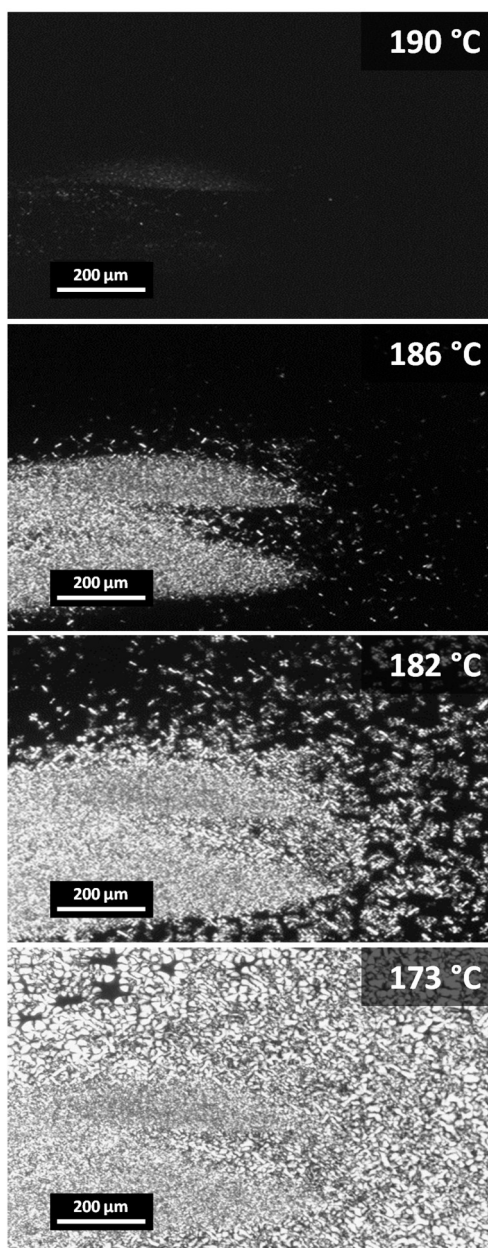


Figure 86. Optical micrographs from polarized light microscopy of a PA6 film with a small amount of Tetrabutylammonium hexafluorophosphate **3a**. Samples were heated, kept at 250 °C for 5 minutes, cooled at a rate of 10 K/min and observed at different temperatures. The additive was dissolved and is not visible in the top picture. The additive did not crystallize upon cooling. Areas where the additive was dissolved crystallized at much lower temperatures than areas where no additive is available.

The image at 190 °C shows molten PA6 starting to crystallize on the left side of the image. The black regions correspond to the optical isotropic polymer melt. The dissolved salt is not visible. Upon cooling, the polymer crystallized starting in the region without the additive. At around 186 °C the region without additive was fully crystallized, whereas the region

containing the ammonium salt revealed just a few spherulites. Upon further cooling, spherulites slowly emerged in the additive rich section. At a temperature of 173 °C almost the whole sample crystallized. The additivated region shows larger spherulites compared to the region of the neat polymer. Similar observations were made for the Nigrosine compound in chapter 5.1.

In order to verify the anti-nucleation effect, a concentration series of PA6 comprising **3a** was prepared in a concentration range of 0.01 wt% to 1.5 wt%. The polymer crystallization temperatures and melting temperatures were obtained from DSC measurements. Figure 87 presents the polymer crystallization temperatures and melting temperatures of PA6 comprising **3a** as function of the additive concentration.

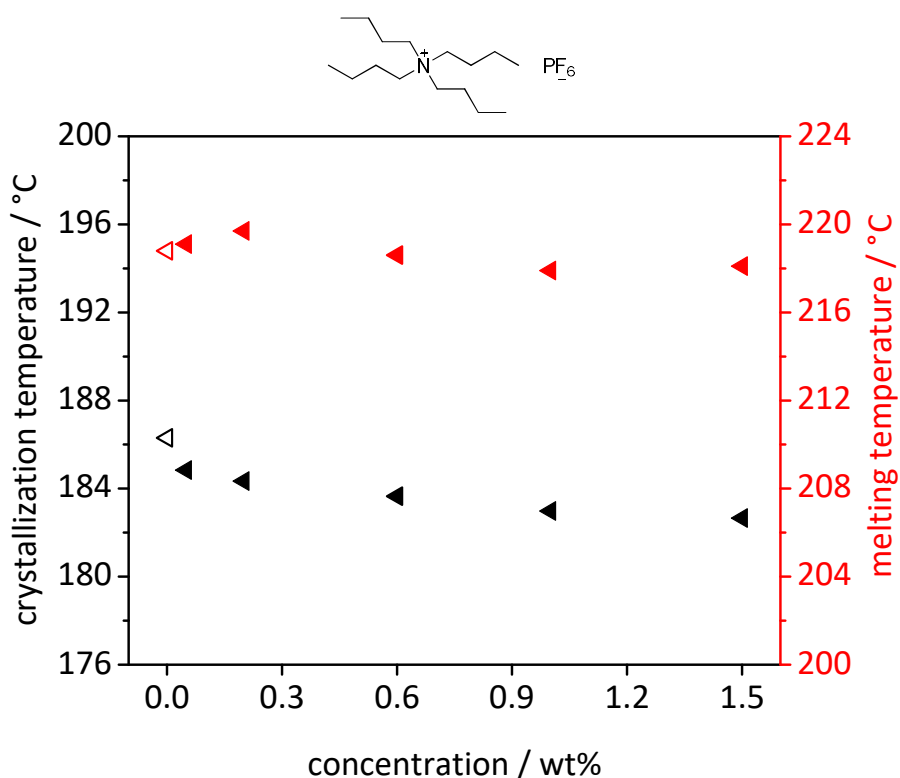


Figure 87. Polymer crystallization temperatures and melting temperatures of PA6 comprising Tetrabutylammonium hexafluorophosphate **3a** as function of the additive concentration. The blank triangles indicate the polymer crystallization temperature and melting temperature of neat PA6 (reference). Polymer melt temperature during processing: 245 °C. DSC heating and cooling rate: 10 K/min.

It clearly shows that in the presence of **3a** the polymer crystallization temperature was significantly reduced. The values for the polymer crystallization temperatures drop slowly with increasing additive concentration from 186 °C for neat PA6 to 182 °C at a concentration of 1.5 wt%. The polymer melting temperature stayed almost constant at temperatures around 218 °C, even at increased additive concentrations. Summarizing the

above, it can be said that, a reduction of 4 °C of the polymer crystallization temperature was realized without reducing the polymer melting temperature.

In order to explore the influence of additive concentrations above 1.5 wt%, a further concentration series with concentrations from 1.5 wt% to 20.0 wt% was prepared. The results are presented in Figure 88.

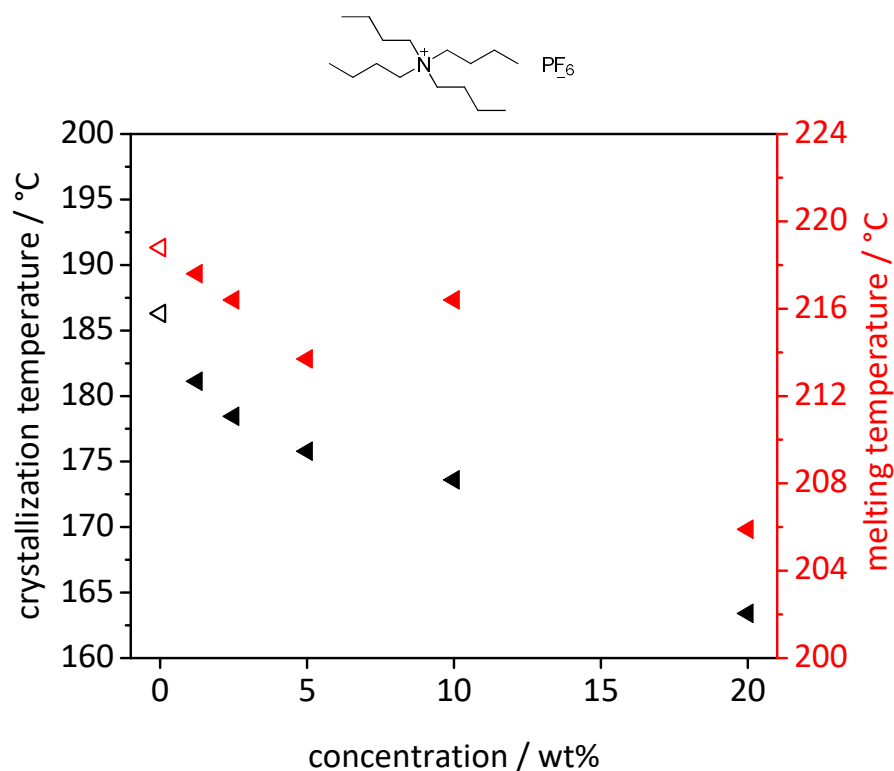


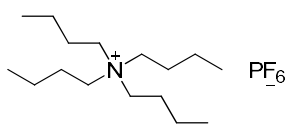
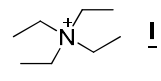
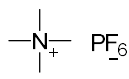
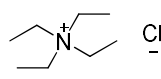
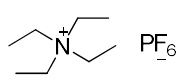
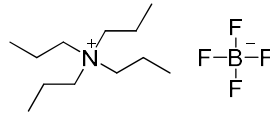
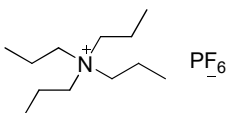
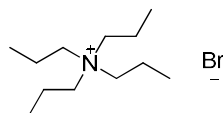
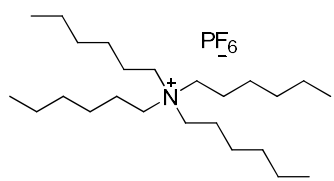
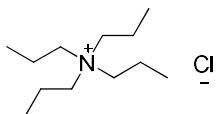
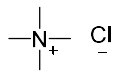
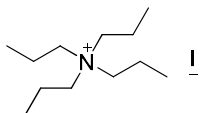
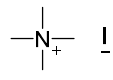
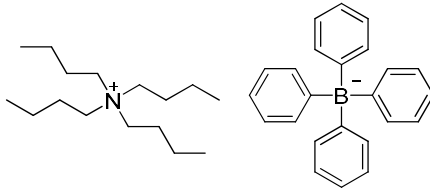
Figure 88. Polymer crystallization temperatures and melting temperatures of PA6 comprising Tetrabutylammonium hexafluorophosphate **3a** as function of the additive concentration. The blank triangles indicate the polymer crystallization temperature and melting temperature of neat PA6 (reference). Polymer melt temperature during processing: 245 °C. DSC heating and cooling rate: 10 K/min.

By increasing the concentration of **3a**, the crystallization temperature of PA6 could be reduced remarkably. At a concentration of 2.0 wt% the crystallization temperature was already reduced by 7 °C and reached its maximum reduction by 23 °C at 20.0 wt%. Nevertheless, a simultaneous decline of the melting temperature was observed, which leads to a loss of several properties of the polymer. Merely, the value at 10.0 wt% displays an anomaly and showed only a reduction of the melting temperature by 2 °C. These results show that additive concentrations above 1.5 wt% are not reasonable.

However, the ammonium salt **3a** revealed a slight anti-nucleation effect at concentrations up to 1.5 wt% with no decrease of the polymer melting temperature. Therefore, in the following, several ammonium salts with varying alkyl chain lengths and different counter

ions are investigated with respect to their anti-nucleation ability. By varying the substituents and/or counter ions, the properties of the ammonium salts are influenced and might show different anti-nucleation effects in PA6. Table 23 summarizes the investigated ammonium salts with the corresponding labels used in this work.

Table 23. Labels and structures of investigated ammonium salts.

No.	Compound	No.	Compound
3a		3h	
3b		3i	
3c		3j	
3d		3k	
3e		3l	
3f		3m	
3g		3n	

Before investigating the anti-nucleation ability, the thermal properties of the ammonium salts were simultaneously determined by means of combined thermogravimetric analysis



(TGA) and differential thermal analysis (DTA). With respect to the thermal properties, the investigated ammonium salts can be categorized into two categories that will be described in detail in the following.

Compounds in category **A** showed a melting transition, followed by the evaporation from the liquid phase and subsequent sublimation and degradation which is indicated by a kink of the TGA curve at elevated temperatures. Complete evaporation is displayed by a weight loss of 100% upon further heating. Figure 89 shows the TGA/DTA diagram of **3f**, which has a melting transition at 274 °C. The five percent weight loss ( $T_{-5 \text{ wt\%}}$ ) is at 330 °C. Similar thermal behavior was observed for compounds **3h**, **3j**, and **3n**. The appearing thermal transitions were confirmed by polarized light microscopy and a melting point system (MP90, Mettler Toledo) for all investigated compounds.

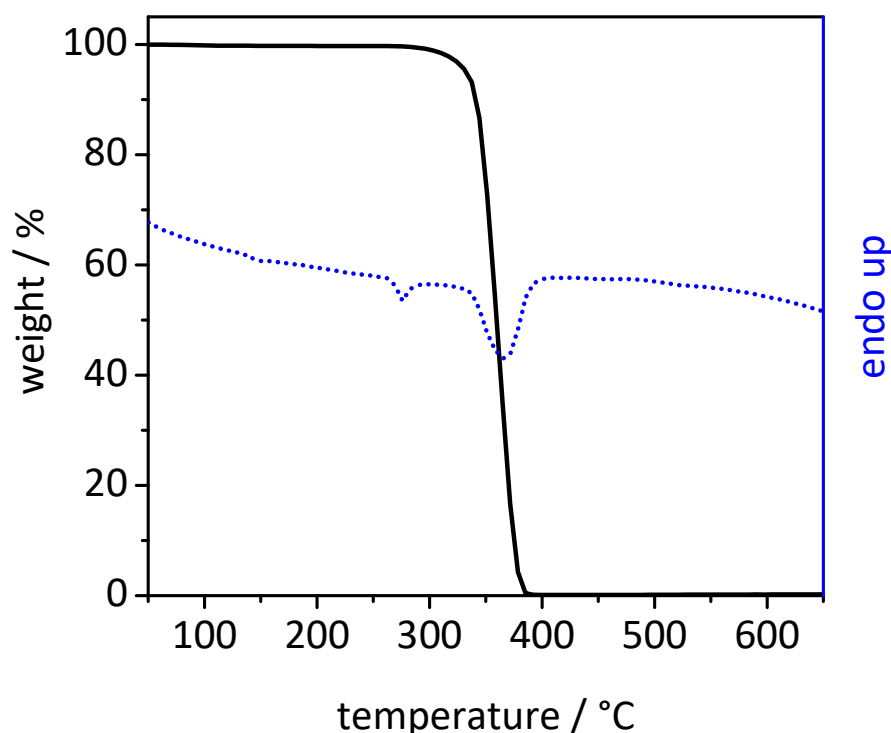


Figure 89. Thermogravimetric (solid line) and simultaneous differential thermal analysis (dashed line) of Tetramethylammonium chloride **3f** measured under nitrogen atmosphere at a heating rate of 10 K/min.

In category **B** no melting, but sublimation of the ammonium salts was detected followed by thermal decomposition at elevated temperatures. Thermal decomposition was confirmed by polarized light microscopy and is indicated by the kink of the TGA curve. Figure 90 shows exemplarily the TGA/DTA curves of **3g** which started to sublime around 300 °C and thermal decomposition occurred above 400 °C. As sublimation and thermal

degradation coincide, a total weight loss of nearly 100% is observed. The same trend was found for the compounds **3a**, **3b**, **3c**, **3d**, **3e**, **3g**, **3i**, **3k**, **3l** and **3m**. For compounds **3i**, **3k**, **3l** and **3m** melting transitions could be detected by polarized light microscopy and the melting point system. These melting transitions were observed at temperatures where already weight loss occurred by sublimation. For that reason it was difficult to detect these melting temperatures by TGA/DTA. For compounds **3a**, **3b**, **3c**, **3d**, and **3e** no melting transitions were observed.

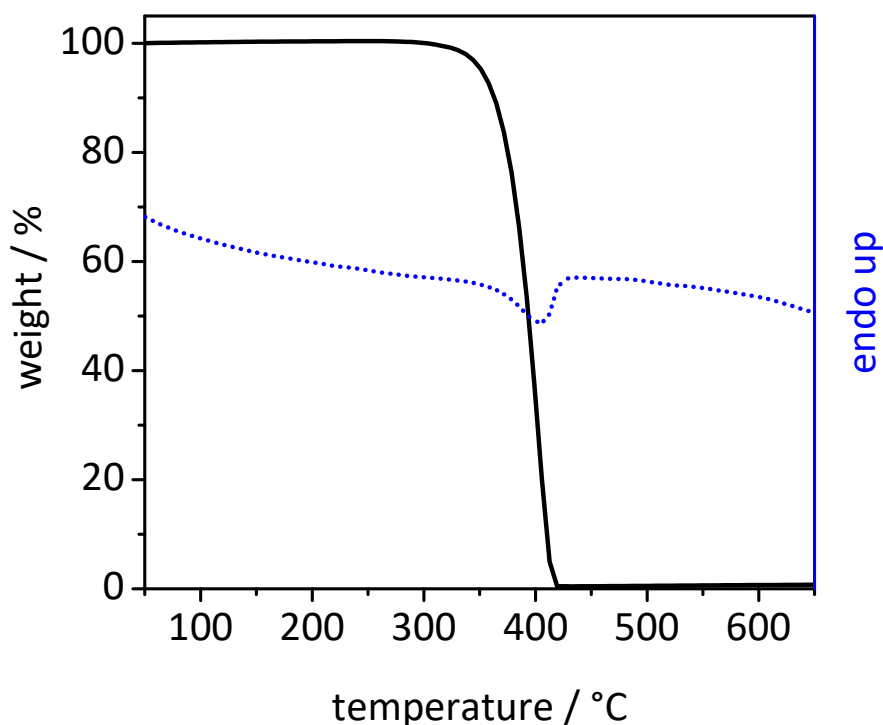


Figure 90. Thermogravimetric (solid line) and simultaneous differential thermal analysis (dashed line) of Tetramethylammonium iodide **3g** measured under nitrogen atmosphere at a heating rate of 10 K/min.

Table 24 summarizes the results from TGA/DTA measurements. No correlation between varying substituents or counter ions and thermal stability could be established. Merely, the temperature at five percent weight loss seems to be higher for compounds with shorter alkyl chain lengths. The propyl substituted ammonium salts **3k**, **3l** and **3m** revealed the lowest thermal stability and displayed weight losses below 250 °C which originated mainly from moisture as already shown for LiCl before. Nevertheless, these ammonium salts are thermally stable up to 250 °C, taking the moisture content into account. In order to avoid sublimation or thermal degradation, low processing temperatures of 245 °C should be selected and the compounds have to be dried prior to compounding. Higher melt temperatures during processing might be applied for the other compounds. However, in

order to ensure comparability concerning the processing conditions, all compounds were processed at 245 °C.

Table 24. Investigated salts, their melting temperatures  $T_m$  (DTA) and temperatures at 5 % weight loss  $T_{-5 \text{ wt\%}}$  (TGA,  $N_2$  atmosphere, 10 K/min).

No.	Compound	$T_m$ [°C]	$T_{-5 \text{ wt\%}}$ [°C]
<b>3a</b>	Tetramethylammonium hexafluorophosphate	-	488
<b>3b</b>	Tetraethylammonium hexafluorophosphate	-	390
<b>3c</b>	Tetrapropylammonium hexafluorophosphate	-	282
<b>3d</b>	Tetrabutylammonium hexafluorophosphate	-	317
<b>3e</b>	Tetrahexylammonium hexafluorophosphate	-	351
<b>3f</b>	Tetramethylammonium chloride	274	330
<b>3g</b>	Tetramethylammonium iodide	-	351
<b>3h</b>	Tetraethylammonium iodide	200	282
<b>3i</b>	Tetraethylammonium chloride	292	262
<b>3j</b>	Tetrapropylammonium tetrafluoroborate	248	350
<b>3k</b>	Tetrapropylammonium bromide	277	244
<b>3l</b>	Tetrapropylammonium chloride	243	227
<b>3m</b>	Tetrapropylammonium iodide	248	227
<b>3n</b>	Tetrabutylammonium tetraphenylborate	241	333

Figure 91 summarizes the crystallization temperatures of PA6 comprising different tetraalkylammonium salts with varying alkyl chain lengths and varying counter ions as function of the additive concentration. The substituents were varied from methyl, ethyl, propyl to butyl and different counter ions such as chloride, iodide, bromide, tetrafluoroborate and tetraphenylborate were used.

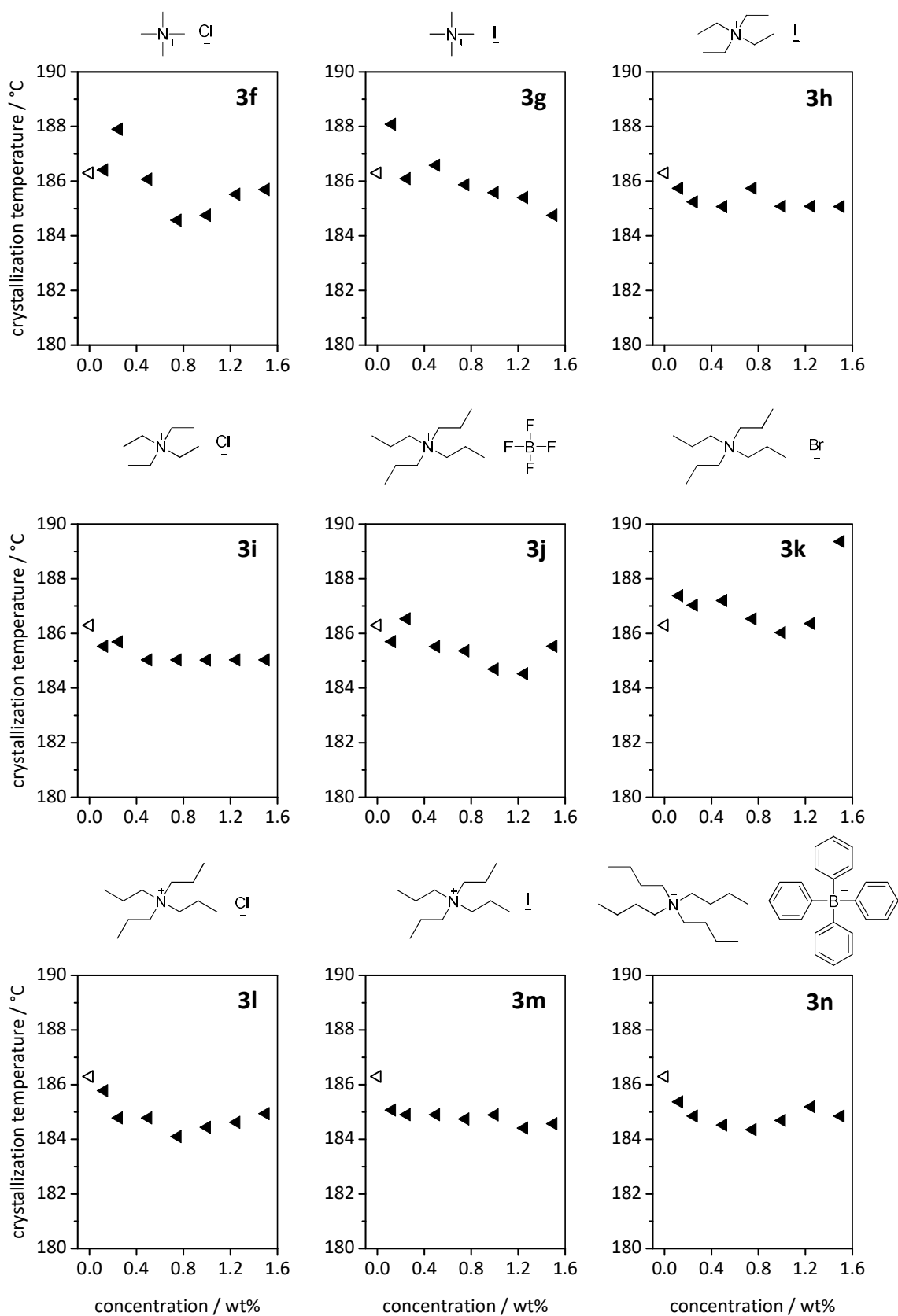


Figure 91. Polymer crystallization temperatures of PA6 comprising tetraalkylammonium salts with varying alkyl chain lengths and varying counter ions as function of the additive concentration. The blank triangle indicates the polymer crystallization temperature of neat PA6 (reference). Polymer melt temperature during processing: 245 °C. DSC heating and cooling rate: 10 K/min.

The tetraalkylammonium salts **3f** – **3j** show almost no anti-nucleation effect. With increasing additive concentration no significant decrease of the polymer crystallization temperature could be observed. A maximum reduction of 1-2 °C was determined, which is almost within the limit of the measurement accuracy of the DSC. Moreover, high fluctuations around 186 °C were especially observed for compounds **3f** and **3g**. The ammonium salt **3k** even showed a slight nucleation effect with a maximum crystallization temperature of 189 °C at 1.5 wt%.

The ammonium salts **3l**, **3m** and **3n** showed a slightly enhanced and more constant anti-nucleation effect compared to the previous ammonium salts **3f** -**3k**. However, a reduction of the polymer crystallization temperature of only 3 °C at its maximum could be achieved. These investigations revealed no relationship with respect to the alkyl chain lengths and particularly the counter ions.

In order to investigate the influence of the alkyl chain length on the anti-nucleation ability of organic ammonium salts in detail, a further series of experiments was conducted based on the results of Tetrabutylammonium hexafluorophosphate **3a** which showed the best results so far. Therefore, several tetraalkylammonium salts with varying alkyl chain length and hexafluorophosphate as counter ion were investigated with respect to their anti-nucleation ability in PA6. Different alkyl substituents come along with a different behavior of the additive in the polymer matrix which may have influence on the crystallization behavior of the polymer. Figure 92 presents the polymer crystallization temperatures of PA6 comprising tetraalkylammonium hexafluorophosphates with varying alkyl chain length (from methyl to hexyl) as function of the additive concentration.

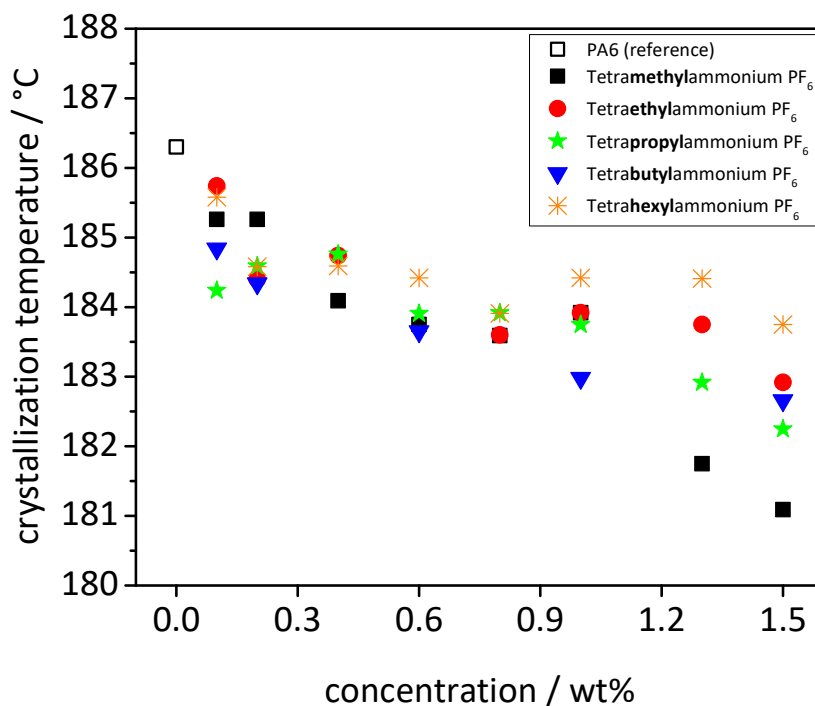


Figure 92. Polymer crystallization temperatures of PA6 comprising tetraalkylammonium hexafluorophosphates with varying alkyl chain lengths (from methyl to hexyl) as function of the additive concentration. The blank square indicates the polymer crystallization temperature of neat PA6 (reference). Polymer melt temperature during processing: 245 °C. DSC heating and cooling rate: 10 K/min. For Tetrabutylammonium PF<sub>6</sub> (blue triangles) no samples were prepared at concentrations of 0.4, 0.8 and 1.3 wt%.

Figure 92 indicates, that all tetraalkylammonium hexafluorophosphates showed anti-nucleation ability in PA6. All investigated additives revealed a decrease of the polymer crystallization temperature with increasing additive concentration. However, no significant correlation between the anti-nucleation effect and the alkyl chain length was observed. The hexyl substituted ammonium salt **3e** showed the worst effect with a maximum reduction of the polymer crystallization temperature by 2 °C at an additive concentration of 1.5 wt%. Whereas the methyl substituted compound **3b** revealed the best anti-nucleation effect with a reduction of the polymer crystallization temperature by 5 °C at the highest additive concentration of 1.5 wt%. All in all, no correlation between alkyl chain length and anti-nucleation effect could be examined.

As already described and investigated before, salts tend to reduce the polymer crystallization temperature as well as the melting temperature at a certain amount of additive. Therefore, the influence of increased amounts of the methyl substituted ammonium salt **3b** on the thermal properties of PA6 were determined. The polymer

crystallization temperature as well as the melting temperature are presented in Figure 93 as function of the additive concentration.

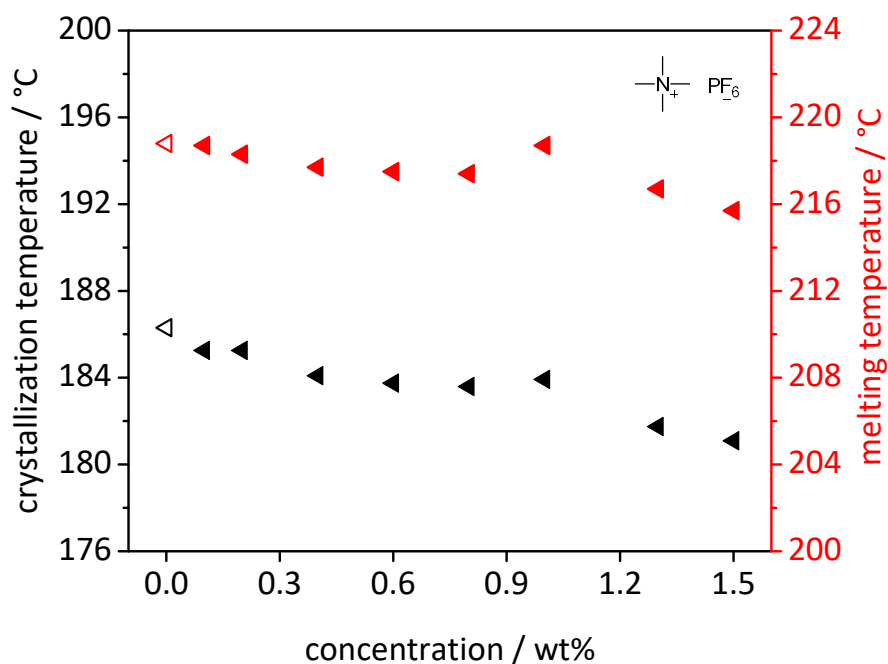


Figure 93. Polymer crystallization temperatures and melting temperatures of PA6 comprising Tetramethylammonium hexafluorophosphate **3b** as function of the additive concentration. The blank triangles indicate the polymer crystallization temperature and melting temperature of neat PA6 (reference). Polymer melt temperature during processing: 245 °C. DSC heating and cooling rate: 10 K/min.

Figure 87 clearly demonstrates that the melting temperature stayed nearly constant around 218 °C up to an additive concentration of 1.0 wt%. With increasing concentration the polymer crystallization temperature was further lowered but also the melting temperature started to drop significantly. This effect is highly undesirable due to a decline of the properties of the polymer.

In conclusion, the investigated organic ammonium salts represent a class of colorless anti-nucleating agents which can reduce the crystallization temperature of PA6 by up to 4 °C without affecting the melting temperature and hence the polymer properties. However, the intensity of Nigrosine as anti-nucleation agent cannot be achieved by the investigated ammonium salts. Depending on the usage, one may face a tradeoff between the strength of the anti-nucleation effect and free choice of color. Possibly, polymers with just a slightly lower polymer crystallization temperature but free choice of color are preferred in some cases.

## 5.3 Azine dyes as anti-nucleating agents for PA6

Takeuchi et al. patented several polycyclic compounds as nucleation inhibitors for semi-crystalline polyamides.<sup>[15]</sup> These compounds exhibit a scaffold consisting of multiple cyclic structures such as phenyl- or cyclohexyl groups leading to a planar and mostly rigid molecule. This work demonstrates that besides charged compounds, planar and rigid structures are also capable of anti-nucleating polyamides. Nigrosine combines both properties within one molecule class. Besides a mostly rigid and planar scaffold, charged groups are present as well. Additionally, Nigrosine contains hetero atoms such as nitrogen. The aim of the following chapter is to combine these structure elements systematically. In order to identify the leading structure elements which are responsible for the anti-nucleation effect, a systematical screening was conducted. Based on Anthracene, as the simplest structure of the Nigrosine scaffold, heteroatoms and finally charges and further substituents are introduced. This series of molecules consists of the commercially available Anthracene, Acridine, Phenazine and Safranin O (Figure 94).

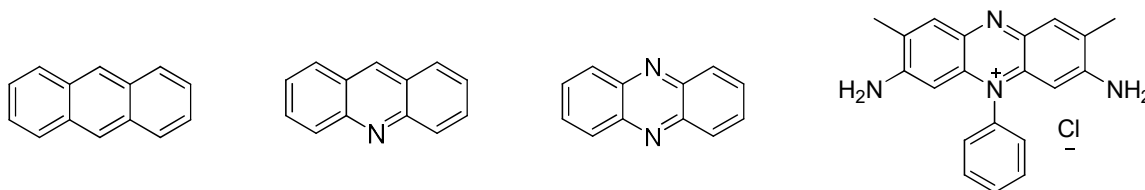


Figure 94. Structures of investigated compounds based on the Nigrosine central core unit: Anthracene, Acridine, Phenazine and Safranin O.

In order to examine their anti-nucleation ability, four concentration series with each compound were prepared. The additives were investigated in a concentration range from 0.01 wt% to 1.5 wt%. In the following, structure-property relations will be systematically discussed. The polymer crystallization temperatures as function of the additive concentrations are presented in Figure 95.



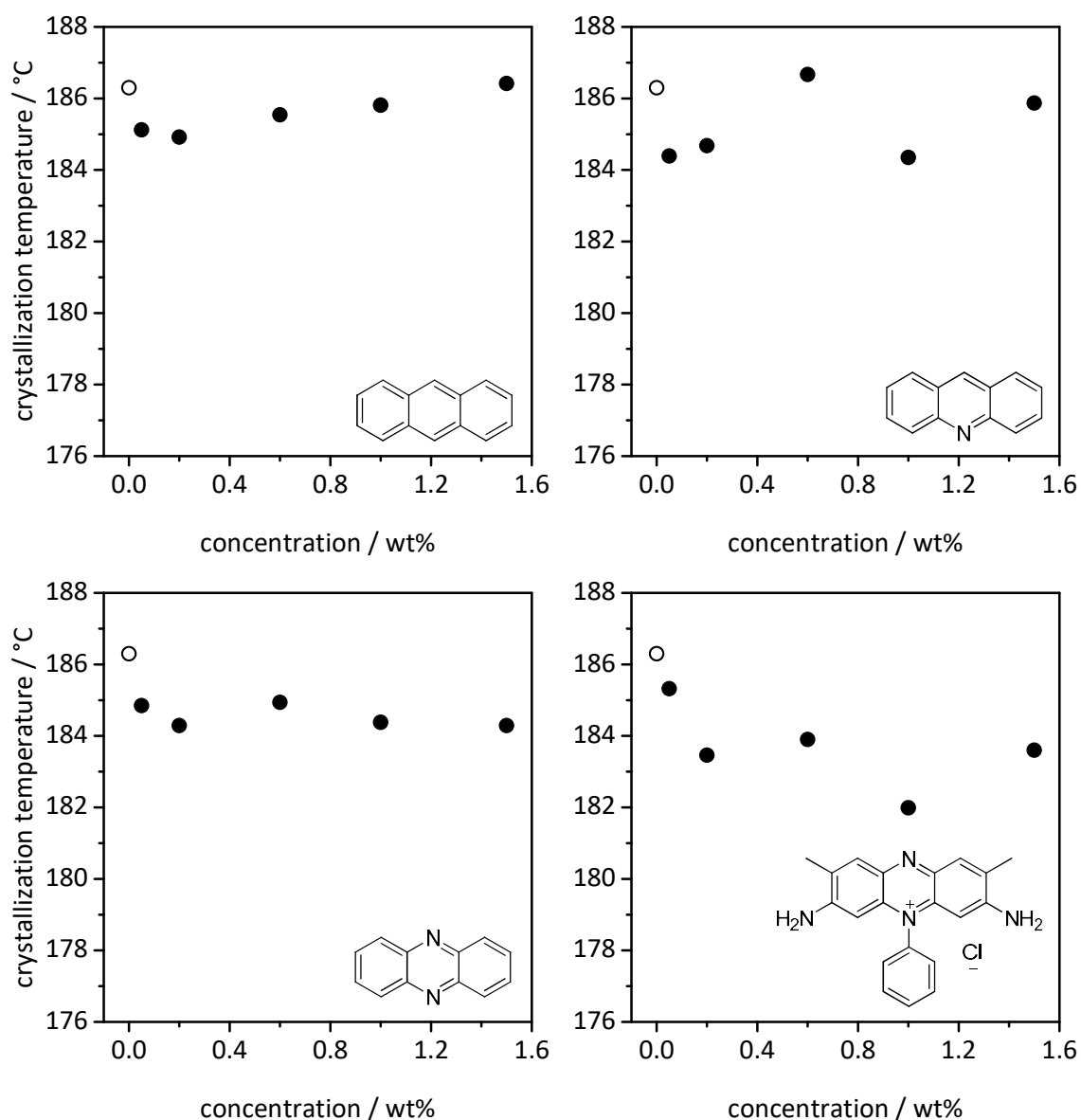


Figure 95. Polymer crystallization temperatures of PA6 comprising Anthracene, Acridine, Phenazine and Safranin O as function of the additive concentration. The blank circles at 186 °C represent the crystallization temperature of neat PA6. Polymer melt temperature during processing: 245 °C. DSC heating and cooling rate: 10 K/min.

The investigations presented in Figure 95 clearly demonstrate that the anti-nucleation ability increases from Anthracene, Acridine, Phenazine to Safranin O. Anthracene showed no significant decrease of the polymer crystallization. Acridine revealed a slight, but extremely inconsistent anti-nucleation effect. The polymer crystallization temperature was decreased by a maximum of 2 °C. Phenazine showed the same strength of anti-nucleation effect as Acridine, but considerably more constant. Safranin O exhibits the highest reduction of the polymer crystallization temperature of PA6 by up to 5 °C at an additive

concentration of 1.0 wt%. Compared to the other compounds, Safranin O exhibits a charged unit and several substituents, such as two amino groups.

By comparing the investigated compounds, it becomes apparent that by introducing nitrogen atoms and finally amino groups, the anti-nucleation effect essentially increased. It is assumed that these structure elements are interacting with the polymer chain. Due to the screening of the amide groups of the polymer by the additives, the polymer crystallization process might be retarded and anti-nucleation is observed. A similar effect was detected by Lin et al. for PA66 additivated with acid dyes.<sup>[33]</sup> Here, a decrease of the crystallization temperature of PA66 was attributed to the formation of coordinate bonds between metal ions of the acid dyes and the amide groups of the polymer chains. This effect was explained by a restriction of the mobility of polymer chains due to the additives, which leads to a retarded crystallization of the polymer.

Based on the good results for Safranin O, in the following chapter several azine dyes will be investigated with respect to their thermal properties and their anti-nucleation ability in PA6.

## 5.3.1 Properties of azine dyes

Previous studies indicate that planar, rigid or charged compounds exhibit the best properties to anti-nucleate polyamides.<sup>[11,15,19,31–33]</sup> For example Takeuchi et al. showed that azine dyes are able to anti-nucleate PA66.<sup>[15]</sup> The huge molecule class of azine dyes represents a type of compound which includes these properties within one molecule. The compounds are mostly rigid and planar, bear charged units and possess functional groups, such as amino substituents. Figure 96 shows the general formula of azine dyes. In this formula  $D^1$  and  $D^2$  stand for an auxochrome group, usually an amino, arylamino, monoalkylamino, dialkylamino, or hydroxyl group. X stands for oxygen, sulphur, or nitrogen with a substituent R (R = hydrogen, alkyl, aryl). Furthermore, the azine dyes include cationic, anionic, and neutral dyes, depending on the kinds of auxochrome groups and substituents.<sup>[147]</sup>

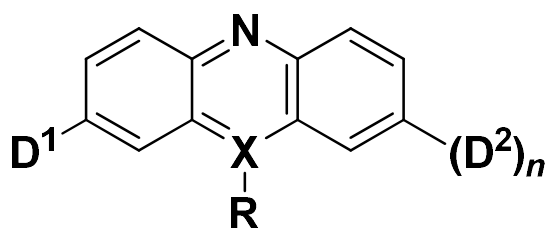


Figure 96. General formula of azine dyes.  $D^1$  and  $D^2$  stand for an auxochrome group. X stands for oxygen, sulphur, or nitrogen with a substituent R (R = hydrogen, alkyl, aryl).

The azine dyes include phenazine, oxazine and thiazine dyes. Those derivatives exhibit good thermal stability and are already used for staining in medicine, bacteriology and microscopy.<sup>[147]</sup> Furthermore, azine dyes are applied for coloring wool, leather, inks and polymer resins.<sup>[147]</sup>

These are all reasons to test the applicability of azine dyes as anti-nucleating agent for PA6. Therefore, various compounds with varying substituents and different functional groups are investigated systematically within the following chapter. Besides nitrogen, these azine dyes contain also sulphur and oxygen atoms. Moreover, all investigated compounds exhibit amine groups. Besides sulfonate and ferrate anions, most of the compounds exhibit chloride counter ions. Table 25 summarizes the molecular formulas of the investigated compounds.

Table 25. Labels and structures of investigated compounds for anti-nucleation of PA6.

No.	compound	No.	compound
4a		4g	
4b		4h	
4c		4i	
4d		4j	
4e		4k	
4f			

First, the thermal properties of the investigated compounds were determined to verify the suitability of the compounds at the applied processing temperatures. Therefore, combined thermogravimetric analysis (TGA) and differential thermal analysis (DTA) of the neat compounds was conducted. With respect to the thermal properties, the investigated

compounds can be categorized into two categories that will be described in detail in the following.

Compounds in category **A** showed a melting transition followed by the evaporation from the liquid phase and subsequent degradation which is indicated by the kink of the TGA curve at elevated temperatures. A weight loss of 100% was observed for none of the investigated compounds. At temperatures around 650 °C all compounds exhibited a weight loss between 40% to 60%. Figure 97 shows the TGA/DTA diagram exemplarily for category **A** of Azure A Chloride **4h**, which has a melting transition at 194 °C. The five percent weight loss ( $T_{-5\text{wt}\%}$ ) is at 221 °C. Weight loss occurred already at temperatures around 100 °C, which can be ascribed to volatile low molecular compounds, water or solvent residuals. These impurities falsify the value for the five percent weight loss. By studying the TGA curve it becomes clear that weight loss induced due evaporation, sublimation or degradation of the compound starts first at around 250 °C. Similar thermal behavior was observed for compounds **4b**, **4e**, **4f**, **4g**, **4i** and **4j**. However, it has to be considered that these compounds might comprise volatiles, and hence have to be dried before compounding.

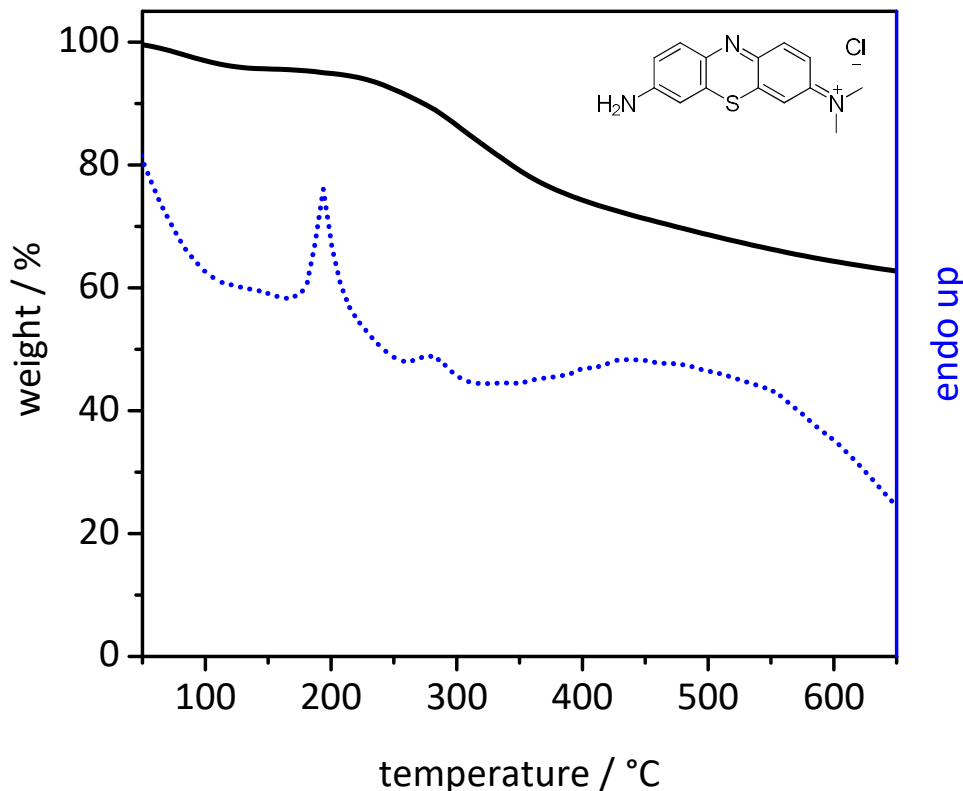


Figure 97. Thermogravimetric analysis (solid line) and simultaneous differential thermal analysis (dotted line) of Azure A Chloride **4h**, measured under nitrogen atmosphere at a heating rate of 10 K/min.

In category **B** no melting, but sublimation of the azine dyes was detected, followed by thermal decomposition at elevated temperatures which is indicated by the kink of the TGA curve. Figure 98 shows the TGA/DTA curves exemplarily for category **B** of Safranin O **4a**, which started to sublime at around 300 °C and thermal decomposition occurred above 350 °C. A weight loss of 100% was observed for none of the investigated compounds. At temperatures around 650 °C all compounds exhibited a weight loss between 40% to 60%. The same trend was found for the compounds **4c**, **4d** and **4k**. For compounds **4d** and **4k** also a weight loss occurred already at temperatures around 100 °C which can be ascribed to volatiles as already described for category **A**. However, it has to be considered that these compounds have to be dried before compounding.

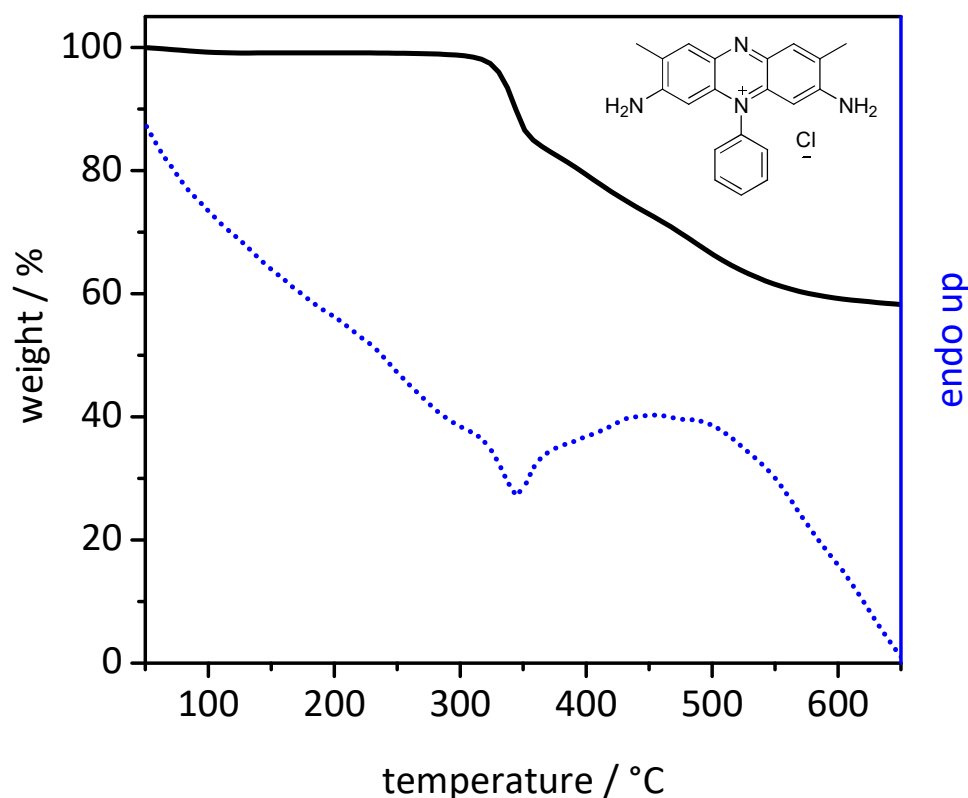


Figure 98. Thermogravimetric analysis (solid line) and simultaneous differential thermal analysis (dotted line) of Safranin O **4a**, measured under nitrogen atmosphere at a heating rate of 10 K/min.

Table 26 summarizes the results of the TGA/DTA measurements. By taking the weight loss induced by volatiles at low temperatures into account, all azine dyes are thermally stable up to 250 °C and hence suitable for the addition of PA6. In order to avoid impurities during polymer processing all investigated compounds were dried prior to compounding.

Table 26. Investigated azine dyes, melting temperatures  $T_m$  (DTA) and temperatures at 5 % weight loss  $T_{-5 \text{ wt\%}}$  (TGA, 10 K/min,  $N_2$  atmosphere).

No.	Compound	$T_m$ [°C]	$T_{-5 \text{ wt\%}}$ [°C]
<b>4a</b>	Safranine O	-	330
<b>4b</b>	Methylene Violet 3RAX	289	282
<b>4c</b>	Induline	-	235
<b>4d</b>	Darrow Red	-	139
<b>4e</b>	Pyronin B	248	255
<b>4f</b>	Nile Blue Chloride	282	260
<b>4g</b>	Nile Blue A	276	228
<b>4h</b>	Azure A Chloride	194	221
<b>4i</b>	Giemsa Stain	200	235
<b>4j</b>	Toluidine Blue O	208	235
<b>4k</b>	Pyronin Y	-	201

## 5.3.2 Anti-nucleation of PA6 by azine dyes

In the following, investigations on the influence of various azine dyes on the thermal properties of PA6 will be discussed. Nigrosine, which can be assigned to the class of azine dyes, showed its best anti-nucleation effect at temperatures around 270 °C. At this temperature, enhanced solubility of the additive and an increase of the anti-nucleation effect was observed. In order to avoid possible solubility issues for the subsequent compounding experiments, four different melt temperatures during processing were applied to identify the ideal processing conditions for each compound. For each processing temperature (measured melt temperature during compounding) one sample with an additive concentration of 1.5 wt% was prepared. The polymer crystallization and melting temperatures were obtained from DSC measurements. The polymer crystallization temperatures are reported as the temperature at the exothermic minimum of the cooling curve and melting temperatures are reported at the endothermic maximum of the heating curve. Exemplary, DSC heating and cooling curves of PA6 comprising 1.5 wt% Safranin O **4a** processed at 245 °C, 259 °C, 273 °C and 283 °C are presented in Figure 99.

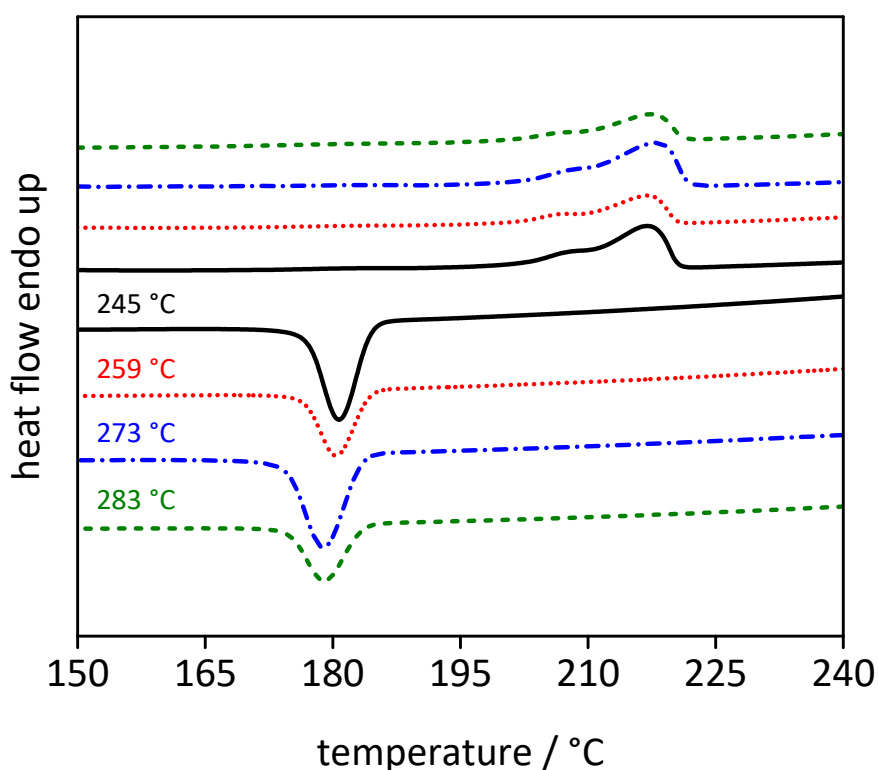


Figure 99. Second heating and cooling curves of PA6 comprising 1.5 wt% Safranin O **4a** processed at temperatures as indicated. DSC heating and cooling rate: 10 K/min.



In order to get a better overview, the results are presented in a simplified way by plotting the crystallization and melting temperatures as function of the melt temperatures during processing for each polymer/additive compound. Figure 100 shows the results for Safranin O.

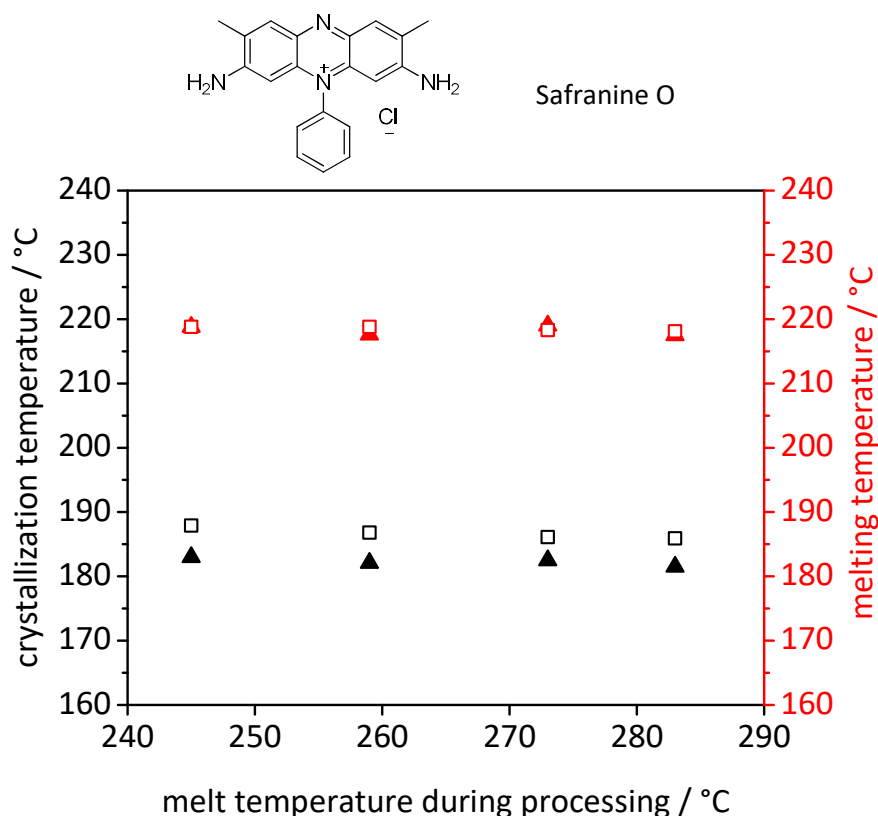


Figure 100. Crystallization and melting temperatures of neat PA6 (□ crystallization, □ melting) and PA6 comprising 1.5 wt% Safranin O **4a** (▲ crystallization, ▲ melting) as function of the melt temperature during processing. DSC heating and cooling rate: 10 K/min.

As demonstrated above, Safranin O revealed a reduction of the polymer crystallization temperature by 5 °C with no influence on the melting temperature of PA6. The variation of the melt temperature during processing induced no enhancement of the anti-nucleation ability.

Figure 101 presents the results for compounds **4b** and **4c**. Both dyes showed quite similar effects on the thermal behavior of PA6. The polymer crystallization temperature was slightly decreased by 2 °C. The polymer melting temperature stayed almost unaffected and different processing temperatures had no influence on the additive performance.

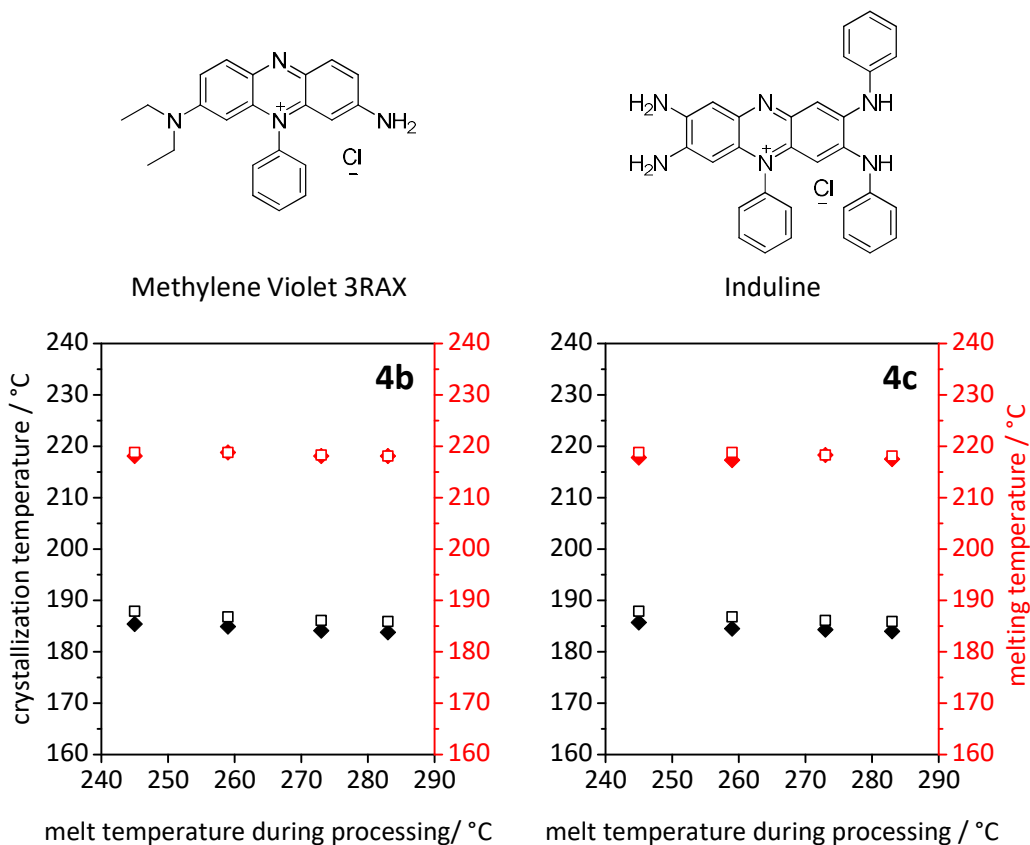


Figure 101. Crystallization and melting temperatures of neat PA6 (□ crystallization, □ melting) and PA6 comprising 1.5 wt% Methylene Violet 3RAX **4b**, and Induline **4c** (◆ crystallization, ◆ melting) as function of the melt temperature during processing. DSC heating and cooling rate: 10 K/min.

By comparing the chemical structures of **4a** - **4c**, all compounds exhibit a four ring-membered scaffold and chloride as counter ion. However, all structures differ concerning their substituents. Here, some reasons for the different effect in PA6 may be derived. Methylene Violet 3RAX holds one amino group, whereas Safranin O and Induline exhibit two amino groups. Besides the ionic character, these amino groups may be able to interact with the polyamide chain and retard the polymer crystallization process. In contrast to Induline, Safranin O revealed a significant better anti-nucleation effect. This effect might be explained by the position of the amino groups. It can be assumed that Safranin O is able to interact with two polymer chains at the same time, whereas Induline interacts only with one amide group of the polymer.

Compared to the compounds **4a** - **4c**, the compounds **4d** - **4g** are based on a three ring-membered scaffold with an ether and nitrogen group, called phenoxazines. As shown in Figure 102, the crystallization temperatures could be decreased by 3 °C for Pyronin B, 4 °C for Darrow Red, 5 °C for Nile Blue A and 6 °C for Nile Blue Chloride. Furthermore, the

polymer melting temperatures were also slightly decreased between 1 °C and 2 °C. The different processing temperatures did not influence the performance of the additives.

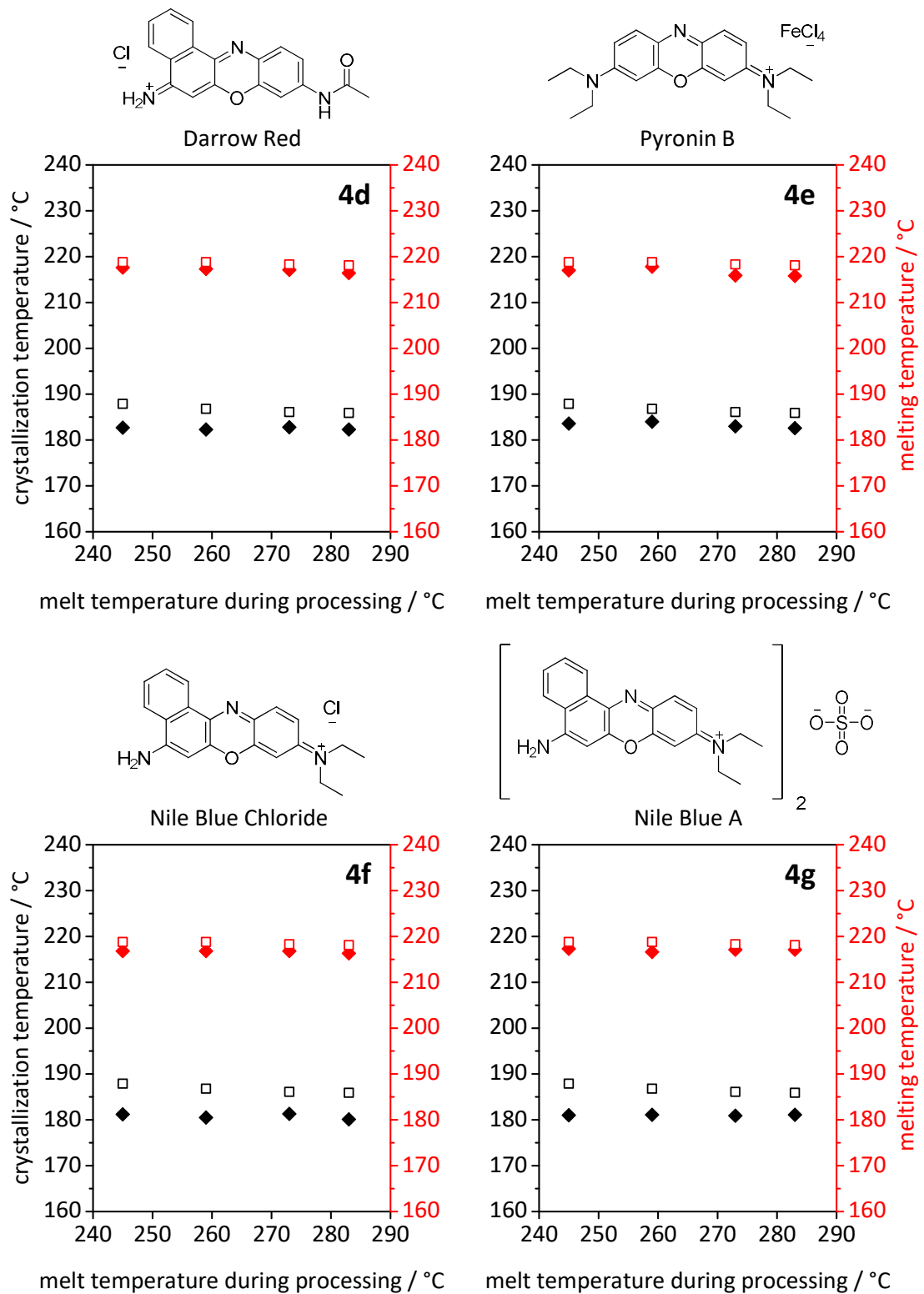


Figure 102. Crystallization and melting temperatures of neat PA6 (□ crystallization, □ melting) and PA6 comprising 1.5 wt% Darrow Red, Pyronin B, Nile Blue Chloride and Nile Blue A (◆ crystallization, ◆ melting) as function of the melt temperature during processing. DSC heating and cooling rate: 10 K/min.

By comparing the chemical structures of the additives, Pyronin B is the only compound with ferrate as counter ion and no amino group. Moreover, Pyronin B revealed the worst anti-nucleation effect compared to **4d**, **4f** and **4g**. By the lack of the amino group, less interaction with the polymer chain might lead to a less pronounced anti-nucleation effect. However, compared to compounds **4b** – **4c**, derivatives **4d** – **4g** revealed a significant reduction of the polymer crystallization temperature. Moreover, it was confirmed that compounds with structure elements such as sulphur-, amino-, and ionic groups are capable of anti-nucleating PA6.

Figure 103 presents the influence of phenothiazines **4h** – **4j**, and the phenoxazine **4k** on the thermal properties of PA6. The phenothiazines are similar to phenoxazines and distinguish themselves by a sulphur instead of the ether bridge. Compounds **4h** – **4k** showed a significant effect on the crystallization temperature of PA6. The polymer crystallization temperatures could be decreased by up to 8 °C for all compounds. Elevated melt temperatures during processing showed no enhancement of the anti-nucleation performance of the additives. The melting temperatures of the polymer were slightly decreased by 1 °C for Azure A Chloride **4h** and Toluidine Blue O **4j**, and by 2 °C for Giemsa Stain **4i** and Pyronin Y **4k**. These deviations of the polymer melting temperatures should be tolerable and not significantly influence further polymer properties.

Compared to compounds **4d** – **4g**, the azine dyes **4h** – **4k** showed significantly enhanced anti-nucleation properties. This effect might be explained by the differing substituents. Compounds **4d** – **4g** exhibit phenyl rings and ethanaminium substituents. Compounds **4h** – **4k** merely bear methyl groups and methanaminium substituents which are distinctly less steric. The aminium ions of the ethanaminium groups are screened by the ethyl substituents, and thus may be less effective in interacting with the polymer. Consequently, it can be assumed that compounds **4h** – **4k** are more flexible in interacting with the polyamide chains and hence represent more effective anti-nucleating agents.

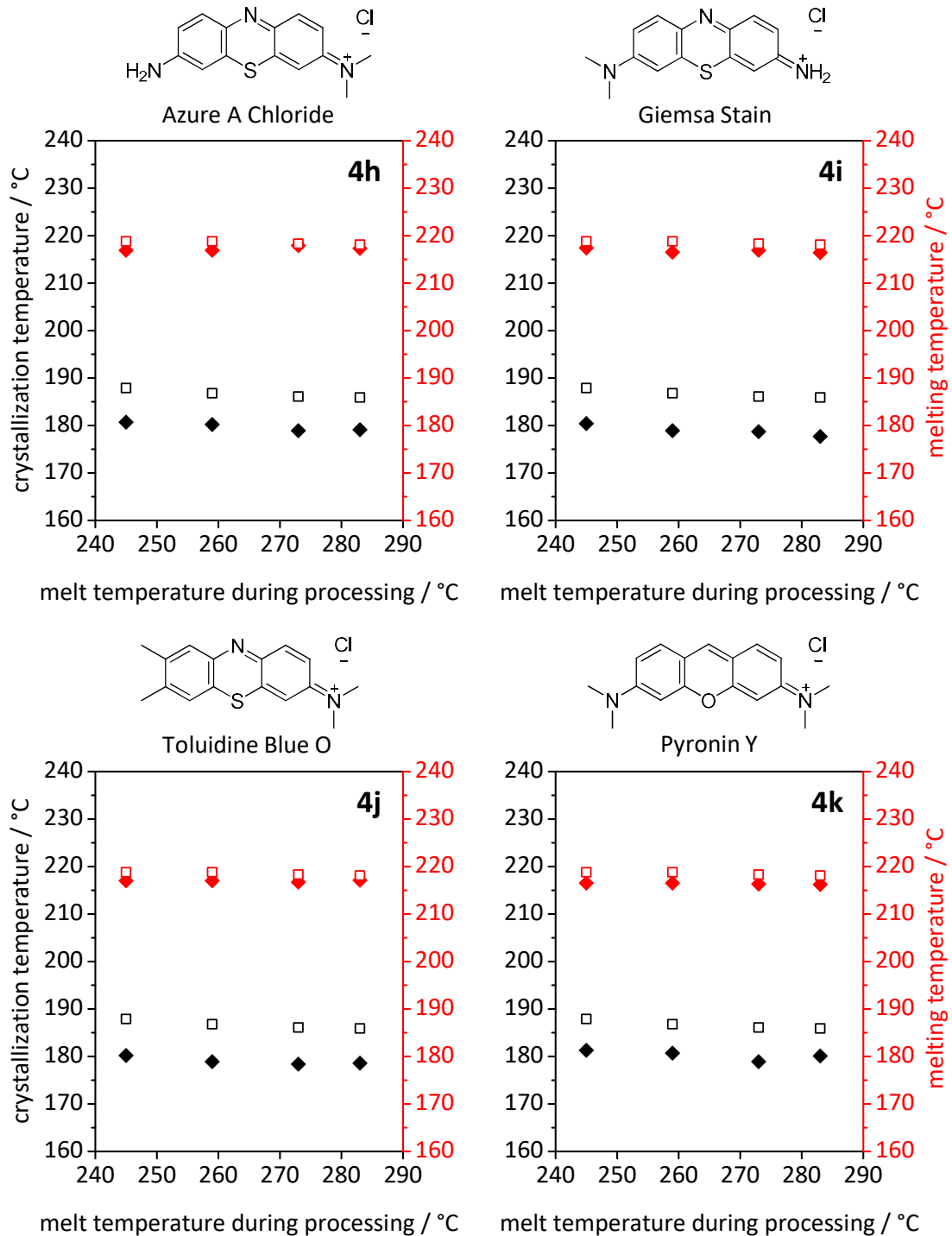


Figure 103. Crystallization and melting temperatures of neat PA6 (□ crystallization, □ melting) and PA6 comprising 1.5 wt% Azure A Chloride, Giemsa Stain, Toluidine Blue O and Pyronin Y (◆ crystallization, ◆ melting) as function of the melt temperature during processing. DSC heating and cooling rate: 10 K/min.

All compounds within this chapter were investigated at four different processing temperatures at a concentration of 1.5 wt%. In order to test the influence of the concentration on the thermal properties of PA6, exemplarily a concentration series of Pyronin Y was prepared. The detailed procedure is explained in the experimental section.

The polymer melt temperature during processing for this experiment was set to 259 °C. The results are presented in Figure 104.

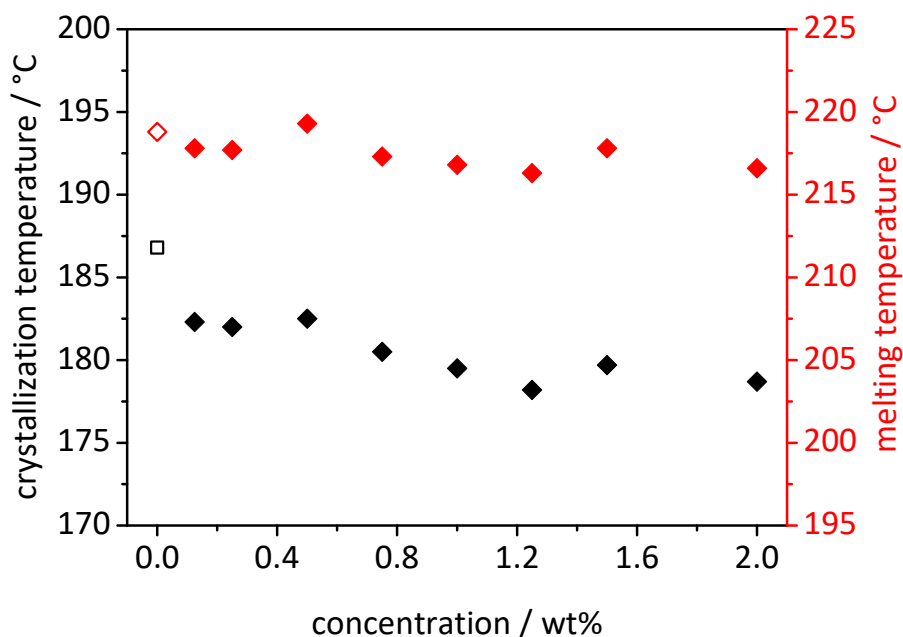


Figure 104. Crystallization temperatures and melting temperatures of PA6 comprising Pyronin Y as function of the additive concentration. The blank squares indicate the polymer crystallization temperature and melting temperature of neat PA6 (reference). Polymer melt temperature during processing: 259 °C. DSC heating and cooling rate: 10 K/min.

Figure 104 shows an increasing anti-nucleation ability with increasing additive concentration. However, already at low concentrations of 0.1 wt% a reduction of the polymer crystallization temperature by 4 °C could be achieved. At an additive concentration of 1.25 wt% the polymer crystallization temperature was reduced to 178 °C which implies a decrease by 8 °C. The melting temperature exhibited a decline of 2 °C. At concentrations above 1.25 wt% no further enhancement of the anti-nucleation ability was achieved. It can be assumed that additive concentrations above 2.0 wt% might decrease the polymer crystallization temperature even more, but a coincident decline of the melting temperature can be expected.

The investigations within this chapter confirmed the aforementioned assumptions. Compounds with a mostly planar and rigid structure as well as ionic character are good anti-nucleating agents. Especially, units which are capable of interacting with the hydrogen bonding units of the polymer chains during the crystallization process seem to be of particular importance. These include sulphur-, amino-, or ionic groups. Furthermore, attention should be paid to compounds which show good solubility in the polymer melt in

order to achieve ideal efficiencies of the additives. In contrast to supramolecular nucleating agents, self-assembly or aggregation of the anti-nucleation additives is undesirable. The groups which seem to be responsible for the retardation of the crystallization process should be accessible for the amide groups of the polyamide chain and not be blocked due to steric substituents. Figure 105 summarizes the achievable crystallization temperatures of PA6 with 1.5 wt% of the investigated azine dyes.

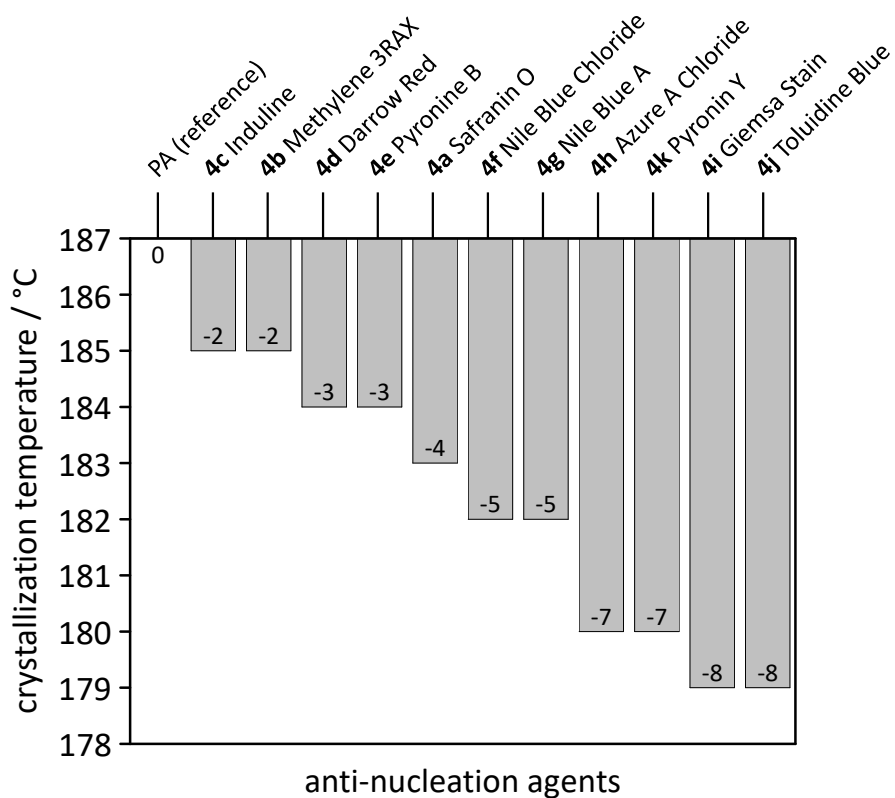


Figure 105. Crystallization temperatures of PA6 comprising the investigated anti-nucleation agents with a concentration of 1.5 wt% and processed at 273 °C.

#### 5.4 Neutral Red as anti-nucleating agent for PA6

The previous chapter revealed azine dyes as good anti-nucleation agents. This class of compounds combines all features required for an effective anti-nucleating agent. Besides a rigid and planar structure, hydrogen bonding units such as amino groups as well as charged groups are unified within one molecule. These properties seem to be indispensable in order to retard the polymer crystallization of polyamides.

The following chapter will give a detailed insight concerning the way of functioning of an anti-nucleating agent on the basis of Neutral Red. Neutral Red belongs to the class of azine dyes and exhibits all features required to anti-nucleate PA6 effectively. Figure 106 shows the structural formula of Neutral Red.

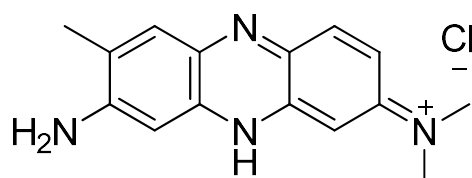


Figure 106. Structural formula of Neutral Red.

First, significant properties of neat Neutral Red are presented and thermal properties are determined. Furthermore, the influence of various processing conditions on the anti-nucleation behavior of Neutral Red in PA6 will be investigated in detail. Additionally, morphology investigations will be conducted and the influence on properties such as crystal modification, degree of crystallinity, and glass transition temperature are examined.



## 5.4.1 Properties of Neutral Red

Neutral Red belongs to the class of eurohodines, which are a subcategory of the class of diaminophenazine dyes. The eurohodines bear a hydrogen atom or an alkyl group on the azine nitrogen atom.<sup>[147]</sup> Neutral Red features several elements which are essential for anti-nucleating polyamides. Besides three amine groups, a methylaminium group with chloride as counter ion are available. Additionally, no steric substituents which might screen these groups are existing. Neutral Red is synthesized by condensation of p-nitrosodimethylaniline hydrochloride and 2,4-diaminotoluene yielding a dark-green powder.<sup>[147,150,163]</sup> The reaction pathway is schematically presented in Figure 107.

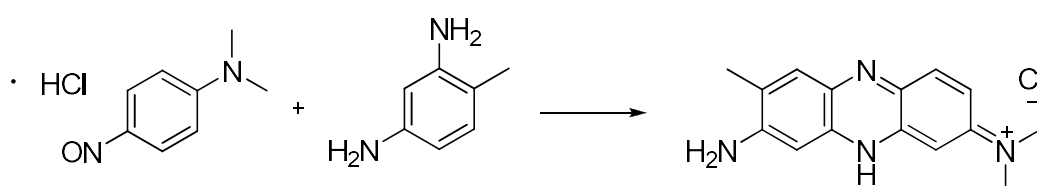


Figure 107. Synthesis route of Neutral Red by condensation of p-nitrosodimethylaniline and 2,4-diaminotoluene in presence of hydrochloric acid.

Neutral Red is known to be used for cell staining or coloring wool, cellulose, polyamides or polyolefines. Moreover, Neutral Red is applicable as a pH indicator, changing from red to yellow between pH 6.8 and 8.0.<sup>[147,150]</sup>

Extensive literature research revealed no publications regarding the influence of Neutral Red on the thermal behavior of polyamides. Before investigating the anti-nucleation ability of Neutral Red in PA6, the thermal properties were determined by means of combined thermogravimetric analysis (TGA) and differential thermal analysis (DTA) to verify the suitability of the compound at processing temperatures of PA6. Figure 108 shows the thermogravimetric analysis (solid line) and simultaneous thermal analysis (dotted line) of Neutral Red.

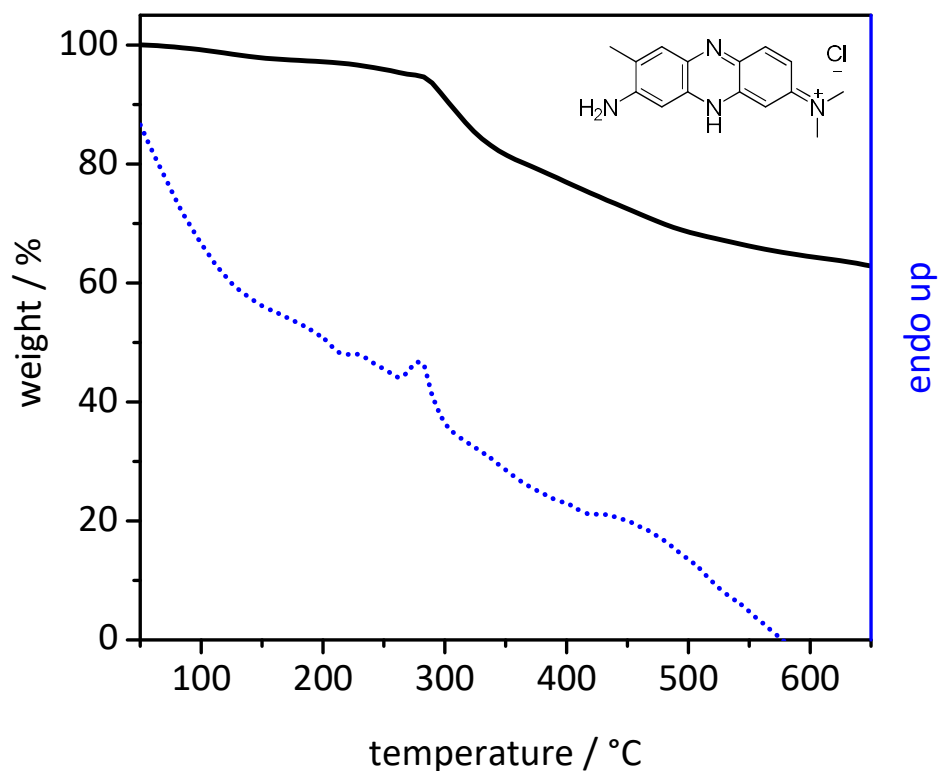


Figure 108. Thermogravimetric (solid line) and simultaneous differential thermal analysis (dashed line) analysis of Neutral Red, measured under nitrogen atmosphere at a heating rate of 10 K/min.

The thermal analysis of Neutral Red revealed a slight weight loss at temperatures around 150 °C which drastically increased at temperatures above 290 °C. The weight loss at lower temperatures can be ascribed to volatile low molecular compounds or solvent residuals, whereas the weight loss above 290 °C indicates evaporation with subsequent thermal degradation at elevated temperatures. These observations can be confirmed by the DTA curve which shows a melting endotherm at 290 °C. The results reveal a thermal stability of Neutral Red up to 300 °C.

#### 5.4.2 Anti-nucleation of PA6 by Neutral Red

In the following, the anti-nucleation ability of Neutral Red in PA6 will be discussed in detail. The influence of Neutral Red on the thermal behavior of PA6 will be investigated at different processing temperatures and processing times as well as various additive concentrations. Here, the focus is on the enhancement of the solubility of the additive in the polymer melt, which is verified by optical polarized microscopy. The polymer crystallization and melting temperatures are obtained from DSC measurements. Furthermore, the influence of Neutral Red on the polymer morphology of PA6 is determined by means of polarized light microscopy. For experimental parameters and details refer to chapter 8.

##### *Standard processing conditions*

Figure 109 presents the polymer crystallization temperatures of PA6 comprising Neutral Red as function of the additive concentration processed at 245 °C. The sample for optical microscopy was obtained by melting a polymer pellet of the extruded compound between two glass slides at 250 °C and subsequent quenching to room temperature.

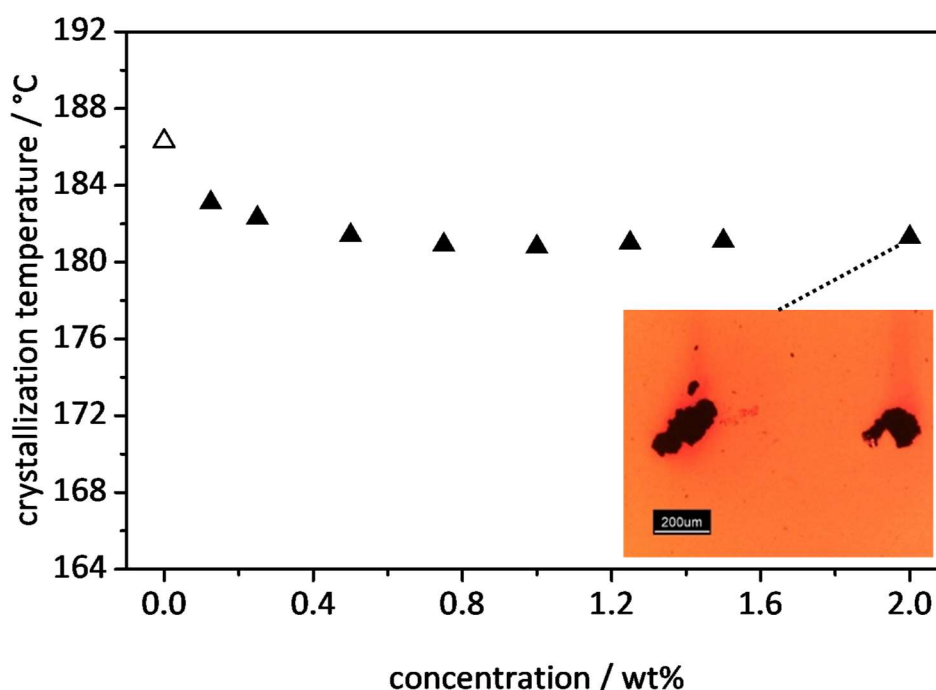


Figure 109. Polymer crystallization temperatures of PA6 comprising Neutral Red as function of the additive concentration and optical micrograph from polarized light microscopy of PA6 with 2.0 wt% of Neutral Red. The non-dissolved additive shows up as black aggregates. The blank triangle indicates the polymer crystallization temperature of neat PA6 (reference). Polymer melt temperature during processing: 245 °C. DSC heating and cooling rate: 10 K/min.

Figure 109 demonstrates a decrease of the polymer crystallization temperature with increasing concentration of Neutral Red to a minimum crystallization temperature of 181 °C. At additive concentrations above 0.8 wt% no further enhancement of the anti-nucleation effect was observed. The crystallization temperatures stayed constant for additive concentrations up to 2.0 wt% at 181 °C.

By examining the compounded samples by polarized light microscopy, micrographs revealed black aggregates. The image in Figure 109 shows a sample of PA6 comprising 2.0 wt% Neutral Red containing black crumbs with diameters up to 250  $\mu\text{m}$ . These aggregates must originate from poorly dissolved Neutral Red. Due to the fast quenching, no spherulites are visible. These results lead to the conclusion that a small portion of Neutral Red is soluble in the polymer melt at processing temperatures of 245 °C. Consequently, a slight anti-nucleation effect was observed. Similar observation were made for Colorant Black 500 in chapter 5.1.

In order to increase the solubility of Neutral Red, the processing time was increased up to 60 min. Figure 110 presents the crystallization and melting temperatures of PA6 comprising 1.5 wt% Neutral Red as function of the processing time. The processing time is defined as time how long the polymer remains in the extruder during compounding.

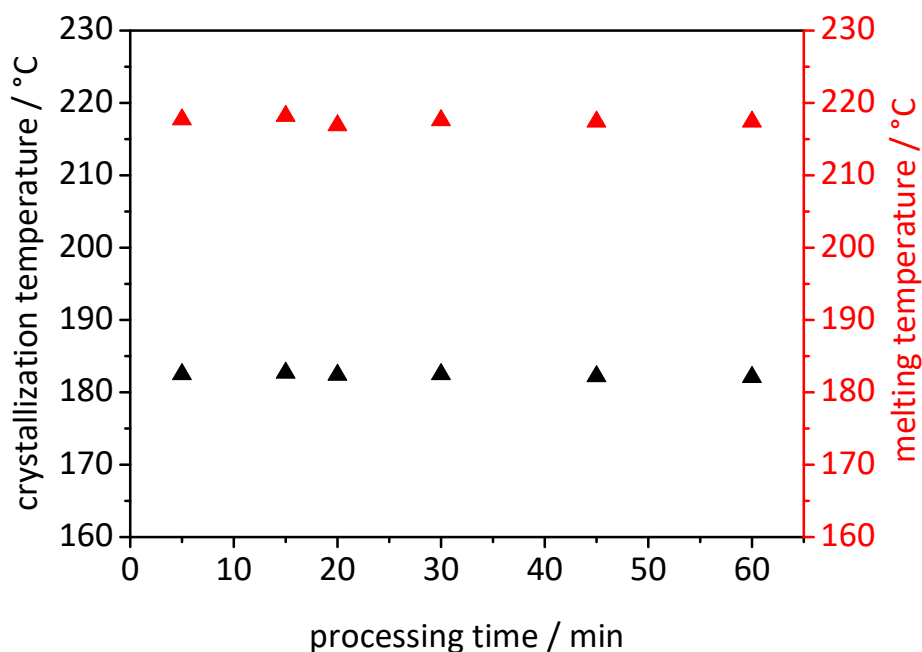


Figure 110. Crystallization and melting temperatures of PA6 comprising 1.5 wt% Neutral Red as function of the processing time. The processing time is defined as time how long the polymer remains in the extruder during compounding. Polymer melt temperature during processing: 245°C. DSC heating and cooling rate: 10 K/min.

As shown in Figure 110, the processing time had no influence of the anti-nucleation performance of Neutral Red at a processing temperature of 245 °C. It can be assumed that no better solubility of Neutral Red was achieved.

#### *Elevated melt temperatures during processing*

The investigations of the thermal properties of neat Neutral Red revealed a melting temperature of Neutral Red around 290 °C. This might lead to the assumption that the melt temperature during processing of 245 °C is too low to dissolve the compound well enough. Similar investigations were made for Colorant Black 500 in chapter 5.1.

Task of this chapter will be to enhance the anti-nucleation effect of Neutral Red by increasing the solubility of Neutral Red in the polymer melt due to increased melt temperatures during processing. Therefore, PA6 comprising 1.5 wt% Neutral Red was processed at elevated processing temperatures of 245 °C, 259 °C, 273 °C and 283 °C. Figure 111 presents the corresponding polymer crystallization and polymer melting temperatures as function of the melt temperature during processing.

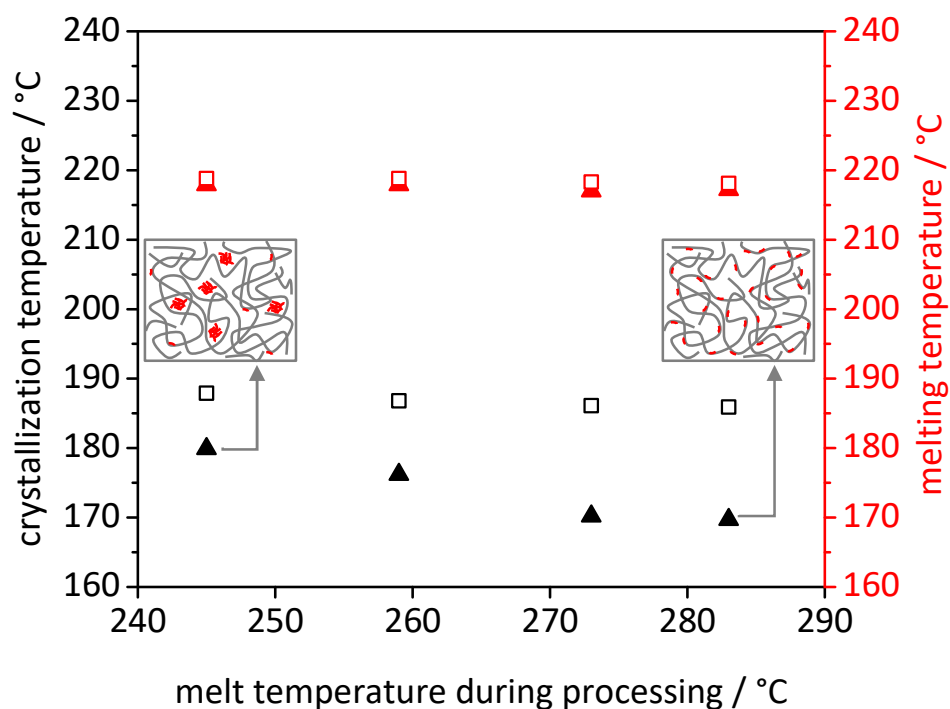


Figure 111. Crystallization and melting temperatures of neat PA6 (□ crystallization, □ melting) and PA6 comprising 1.5 wt% Neutral Red (▲ crystallization, ▲ melting) as function of the melt temperature during processing. The insets show the schematic state of the additive in the polymer melt at the corresponding processing temperature. DSC heating and cooling rate: 10 K/min.

As shown in Figure 111, a significant influence of the melt temperature during processing on the crystallization temperature of PA6 comprising Neutral Red was observed. The polymer crystallization temperature was reduced from 180 °C at a processing temperature of 245 °C to a polymer crystallization temperature of 170 °C for a processing temperature of 283 °C. This means a reduction of 10 °C for the polymer crystallization temperature due to elevated processing temperatures with the same amount of additive. These results may confirm the assumptions that elevated melt temperatures during processing lead to a better solubility of additive which results in an enhanced anti-nucleation performance. The effect is schematically indicated by the images in Figure 111. Besides a reduction of the polymer crystallization temperature, a special benefit is the retention of the melting temperature for the additivated PA6 at elevated processing temperatures.

In order to investigate this positive effect in detail, four concentration series of PA6 comprising Neutral Red at four different processing temperatures were conducted and the obtained samples were observed by polarized light microscopy. The results are summarized in Figure 112.

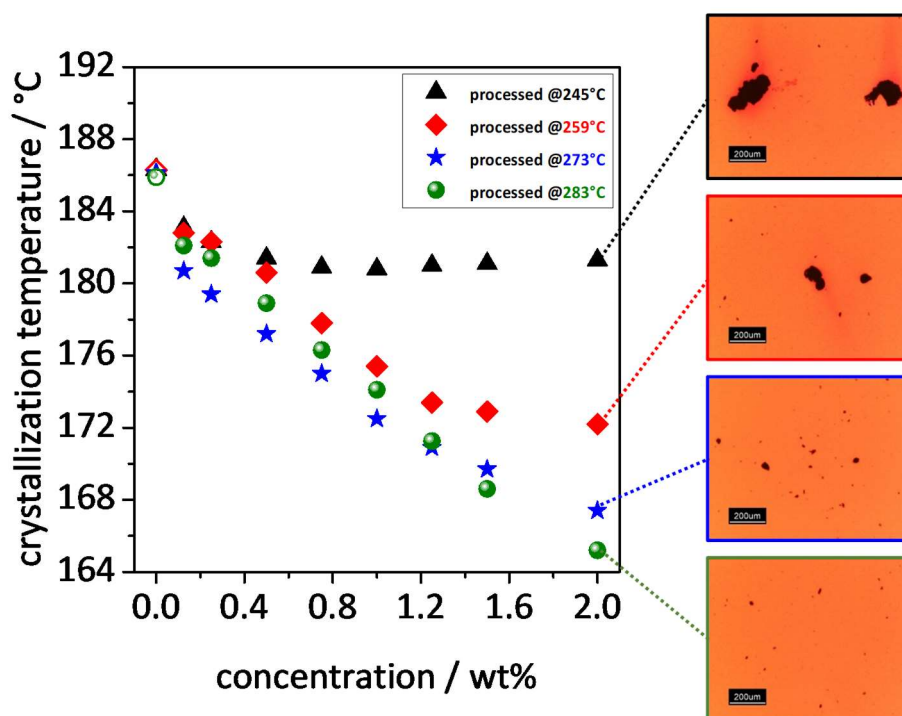


Figure 112. Left: Crystallization temperatures of PA6 containing Neutral Red as function of the additive concentration. Different symbols indicate different processing temperatures: 245 °C (triangles), 259 °C (diamonds), 273 °C (stars) and 283 °C (circles). DSC heating and cooling rate: 10 K/min. Right: Optical micrographs from polarized light microscopy of PA6 with 2.0 wt% of Neutral Red processed at different temperatures. The compounded polymer pellets were heated, kept at 250 °C for 5 min and quenched to room temperature. The polymer appears orange due to the  $\lambda/4$  platelet. The non-dispersed additive shows up as black aggregates.

Figure 112 substantiates the previously made results. At low additive concentrations no significant difference of the polymer crystallization could be made. However, when considering higher additive concentrations significant influence of the processing temperatures occurred. This approves the suspicion that a small amount of Neutral Red is well dissolved even at low melt temperatures during processing. This leads to a slight anti-nucleation effect. With increasing additive concentration the influence of the processing temperature rises and the polymer crystallization temperatures differ significantly for the same amount of additive, but different processing temperatures. The polymer crystallization temperature could be decreased from 181 °C for PA6 processed at 245 °C to 165 °C for PA6 processed at 283 °C at an equal additive concentration of 2.0 wt%. This means a decrease of the polymer crystallization temperature by 16 °C which is an enormous enhancement of the additive performance. Furthermore, the polymer crystallization temperature was reduced by additional 3 °C compared to Colorant Black 500 at the same processing conditions.

The images obtained from polarized light microscopy explain this improvement visually. The increased processing temperatures have led to an enhanced solubility of Neutral Red. With increasing melt temperatures during processing, much smaller and especially less aggregates are visible. Due to this effect, a better interaction of the additive with the polymer chain is assumed and an enhancement of the additive performance is achieved.

As already observed prior in this work, some additives evoke a decrease of the polymer crystallization temperature with a coincident decline of the polymer melting temperature. Therefore, Figure 113 presents the DSC heating and cooling curves for a concentration series of PA6 comprising Neutral Red processed at 283 °C.

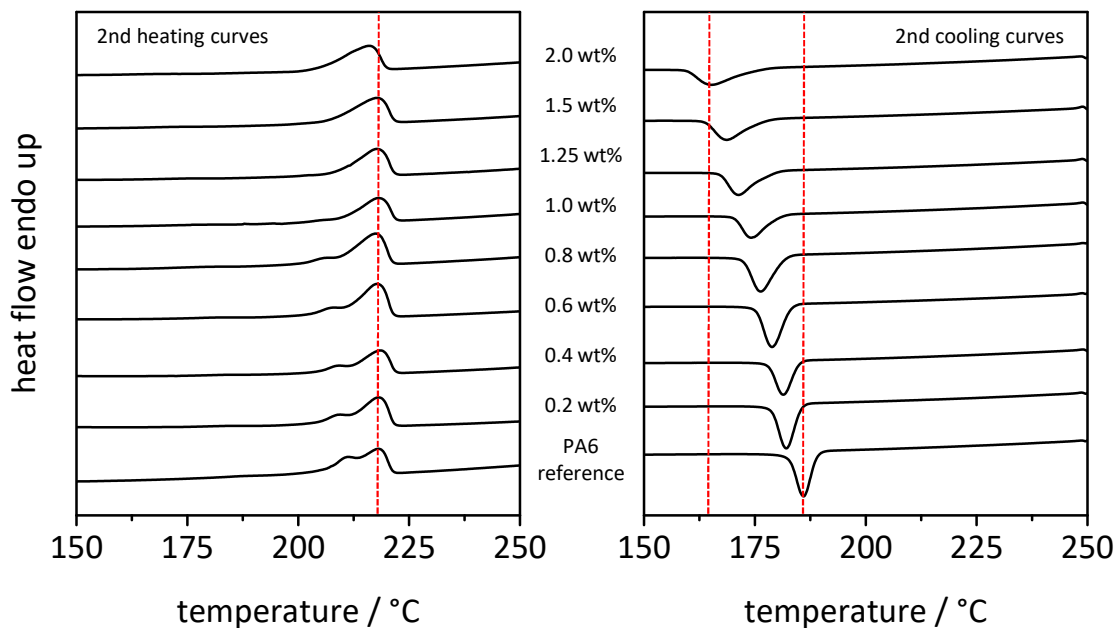


Figure 113. DSC heating and cooling curves of neat PA6 and PA6 comprising Neutral Red. Polymer melt temperature during processing: 283 °C. DSC heating and cooling rate: 10 K/min.

The results presented in Figure 113 clearly show that a significant decrease of the polymer crystallization temperatures with no change of the melting temperatures with increasing additive concentrations was observed. Merely the melting temperature at a concentration of 2.0 wt% Neutral Red was slightly shifted to lower temperatures.

The above made results lead to the conclusion that elevated melt temperatures during processing seem to have enormous influence on the solubility of Neutral Red in PA6. Elevated processing temperatures also caused an increased additive performance of the commercially applied Nigrosine in chapter 5.1. Unfortunately, it has been not possible to investigate the solubility of Nigrosine in the polymer matrix. Due to the addition of Nigrosine to the polymer the compound was dyed dark black, and hence hindered the observation of undissolved particles in the polymer melt.

With the aid of the detailed investigations of PA6 comprising Neutral Red and the results of the DSC measurements of PA6 comprising Nigrosine, the assumed solubility behavior of certain anti-nucleating agents in the polymer matrix at different stages of the polymer processing is presented schematically in Figure 114.



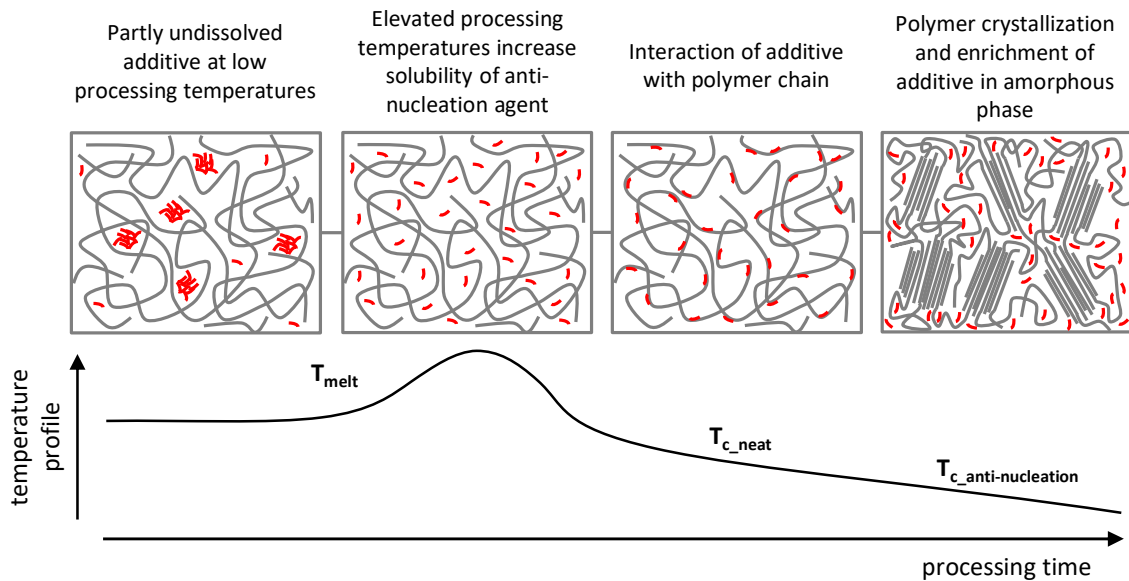


Figure 114. Top: Schematic illustration of the solubility behavior of an anti-nucleation agent in the polymer matrix. The grey lines symbolize the polymer chains and the red dashes indicate the polymer additive. Bottom: Schematic temperature profile during polymer processing.  $T_{melt}$  indicates the temperatures when the polymer is molten,  $T_{c\_neat}$  the crystallization temperature of neat PA6 and  $T_{c\_anti-nucleation}$  the crystallization temperature of anti-nucleated PA6.

The first picture in Figure 114 shows partly undissolved additive (red) at low polymer melt temperatures during processing. Here, the temperatures are too low to achieve passable solubility of the polymer additive. Hence, only weak interactions between the polymer chains and additive molecules are assumed, which would result in low additive performance upon cooling from this stage. The second picture shows well dissolved additive at elevated melt temperatures during processing. This effect might be reached by an increase of the polymer melt temperature during processing, and thus an improved solubility of the additive within the polymer melt. The aim is to enhance the solubility of the additive to generate a huge quantity of free molecules which are capable of interacting with the polymer chain, and hence retard the polymer crystallization. Upon cooling from this stage, the additive molecules are suspected of interacting with the polymer chain and retard the crystallization process, which leads to an anti-nucleation effect (third image in Figure 114). Upon further cooling, the additive molecules are repressed to the amorphous phase and the polymer crystallization takes place (fourth image in Figure 114). A prerequisite is, however, that the applied additives exhibit a high thermal stability not to evoke any side reactions or degradation which may lead to a loss of the polymer properties.

*Crystallization behavior and morphology of PA6 comprising Neutral Red*

As already observed for Nigrosine as well as for the ammonium salts, the spherulitic morphology and the crystallization behavior of polyamide is strongly influenced by anti-nucleating agents. Therefore, the influence of Neutral Red on the crystallization behavior of PA6 was studied isothermally by DSC and polarized light microscopy. Additionally, the macroscopic morphology of PA6 comprising Neutral Red was studied on thin films.

Figure 115 presents the micrographs obtained by polarized light microscopy of PA6 comprising 2.0 wt% Neutral Red at 200 °C after 0 min, 17 min, 25 min, 40 min, 90 min and 150 min and the corresponding isothermal DSC curve. For experimental details refer to chapter 5.1.2 and 8.

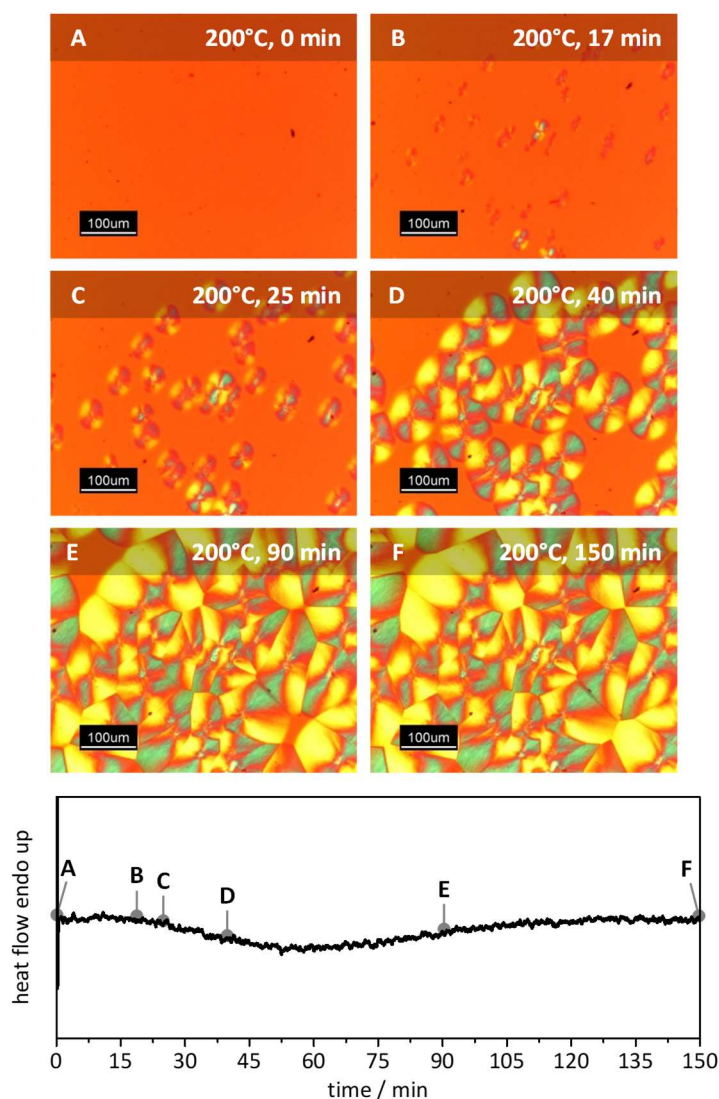


Figure 115. Top: Polarized optical micrographs of a PA6 film comprising 2.0 wt% Neutral Red at 200 °C after 0 min, 17 min, 25 min, 40 min, 90 min and 150 min. The compounded polymer pellets were heated and pressed, kept at 250 °C for 5 min and cooled to 200 °C with 10 K/min. Bottom: Isothermal DSC curve at 200 °C of PA6 comprising 2.0 wt% Neutral Red processed at 283 °C.

The picture at 0 min shows the optical isotropic polymer melt which appears orange due to the  $\lambda/4$  platelet. The second image after 17 min shows several yellowish and greenish structures which can be attributed to the spherulitic structure of PA6. The corresponding DSC curve started to drop at 15 min which describes the onset of the crystallization process of the polymer. After 40 min no further spherulites emerged within the observed image section, but the already existing have grown. As it appears from the images, the growth rate of the spherulites was very slow and very few nuclei were formed. This incident leads to large spherulites. The spherulites reached diameters of several hundreds of microns before the growth was stopped by collision with each other. At 150 min the micrograph shows an almost fully crystallized polymer film and the endset of the crystallization peak of the DSC measurement is around 135 min. In comparison, neat PA6 was fully crystallized after 9 min and PA6 comprising 2.0 wt% Colorant Black 500 revealed its endset after 140 min.

This experiment clearly showed the influence of Neutral Red on the crystallization behavior and also on the spherulitic morphology of PA6. The images present vividly the partial suppression of forming nuclei and thus the retardation of polymer crystallization due to the addition of Neutral Red as anti-nucleating agent. Moreover, the visual results were confirmed by isothermal DSC measurements of the same compounds under equal temperature conditions. Almost the same observations were made for Nigrosine previously in this work.

In order to show the influence of Neutral Red on the macroscopic morphology of PA6 under dynamic cooling conditions, films were investigated by polarized light microscopy. Samples were prepared by melting a polymer pellet of the extruded and additivated compound between two glass slides at 250 °C, pressed for 2 minutes and quenched to room temperature. The so obtained films were inserted to the hot stage, heated rapidly to 250 °C, held there for 5 min and cooled to room temperature with 10 K/min. Optical micrographs were recorded by a digital camera to monitor the crystallization process.

Figure 116 presents the crystallization temperatures of PA6 comprising Neutral Red as function of the additive concentration. The optical micrographs show the spherulitic morphology of PA6 comprising different additive concentrations (0.0 wt%, 0.125 wt%, 1.0 wt% and 2.0 wt%) at temperatures as indicated.

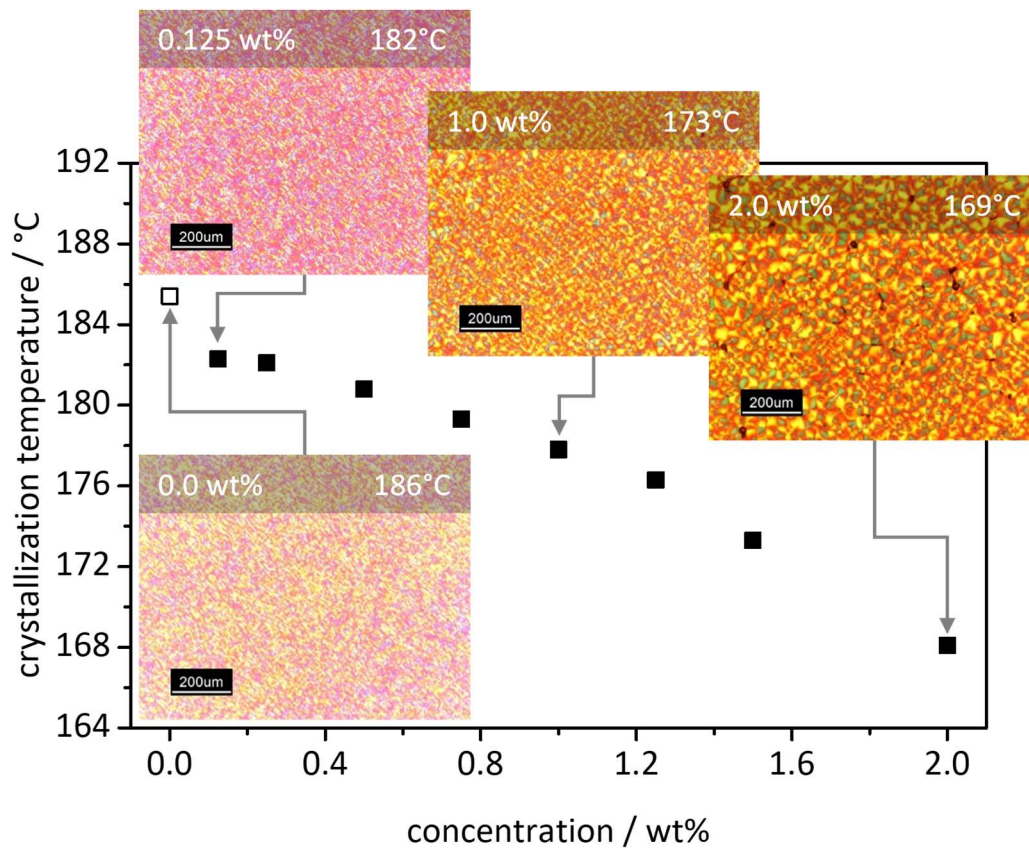


Figure 116. Crystallization temperatures of PA6 comprising Neutral Red as function of the additive concentration processed at 283 °C. Optical micrographs from polarized light microscopy of PA6 with 0.0 wt%, 0.125 wt%, 1.0 wt% and 2.0 wt% Neutral Red. Samples were heated and pressed, kept at 250 °C for 5 min, cooled with a rate of 10 K/min and observed at the indicated temperature.

With increasing additive concentration the polymer crystallization temperatures decreased constantly, as well as the spherulitic morphology changed significantly. With increasing additive concentration, the amount of spherulites decreased but the spherulite size increased distinctly. These observations again confirm the assumptions that anti-nucleating agents retard the crystallization process of polyamides by inhibiting the generation of nuclei.

### 5.4.3 Properties of PA6 containing Neutral Red

As already shown above, Neutral Red has a significant influence on the morphology of PA6. Therefore, the following chapter will examine the influence of Neutral Red on further properties of PA6 such as crystal modification, degree of crystallinity and glass transition temperature. Therefore, methods such as WAXS, DSC and DMTA were applied.

#### *Crystal modification*

In order to figure out the crystal modifications, WAXS measurements were conducted. Figure 117 shows the WAXS pattern of 1.1 mm thick injection molded platelets of neat PA6 and PA6 comprising 1.5 wt% Neutral Red.

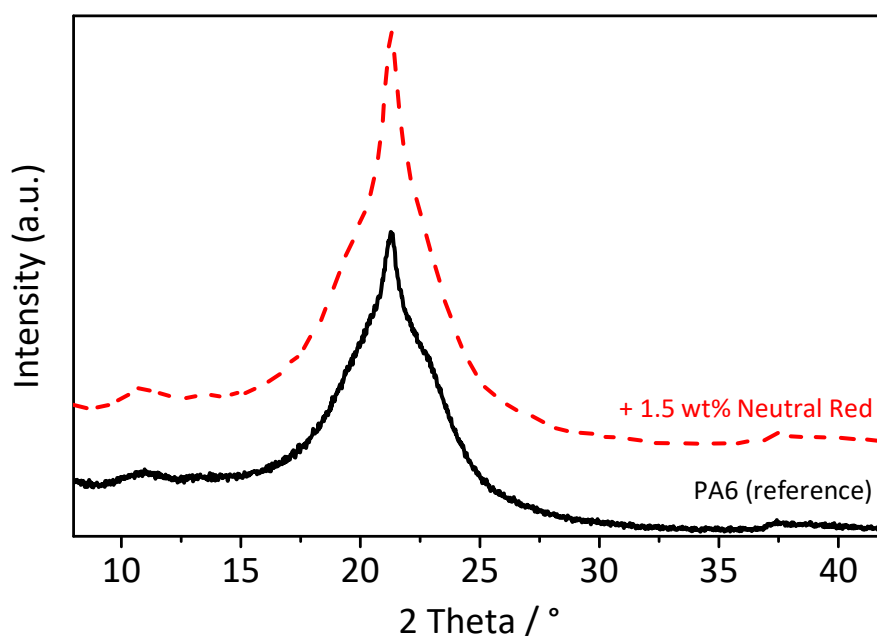


Figure 117. WAXS pattern of neat PA6 (line) and PA6 containing 1.5 wt% Neutral Red (dashed line). Measurements were performed at room temperature on 1.1 mm thick injection molded specimen.

As already described in chapter 3.4, PA6 can crystallize into  $\alpha$ -,  $\gamma$ - or the metastable  $\beta$ -phase. As apparent from Figure 117 both compounds, neat PA6 and PA6 comprising Neutral Red, crystallize predominantly in the  $\gamma$ -phase. The WAXS pattern of neat PA6 shows a hint of the  $\alpha$ -peak around  $23^\circ$ , whereas PA6 comprising Neutral Red exhibits almost no  $\alpha$ -peak. All in all, no significant variation of the crystal modification was observed. Almost the same observation were made for PA6 comprising Nigrosine.

### *Degree of crystallinity*

In addition to the crystal modification of a polymer, the degree of crystallinity is another important parameter, especially for semi-crystalline polymers. Therefore, the degree of crystallinity was determined by DSC. The detailed procedure is explained in chapter 3.4. The degree of crystallinity for both neat PA6 and PA6 comprising 1.5 wt% Neutral Red just vary slightly from each other. The deviations in this dimension can be associated with a measuring error. The results are summarized in Table 27.

Table 27. Melt enthalpies  $\Delta H_f$  and degree of crystallinity of neat PA6 and PA6 comprising 1.5 wt% Neutral Red determined by DSC. Both samples were processed at 283 °C. DSC heating and cooling rate: 10 K/min.

Compound	$\Delta H_f$ [J/g]	Degree of crystallinity [%]
PA6 (reference)	68	36
+ 1.5 wt% Neutral Red	64	34

### *Glass transition temperature*

A further very important property of polymers is the glass transition temperature. The glass transition temperature determines the temperature range where a polymer is applicable. Besides additives, water absorption has a great influence on the glass transition temperature. Therefore, throughout the whole work samples were measured after equilibrium water uptake (70 °C, 62 rh%), with a frequency of 1 Hz and a heating rate of 2 K/min. Figure 118 presents the plot of the storage modulus  $E'$ , and loss factor  $\tan \delta$  as a function of temperature for PA6 comprising 1.5 wt% Neutral Red.

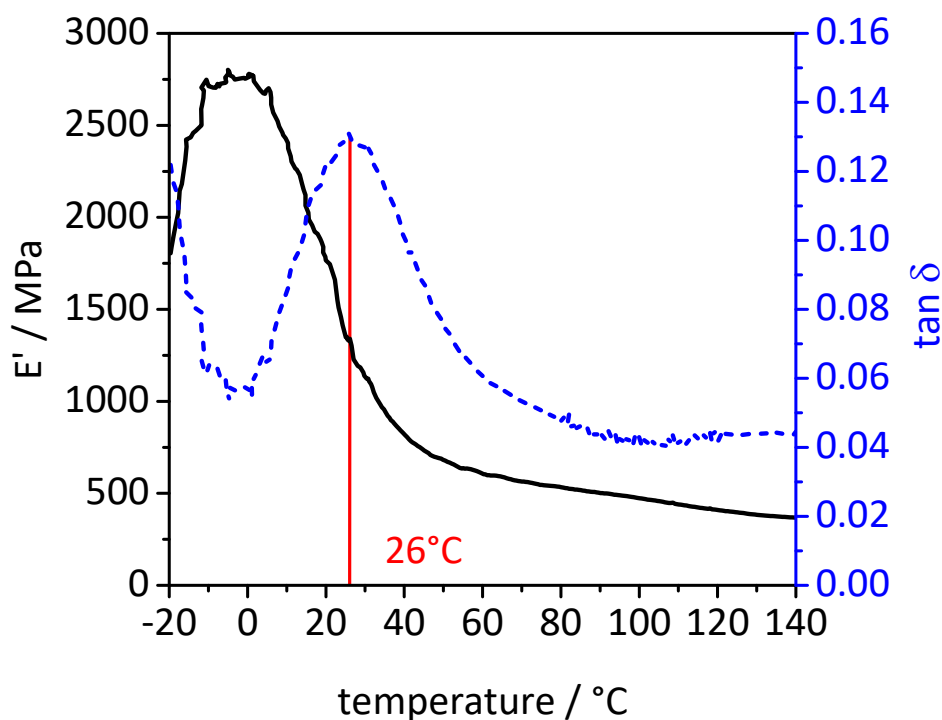


Figure 118. DMTA measurements of PA6 comprising 1.5 wt% Neutral Red after equilibrium water uptake (70 °C, 62 rh%) measured at 1 Hz, 2 K/min. Solid, black line: storage modulus  $E'$ ; Dashed, blue line:  $\tan \delta$ . The red solid line indicates the glass transition temperature determined from the maximum of  $\tan \delta$ .

The value for the glass transition temperature was determined from the peak of  $\tan \delta$ . The red line indicates the glass transition temperature of PA6 comprising 1.5 wt% Neutral Red at 26 °C. By comparison, neat PA6 exhibits a glass transition temperature of 20 °C under the same storing and measurements conditions. This means an increase of the glass transition temperature for PA6 by 6 °C.

The increase of the glass transition temperature might originate from Neutral Red molecules which are in the amorphous phase of PA6 after the crystallization process. These molecules are assumed to be responsible for restricting the movement of the polymer chains. This effect would explain an increase of the glass transition temperature from 20 °C for neat PA6 to 26 °C for PA6 comprising 1.5 wt% Neutral Red. Similar observations were made by Schmack et al. for PA6 comprising LiCl. Here, an coincident decrease of crystallinity and a decline of the melting temperature by increasing glass transition temperature was observed for PA6 comprising LiCl.<sup>[164]</sup> Investigations above would confirm this theory. A slight decrease of the degree of crystallinity was observed for PA6 comprising 1.5 wt% Neutral Red as well. However, the melting temperature stayed almost unaffected.

All in all, a significant decrease of the crystallization temperature of PA6 comprising

Neutral Red was observed. By adapting the processing temperatures, an enhanced solubility of the additive and a coincident reduction of the polymer crystallization temperature were achieved while almost no change of the melting temperature was observed. The crystal modification stayed unaffected, whereas the degree of crystallinity and glass transition temperature revealed changes. The degree of crystallinity slightly decreased by 2% and the glass transition temperature increased by 6 °C. WAXS measurements revealed no change of the crystal modification

In conclusion, Neutral Red acts as an excellent anti-nucleating agent having no negative influence on the properties of PA6. Moreover, it is a cheap and commercially available compound.

Table 28. Summary of characteristic values of neat PA6 and PA6 comprising 1.5 wt% Neutral Red. Melt temperature during processing for all data is 283 °C.

	PA6 (reference)	+ 1.5 wt% Neutral Red @ 283 °C
Melting temperature $T_m$	218 °C	217 °C
Crystallization temperature $T_c$	186 °C	169 °C
Degree of crystallinity	36%	34%
Glass transition temperature $T_g$	20 °C	26 °C
Main crystal modification	$\gamma$ -modification	$\gamma$ -modification

---



### 5.5 Improving anti-nucleating agents by LiCl

Previous investigations revealed that well dissolved anti-nucleating agents exhibit significantly higher efficiencies than poorly dissolved ones. This effect was explained by the increased amount of free molecules for a well dissolved additive in the polymer melt. These molecules are assumed to be capable of interacting with the polymer chains and thus retard the crystallization process. If the polymer additives are present as aggregates, distinctly less molecules are available to interact with the polymer, and consequently lower efficiencies of the additives can be reached.

One approach to solve this issue was to adapt the polymer melt temperatures during processing. Due to higher processing temperatures an enhanced dissolution of the polymer additives was observed. However, elevated processing temperatures implicate high thermal stress for both, the polymer and the additive. Furthermore, higher processing temperatures cause high energy costs and are not economically. In order to avoid these negative side effects, a further approach was developed. Lithium Chloride (LiCl) is well known to disturb hydrogen bonds and is often used to increase the solubility and to modify the reactivity of certain compounds during synthesis.<sup>[165]</sup> In the frame of this work, LiCl was examined with respect to its anti-nucleation ability in polyamides. Likewise to earlier investigations, LiCl evoked a decline of several polymer properties at high additive concentrations. But for all that, LiCl showed no negative effects at concentrations below 0.25 wt%. With this knowledge, a new approach enhancing anti-nucleating agents even at low processing temperatures was tested. A combination of already well functioning anti-nucleating agents and small amounts of LiCl was investigated with respect to its anti-nucleation ability in PA6.

Therefore, the anti-nucleation ability of Neutral Red in PA6 with and without LiCl is investigated at different melt temperatures during processing. The compounds were processed at 245 °C, 259 °C, 273 °C and 283 °C in order to determine an enhancement of the additive performance at low processing temperatures. Figure 119 presents the corresponding polymer crystallization and melting temperatures. Squares indicate neat PA6, triangles represent PA6 comprising 1.5 wt% Neutral Red and circles show the results for PA6 comprising 1.5 wt% Neutral Red and 0.25 wt% LiCl. The initial Neutral Red/LiCl

powder mixtures as well as the polymer/additive powder mixtures were ground with a pestle and mortar prior to compounding to guarantee a homogenous mixture.

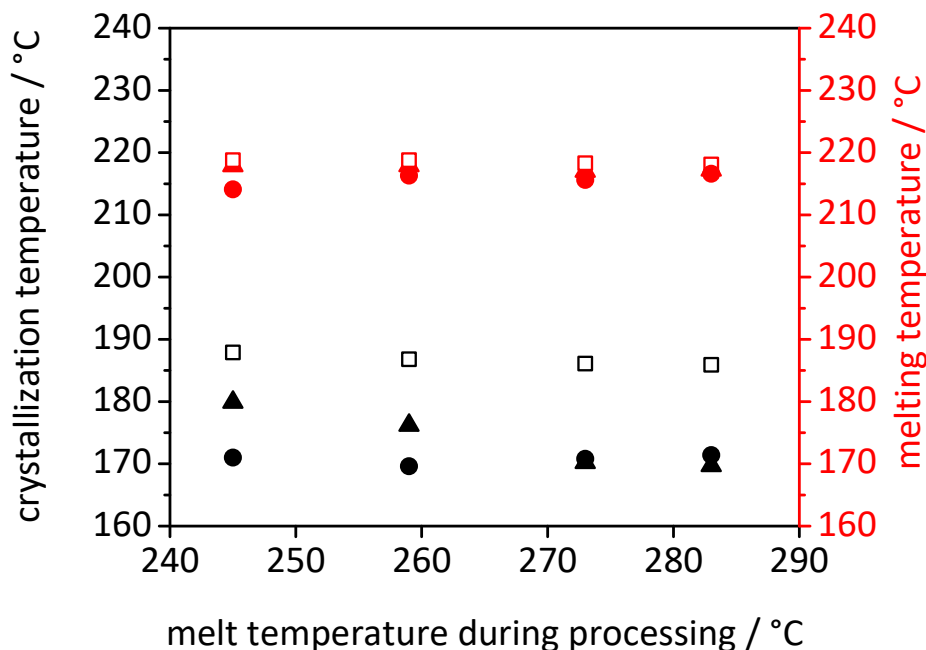


Figure 119. Crystallization and melting temperatures of neat PA6 (□ crystallization, □ melting), PA6 containing 1.5 wt% Neutral Red (▲ crystallization, ▲ melting) and PA6 containing 1.5 wt% Neutral Red + 0.25 wt% LiCl (● crystallization, ● melting) as function of the melt temperature during processing. DSC heating and cooling rate: 10 K/min.

Figure 119 reveals a significant enhancement of the anti-nucleation ability of Neutral Red in PA6 due to the addition of LiCl. The crystallization temperature dropped from 180 °C to 170 °C at a processing temperature of 245 °C. At a processing temperature of 259 °C a decrease of the polymer crystallization temperature by 7 °C was observed. Investigations of chapter 5.2.1 demonstrated that a concentration of 0.25 wt% pure LiCl in PA6 reached a decrease of the polymer crystallization temperature by only up to 3 °C. Taking those results into account, still a massive enhancement of the anti-nucleation effect of Neutral Red can be observed. At processing temperatures of 273 °C and 283 °C no significant enhancement was observed due to the addition of LiCl. Considering the polymer melting temperatures of the compounds, it is notable that the melting temperature for PA6 comprising Neutral Red and LiCl at a processing temperature of 245 °C showed a decline of 3 °C compared to neat PA6. As the values of the polymer melting temperature for the compounds at elevated melt temperatures during processing revealed only a slight decrease of the polymer melting temperature by 1 °C - 2 °C, this effect can be assumed as a measuring error.

These results clearly show a massive enhancement of the performance of Neutral Red at low processing temperatures by the addition of a small amount of LiCl and emphasize the previously made assumptions. In order to confirm these, further investigations were conducted. Therefore, the samples obtained by the compounding experiments were examined by polarized light microscopy. The samples were prepared by melting polymer pellets of the extruded compounds between two glass slides at 250 °C and subsequent quenching to room temperature which leads to thin polymer films with almost no spherulites visible. The results are presented in Figure 120.

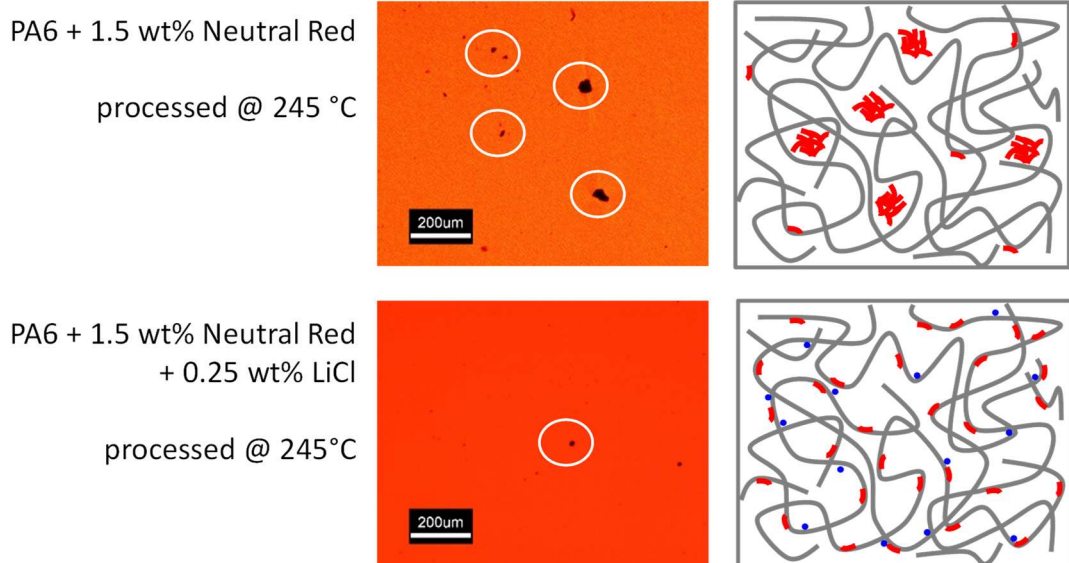


Figure 120. Optical micrographs from polarized light microscopy of PA6 with 1.5 wt% of Neutral Red and with 1.5 wt% Neutral Red/0.25 wt% LiCl processed at 245 °C. The compounded polymer pellets were heated, kept at 250 °C for 5 min and quenched to room temperature. The polymer appears orange due to the  $\lambda/4$  platelet. The non-dissolved additive shows up as black aggregates. The state of the additives in the polymer melt can be seen schematically in the right images. The red aggregates indicate Neutral Red and the blue dots indicate LiCl.

Figure 120 shows two optical micrographs of PA6 comprising 1.5 wt% Neutral Red and PA6 comprising 1.5 wt% Neutral Red and 0.25 wt% LiCl. Both compounds were processed at 245 °C. The top image, without LiCl, revealed several black aggregates which can be referred to Neutral Red, whereas the bottom image, with LiCl, showed almost no crumbles of undissolved Neutral Red. These images are an evidence for the dissolution of additive aggregates by the addition of LiCl. This effect is schematically shown at the right side of Figure 120.

In order to show both, the effect of LiCl and the effect of elevated processing temperatures on the solubility of Neutral Red, Figure 121 presents the optical micrographs of all additivated samples of Figure 119.

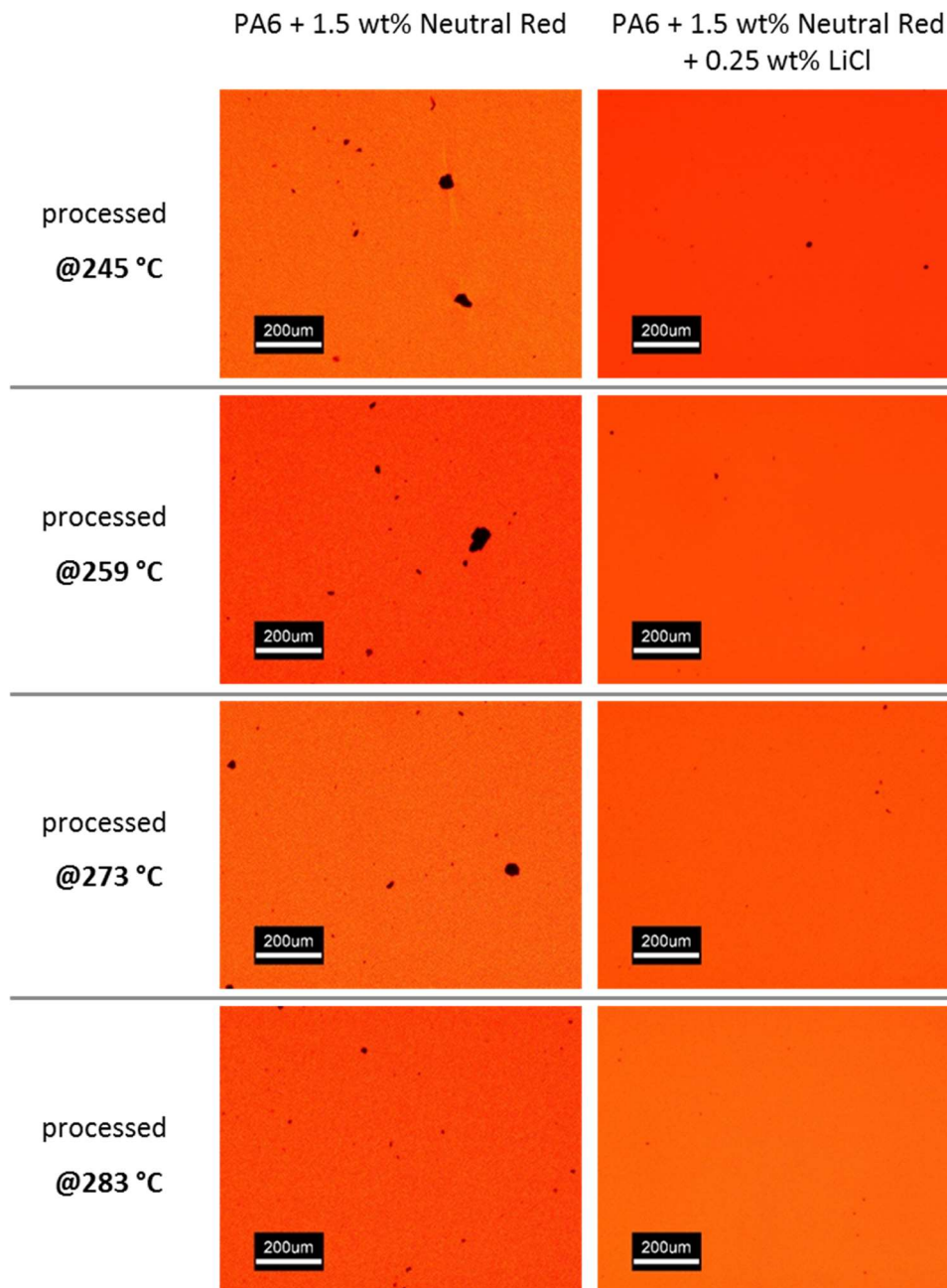


Figure 121. Optical micrographs from polarized light microscopy of PA6 with 1.5 wt% of Neutral Red and with 1.5 wt% Neutral Red/0.25 wt% LiCl processed at different temperatures. The compounded polymer pellets were heated and pressed, kept at 250 °C for 5 min and quenched to room temperature. The polymer appears orange due to the  $\lambda/4$  platelet. The non-dissolved additive shows up as black aggregates.

It becomes clear that the dissolution of additive aggregates is achievable by increasing the melt temperature during processing, as well as by the addition of LiCl as co-additive for Neutral Red. Figure 121 demonstrates a significant reduction of aggregates with increasing

processing temperature (left). In the case of Neutral Red additivated with LiCl almost no aggregates at any processing temperature could be observed (right).

Based on the above made observations and results, the assumed process of the enhancement of an anti-nucleating agent by the addition of LiCl is presented schematically in Figure 122.

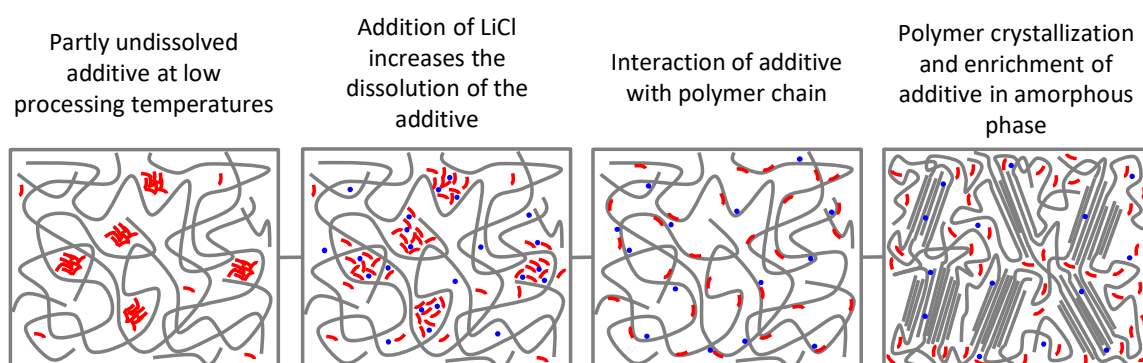


Figure 122. Schematic illustration of enhancement of an anti-nucleating agent in the polymer melt by adding LiCl. The grey lines symbolize the polymer chains, the red dashes the polymer additive and the blue dots indicate LiCl.

The first picture in Figure 122 shows partly undissolved additive which leads to weak interactions between the polymer chains and the additive molecules. In order to resolve those additive aggregates, the polymer additive is mixed with a small amount of LiCl. By adding LiCl, the interactions between the additive molecules are disturbed which leads to an enhanced solubility of the additive in the polymer melt (second image). As a result, more free additive molecules are available which are capable of interacting with the polymer chains upon cooling, and thus retard the polymer crystallization (third picture). Upon further cooling, the additive molecules are repressed to the amorphous phase and the polymer crystallization takes place.

This approach might be a smart way to resolve the dissolution issues of anti-nucleating agents and make the already existing anti-nucleating agents extremely efficient. A further advantage might be the use of a reduced amount of additive due to the enhancement of the polymer additive by LiCl as co-additive.

However, the highest priority is not to evoke any bad influence on the polymer properties by adding an anti-nucleating agent. It was revealed previously, that the addition of certain amounts of LiCl significantly decreased the melting temperature of PA6 as well as the degree of crystallinity. Therefore, the influence of the additive system Neutral Red/LiCl on

the polymer properties of PA6, such as crystal modification, degree of crystallinity and glass transition temperature was investigated. The corresponding values are summarized in Table 29.

Table 29. Summary of characteristic values of neat PA6, PA6 comprising 1.5 wt% Neutral Red, and PA6 comprising 1.5 wt% Neutral Red and 0.25 wt% LiCl. Melt temperature during processing for all data is 283 °C.

	PA6 (reference)	+ 1.5 wt% Neutral Red	+ 1.5 wt% Neutral Red + 0.25 wt% LiCl
Melting temperature	218 °C	217 °C	217 °C
Crystallization temperature	186 °C	170 °C	170 °C
Degree of crystallinity	36%	33%	34%
Glass transition temperature	20 °C	26 °C	28 °C
Main crystal modification	$\gamma$ -modification	$\gamma$ -modification	$\gamma$ -modification

The values for the Neutral Red/LiCl additive system show almost no difference compared to the values for pure Neutral Red as anti-nucleating agent. Merely, the glass transition temperature increased by 2 °C for the additive system compared to pure Neutral Red. Schmack et al. reported an increase of the glass transition temperature for PA6 by addition of LiCl (1.0 wt% and 3.0 wt%) and explained this effect due to polar bonds between the polyamide chain and LiCl which act as physical crosslinking and thus increase the glass transition temperature.<sup>[164]</sup>

These tremendous results underline the positive effect of small amounts of LiCl on the additive performance of slightly dissolved Neutral Red without affecting further polymer properties in a bad way.

Based on the remarkable results, the concept of LiCl as co-additive was transferred to the commercially applied Nigrosine compound. In order to guarantee a better comparability,

compounds with 0.25 wt% pure LiCl, 1.0 wt% pure Colorant Black 500 and a compound with the combination of both, 0.25 wt% LiCl and 1.0 wt% Colorant Black were prepared. The results are summarized in Figure 123.

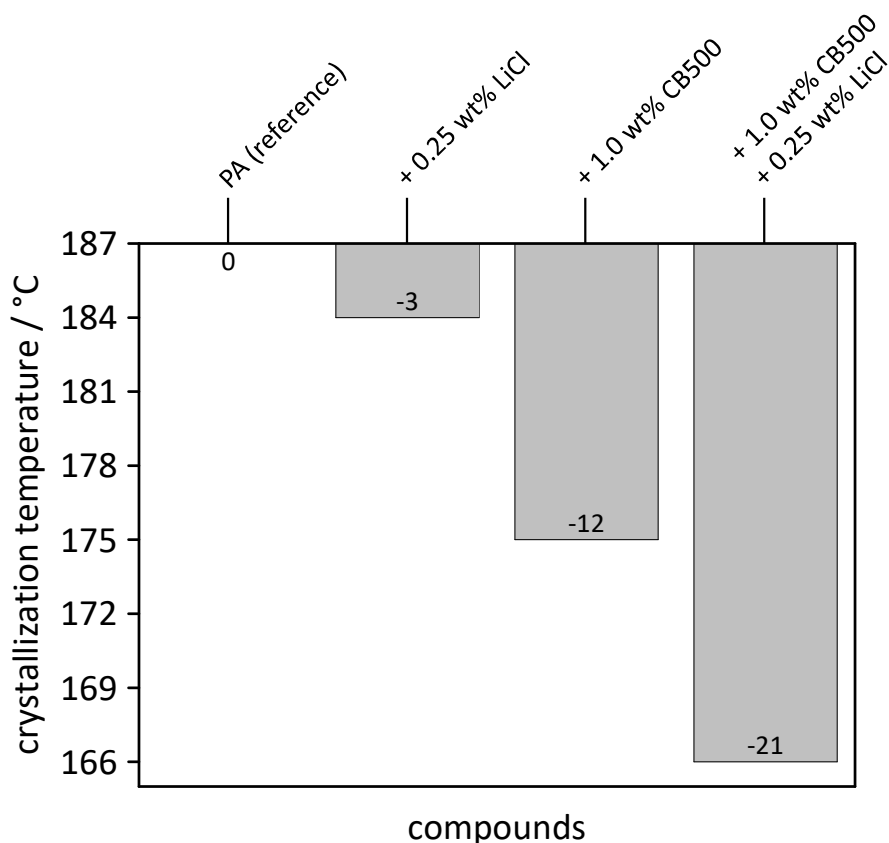


Figure 123. Crystallization temperatures of neat PA6, PA6 comprising 0.25 wt% LiCl, PA6 comprising 1.0 wt% Colorant Black 500 and PA6 comprising both 1.0 wt% Colorant Black 500 and 0.25 wt% LiCl. Polymer melt temperature during processing: 245 °C.

The above presented results show the enormous influence of LiCl on the anti-nucleation performance of Colorant Black 500. Neat LiCl at a concentration of 0.25 wt% decreased the polymer crystallization temperature of PA6 by 3 °C. Neat Colorant Black 500 showed a reduction of the polymer crystallization temperature by 12 °C at a concentration of 1.0 wt%. By adding up both values an overall decrease of the polymer crystallization temperature would be 15 °C, but the combination of both compounds revealed a reduction of the polymer crystallization temperature by 21 °C. This result demonstrates the massive influence of LiCl on the additive performance of Nigrosine. It can be assumed that the addition of LiCl to Colorant Black 500 causes a disturbance of the interactions within the Nigrosine compound and thus lead to an enhanced solubility.

At this point it should be mentioned that PA6 comprising 1.0 wt% Colorant Black 500 in chapter 5.1.2 revealed a reduction of the polymer crystallization temperature by 5 °C instead of 12 °C as shown in Figure 123. This is a clear indication that the reproducibility of the anti-nucleation effect of Nigrosine at low processing temperatures is poor. These differences concerning the polymer crystallization temperatures may arise from the bad solubility of the Nigrosine compound. Due to the application of LiCl as co-additive good solubility and hence reproducibility even at low processing temperatures is ensured.

After completing the practical work of this thesis, a patent was published by Pfaendner et al. also dealing with the enhancement of Nigrosine by the addition of metal salts such as LiCl.<sup>[149]</sup> Here, a synergistic effect due to the combination of Nigrosine and LiCl could be observed as well, but was not investigated in detail. However, this patent substantiates the results made within this thesis and encourage the importance of anti-nucleating agents for industry.



## 5.6 Water absorption and mechanical properties

Polyamides crystallize due to hydrogen-bonds between the polymer chains. These hydrogen bonds can be influenced by the addition of additives. In the case of anti-nucleating agents the amide groups of polyamides interact with the additive molecules. Thus, the polymer additive stays within the polymer matrix. This modification of the polymer might lead to an influence of the polymer properties. Polyamides are known to absorb water in a certain amount, depending on the polyamide type, temperature, crystallinity and sample dimensions. By addition of polymer additives, the affinity to absorb water might be influenced. Particularly the mechanical properties, such as the elastic modulus, are strongly governed by the amount of water.<sup>[2,131]</sup>

Therefore, in the following the influence of additives on the water absorption and the mechanical properties of PA6 are studied. The influence of the most efficient anti-nucleating agents, namely Colorant Black 500, Neutral Red and Neutral Red/LiCl, on the properties of PA6 were investigated at additive concentrations of 1.5 wt% and 0.25 wt% LiCl, respectively.

### *Water absorption*

Water absorption experiments were conducted on 1.1 mm thick injection molded platelets with diameters of 25 mm. Samples were dried for 8 days at 80 °C under vacuum. The dried samples were weighed and stored at 30 °C and 50 rh% in a thermocabinet. In the following, samples were weighed every 24 h until saturation was reached.

Figure 124 presents the water uptake of injection molded platelets of PA6 comprising the above mentioned additives as function of the time stored at 30 °C and 50 rh%. In the period of the first three days an almost linear increase of the water uptake up to 1.25 % for all samples could be observed. With increasing storage time the process flattens and the water uptake reached a plateau at a maximum water uptake around 3.1% after 30 days. It should also be noted, that at a storage time above 18 days, the water uptake slightly differs for the specific samples. Neat PA6 revealed the lowest water uptake of 3.1% after 36 days. The compound comprising the additive system Neutral Red/LiCl showed the maximum water uptake with 3.3%. The compounds comprising Neutral Red and Colorant Black 500 revealed quite similar values and reached their saturation at 3.2%.

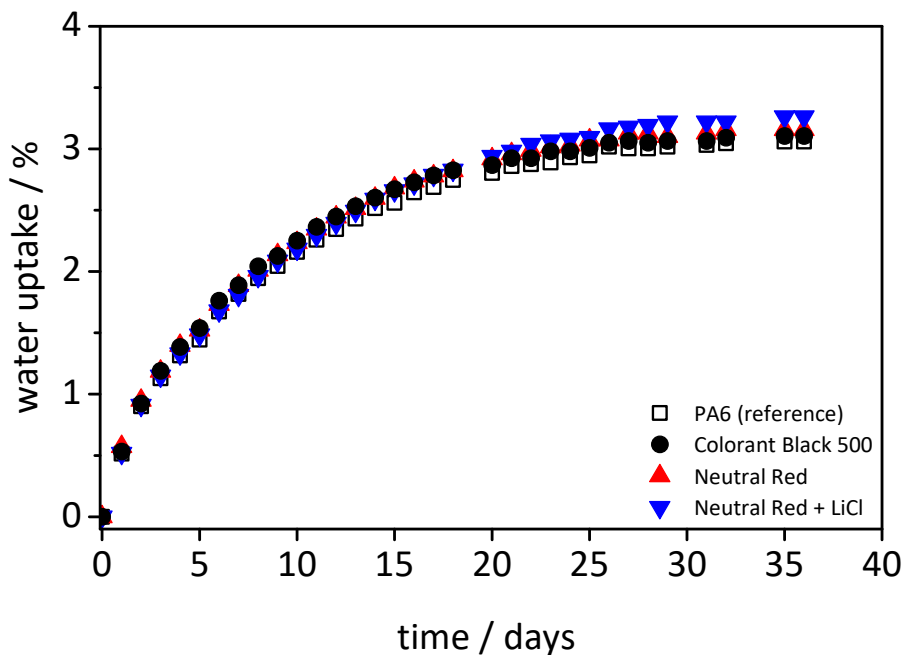


Figure 124. Water uptake of dried injection molding platelets (1.1 mm thickness; 25 mm diameter) as function of the time at 30 °C at 50 rh%.

All in all, in consideration of the measuring error, no significant deviations could be observed among neat PA6 and PA6 comprising the polymer additives. Merely, the additive system comprising LiCl showed a slightly higher water uptake which can be attributed to the strong hygroscopy of LiCl.

### *Mechanical properties*

Tensile tests were conducted on conditioned specimen (4 days, 70 °C, 62 %rh) by an Instron 5565 universal tester with a camera (Instron 2663-821 Advanced Video Extensometer), pneumatic clamps and a 1 kN load cell. Tensile rods with a measuring section of 30 mm x 5 mm x 2 mm were tested at an initial strain rate of 0.3 mm/s (up to 0.5% strain; video measurement) and then increased to 50.0 mm/s. The reported moduli were calculated from the initial slope between 0.15% and 0.35%. The average of at least four samples is reported. Figure 125 presents a typical stress-strain curve of a conditioned PA6 specimen with characteristic values as indicated.

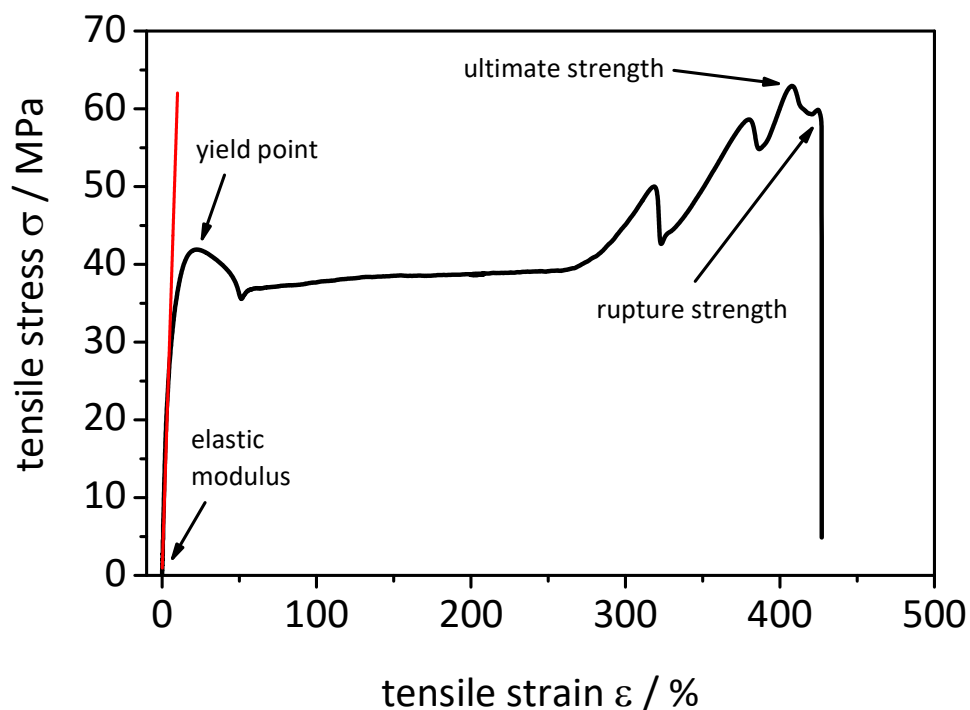


Figure 125. Typical stress-strain curve of a conditioned PA6 specimen with characteristic measurable values: Elastic modulus, yield point, ultimate strength and rupture strength.

The characteristic values, for each of the investigated compounds, such as elastic modulus, ultimate strength, rupture strength and elongation at break are summarized in Table 30.

Table 30. Summary of the tensile properties of the investigated compounds. All samples were conditioned prior to the experiments. The average of at least four samples is reported.

Compound	Elastic modulus [MPa]	Ultimate strength [MPa]	Rupture strength [MPa]	Elongation at break [%]
PA6 (reference)	633 ± 25	69 ± 4	66 ± 5	499 ± 48
+ 1.5 wt% Colorant Black 500	628 ± 14	75 ± 8	74 ± 8	648 ± 46
+ 1.5 wt% Neutral Red	539 ± 24	61 ± 5	59 ± 5	507 ± 54
+ 1.5/0.25 wt% Neutral Red/LiCl	502 ± 16	63 ± 2	61 ± 2	455 ± 24

Comparing the elastic moduli of the compounds revealed that neat PA6 exhibits with 633 MPa the highest value and PA6 comprising Neutral Red/LiCl with 502 MPa the lowest value. It is well known from the literature that with increasing moisture content a coincident decrease of the elastic modulus occurs.<sup>[2]</sup> Previously, the water absorption experiments revealed that the compound comprising the Neutral Red/LiCl system presented the highest amount of moisture. These observations would confirm the differences for the elastic moduli between the investigated samples. The values for the ultimate strength are around 70 MPa, with slightly lower values for the Neutral Red compounds which are around 63 MPa. Furthermore, the rupture strength for neat PA6 exhibits a value of 66 MPa. The values for the additivated samples range from 59 MPa for PA6 comprising Neutral Red to 74 MPa for PA6 comprising Colorant Black 500. However, by consideration of the measuring error, all samples are in the same range. Finally, the elongation of break was determined. Here, an average value of 499% for neat PA6 provides guidance for the additivated samples. Colorant Black 500 showed the largest elongation to 648%, followed by Neutral Red with 507%. PA6 comprising the Neutral Red/LiCl system revealed slightly lower elongations compared to neat PA6.

In conclusion it can be said, that the slight tendencies of the affinity of water absorption of PA6 comprising different additives was reflected by the values of the elastic modulus. Here, PA6 comprising Neutral Red/LiCl presented the lowest value. Further results for this compound are only slightly lower compared to neat PA6. However, PA6 comprising Colorant Black 500 revealed continuously higher values than neat PA6, whereas PA6 comprising Neutral Red showed slightly lower values as for neat PA6, but revealed a gently higher elongation at break.

## 5.7 Anti-nucleation of polyamide 66

Besides polyamide 6, polyamide 66 is the most frequently used nylon. PA66 exhibits a distinctly higher melting and crystallization temperature than PA6 which can be attributed to a difference of their hydrogen bonding pattern. In the case of PA 66, the carbonyl groups are arrayed alternately and are capable of forming hydrogen bonds without distorting the polymer chain. In PA6, only every second carbonyl group is able to form hydrogen bonds with an adjacent amide group. Consequently, PA66 exhibits a distinctly higher melting and crystallization temperature. The mechanical properties differ slightly for PA6 and PA66. For instance, PA66 reveals increased stiffness but less impact strength compared to PA6.<sup>[2]</sup> Moreover, the processing conditions and thermal stability are more favorable for PA6.<sup>[2,166]</sup> In the following chapter, the most efficient anti-nucleating agents previously studied, will be tested with respect to their anti-nucleation ability in PA66. Therefore, Nigrosine as reference, and three compounds, namely Safranin O, Neutral Red and Tetrabutylammonium hexafluorophosphate, were investigated at concentrations from 0.1 wt% to 2.0 wt%.

But first of all, the thermal properties of the PA66 grade used in this work are determined by means of DSC. To explore effects such as degradation and thus possible changes of melting or crystallization temperatures of the neat polymer due to the retention time in the extruder, a blank concentration series without any additive was conducted.

Figure 126 presents the melting and crystallization temperatures of PA66 versus the corresponding run number. All measured temperatures are almost within 0.5 °C. No significant changes of the melting or crystallization temperature with increasing run number were detected. The calculated mean values are listed in Table 31.

Table 31. Melting and crystallization temperatures for PA66 processed at 280 °C. DSC heating and cooling rate: 10 K/min.

	PA66 (reference)
Melting temperature $T_m$	260 °C
Crystallization temperature $T_c$	231 °C

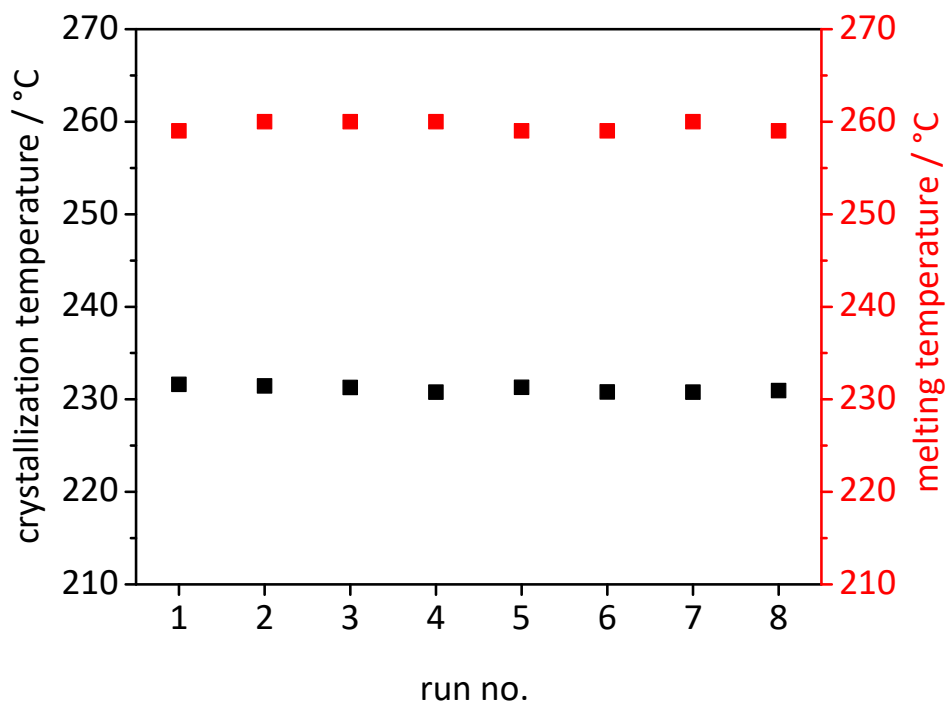


Figure 126. Crystallization temperatures (black squares) and melting temperatures (red squares) of neat PA66 versus the number of processing runs. For each run the samples were compounded for 5 min at 280 °C. DSC heating and cooling rate: 10 K/min.

In order to test if the anti-nucleating agents for PA6 are also valid for PA66, the additive screening process already described in chapter 5.1 was applied. Figure 127 presents micrographs of PA66 partly comprising Neutral Red recorded between crossed polarizers at temperatures as indicated. The image at 25 °C shows a PA66 film at room temperature comprising partly Neutral Red (left). The second picture reveals the isotropic polymer melt at 234 °C, upon cooling from 280 °C. Upon further cooling, the polymer crystallized at 231 °C starting in the region without additive (right side). At a temperature of 224 °C almost the whole sample crystallized. The additivated region shows distinctly larger spherulites compared to the region of the neat polymer. Similar observations were made previously in this work for PA6.

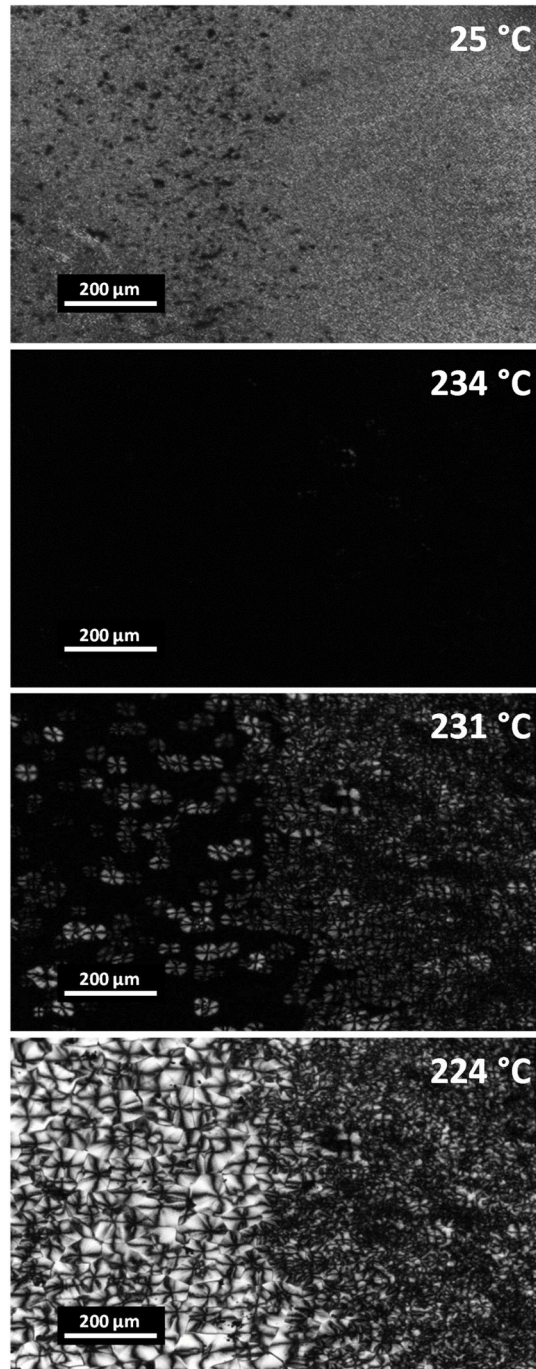


Figure 127. Optical micrographs from polarized light microscopy of a PA66 film with a small amount of Neutral Red. Samples were heated, kept at 280 °C for 5 minutes, cooled with a rate of 10 K/min and observed at different temperatures. The additive is visible in the top picture. During heating the additive diffuses into the PA66 melt and does not crystallize upon cooling. Areas where the additive is dissolved crystallize at much lower temperatures than areas where no additive is available.

In the following, the anti-nucleation ability of Colorant Black 500, Safranin O, Neutral Red and Tetrabutylammonium hexafluorophosphate are determined by DSC. All of these additives induced good anti-nucleation effects in PA6. Due to the fact that PA66 requires significantly higher melt temperatures during processing in contrast to PA6, all further

experiments are merely conducted at polymer melt temperatures during processing of 280 °C. Higher processing temperatures would be rarely possible due to the thermal stability of the additives. The chemical structures and the polymer crystallization and melting temperatures as function of additive concentrations are compared in Figure 128. The values for neat PA66 are plotted as unfilled squares.

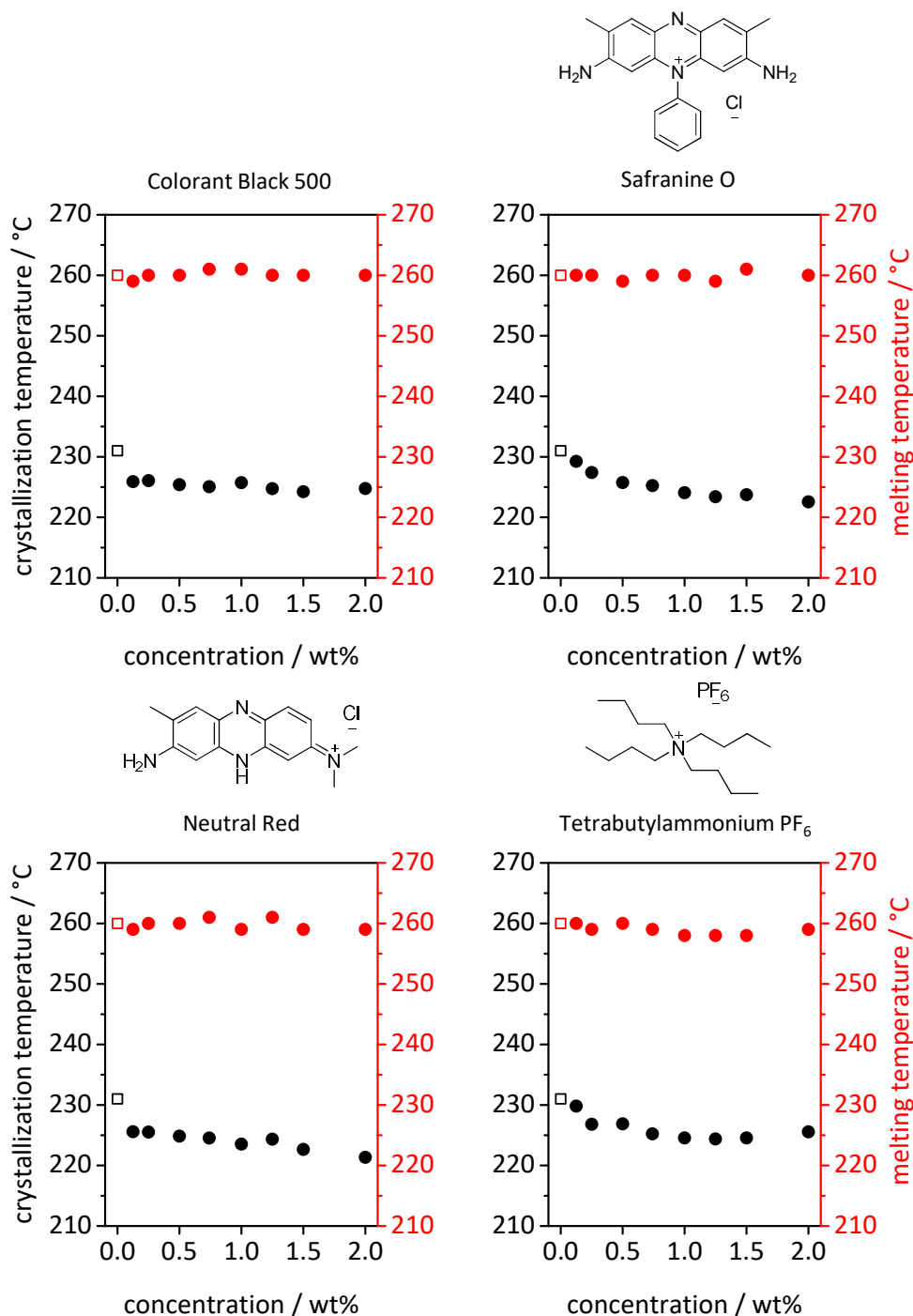


Figure 128. Crystallization and melting temperatures of PA66 comprising Colorant Black 500, Safranin O, Neutral Red and Tetrabutylammonium PF<sub>6</sub> as function of the additive concentration. The blank squares represent the crystallization and melting temperature of neat PA66. DSC heating and cooling rate: 10 K/min.



All compounds showed good anti-nucleation abilities in PA66. Colorant Black 500 and Neutral Red decreased the polymer crystallization temperature of PA66 by 5 °C even at low concentrations of 0.1 wt%. Colorant Black 500 reached its maximum at 1.5 wt% with a decrease of the polymer crystallization temperature by 6 °C, whereas Neutral Red revealed a significant higher influence on the crystallization behavior of PA66 and reduced the polymer crystallization temperature by 10 °C at an additive concentration of 2.0 wt%. Safranin O and Tetrabutylammonium PF<sub>6</sub> showed quite similar effects. Here, with increasing additive concentrations an enhanced anti-nucleation ability was observed. Safranin O was capable of reducing the polymer crystallization temperature by 8 °C at an additive concentration of 2.0 wt%, whereas the ammonium salt reached its maximum at 1.5 wt% with a decrease of the polymer crystallization temperature by 6 °C. Moreover, all additives showed no significant influence on the polymer melting temperature of PA66. In conclusion, all investigated compounds anti-nucleated PA66 effectively without affecting the polymer melting temperature.

## 5.8 Summary

Nigrosine is the only commercially applied anti-nucleating agent for polyamides although the existence of anti-nucleation is known since the early 70s. The aim of this chapter was to investigate the phenomenon of anti-nucleation and to develop structure-property relations and a possible mechanism explaining this almost unknown effect. The major challenge was to develop anti-nucleating agents which decrease the polymer crystallization temperature without affecting the melting temperature of the polymer, and hence retain other polymer properties. Based on the structure elements of the commercially applied anti-nucleating agent Nigrosine, several approaches were perused systematically to develop new anti-nucleating agents.

First, Nigrosine was investigated in detail as reference material. Here, a significant effect of the polymer processing temperatures on the additive performance was observed. By increasing the processing temperatures, a reduction of the PA6 crystallization temperature by 18 °C from 187 °C to 169°C was observed.

Second, the influence of salts as lithium chloride (LiCl) and various organic ammonium salts on the crystallization temperature of PA6 was examined. The investigations showed that LiCl is capable of anti-nucleating PA6 slightly by 3 °C at concentrations below 0.25 wt% with almost unchanged PA6 properties. However, higher concentrations led to a loss of several polymer properties, such as a reduced melting temperature or degree of crystallinity. Additionally, fourteen organic ammonium salts were investigated and showed a slight decrease of the polymer crystallization temperature of PA6 by up to 4 °C from 187 °C to 183 °C without affecting the polymer melting temperature.

To combine the basic structural elements of Nigrosine, sixteen azine dyes were investigated with respect to their anti-nucleation ability in PA6. Here, the polymer crystallization temperature was decreased by up to 8 °C from 187 °C to 179 °C at 1.5 wt% with the azine dyes Giemsa Stain and Toluidine Blue. Among the investigated azine dyes, Neutral Red represents a particular efficient anti-nucleating agent. A reduction of the polymer crystallization temperature by 21 °C from 187 °C to 166 °C was achieved at additive concentrations of 2.0 wt% without affecting other polymer properties. It was also demonstrated that the processing temperature strongly affected the anti-nucleation performance of the additive. Neutral Red as well as Nigrosine revealed dissolution

problems during melt processing. Therefore, a new approach was developed to enhance the additive performance even at low processing temperatures. This approach was based on an additive system consisting of an anti-nucleating agent and lithium chloride as co-additive. It was demonstrated that small amounts of LiCl increased the solubility of Neutral Red in the polymer melt especially at low processing temperatures. The polymer crystallization temperature dropped by 10 °C from 180 °C (PA6 + 1.5 wt% Neutral Red) to 170 °C (PA6 + 1.5 wt% Neutral Red + 0.25 wt% LiCl) at a processing temperature of 245 °C. Hence, this approach was transferred to the commercially applied Nigrosine. Here, a decrease of the polymer crystallization temperature from 175 °C (PA6 + 1.0 wt% Nigrosine) to 166 °C (PA6 + 1.0 wt% Nigrosine + 0.25 wt% LiCl) was achieved.

In addition, water absorption experiments and tensile tests of additivated PA6 were conducted. The most efficient additives, namely Nigrosine, Neutral Red and Neutral Red/LiCl, were investigated at additive concentrations of 1.5 wt% and 0.25 wt% LiCl, respectively. The water absorption experiments revealed no significant differences between neat PA6 and PA6 comprising the polymer additives. The mechanical properties for PA6 comprising Nigrosine revealed slightly improved properties, such as a small increase of the elongation at break from 499% to 648%. However, the elastic modulus for PA6 comprising Neutral Red decreased from 633 MPa to 539 MPa.

Furthermore, the most efficient anti-nucleating agents found in this thesis for PA6 were tested also with respect to their anti-nucleation ability in PA66. Neutral Red showed the best results and reduced the crystallization temperature of PA66 by 10 °C from 231 °C to 221 °C at an additive concentration of 2.0 wt%.

In summary, several new anti-nucleation agents were found and an approach to significantly enhance the commercially applied Nigrosine was developed. By investigations of different compounds, namely Nigrosine, inorganic and organic salts, and azine dyes, structure-property relations could be established concerning the anti-nucleation performance in PA6: Predominantly planar and rigid structures bearing units capable of interacting with the hydrogen bonds of polyamides, such as amino or ionic groups, are the most efficient anti-nucleation agents. These results are indicative for interactions between the anti-nucleating agents and the polymer chains which lead to a retarded polymer

crystallization. Mostly, these compounds do not sacrifice other polymer properties such as polymer melting temperature and degree of crystallinity.

## 6 Summary

The application of additives to enhance processability and end properties of a polymer is an important field in plastics technology and industry. The macroscopic properties of a semi-crystalline polymer strongly depend on the crystal structure and morphology which can be controlled by additives. On the one hand, *nucleating agents increase the polymer crystallization temperature*. On the other hand, *anti-nucleating agents decrease the polymer crystallization temperature* and retard the polymer crystallization.

Process and product requirements can be improved and adapted for specific applications by the control of the crystallization behavior. *Nucleating agents*, for example, reduce cycle times during melt processing, increase the mechanical properties and can improve the optical properties of polymers. In contrast, *anti-nucleating agents* evoke good fluidity and molding precision during injection molding and are able to improve the surface gloss and texture of injection molded products. Ideally, anti-nucleating agents do not influence other polymer properties, such as melting temperature or degree of crystallinity.

In this thesis nucleating and anti-nucleating agents were used to influence the crystallization behavior and the macroscopic properties of semi-crystalline polyamides.

In the first part of this thesis, the influence of different ***processing conditions on the properties of polyamide 6 (PA6)*** was examined. The investigations revealed no significant influence on the polymer properties such as melting and crystallization temperature, degree of crystallinity, glass transition temperature and crystal modification under the applied processing conditions. These values were then used as reference to study the influence of additives on polyamides.

The second part of this thesis deals with the ***nucleation and clarification of polyamide 6***. Different processing techniques require different processing temperatures. Therefore, the thermal stability of a bisurea derivative and the nucleation and clarification efficiency in PA6 at elevated melt temperatures during processing were investigated. It was observed that increasing processing temperatures induced an increase of the haze value linearly from below 20% at 245 °C to 50% at 283 °C. GC-MS investigations revealed thermal degradation of the bisurea additive at temperatures above 245 °C. Based on these

investigations, processing temperatures around 245 °C turned out to be best to clarify PA6 without an increase of the haze value.

Additionally, for the first time, the influence of a nucleating agent on the spherulitic morphology of PA6 was observed at the nanoscale by scanning electron microscopy of thin films.

Furthermore, a new class of clarifying agents for polyamides was developed. The concept and structural motif of bisurea compounds was transferred to a related class of **bisthioureas**. Four bisthiourea derivatives were synthesized, characterized and investigated with regard to their nucleation and clarification ability in PA6. Nucleation efficiencies up to 70% at concentrations of 1.5 wt% were achieved. Additionally, an enhancement of the optical properties (haze and clarity) was achieved by all investigated compounds. For example, 1,1'-(*trans*-1,4-cyclohexane)bis(3-*tert*-butylthiourea) at a concentration of 1.5 wt% gained a reduction of the haze value from 98% to 45% for a 1.1 mm thick sample. Furthermore, morphology investigations showed a significant decrease of the spherulite size and the initial  $\gamma$ -modification transferred to the  $\alpha$ -form for PA6 comprising the bisthiourea additives. Mechanical investigations revealed an increase of the elastic modulus from 633 MPa to 717 MPa for PA6 comprising 1,1'-(*trans*-1,4-cyclohexane)bis(3-*tert*-butylthiourea).

The third part of the thesis addresses the **anti-nucleation of polyamide 6**. Based on the structure elements of the commercially applied anti-nucleating agent *Nigrosine* (*Colorant Black 500*), such as amino or ionic groups, several approaches were pursued to develop new anti-nucleating agents.

First, ***Nigrosine*** was investigated in detail as reference material. Here, a significant effect of the polymer processing temperatures on the additive performance was observed. By increasing the processing temperatures, a reduction of the PA6 crystallization temperature by 18 °C from 187 °C to 169 °C was observed.

Second, the influence of salts as ***lithium chloride*** (*LiCl*) and various organic **ammonium salts** on the crystallization temperature of PA6 was examined. The investigations showed that *LiCl* is capable of anti-nucleating PA6 slightly by 3 °C at concentrations below 0.25 wt% with almost unchanged PA6 properties. However, higher concentrations led to a loss of several polymer properties, such as a reduced melting temperature or degree of crystallinity.

Additionally, fourteen organic **ammonium salts** were investigated and showed a slight decrease of the polymer crystallization temperature of PA6 by up to 4 °C from 187 °C to 183 °C without affecting the polymer melting temperature.

To combine the basic structural elements of *Nigrosine*, sixteen **azine dyes** were investigated with respect to their anti-nucleation ability in PA6. Here, the polymer crystallization temperature was decreased by up to 8 °C from 187 °C to 179 °C at 1.5 wt% with the *azine dyes Giemsa Stain* and *Toluidine Blue*. Among the investigated *azine dyes*, **Neutral Red** represents a particular efficient anti-nucleating agent. A reduction of the polymer crystallization temperature by 21 °C from 187 °C to 166 °C was achieved at additive concentrations of 2.0 wt% without affecting other polymer properties. It was also demonstrated that the processing temperature strongly affected the anti-nucleation performance of the additive. *Neutral Red* as well as *Nigrosine* revealed dissolution problems during melt processing. Therefore, a new approach was developed to enhance the additive performance even at low processing temperatures. This approach was based on an additive system consisting of an **anti-nucleating agent and lithium chloride as co-additive**. It was demonstrated that small amounts of *LiCl* increased the solubility of *Neutral Red* in the polymer melt especially at low processing temperatures. The polymer crystallization temperature dropped by 10 °C from 180 °C (PA6 + 1.5 wt% *Neutral Red*) to 170 °C (PA6 + 1.5 wt% *Neutral Red* + 0.25 wt% *LiCl*) at a processing temperature of 245 °C. Hence, this approach was transferred to the commercially applied *Nigrosine*. Here, a decrease of the polymer crystallization temperature from 175 °C (PA6 + 1.0 wt% *Nigrosine*) to 166 °C (PA6 + 1.0 wt% *Nigrosine* + 0.25 wt% *LiCl*) was achieved.

In addition, water absorption experiments and tensile tests of additivated PA6 were conducted. The most efficient additives, namely *Nigrosine*, *Neutral Red* and *Neutral Red/LiCl*, were investigated at additive concentrations of 1.5 wt% and 0.25 wt% *LiCl*, respectively. The water absorption experiments revealed no significant differences between neat PA6 and PA6 comprising the polymer additives. The mechanical properties for PA6 comprising *Nigrosine* revealed slightly improved properties, such as a small increase of the elongation at break from 499% to 648%. However, the elastic modulus for PA6 comprising *Neutral Red* decreased from 633 MPa to 539 MPa.

Furthermore, the most efficient anti-nucleating agents found in this thesis for PA6 were tested also with respect to their anti-nucleation ability in **PA66**. *Neutral Red* showed the best results and reduced the crystallization temperature of *PA66* by 10 °C from 231 °C to 221 °C at an additive concentration of 2.0 wt%.

In summary, several new anti-nucleation agents were found and an approach to significantly enhance the commercially applied *Nigrosine* was developed. By investigations of different compounds, namely ***Nigrosine, inorganic and organic salts, and azine dyes***, structure-property relations could be established concerning the anti-nucleation performance in PA6: Predominantly planar and rigid structures bearing units capable of interacting with the hydrogen bonds of polyamides, such as amino or ionic groups, are the most efficient anti-nucleation agents. These results are indicative for interactions between the anti-nucleating agents and the polymer chains which lead to a retarded polymer crystallization. Mostly, these compounds do not sacrifice other polymer properties such as polymer melting temperature and degree of crystallinity.



## 7 Zusammenfassung

Der Einsatz von Additiven zur Verbesserung der Prozessierbarkeit und der Endigenschaften eines Polymers stellt ein wichtiges Forschungsgebiet der Kunststoffindustrie dar. Die makroskopischen Eigenschaften eines teilkristallinen Polymers werden von der Kristallstruktur sowie der Morphologie bestimmt und können durch Additive kontrolliert werden. So können zum Beispiel *Nukleierungsmittel die Kristallisationstemperatur eines Polymers erhöhen*, wohingegen *Anti-Nukleierungsmittel die Kristallisationstemperatur herabsetzen* indem sie den Kristallisationsprozess verzögern. Prozess- und Produkthanforderungen für spezielle Anwendungen können durch die Kontrolle des Kristallisationsverhaltens verbessert und angepasst werden. *Nukleierungsmittel* zum Beispiel verkürzen die Zykluszeiten im Spritzguss, verbessern die mechanischen Eigenschaften und können in manchen Fällen die optischen Eigenschaften eines Polymers verbessern. *Anti-Nukleierungsmittel* hingegen erhöhen den Oberflächenglanz spritzgegossener Produkte, führen zu verbesserten Fließeigenschaften der Polymerschmelze und können somit die Formgenauigkeit im Spritzguss steigern. Im Idealfall führt der Einsatz von Anti-Nukleierungsmitteln zu keiner Verschlechterung weiterer Eigenschaften des Polymers, wie z.B. einer Senkung der Schmelztemperatur oder des Kristallisationsgrads.

In dieser Arbeit wurden sowohl *Nukleierungsmittel* als auch *Anti-Nukleierungsmittel* zur Beeinflussung des Kristallisationsverhaltens und der makroskopischen Eigenschaften von teilkristallinen Polyamiden untersucht.

Im ersten Teil dieser Arbeit wurde der ***Einfluss verschiedener Verarbeitungsbedingungen auf die Eigenschaften von reinem Polyamid 6 (PA6)*** untersucht. Die Untersuchungen zeigten unter den angewendeten Prozessbedingungen keinen signifikanten Einfluss auf die Polymereigenschaften, wie Schmelz- und Kristallisationstemperatur, Kristallisationsgrad, Glasübergangstemperatur und Kristallmodifikation. Die ermittelten Werte dienten als Referenz für die nachfolgenden Untersuchungen des Einflusses von Additiven auf PA6.

Der zweite Teil der Arbeit umfasst die ***Nukleierung und Klarmodifikation von Polyamid 6***. Da unterschiedliche Verarbeitungsprozesse unterschiedliche Verarbeitungstemperaturen erfordern, wurden die thermische Stabilität eines Bisharnstoffderivats, dessen

Nukleierungseffizienz in PA6 sowie der Einfluss auf die optischen Eigenschaften (Haze und Clarity) von PA6 unter erhöhten Verarbeitungstemperaturen untersucht. Es konnte beobachtet werden, dass mit der Erhöhung der Schmelzetemperaturen während der Polymerverarbeitung eine Zunahme des Haze-Wertes von unter 20% bei 245 °C auf 50% bei 283 °C einhergeht. GC-MS Untersuchungen zeigten thermischen Abbau des Bisharnstoffs bei Temperaturen über 245 °C. Basierend auf diesen Erkenntnissen haben sich Verarbeitungstemperaturen um 245 °C als ideal erwiesen um den Haze-Wert von PA6 möglichst gering zu halten.

Des Weiteren konnte erstmals der Einfluss eines Nukleierungsmittels auf die Sphärolithmorphologie von PA6 im Nanometerbereich mittels Rasterelektronenmikroskopie an dünnen PA6-Filmen gezeigt werden.

Darüber hinaus wurde eine neue Klasse an Klarmodifizierern für Polyamide entwickelt. Hierfür wurden das Konzept und der strukturelle Aufbau der Bisharnstoffe auf die verwandte Klasse der **Bisthioharnstoffe** übertragen. Vier Bisthioharnstoffderivate wurden synthetisiert, charakterisiert und hinsichtlich der Nukleierung und Klarmodifizierung von PA6 untersucht. Hierbei konnten Nukleierungseffizienzen von bis zu 70% bei einer Additivkonzentration von 1,5 Gew.-% erreicht werden. Zudem konnten die optischen Eigenschaften (Haze und Clarity) von PA6 durch alle Bisthioharnstoffe verbessert werden. Mit 1,1'-(*trans*-1,4-cyclohexane)bis(3-*tert*-butylthiourea) zum Beispiel ist es gelungen den Haze einer 1,1 mm dicken Probe von 98% auf 45% bei einer Additivkonzentration von 1,5 Gew.-% zu senken. Des Weiteren wurde eine signifikante Reduktion der Sphärolithgröße festgestellt und alle eingesetzten Bisthioharnstoffe nukleierten die  $\alpha$ -Form von PA6. Außerdem konnte am Beispiel von PA6 und 1,1'-(*trans*-1,4-cyclohexane)bis(3-*tert*-butylthiourea) ein Anstieg des E-Moduls von 633 MPa auf 717 MPa mittels statistischer Zugprüfung gezeigt werden.

Der dritte Teil der Arbeit befasst sich mit der **Anti-Nukleierung von Polyamid 6**. Basierend auf den Strukturelementen des kommerziell eingesetzten Anti-Nukleierungsmittels Nigrosine (Colorant Black 500), wie Amino-oder ionische Gruppen, wurden mehrere Ansätze verfolgt um neue Anti-Nukleierungsmittel zu entwickeln.

Zu Beginn wurde **Nigrosin** als Referenz ausführlich untersucht. Hierbei konnte ein signifikanter Einfluss der Verarbeitungstemperaturen bezüglich der Anti-Nukleierung

beobachtet werden. Durch eine Erhöhung der Schmelztemperatur während der Verarbeitung konnte eine Reduktion der Polymerkristallisationstemperatur um 18 °C von 187 °C auf 169 °C erreicht werden.

Weiterhin wurde der Einfluss von **Lithiumchlorid** (LiCl) und verschiedenen organischen **Ammoniumsalzen** auf das Kristallisationsverhalten von PA6 getestet. Die Untersuchungen zeigten, dass durch LiCl-Konzentrationen unter 0,25 Gew.-% die Kristallisationstemperatur von PA6 um bis zu 3 °C gesenkt werden kann ohne weitere Polymereigenschaften signifikant zu beeinflussen. Höhere Konzentrationen führten jedoch zur Verschlechterung mehrerer Polymereigenschaften, wie z.B. eine Verringerung der Schmelztemperatur oder des Kristallisationsgrades. Des Weiteren wurden vierzehn organische Ammoniumsalze untersucht. Hierbei konnte eine Reduktion der Polymerkristallisationstemperatur um bis zu 4 °C von 187 °C auf 183 °C erzielt werden ohne weitere Polymereigenschaften zu beeinflussen.

Um die elementaren Strukturbausteine von Nigrosin zu verbinden, wurden sechzehn **Azinfarbstoffe** bezüglich ihres anti-nukleierenden Effekts in PA6 untersucht. Durch die Verbindungen *Giemsa Stain* und *Toluidine Blue* konnte eine Verringerung der Kristallisationstemperatur von PA6 um 8 °C von 187 °C auf 179 °C bei einer Additivkonzentration von 1,5 Gew.-% erreicht werden. Unter den untersuchten Azinfarbstoffen stellt **Neutral Rot** ein besonders effizientes Anti-Nukleierungsmittel dar. Durch die Zugabe von Neutral Rot konnte eine Verringerung der Kristallisationstemperatur von PA6 um 21 °C von 187 °C auf 166 °C mit einer Additivkonzentration von 2,0 Gew.-% erzielt werden ohne weitere Polymereigenschaften zu beeinflussen. Weiterhin wurde gezeigt, dass die Verarbeitungstemperaturen die Anti-Nukleierung von PA6 durch Neutral Rot stark beeinflussen. Neutral Rot, wie auch Nigrosin, offenbarten Löslichkeitsprobleme während der Polymerverarbeitung, was eine vollständige Ausschöpfung des Additivpotentials verhinderte. Aus diesem Grund wurde eine neue Methode entwickelt um die Additive auch bei niedrigen Verabreichungstemperaturen zu verbessern. Dieser Ansatz basiert auf einem Additivsystem bestehend aus einem **Anti-Nukleierungsmittel und Lithiumchlorid als Co-Additiv**. Es konnte gezeigt werden, dass kleine Mengen LiCl die Löslichkeit von Neutral Rot in der Polymerschmelze, besonders bei niedrigen Verarbeitungstemperaturen, deutlich erhöhen. Durch den Einsatz von 0,25 Gew.-% LiCl als

Co-Additiv bei einer Neutral Rot-Konzentration von 1,5 Gew.-% wurde die Kristallisationstemperatur von PA6 um 10 °C von 180 °C (PA6 + 1,5 Gew.-% Neutral Rot) auf 170 °C (PA6 + 1,5 Gew.-% Neutral Rot + 0,25 Gew.-% LiCl), bei einer Verarbeitungstemperatur von 245 °C, reduziert. Infolgedessen wurde diese Methode für das kommerziell eingesetzte Nigrosin getestet. Hierbei konnte durch 0,25 Gew.-% LiCl als Co-Additiv und einer Nigrosin-Konzentration von 1,0 Gew.-% eine Verringerung der Kristallisationstemperatur von PA6 von 175 °C (PA6 + 1,0 Gew.-% Nigrosin) auf 166 °C (PA6 + 1,0 Gew.-% Nigrosin + 0,25 Gew.-% LiCl) erreicht werden.

Weiterhin wurden die Wasseraufnahme und die mechanischen Eigenschaften von additiviertem PA6 untersucht. Die effizientesten Additive, *Nigrosine*, *Neutral Rot* und das *Additivsystem Neutral Rot/LiCl*, wurden bei Konzentrationen von 1,5 Gew.-% bzw. 0,25 Gew.-% LiCl in PA6 untersucht. Die Wasseraufnahme der einzelnen Zusammensetzungen zeigte keine signifikante Abweichung im Vergleich zu reinem PA6. Die mechanischen Eigenschaften für das System *PA6/Nigrosin* zeigten sich leicht verbessert im Vergleich zu reinem PA6. Hier konnte ein Anstieg der Bruchdehnung von 499% auf 648% beobachtet werden. Der E-Modul für das System *PA6/Neutral Rot* nahm von 633 MPa auf 539 MPa ab.

Die effizientesten Anti-Nukleierungsmittel für PA6 wurden im Verlauf dieser Arbeit auch auf ihre ***anti-nukleierende Wirkung in Polyamid 66*** analysiert. Hierbei erzielte Neutral Rot die besten Ergebnisse und verringerte die Kristallisationstemperatur um 10 °C von 231 °C auf 221 °C bei einer Additivkonzentration von 2,0 Gew.-%.

Im Rahmen dieser Arbeit wurde eine Vielzahl neuer Anti-Nukleierungsmittel gefunden und eine Methode zur signifikanten Verbesserung des kommerziell eingesetzten Nigrosins entwickelt. Durch die systematischen Untersuchungen verschiedener Verbindungen, wie ***Nigrosin, anorganischen und organischen Salzen*** sowie ***Azinfarbstoffen***, konnten Struktur-Eigenschaftsbeziehungen hinsichtlich des Anti-Nukleierungspotentials in PA6 festgestellt werden. Die Forschungsarbeiten haben gezeigt, dass vorwiegend planare und starre Strukturen mit Substituenten, welche in der Lage sind mit den Wasserstoffbrücken der Polyamidketten zu interagieren, die effizientesten Anti-Nukleierungsmittel darstellen. Hierbei haben besonders Verbindungen mit Amino- oder ionische Gruppen die besten Resultate erzielt. Diese Ergebnisse deuten darauf hin, dass Wechselwirkungen zwischen

den Anti-Nukleierungsmitteln und den Polymerketten auftreten was zu einem verzögertem Kristallisationsprozess des Polymers führt. Weitestgehend werden durch diese Verbindungen keine weiteren Eigenschaften des Polymers, wie z.B. eine Verringerung der Schmelztemperatur oder des Kristallisationsgrad, beeinflusst.



## 8 Experimental part

### 8.1 Materials and equipment

#### *Polymers*

In the frame of this work the influence of additives on the crystallization behavior of semi-crystalline polyamides was studied. All polymer resins were provided by BASF SE and contained no further additives. The polymer granulates were pulverized in a freezer mill (Retsch ZM100, Schieritz & Hauenstein AG) prior to use through a 1 mm sieve. The following polymers were investigated:

- Polyamide 6 (PA6), Ultramid® B27 E; a low-viscosity grade for compounding and the production of monofilaments.
- Polyamide 66 (PA66), Ultramid® A27 E 01; a low-viscosity grade for compounding and the production of monofilaments and bristles.

#### *Chemicals and solvents*

All chemicals (except the bisurea) were purchased from Sigma Aldrich and used without further purification.

1,1'-(*trans*-1,4-cyclohexylene)bis(3-*tert*-butylurea)

(synthesized by Richter, Chair MCI, University of Bayreuth)

1,4,5,8-Naphthalenetetracarboxylic dianhydride

4,7-Dimethyl-1,10-phenanthroline (98%)

Acid Black 2

Acridine (97%)

Azure A Chloride (dye content, 80%)

Anthracene (97%)

Bathocuproine (96%)

Darrow Red (dye content, ≥ 65%)

Ethyl isothiocyanate (97%)

Giemsa Stain

Induline

Isopropyl isothiocyanate (97%)

Potassium hexafluorophosphate (98%)  
Lithium chloride (anhydrous, 99%)  
Methylene Blue (dye content,  $\geq 82\%$ )  
Methylene Violet 3RAX (dye content, 90%)  
Methyl isothiocyanate (97%)  
N,N-Dimethylmethyleiminium chloride ( $\geq 95\%$ )  
Neutral Red (dye content,  $\geq 58\%$ )  
Nile Blue A (dye content,  $\geq 75\%$ )  
Nile Blue Chloride (dye content,  $\geq 85\%$ )  
Phenazine (98%)  
Pyronin B (dye content,  $\geq 30\%$ )  
Pyronin Y (dye content,  $\geq 50\%$ )  
Safranin O (dye content,  $\geq 85\%$ )  
Solvent Black 5  
Solvent Black 7 / Colorant Black 500  
Tetrahydrofuran (anhydrous,  $\geq 99.9\%$ )  
*tert*-Butyl isothiocyanate (99%)  
Tetrabutylammonium bromide ( $\geq 98\%$ )  
Tetrabutylammonium chloride ( $\geq 97\%$ )  
Tetrabutylammonium hexafluorophosphate ( $\geq 99\%$ )  
Tetrabutylammonium iodide ( $\geq 98\%$ )  
Tetrabutylammonium tetraphenylborate ( $\geq 99\%$ )  
Tetraethylammonium chloride ( $\geq 99\%$ )  
Tetraethylammonium hexafluorophosphate ( $\geq 99\%$ )  
Tetraethylammonium iodide ( $\geq 98\%$ )  
Tetrahexylammonium hexafluorophosphate ( $\geq 97\%$ )  
Tetramethylammonium chloride ( $\geq 99\%$ )  
Tetramethylammonium hexafluorophosphate ( $\geq 98\%$ )  
Tetramethylammonium iodide (99%)  
Tetrapropylammonium hexafluorophosphate  
Tetrapropylammonium tetrafluoroborate ( $\geq 98\%$ )



Toluidine Blue O (dye content, 80%)

*trans*-1,4-diaminocyclohexane ( $\geq 98\%$ )

### Equipment

$^1\text{H}$ -NMR-spectroscopy	Bruker Avance 300 (300 MHz)
Compounding	Co-rotating twin-screw compounder DSM Xplore 15 mL
DMTA	Rheometric Scientific DMTA IV
DSC	Perkin Elmer Diamond DSC with autosampler; Standard heating and cooling rates of 10 K/min
GC-MS	Agilent 5977A MSD with Gerstel autosampler
Haze-Meter	BYK Gardener Haze Gard plus Calibration by clarity and haze standard
Injection molding	Micro-injection molding machine DSM Xplore 12 mL
Mass spectrometry	Finnigan Mat 112S (70 eV)
Melting Point System	Mettler Toledo MP90
Microtome	Leica RM 2255 rotary microtome
Polarized light microscopy	Nikon, DIAPHOT 300 (microscope) Mettler, FP82HT (hot stage) Nikon, DMX1200 (digital camera)
Powder mill	Schieritz & Hauenstein AG, Retsch ZM100, freezer mill
SEM	Zeiss 1530 FESEM Cressington Sputter Coater 208HR
Tensile testing	Instron 5565 universal tester
TGA	Mettler Toledo TGA/SDTA851e; Standard heating and cooling rates of 10 K/min
Tumble mixer	Heidolph Reax 2
WAXS	Bruker D8 Advance CuK $\alpha$ radiation ( $\lambda = 1.54 \text{ \AA}$ )

### 8.2 Methods and procedures

The main focus of this work is on the investigation of polymer crystallization, polymer morphology and the improvement of the macroscopic properties influenced by various polymer additives.

The basic molecular characterizations were carried out by standard techniques such as  $^1\text{H}$ -NMR- and mass spectrometry, gas chromatography–mass spectrometry, thermogravimetric analysis and differential thermal analysis. In order to evaluate the effect of different polymer additives on the thermal behavior and morphology of polyamides, efficient and reliable methods and procedures were applied. Most of the procedures presented in the following have already been established by coworkers from the Chair Macromolecular Chemistry I for polyamides<sup>[14]</sup> and were adjusted to optimize the effect of various additives. With these procedures it is possible to obtain significant information with small amounts of material. The polymer crystallization and melting temperatures were characterized by differential scanning calorimetry after microscale polymer processing. The optical and mechanical properties were obtained from injection molded platelets and tensile rods. The polymer morphology was investigated by means of polarized light microscopy and electron microscopy.

In the following the applied techniques and conditions will be briefly summarized:

- Compounding
- Injection molding
- Thermal analysis
- Nuclear magnetic resonance spectroscopy
- Gas chromatography–mass spectrometry
- Polarized light microscopy
- Scanning electron microscopy
- Optical characterization
- Wide angle X-ray diffraction
- Mechanical analysis
- Dynamic mechanic thermal analysis
- Water absorption experiments

### 8.2.1 Compounding

To guarantee easy filling of the polymer to the micro-compounder and homogeneous melting while compounding the polymer granulate was first pulverized with a freezer mill. The obtained powder was dried at least for 24 h at 80 °C before compounding with a co-rotating twin-screw compounder (DSM Xplore 15 mL) under nitrogen atmosphere. The micro-compounder has three heating zones which can be controlled separately. The heating zones were set to the desired melt temperatures of the polymer as listed below. After a defined processing time, the melt was discharged and collected either as polymer strand or transferred directly to the injection molding unit. The standard processing parameters for PA6 and PA66 are listed in Table 32.

Table 32. Standard processing parameters for the investigated polymers and their measured melt temperature.

Polymer	Temperature profile (T <sub>1</sub> -T <sub>2</sub> -T <sub>3</sub> ) [°C]	Melt temperature during processing [°C]	Compounding time [min]	Rotational speed [rpm]
PA6	230-260-260	245	5	50
PA66	260-300-300	280	5	50

In the course of this thesis various compounding experiments for PA6 with varying compounding parameters were conducted. Either the melt temperature during processing or the processing time were varied. Table 33 summarizes the parameters for the extrusion experiments with varying melt temperature and constant compounding time, while Table 34 summarizes the parameters for the extrusion experiments with constant melt temperature during processing and varying compounding time.

Table 33. Processing parameters for the extrusion experiments with varying melt temperature during processing and constant compounding time for PA6.

Temperature profile (T <sub>1</sub> -T <sub>2</sub> -T <sub>3</sub> ) [°C]	Melt temperature during processing [°C]	Compounding time [min]	Rotational speed [rpm]
230-260-260	245		
240-275-275	259		
250-290-290	273	5	50
270-300-300	283		

Table 34. Processing parameters for the extrusion experiments with varying processing time and constant melt temperature during processing for PA6.

Temperature profile ( $T_1$ - $T_2$ - $T_3$ ) [°C]	Melt temperature during processing [°C]	Processing time [min]	Rotational speed [rpm]
230-260-260	245	5	50
		10	
		20	
		30	
		60	

The additives were investigated in a concentration range from 2.0 wt% or 1.5 wt% to 0.1 wt%. In the following the calculation, preparation and initial weights are exemplarily shown for a concentration series from 1.5 wt% to 0.1 wt%.

The different concentrations were prepared by diluting the initial additive concentration of 1.5 wt% with a mixture of the initial PA6/additive powder blend and neat PA6, yielding the following dilution series: 1.3 wt%, 1.0 wt%, 0.8 wt%, 0.6 wt%, 0.4 wt%, 0.2 wt% and 0.1 wt%. The preparation steps and initial weights for a concentration series are shown in Table 35 and are explained below.

Table 35. Initial weights and additive concentration for a concentration series in PA6.

Run	Comment	$m_{\text{powder mixture}}$ [g]	$m_{\text{neat polymer}}$ [g]	$C_{\text{additive}}$ [wt%]
1	cleaning	14.0	0.0	1.50
2	1st sample	8.6	0.0	1.50
3	1st dilution	6.8	1.8	1.30
4	2nd dilution	4.7	3.9	1.00
5	3rd dilution	3.9	4.7	0.80
6	4th dilution	2.7	5.9	0.60
7	5th dilution	1.6	7.0	0.40
8	6th dilution	0.5	8.1	0.20
9	7th dilution	0.2	8.4	0.10

For the cleaning run and the first sample run a blend with a concentration of 1.5 wt% additive was used. For the following runs the initial additive concentration was diluted by neat PA6 and the initial powder blend to obtain the requested concentrations. With a dead volume of 5.4 g the exact additive concentrations of the extrudates could be calculated according to Richter et al.:<sup>[14]</sup>

With an initial additive concentration of 1.5 wt% and a dead volume of 5.4 g (for PA6 and the compounder used for this work), the amount of additive within the dead volume is 0.081 g. To obtain an additive concentration of 1.3 wt%, 6.8 g of the initial powder mixture with 1.5 wt% of additive and 1.8 g of neat PA6 are added. The amount of additive in 6.8 g of the initial powder mixture is 0.102 g. Consequently, the total amount of additive within the compounder in the first dilution run is 0.183 g. The exact additive concentration results from the total amount of additive divided by the amount of polymer:

$$\left( \frac{0.081 \text{ g} + 0.102 \text{ g}}{5.4 \text{ g} + 6.8 \text{ g} + 1.8 \text{ g}} \right) \cdot 100\% = \left( \frac{0.183 \text{ g}}{14 \text{ g}} \right) \cdot 100\% = 1.31\%$$

### 8.2.2 Injection molding

Injection molding platelets were produced using a DSM Xplore 12mL injection molding machine to obtain specimen for the determination of optical properties, morphology investigations, WAXS, and mechanical measurements. The injection molding unit was directly filled with the discharged polymer melt from the twin-screw compounder. Specimen with a diameter of 25 mm and a thickness of 1.1 mm were prepared under nitrogen atmosphere using an injection mold with a thickness of 1.1 mm. Tensile rods with a measuring section of 30 mm x 5 mm x 2 mm were prepared in the same way. The standard injection molding conditions for PA6 and PA66 are listed in Table 36.

Table 36. Standard injection molding parameters for PA6 and PA66.

Polymer	Barrel temperature [°C]	Mold temperature [°C]	Injection pressure [bar]	Injection time [sec]	Holding time [sec]
PA6	250	100	6	10	10
PA66	260	100	6	10	10

### 8.2.3 Thermal analysis

Thermogravimetric analyses (TGA) of the additives were performed on a Mettler Toledo TGA/SDTA851e under nitrogen atmosphere (60mL/min) at a heating rate of 10 K/min between 30 °C and 700 °C. Melting temperatures of the additives were determined by simultaneous differential thermal analysis (DTA).

Differential scanning calorimetry (DSC) measurements for the determination of the polymer melting and crystallization temperatures were conducted on a Perkin-Elmer Diamond DSC with autosampler under nitrogen (20 mL/min) at heating and cooling rates of 10 K/min. Samples were taken either from the polymer strand or from the sprue of the injection molding platelets. Two heating and cooling runs were performed. To erase the thermal history, samples were held well above the equilibrium melting temperature for 5 min before each cooling run. Values for the polymer melting temperatures were determined at the endothermic peak maximum of the second heating scan and values for the polymer crystallization temperatures were determined at the exothermic peak minimum of the second cooling scan.

Table 37. Starting and end temperatures for the DSC measurements of PA6 and PA66. For each sample two heating and cooling scans were performed under nitrogen at 10 K/min. Samples were held at the end temperature for 5 min before each cooling run.

Polymer	Starting temperature [°C]	End temperature [°C]
PA6	30	250
PA66	30	280

### 8.2.3 Nuclear magnetic resonance spectroscopy

Spectra were recorded on a Bruker AC spectrometer (300 MHz) at room temperature using CDCl<sub>3</sub> or (CD<sub>3</sub>)<sub>2</sub>SO as solvent and internal standard. Chemical shifts are reported in ppm relative to residual protons in the deuterated solvent.

### 8.2.4 Gas chromatography–mass spectrometry

In order to identify impurities or degradation products within the investigated compounds gas chromatography–mass spectrometry (Agilent 5977A MSD with Gerstel Autosampler) was used. Therefore 4 -5 mg polymer strand was placed in a μ-vial. This μ-vial was inserted to a glass capillary called “twister-desorption-liner” (TDU) and stored in the autosampler of

the GC-MS machine. The TDU was heated to the requested temperature and held there for 5 min. After 5 min the TDU was purged with helium gas (1 mL/min) to transfer the degassed substances to the gas chromatography column ((5%-Phenyl)-methylpolysiloxane column). A chromatogram was recorded for 38 min. The eluant was analyzed by mass spectrometry with a rate of seven mass spectra per second. Only one sample was used to measure at different temperatures. For this purpose the sample was heated to the lowest required measuring temperature, held there for 5 min and then cooled to room temperature. After 38 min, when the first measurement was finished, the sample was heated to the second highest measuring temperature. This procedure was repeated for each temperature ending with the highest measuring temperature.

#### 8.2.5 Polarized light microscopy

Polarized light microscopy was applied to investigate the crystallization process of the compounds, to screen promising additives quickly and to investigate the morphology of the compounds more detailed. Therefore, three different types of experiments were conducted and are explained below. All experiments were performed using an optical microscope (Nikon, DIAPHOT 300) equipped with a hot stage (Mettler, FP82HT). Optical micrographs were recorded by a Nikon ACT-1 software using a digital camera (Nikon, DMX1200).

##### *Additive screening method*

In order to evaluate the anti-nucleation ability of a large number of compounds a fast screening method was of great interest. In this work an additive screening process established by Abraham et. al.<sup>[29]</sup> to identify suitable compounds for the use as nucleating agents was applied to screen anti-nucleating agents. For this purpose samples were prepared by melting a polymer pellet between two glass slides at 250 °C (PA6; PA66: 280 °C). Afterwards the sample was pressed for 2 minutes at 250 °C (PA6; PA66: 280 °C) and quenched to room temperature. Up next the cover glass was removed and a small amount of additive was positioned in the middle of the film. The whole setup was covered again and inserted to the hot stage under a polarized optical microscope. The samples were heated well above the melting temperature of the polymer for 5 min whereas the additives partly dissolve and diffuse into the surrounding polymer melt. The setup was slowly cooled at 10 K/min to monitor the crystallization processes of both the additives and the polymer.

### *Crystallization of extruded compounds*

In order to investigate the crystallization behavior of samples with homogenous distributed additives, similar experiments as described for the additive screening method, were conducted. Samples were prepared by melting a polymer pellet of the extruded and additivated compounds between two glass slides at 250 °C (PA6; PA66: 280 °C). Afterwards, the sample was pressed for 2 minutes at 250 °C (PA6; PA66: 280 °C) and quenched to room temperature. The so obtained sample was inserted to the hot stage. The crystallization and dissolution temperatures of the compounds were determined at the disappearance and reappearance of birefringent structures (spherulites) at heating and cooling rates of 10 K/min. Besides dynamic DSC measurements, also isothermal DSC measurements were conducted. The samples were heated rapidly to 250 °C, held there for 5 minutes and cooled to the desired isothermal temperature with 20 K/min. The sample was held at this temperature for the requested time and then cooled to room temperature.

### *Thin sections*

In order to explore the morphology of injection molding samples by polarized light microscopy, thin sections with a thickness of 10 µm were cut (Leica RM 2255 rotary microtome) parallel to the direction of injection (flow direction). These thin sections were placed between two object slides and fastened with a tape and analyzed with a polarized optical microscope.

### 8.2.6 Scanning electron microscopy

Samples for morphological studies were prepared by dissolving PA6 in formic acid with subsequent dropcasting on a silicon waver. The waver was shortly placed on a hot stage at 250 °C and quenched to room temperature to obtain a homogenous film. For the additivated film as little as possible of the additive was placed onto the molten film by a pin and quenched to room temperature after 60 seconds. The dried samples were sputtered with platinum (0.8 nm) by a Cressington Sputter Coater 208HR. Scanning electron micrographs were recorded using a Zeiss 1530 FESEM (SEM imaging).



### 8.2.7 Optical characterization

The optical properties were determined according to ASTM D-1003 on 1.1 mm thick injection molded platelets with diameters of 25 mm using a Haze-Gard Plus instrument (BYK Gardner GmbH, Germany). The average of at least three samples is reported.

### 8.2.8 Wide angle X-ray diffraction

WAXS measurements were conducted on 1.1 mm thick injection molding platelets with diameters of 25 mm with a Bruker D8 Advance X-ray diffractometer using  $\text{CuK}\alpha$  radiation ( $\lambda = 1.54 \text{ \AA}$ ). Data was recorded in the range of 5-40° (2 Theta) with a step size of 0.05° and a step time of 10 sec.

### 8.2.9 Mechanical analysis

Tensile tests were conducted on conditioned (4 days, 70 °C, 62 %rh) specimen on an Instron 5565 universal tester with a camera (Instron 2663-821 Advanced Video Extensometer), pneumatic clamps and a 1 kN load cell. Tensile rods with a measuring section of 30 mm x 5 mm x 2 mm were tested at an initial strain rate of 0.3 mm/s (up to 0.5% strain; video measurement) and then increased to 50.0 mm/s. The reported moduli were calculated from the initial slope between 0.15% and 0.35%. The average of at least four samples is reported.

### 8.2.10 Dynamic mechanic thermal analysis

Glass transition temperatures were measured by dynamic mechanic thermal analysis (DMTA) using a Rheometric Scientific DMTA IV. Measurements were performed in tension geometry from – 20 °C to 140 °C with a heating rate of 2 K/min and a frequency of 1 Hz. The specimen were punched out from an injection molding platelet and conditioned at 70 °C and 62 rh% for 4 days corresponding to DIN ISO 527-2.<sup>[65]</sup> The sample dimensions were 1.11 mm x 10.00 mm x 1.96 mm. The value for the glass transition temperature is determined from the peak maximum of  $\tan \delta$ .

### 8.2.11 Water absorption experiments

Water absorption experiments were conducted on 1.1 mm thick injection molding platelets with diameters of 25 mm. Samples were dried for 8 days at 80 °C under vacuum atmosphere. The dried samples were weighed and then stored at 30 °C and 50 rh%. In the

following, samples were weighed every 24 h until no more increase in weight could be determined.

## 8.3 Synthesis and characterization of bithiourea derivatives

Tetrahydrofuran (THF) was purified and dried prior to use according to standard procedures. The starting materials were purchased Sigma Aldrich and used as received.  $^1\text{H}$ -NMR spectra were recorded on a Bruker Avance 300 spectrometer. The chemical shifts are reported in ppm ( $\delta$ ). Mass spectra were recorded on a Finnigan Mat 112S instrument (70 eV) with direct probe inlet at the central analytic laboratory of the University of Bayreuth. All spectra were recorded at 298 K. The thermal properties were simultaneously determined by means of combined thermogravimetric (TGA) and differential thermal analysis (DTA) on a Mettler Toledo TGA/SDTA851e between 30 °C and 700 °C with a heating rate of 10 K/min under nitrogen atmosphere.

*General synthetic route to trans-1,4-cyclohexyl-bithiourea derivatives*

*Trans*-1,4-diaminocyclohexane was added in a flame-dried Schlenk flask and dissolved in THF under argon atmosphere. The solution was cooled to 0 °C in an ice bath and the corresponding isocyanate, diluted in THF, was added slowly under heavy stirring. The reaction mixture was heated to reflux and, unless indicated otherwise, maintained at this temperature for 12 h. After cooling the precipitated white solid was filtered off and dried under vacuum for 2 h (70 °C, 100 mbar).

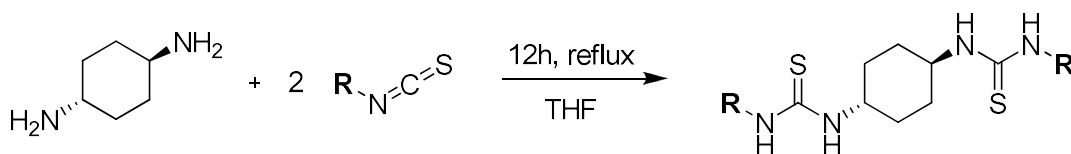


Figure 129. Synthetic route to *trans*-1,4-cyclohexyl-bithiourea derivatives starting from *trans*-1,4-diaminocyclohexane.

**1,1'-(*trans*-1,4-cyclohexane)bis(3-*tert*-butylthiourea) 2a**

Molecular formula: C<sub>16</sub>H<sub>32</sub>N<sub>4</sub>S<sub>2</sub>; M = 344.58 g/mol

Internal notebook number: HH21

*Reaction batch:*

1.14 g (10 mmol) *trans*-1,4-diaminocyclohexane

2.65 g (23 mmol) *tert*-butyl isothiocyanate

200 mL THF

*Characterization:*

<sup>1</sup>H-NMR (300 MHz, DMSO d<sub>6</sub>): δ [ppm] = 6.9-7.1 (m, 4H), 3.9 (m, 2H), 1.9 (m, 4H), 1.4 (s, 18H), 1.1 (m, 4H)

MS (70 eV), m/z (%): 344 (100); 213 (31); 155 (36); 138 (23); 133 (48); 96 (95); 77 (65); 57 (49); 41 (33)

Melting point: T<sub>m</sub> = subl.

Temperature at 5 % weight loss: T<sub>-5 wt%</sub> = 241 °C

**1,1'-(*trans*-1,4-cyclohexane)bis(3-isopropylthiourea) 2b**

Molecular formula: C<sub>14</sub>H<sub>28</sub>N<sub>4</sub>S<sub>2</sub>; M = 316.53 g/mol

Internal notebook number: HH23

*Reaction batch:*

1.44 g (12.65 mmol) *trans*-1,4-diaminocyclohexane

2.56 g (25.30 mmol) isopropyl isothiocyanate

250 mL THF

*Characterization:*

<sup>1</sup>H-NMR (300 MHz, DMSO d<sub>6</sub>): δ [ppm] = 7.1 (m, 4H), 3.7-4.2 (m, 4H), 1.9 (m, 4H), 1.2 (m, 4H), 1.1 (s, 12H)

MS (70 eV), m/z (%): 316 (100); 214 (6); 199 (33); 180 (6); 155 (10); 119 (93); 96 (38); 81 (17); 58 (30); 44 (18)

Melting point: T<sub>m</sub> = subl.

Temperature at 5 % weight loss: T<sub>-5 wt%</sub> = 269 °C

**1,1'-(trans-1,4-cyclohexane)bis(3-ethylthiourea) 2c**Molecular formula: C<sub>12</sub>H<sub>24</sub>N<sub>4</sub>S<sub>2</sub>; M = 288.48 g/mol

Internal notebook number: HH24

*Reaction batch:*1.58 g (13.88 mmol) *trans*-1,4-diaminocyclohexane

2.42 g (27.76 mmol) ethyl isothiocyanate

250 mL THF

*Characterization:*<sup>1</sup>H-NMR (300 MHz, CDCl<sub>3</sub>): δ [ppm] = 7.9 (m, 4H), 3.7 (m, 2H), 3.5 (m, 4H), 2.0 (m, 4H), 1.5 (m, 4H), 1.3 (m, 6H)

MS (70 eV), m/z (%): 288 (100); 184 (32); 155 (9); 150 (5); 105 (82); 96 (37); 81 (19); 60 (16); 45 (16)

Melting point: T<sub>m</sub> = subl.Temperature at 5 % weight loss: T<sub>-5 wt%</sub> = 265 °C**1,1'-(trans-1,4-cyclohexane)bis(3-methylthiourea) 2d**Molecular formula: C<sub>10</sub>H<sub>20</sub>N<sub>4</sub>S<sub>2</sub>; M = 260.42 g/mol

Internal notebook number: HH25

*Reaction batch:*1.75 g (15.38 mmol) *trans*-1,4-diaminocyclohexane

2.25 g (30.76 mmol) methyl isothiocyanate

250 mL THF

*Characterization:*<sup>1</sup>H-NMR (300 MHz, CDCl<sub>3</sub>/CF<sub>3</sub>COOD): δ [ppm] = 11.4 (m, 2H), 8.0 (m, 2H), 3.6 (m, 2H), 3.1 (m, 6H), 2.0 (m, 4H), 1.5 (m, 4H)

MS (70 eV), m/z (%): 260 (100); 193 (7); 170 (37); 152 (7); 137 (6); 129 (7); 91 (79); 81 (20); 74 (27); 57 (22); 24 (10)

Melting point: T<sub>m</sub> = subl.Temperature at 5 % weight loss: T<sub>-5 wt%</sub> = 242 °C



## 9 Literature

- [1] W. H. Carothers **1937**.
- [2] M. I. Kohan (Ed.), *Nylon plastics handbook*, Hanser, Munich **1995**.
- [3] G. Abts, *Kunststoff-Wissen für Einsteiger*, Hanser, München **2014**.
- [4] M. Dexter, R. W. Thomas, R. E. King, in *Encyclopedia of polymer science and technology*, Wiley Interscience. Hoboken, NJ **2004**.
- [5] *Additives for Polymers* **2016**, 2016, 2.
- [6] G. Beyer, *Plastics, Additives and Compounding* **2002**, 4, 22.
- [7] E. C. Achilleos, G. Georgiou, S. G. Hatzikiriakos, *J Vinyl Addit Technol* **2002**, 8, 7.
- [8] R. A. Charvat, *Coloring of plastics*, Wiley-Interscience, New York **2004**.
- [9] R. A. Mustalish, *Studies in Conservation* **2013**, 45, 133.
- [10] S. E. Amos, *Plastics additives handbook*, Hanser, Munich u.a. **2009**.
- [11] A. Hayashi, *Nigrosine compound, resin composition, molded product, crystallization temperature lowering, fluidity improving and surface gloss improving method*, US 6,395,809 B1.
- [12] F. L. Binsbergen, *Polymer* **1970**, 11, 253.
- [13] J. P. Mercier, *Polym. Eng. Sci.* **1990**, 30, 270.
- [14] F. Richter, *Supramolecular polymer additives to improve the crystallization behavior and optical properties of polybutylene terephthalate and polyamides*, Bayreuth **2013**.
- [15] H. Takeuchi, K. Sukata, *Nucleation effect inhibitor, crystalline resin composition and method of controlling crystallization of crystalline resin composition*, US 2005/0234159 A1.
- [16] G. Topoulos, *Polyamide compositions for flow molding*, US 2012/0177858 A1.
- [17] M. D. Roth, N. Lamberts, B. Hoffmann, *Polyamide moulding compounds and use thereof in the production of moulded articles*, US 2014/0094548 A1.
- [18] S. E. Amos, *Plastics additives handbook*, Hanser, München **2001**.
- [19] K. Sukata, H. Takeuchi, M. Shimada, Y. Agari, *J. Appl. Polym. Sci.* **2006**, 101, 3270.
- [20] M. D. Lechner, *Makromolekulare Chemie*, Birkhäuser, Basel u.a. **2010**.
- [21] J. Cowie, V. Arrighi, *Polymers: Chemistry and Physics of Modern Materials, Third Edition*, CRC Press, Hoboken **2007**.
- [22] S. T. Milner, *Soft Matter* **2011**, 7, 2909.

- [23] G. Menges, *Menges Werkstoffkunde Kunststoffe*, Hanser, München **2011**.
- [24] A. Costantino, V. Pettarin, J. Viana, A. Pontes, A. Pouzada, P. Frontini, *Procedia Materials Science* **2012**, *1*, 34.
- [25] K. Hashimoto, H. Saito, *Polym J* **2008**, *40*, 900.
- [26] L. Li, W. H. de Jeu, *Physical review letters* **2004**, *92*, 75506.
- [27] B. Sun, Y. Qin, Y. Xu, Y. Sun, B. Wang, K. Dai, G. Zheng, C. Liu, J. Chen, *J Mater Sci* **2013**, *48*, 5354.
- [28] K. M. Bernland, *Nucleating and clarifying polymers*, Zürich, ETH **2010**.
- [29] F. Abraham, *Synthesis and structure-property relations of 1,3,5-benzenetrisamides as nucleating agents for isotactic polypropylene and poly(vinylidene fluoride)* **2009**.
- [30] C. Ouyang, W. Xue, D. Zhang, Q. Gao, X. Li, K. Zheng, *Polym Eng Sci* **2015**, *55*, 2011.
- [31] A. Siegmann, Z. Baraam, *J. Appl. Polym. Sci.* **1980**, *25*, 1137.
- [32] A. Siegmann, Z. Baraam, *International Journal of Polymeric Materials and Polymeric Biomaterials* **2006**, *8*, 243.
- [33] W. Lin, Y. Gowayed, *Journal of Applied Polymer Science* **1999**, *74*, 2386.
- [34] BASF, *Datasheet Ultramid B27 E* **2008**,  
[http://www.plasticsportal.net/wa/EU~pl\\_PL/Catalog/ePlastics/doc4/BASF/product/ultramid\\_b27\\_e/.pdf?asset\\_type=pds/pdf&language=EN&urn=urn:documentum:eCommerce\\_sol\\_EU:09007bb280079c22.pdf](http://www.plasticsportal.net/wa/EU~pl_PL/Catalog/ePlastics/doc4/BASF/product/ultramid_b27_e/.pdf?asset_type=pds/pdf&language=EN&urn=urn:documentum:eCommerce_sol_EU:09007bb280079c22.pdf).
- [35] B. Fillon, J. C. Wittmann, B. Lotz, A. Thierry, *Journal of Polymer Science Part B: Polymer Physics* **1993**, *31*, 1383.
- [36] V. Miri, S. Elkoun, F. Peurton, C. Vanmansart, J.-M. Lefebvre, P. Krawczak, R. Seguela, *Macromolecules* **2008**, *41*, 9234.
- [37] N. Avramova, S. Fakirov, I. Avramov, *Journal of Polymer Science: Polymer Physics Edition* **1984**, *22*, 311.
- [38] T. Ferreira, P. E. Lopes, A. J. Pontes, M. C. Paiva, *Polym. Adv. Technol.* **2014**, *25*, 891.
- [39] M. Todoki, T. Kawaguchi, *Journal of Polymer Science: Polymer Physics Edition* **1977**, *15*, 1067.
- [40] J. Gao, G. C. Walsh, D. Bigio, R. M. Briber, M. D. Wetzel, *Polymer Engineering & Science* **2000**, *40*, 227.
- [41] C. Vasile (Ed.), *Handbook of polyolefins*, Dekker, New York u.a. **2000**.



- [42] Gestis Stofdatenbank, *Caprolactam*,  
[http://gestis.itrust.de/nxt/gateway.dll/gestis\\_de/000000.xml?f=templates\\$fn=default.htm\\$3.0](http://gestis.itrust.de/nxt/gateway.dll/gestis_de/000000.xml?f=templates$fn=default.htm$3.0).
- [43] H. K. Reimschuessel, *Journal of Polymer Science: Macromolecular Reviews* **1977**, *12*.
- [44] V. S. Kumar, S. K. Gupta, *Ind. Eng. Chem. Res.* **1997**, *36*, 1202.
- [45] G. C. Ongemach, A. C. Moody, *Anal. Chem.* **1967**, *39*, 1005.
- [46] S. Mori, M. Furusawa, T. Takeuchi, *Anal. Chem.* **1970**, *42*, 661.
- [47] G. C. Ongemach, V. A. Dorman-Smith, W. E. Beier, *Anal. Chem.* **1966**, *38*, 123.
- [48] A. Anton, *J. Appl. Polym. Sci.* **1963**, *7*, 1629.
- [49] M. Kyotani, S. Mitsuhashi, *J. Polym. Sci. A-2 Polym. Phys.* **1972**, *10*, 1497.
- [50] M. Ito, K. Mizuochi, T. Kanamoto, *Polymer* **1998**, *39*, 4593.
- [51] S. Dasgupta, W. B. Hammond, W. A. Goddard, *J. Am. Chem. Soc.* **1996**, *118*, 12291.
- [52] L. Shen, I. Y. Phang, T. Liu, *Polymer Testing* **2006**, *25*, 249.
- [53] N. Vasanthan, D. R. Salem, *Journal of Polymer Science Part B: Polymer Physics* **2000**, *38*.
- [54] Z. MO, B. YANG, H. ZHANG, *Anal. Sci.* **1991**, *7*, 1637.
- [55] S. Polizzi, G. Fagherazzi, A. Benedetti, M. Battagliarin, T. Asano, *European Polymer Journal* **1991**, *27*, 85.
- [56] E. Piorkowska, G. C. Rutledge, *Handbook of Polymer Crystallization*, Wiley, Hoboken **2013**.
- [57] M. Dole, B. Wunderlich, *Makromol. Chem.* **1959**, *34*, 29.
- [58] J. E. Mark (Ed.), *Polymer data handbook*, Oxford University Press, Oxford, New York **2009**.
- [59] B. Wunderlich, *Thermal analysis of polymeric materials*, Springer, Berlin **2005**.
- [60] S. Kazemi, M. R. M. Mojtahedi, W. Takarada, T. Kikutani, *Journal of Applied Polymer Science* **2014**, *131*.
- [61] J. Rieger, *Polymer Testing* **2001**, *20*, 199.
- [62] M. S. Rahman, I. M. Al-Marhubi, A. Al-Mahrouqi, *Chemical Physics Letters* **2007**, *440*, 372.

- [63] Cambridge Polymer Group, *Glass Transition by DMA* **2014**,  
[http://www.campoly.com/files/6114/2850/4047/035\\_Glass\\_Transition\\_by\\_DMA\\_AD\\_MIN-0243\\_v2.0.pdf](http://www.campoly.com/files/6114/2850/4047/035_Glass_Transition_by_DMA_AD_MIN-0243_v2.0.pdf).
- [64] PerkinElmer, *Dynamic Mechanical Analysis (DMA)* **2013**,  
[https://www.perkinelmer.com/CMSResources/Images/44-74546GDE\\_IntroductionToDMA.pdf](https://www.perkinelmer.com/CMSResources/Images/44-74546GDE_IntroductionToDMA.pdf).
- [65] Deutsches Institut für Normung e.V., *Bestimmung der Zugeigenschaften*, 83.080.00  
**1996**.
- [66] Y. C. Kim, C. Y. Kim, S. C. Kim, *Polym. Eng. Sci.* **1991**, *31*, 1009.
- [67] M. Kristiansen, T. Tervoort, P. Smith, H. Goossens, *Macromolecules* **2005**, *38*, 10461.
- [68] L. Han, Y. Wang, L. Liu, F.-m. Xiang, T. Huang, Z.-w. Zhou, *Chin J Polym Sci* **2010**, *28*, 457.
- [69] M. Kristiansen, M. Werner, T. Tervoort, P. Smith, M. Blomenhofer, H.-W. Schmidt, *Macromolecules* **2003**, *36*, 5150.
- [70] A. S. Vaughan, I. L. Hosier, *J Mater Sci* **2008**, *43*, 2922.
- [71] F. Richter, H.-W. Schmidt, *Macromol. Mater. Eng.* **2013**, *298*, 190.
- [72] M. Kristiansen, P. Smith, H. Chanzy, C. Baerlocher, V. Gramlich, L. McCusker, T. Weber, P. Pattison, M. Blomenhofer, H.-W. Schmidt, *Crystal Growth & Design* **2009**, *9*, 2556.
- [73] M. Blomenhofer, S. Ganzleben, D. Hanft, H.-W. Schmidt, M. Kristiansen, P. Smith, K. Stoll, D. Mäder, K. Hoffmann, *Macromolecules* **2005**, *38*, 3688.
- [74] F. Abraham, R. Kress, P. Smith, H.-W. Schmidt, *Macromol. Chem. Phys.* **2013**, *214*, 17.
- [75] A. Thierry, C. Straupé, J.-C. Wittmann, B. Lotz, *Macromol. Symp.* **2006**, *241*, 103.
- [76] M. Nie, R. Han, Q. Wang, *Ind. Eng. Chem. Res.* **2014**, *53*, 4142.
- [77] J. Peng, P. J. Walsh, R. C. Sabo, L.-S. Turng, C. M. Clemons, *Polymer* **2016**, *84*, 158.
- [78] F. Abraham, S. Ganzleben, D. Hanft, P. Smith, H.-W. Schmidt, *Macromol. Chem. Phys.* **2010**, *211*, 171.
- [79] B. Fillon, B. Lotz, A. Thierry, J. C. Wittmann, *J. Polym. Sci. B Polym. Phys.* **1993**, *31*, 1395.
- [80] I. Mudra, G. Balázs, *Journal of Thermal Analysis and Calorimetry* **1998**, *52*, 355.
- [81] G. Gurato, D. Gaidano, R. Zannetti, *Makromol. Chem.* **1978**, *179*, 231.

- [82] Brink, T. Brink, J. L. Cohen, T. K. Sham, *PCT Int. Appl. WO 9824846*.
- [83] Q. Du, R. Wang, W. Chen, L. Wang, *Gaofenzi Cailiao Kexue Yu Gongcheng* **1991**, *7*, **28**.
- [84] Y. P. Khanna, *Polym. Eng. Sci.* **1990**, *30*, 1615.
- [85] Thomas A. Shepard, Carl R. Delsorbo, Richard M. Louth, Jonathan L. Walborn, David A. Norman, Noel G. Harvey, Richard J. Spontak, *Journal of Polymer Science Part B: Polymer Physics* **1997**, *35*, 2617.
- [86] H.-W. Schmidt, M. Blomenhofer, K. Stoll, H.-R. Meier, *WO 2004072168*.
- [87] H.-W. Schmidt, P. Smith, M. Blomenhofer, *WO 2002046300*.
- [88] D. Maeder, K. Hoffmann, H.-W. Schmidt, *WO 2003102069*.
- [89] C. Gabriel, H.-W. Schmidt, F. Richter, H. J. Park, R. Xalter, *WO 2013/139802 A1*.
- [90] ASTM International, *ASTM D1003, Test Method for Haze and Luminous Transmittance of Transparent Plastics*, West Conshohocken **2011**.
- [91] BYK (Ed.), *Qualitätskontrolle für Lacke und Kunststoffe*, 2007.
- [92] C. Gabriel, H.-W. Schmidt, F. Richter, H. J. Park, R. Xalter, *WO 2013/139800 A2*.
- [93] L. Bouteiller, E. Ressouche, S. Pensec, B. Isare, *Compositions containing bisureas to form stable gels*, *WO 2016055751*.
- [94] X. Cao, A. Gao, K. Sun, L. Zhao, *Supramolecular Chemistry* **2015**, *27*, 484.
- [95] B. Isare, S. Pensec, M. Raynal, L. Bouteiller, *Comptes Rendus Chimie* **2016**, *19*, 148.
- [96] F. Lortie, S. Boileau, L. Bouteiller, C. Chassenieux, B. Demé, G. Ducouret, M. Jalabert, F. Lauprêtre, P. Terech, *Langmuir* **2002**, *18*, 7218.
- [97] T. Pinault, B. Andrioletti, L. Bouteiller, *Beilstein journal of organic chemistry* **2010**, *6*, 869.
- [98] E. Sabadini, K. R. Francisco, L. Bouteiller, *Langmuir the ACS journal of surfaces and colloids* **2010**, *26*, 1482.
- [99] M. Schmidt, C. S. Zehe, R. Siegel, J. U. Heigl, C. Steinlein, H.-W. Schmidt, J. Senker, *CrystEngComm* **2013**, *15*, 8784.
- [100] S. van der Laan, B. L. Feringa, R. M. Kellogg, J. van Esch, *Langmuir* **2002**, *18*, 7136.
- [101] J. van Esch, S. de Feyter, R. M. Kellogg, F. de Schryver, B. L. Feringa, *Chem. Eur. J.* **1997**, *3*, 1238.
- [102] R. M. Versteegen, R. P. Sijbesma, E. W. Meijer, *Macromolecules* **2005**, *38*, 3176.
- [103] Y. Xu, L. Wu, *European Polymer Journal* **2013**, *49*, 865.

- [104] N. Zweep, A. Hopkinson, A. Meetsma, W. R. Browne, B. L. Feringa, J. H. van Esch, *Langmuir* **2009**, *25*, 8802.
- [105] D. R. Holmes, C. W. Bunn, D. J. Smith, *J. Polym. Sci.* **1955**, *17*, 159.
- [106] Y. Li, W. A. Goddard, *Macromolecules* **2002**, *35*, 8440.
- [107] T. D. Fornes, D. R. Paul, *Polymer* **2003**, *44*, 3945.
- [108] Masahito Sano, Darryl Y. Sasaki, Toyoki Kunitaket, *Science*, *1992*, 441.
- [109] D. C. Giancoli, *Physik: Lehr- und Übungsbuch*, Pearson Studium **2010**.
- [110] D. C. Schroeder, *Chem. Rev.* **1955**, *55*, 181.
- [111] Asieh Yahyazadeh, Zahra Ghasemi, *Eur. Chem. Bull.* **2013**, *2 (8)*, 573.
- [112] J. J. Klein, S. Hecht, *Organic Letters* **2011**, *14*, 330.
- [113] M. Mushtaque, M. Jahan, M. Ali, M. S. Khan, M. S. Khan, Preeti Sahay, A. Kesarwani, *Journal of Molecular Structure* **2016**, *1122*, 164.
- [114] Mohammad Shoaib, *Pharmacology* **2014**, *3*, 91.
- [115] J. Liu, S. Yang, X. Li, H. Fan, P. Bhadury, W. Xu, J. Wu, Z. Wang, *Molecules (Basel, Switzerland)* **2010**, *15*, 5112.
- [116] A. Saeed, U. Flörke, M. F. Erben, *Journal of Sulfur Chemistry* **2013**, *35*, 318.
- [117] C. Rampalacos, W. D. Wulff, *Advanced synthesis & catalysis* **2008**, *350*, 1785.
- [118] O. V. Serdyuk, C. M. Heckel, S. B. Tsogoeva, *Organic & biomolecular chemistry* **2013**, *11*, 7051.
- [119] Á. Madarász, Z. Dósa, S. Varga, T. Soós, A. Csámpai, I. Pápai, *ACS Catal.* **2016**.
- [120] G. Vo-Thanh, T.-T.-D. Ngo, T.-H. Nguyen, C. Bournaud, R. Guillot, M. Toffano, *Asian J. Org. Chem.* **2016**.
- [121] L.-J. Yan, H.-F. Wang, W.-X. Chen, Y. Tao, K.-J. Jin, F.-E. Chen, *ChemCatChem* **2016**.
- [122] R.T. Loto, C.A. Loto, A.P.I. Popoola, *Journal of Materials and Environmental Science* **2012**, *3 (5)*, 885.
- [123] G. Bian, H. Fan, H. Huang, S. Yang, H. Zong, L. Song, G. Yang, *Organic Letters* **2015**, *17*, 1369.
- [124] G. Bian, H. Fan, S. Yang, H. Yue, H. Huang, H. Zong, L. Song, *The Journal of organic chemistry* **2013**, *78*, 9137.
- [125] M. Breugst, K. N. Houk, *The Journal of organic chemistry* **2014**, *79*, 6302.
- [126] V. Rajendran, J. Uma, *Optical Materials* **2016**, *57*, 249.

- [127] S. Sasi, G. Ramesh, R. Robert, S. Arumugam, C. Inmozhi, *Optik - International Journal for Light and Electron Optics* **2016**, *127*, 759.
- [128] C. Laurence, M. Berthelot, J.-Y. Le Questel, M. J. El Ghomari, *J. Chem. Soc., Perkin Trans. 2* **1995**.
- [129] A. Saeed, S. Ashraf, U. Flörke, Z. Y. D. Espinoza, M. F. Erben, H. Pérez, *Journal of Molecular Structure* **2016**, *1111*.
- [130] P. M. Pihko (Ed.), *Hydrogen bonding in organic synthesis*, Wiley-VCH, Weinheim **2009**.
- [131] M. Zappa, *Mettler Toledo - Thermal Analysis - UserCom* **2006**, *2*.
- [132] R. Ulrich, D. Joachimi, *Polyamide molding compositions*, US 2004/0242757 A1.
- [133] B. Valenti, E. Bianchi, G. Greppi, A. Tealdi, A. Ciferri, *J. Phys. Chem.* **1973**, *77*, 389.
- [134] T. Tsuruhara, A. Hayashi, H. Takeuchi, US6399681 (B1).
- [135] C. P. McAdam, N. E. Hudson, J. J. Liggat, R. A. Pethrick, *J. Appl. Polym. Sci.* **2008**, *108*, 2242.
- [136] M. R. Kamal, N. K. Borse, A. Garcia-Rejon, *Polym. Eng. Sci.* **2002**, *42*, 1883.
- [137] H. Chen, X. Hu, P. Cebe, *J Therm Anal Calorim* **2008**, *93*, 201.
- [138] W. Dong, W. Zhang, G. Chen, J. Liu, *Radiation Physics and Chemistry* **2000**, *57*, 27.
- [139] J.-W. Huang, C.-C. Chang, C.-C. Kang, M.-Y. Yeh, *Thermochimica Acta* **2008**, *468*, 66.
- [140] S. H. Jafari, P. Pötschke, M. Stephan, G. Pompe, H. Warth, H. Alberts, *J. Appl. Polym. Sci.* **2002**, *84*, 2753.
- [141] H.-M. Li, Z.-G. Shen, F.-M. Zhu, S.-A. Lin, *European Polymer Journal* **2002**, *38*, 1255.
- [142] Y. Li, T. Xie, G. Yang, *J. Appl. Polym. Sci.* **2006**, *99*, 335.
- [143] S. Shulin, C. Zhuo, S. Lili, Z. Huixuan, *J. Appl. Polym. Sci.* **2011**, *121*, 909.
- [144] R. T. Tol, V. Mathot, G. Groeninckx, *Polymer* **2005**, *46*, 369.
- [145] P. S. Walia, R. K. Gupta, C. T. Kiang, *Polym. Eng. Sci.* **1999**, *39*, 2431.
- [146] K. Yu, Z. Du, H. Li, C. Zhang, *Polym Eng Sci* **2010**, *50*, 396.
- [147] *Ullmann's Encyclopedia of Industrial Chemistry*, Wiley-VCH Verlag GmbH & Co. KGaA, Weinheim, Germany **2000**.
- [148] Orient Chemicals, <http://www.orient-usa.com/userfiles/file/Nigrosine.pdf>, accessed on, 22.08.2016.

- [149] B. Groos, R. Pfaender, *WO2016091807 A1*.
- [150] F. J. Green, *The Sigma-Aldrich handbook of stains, dyes, and indicators*, Aldrich Chemical Co, Milwaukee, Wis. **1990**.
- [151] <http://www.worlddyevariety.com/acid-dyes/acid-black-2.html>, accessed on, 17.08.2016.
- [152] <http://www.worlddyevariety.com/solvent-dyes/solvent-black-5.html>, accessed on, 17.08.2016.
- [153] <http://www.worlddyevariety.com/solvent-dyes/solvent-black-7.html>, accessed on, 17.08.2016.
- [154] A. Ciferri, E. Bianchi, F. Marchese, A. Tealdi, *Die Makromolekulare Chemie* **1971**, 150.
- [155] Y. Tian, H. Qin, X. Yang, C. Chi, S. Liu, *Materials Letters* **2016**, 180, 200.
- [156] A. Siegmann, Z. Baraam, *Polym. Eng. Sci.* **1981**, 21, 223.
- [157] K. E. Johnson, *The Electrochemical Society Interface* **2007**.
- [158] A. K. Haghi, *Physics and chemistry of classical materials: Applied research and concepts*, Apple Acad. Press, Toronto u.a. **2015**.
- [159] J. Yuen, J. Yung, *Modern Chemistry & Applications* **2013**, 1.
- [160] W. Zhang, Q. Wang, X. Wei, *Pige Yu Huagong* **2015**, 32, 14.
- [161] Y. Xue, H. Xiao, Y. Zhang, *International journal of molecular sciences* **2015**, 16, 3626.
- [162] J. Zhishen, S. Dongfeng, X. Weiliang, *Carbohydrate Research* **2001**, 333, 1.
- [163] Tianjin Chemical Reagent Research Institute Co., Ltd., Peop. Rep. China, *CN 104109129*.
- [164] G. Schmack, R. Vogel, L. Häussler, *Kunststoffe* **1994**, 11, 1590.
- [165] L. A. Paquette (Ed.), *Encyclopedia of reagents for organic synthesis*, Wiley, Chichester **1995**.
- [166] [https://techcenter.lanxess.com/scp/emea/de/docguard/TI\\_2009-017\\_DE\\_Die\\_Zwillinge\\_unter\\_den\\_Polyamiden.pdf?docId=63401](https://techcenter.lanxess.com/scp/emea/de/docguard/TI_2009-017_DE_Die_Zwillinge_unter_den_Polyamiden.pdf?docId=63401), accessed on, 16.09.2016.

## **(Eidesstattliche) Versicherungen und Erklärungen**

(§ 5 Nr. 4 PromO)

*Hiermit erkläre ich, dass keine Tatsachen vorliegen, die mich nach den gesetzlichen Bestimmungen über die Führung akademischer Grade zur Führung eines Doktorgrades unwürdig erscheinen lassen.*

(§ 8 S. 2 Nr. 5 PromO)

*Hiermit erkläre ich mich damit einverstanden, dass die elektronische Fassung meiner Dissertation unter Wahrung meiner Urheberrechte und des Datenschutzes einer gesonderten Überprüfung hinsichtlich der eigenständigen Anfertigung der Dissertation unterzogen werden kann.*

(§ 8 S. 2 Nr. 7 PromO)

*Hiermit erkläre ich eidesstattlich, dass ich die Dissertation selbständig verfasst und keine anderen als die von mir angegebenen Quellen und Hilfsmittel benutzt habe.*

(§ 8 S. 2 Nr. 8 PromO)

*Ich habe die Dissertation nicht bereits zur Erlangung eines akademischen Grades anderweitig eingereicht und habe auch nicht bereits diese oder eine gleichartige Doktorprüfung endgültig nicht bestanden.*

(§ 8 S. 2 Nr. 9 PromO)

*Hiermit erkläre ich, dass ich keine Hilfe von gewerblichen Promotionsberatern bzw. -vermittlern in Anspruch genommen habe und auch künftig nicht nehmen werde.*

.....  
Ort, Datum, Unterschrift